IntechOpen

# Robust Control

## Theoretical Models and Case Studies

*Edited by Moises Rivas López and Wendy Flores-Fuentes*

# ROBUST CONTROL - THEORETICAL MODELS AND CASE STUDIES

Edited by **Moises Rivas López** and **Wendy Flores-Fuentes**

**Robust Control - Theoretical Models and Case Studies**
http://dx.doi.org/10.5772/61622
Edited by Moises Rivas López and Wendy Flores-Fuentes

**Contributors**

Guoliang Wang, Chieh-Chuan Feng, Cheng-Lun Chen, Sheng-Hsiung Yang, Jenq-Lang Wu, Kufre Bassey, Teresa Orłowska-Kowalska, Grzegorz Tarchała, Esmeralda López, Gerardo Romero, Irma Perez, David Lara



**Notice**



First published in Croatia, 2016 by INTECH d.o.o.
eBook (PDF) Published by IN TECH d.o.o.
Place and year of publication of eBook (PDF): Rijeka, 2019.
IntechOpen is the global imprint of IN TECH d.o.o.
Printed in Croatia

Legal deposit, Croatia: National and University Library in Zagreb

Additional hard and PDF copies can be obtained from orders@intechopen.com

Robust Control - Theoretical Models and Case Studies
Edited by Moises Rivas López and Wendy Flores-Fuentes

p. cm.

Print ISBN 978-953-51-2423-8

Online ISBN 978-953-51-2424-5

eBook (PDF) ISBN 978-953-51-5070-1

# Meet the editors

Dr. Rivas López Moisés was born in 1960. He received the BS and MS degrees in Autonomous University of Baja California, Mexico, in 1985 and 1991, respectively, and the PhD degree in Science, Applied Physics, in the same University, in 2010. He has written 5 book chapters and 35 Journal and Proceedings Conference papers in optoelectronics and control applications. Also, he has presented different works in several International Congresses of IEEE, ICROS, SICE, in America and Europe. Dr. Rivas was Dean of Engineering Institute of Autonomous University Baja California (1997–2005) and Rector of Polytechnic University of Baja California (2006–2010). He is a member of National Researcher System and now is the head of Physics Engineering Department, of Engineering Institute of UABC, Mexico.

Dr. Flores-Fuentes was born in Baja California, Mexico on January, 1978. She received the bachelor's degree in Electronic Engineering from the Autonomous University of Baja California in 2001, the master's in Engineering degree from Technological Institute of Mexicali in 2006, and the PhD. degree in Science, Applied Physics, from Autonomous University of Baja California in June 2014. Until now she is the author of 4 journal articles, 2 book chapters, and 13 proceedings articles. Recently she organized and participated as Chair of Special Session on "Machine Vision, Control and Navigation" at IEEE ISIE 2015. She has been incorporated to CONACYT National Research System in 2016.

# Contents

# Preface

From the late 70s we have witnessed a revolution in the field of control, when it was found that the classical and modern control theories did not assure the stability or performance of the system under uncertainty.

Due to the need of being tolerant to changes in the control systems, subject to unknown disturbances or random changes in the operational environment of these systems, the robust control theory started generating new methods that are able to deal with the non-parameterized disturbances of systems, without adapting itself to the system uncertainty, but rather providing stability in the presence of errors bound to a model or dealing directly and effectively with real parameters uncertainty in the control systems.

Robust control applications have been increasing from the mid-80s with the Kharitonov's Theorem for interval polynomials; after this, several applications in aerospace, electrical, mechanical and others fields have been generated. More recently, Hansen and Sargent introduced an approach in the field of economics, which the solution of robustness problem is found implementing a dynamic game.

We could say, that in the last two decades, several questions about stability of systems under uncertainty have been answered. However, the robustness problem will remain a study subject, to improve the technological development and enhance the human quality of life in the world.

With this approach in mind and with the intention to exemplify robust control applications, this book includes selected chapters that describe models of H-infinity loop-shaping, robust stability and uncertainty, among others.

Each robust control method and model discussed in this book is illustrated by a relevant example, which facilitates its use as research reference or practical textbook in graduate programs.

Finally, we are grateful to the authors for their kind contributions and also appreciate the publisher for the support and guidance to publish this book.

**Moises Rivas López**
Engineering Institute
Autonomous University of Baja California, Mexico

**Wendy Flores-Fuentes**
Faculty of Engineering
Autonomous University of Baja California, Mexico

Chapter 1

# Robust Observer-Based Output Feedback Control of a Nonlinear Time-Varying System

Chieh-Chuan Feng

Additional information is available at the end of the chapter

http://dx.doi.org/10.5772/62697

**Abstract**

A class of time-varying systems can be quadratically stabilized with satisfactory performance by a modified time-invariant-based observer. The modified observer driven by the additional adaptation forces with static correction gains is used to estimate the time-varying system states. Under the frame of quadratic stability, the closed-loop systems satisfying induced norm bounded performance criterion are exponentially stabilized while the states are exponentially approaching by the modified observer. This paper deals with the time-varying systems that can be characterized as the multiplicative type of time-invariant and time-varying parts. The time-invariant part is then used to construct the modified observer with additional driving forces, which are ready to adjust time-varying effect coming from the measured outputs feeding into the modified observer. The determination of the adaptation forces can be derived from the minimization of the cost of error dynamics with modified least-squares algorithms. The synthesis of control and observer static correction gains are also demonstrated. The developed systems have been tested in a mass-spring-damper system to illustrate the effectiveness of the design.

**Keywords:** quadratic stablilization, time-invariant-based observer, error dynamics, least-squares algorithm, adaptation forces, time-varying parts

## 1. Introduction

The study of optimal control for time-varying systems involves, in general, the solutions of Riccati differential equations (RDEs) and computations of the time-varying correction gains [1–4]. It is noted that the system is typically computer-implemented system, upon which the RDE and correction gains are calculated. The computations, however, induces unavoidable time

delay. Although the time-delayed control has been considered, it leads to two disadvantages—complication of control mechanism and bulk of the control board. For some systems, for example, hard disk drives (a typically time-varying system) can only tolerate no delayed or very limited time delay control [5, 6] and use very small compartment. Hence, many literatures have focused on the static gain control of time-varying systems or the systems with time-varying or nonlinear uncertainties [7, 8]. It represents the simplest closed-loop control form but still encounters problems. One should aware that static output control is nonconvex, in which iterative linear matrix inequality approaches are exploited after it is expressed as a bilinear matrix inequality formulation( see [9–12]). As a result, it cannot be easily implemented in controlling the time-varying system and time delay problems remain.

It is a great challenge problem to design a linear continuous time-invariant observer with constant correction gains that regulate linear continuous time-varying plants. Although the vast majority of continuous TV control applications are implemented in digital computers [6, 13, 14], there are still opportunities to implement control with Kalman observer in continuous time (i.e., in analog circuits) [Hug88]. In particular, those control systems requiring fast response ask no or little delay effects. The difficulties for setting up those boards are because the algorithm of the design is too complex to implement in board level design, too expensive which can only be realized in a laboratory, or digital computation time induced unsatisfactory delay. It should be noticed that to realize the Kalman observer involves the computation of Riccati differential equations and inversion of matrices, which cause the obstacles of the board level design. A survey of linear and nonlinear observer design for control systems has been conducted in the literatures [15–18] and references therein. For controlling an linear time-invariant (LTI) system, the Lungerber observer [19] design with constant correction gain is straightforward and can be implemented on a circuit board with ease.

Many practical control systems implement time-invariant controllers with observers in the feedback loop, which can be easily realized not only in the laboratory but also in the industrial merchandize [20]. The advantages of realization for the time-invariant controllers and observers are due to the constant parameters, which can be easily assembled by using resistors and other analog integrated elements in circuits board. The use of observers is also essential in industrial controls due to, in some cases, the states can be either not reachable or expensive to be sensed. Therefore, the use of observers are undoubtedly required to estimate unmeasured states since not merely full-state feedback control can be easily implemented but unmeasured states can be monitored [21–25].

With the aforementioned disadvantages and advantages, the control of time-varying systems is naturally arisen by designing a time-invariant observer-based controller that stabilizes, in particular exponentially, this time-varying plant. It is believed that this is a great challenge problem since we found no literatures tackling this problem. In what follows time-varying system control is first reviewed for laying the foundation of the robust control of the system with optimality property.

The feedback control of linear time-varying system has been extensively studied [1, 6, 7, 26–31]. The key observation of early works for exponential stability of time-varying systems requires that the time-dependent matrix-valued functions be bounded and piecewise contin-

http://dx.doi.org/10.5772/62697

uous satisfying Lyapunov quadratic stability [29, 31]. In this regard, many, but not all, of them can be translated to robust control framework since time-dependent matrices are essentially bounded and are treated as uncertainties [8, 32]. This gives an opportunity for the control system design without solving RDEs, although what we pay for the avoiding solving RDEs is the conservative of control. The conservativeness comes from two reasons—solutions of RDEs are avoided and admit fast varying parameters. This, however, can be reduced by designing parameter-dependent type of criterion or introducing slack variables such that reduces the tightness of dependent variables( see, e.g., [33] and reference therein).

This paper is organized as follows. The following section, Section 2, sets up the time-varying systems to be tackled, time-invariant observer to be built, feedback control problems to be solved, and system properties (assumptions) to be with the systems. Section 3 gives the main results for solving the feedback control problems, in which LMIs characterize the quadratically stability of the closed-loop system with $L_2$-gain of the closed-loop system is preserved; in addition, least-squares algorithm is suggested to drive the time-varying observer such that the time-varying plant states can be estimated asymptotically. Consequently, Section 4 demonstrates the synthesis of the static gains of control input and correction gains of observer. To verify the effectiveness, illustrative applications are to test the overall design of the feedback closed-loop system. The last section, Section 5, concludes the overall paper.

## 2. System formulation and problem statement

We consider a nonlinear time-varying system described by a set of equations

$$\begin{aligned} \dot{x}(t) &= A(t)x(t) + B_1u(t) + B_2w(t) \\ z(t) &= \quad Dx(t) \qquad\quad + D_2w(t) \\ y(t) &= \quad Cx(t) \end{aligned} \tag{1}$$

The first equation describes the *plant* with $n$-vector of *state* $x$ and *control input* $u \in \mathbb{R}^m$ and is subject to *exogenous input* $w \in \mathbb{R}^l$, which include *disturbances* (to be rejected) or *references* (to be tracked). The second equation defines the *regulated outputs* $z \in \mathbb{R}^q$, which, for example, may include *tracking error*, expressed as a linear combination of the plant state $x$ and of the exogenous input $w$. The last part is the *measured outputs* $y \in \mathbb{R}^p$. The matrices in (1) are assumed to have the following *system property*:

**(S1)** $A(t)$ denotes the matrix with nonlinear time-varying properties satisfying

$$A(t) = F(t)A, \tag{2}$$

where $A$ is the $n \times n$ constant matrix that extracts from $A(t)$. The $n \times n$ matrix $F(t)$ lumps all time-varying elements associated with plant matrix $A(t)$, and it is possible to find a vertex set $\Psi_1$ defined as follows

$$\Psi_1 = \mathbf{Co}\{F_1, F_2, \cdots, F_i\}$$

such that $F(t) \in \Psi_1$, which is equivalent to saying that $F(t)$ is within the convex set $\Psi_1$ for all time $t \geq 0$.

**(S2)** The matrices $B_1$, $B_2$, $D$, and $D_2$ are all constant matrices, in which $B_1$ and $B_2$ quantify the range spaces of control input $u$ and exogenous input $w$, respectively, and $D_2$ is chosen to be zero matrix that is $D_2 = 0$ for computational simplicity.

**Remark 1**. It is highlighted that $F(t)$ in ($S1$) is not merely to lump all possible time-varying functions but to include the parametric uncertainties. For the parametric uncertainties, it is seen by simply observing that $F(t)$ can be multiplicative uncertainties shown in [8]. For representing time-varying matrix, an example is set as follows. Let

$$A(t) = \begin{pmatrix} -2 & f(t) \\ 0 & -1 \end{pmatrix} = F(t)A,$$

where

$$F(t) = \begin{pmatrix} 1 & -f(t) \\ 0 & 1 \end{pmatrix}, \quad A = \begin{pmatrix} -2 & 0 \\ 0 & -1 \end{pmatrix}.$$

It should be aware that another equally good choice is to use additive type of representation, that is, $A(t) = A + F_1(t)$, where $F_1(t)$ lumps all time-varying factors. As a matter of fact, multiplicative and additive type of representations are interchangeable. Let $F_2(t)$ be such that $F_1(t) = F_2(t)A$. Thus, $A(t)=F(t)A$, where $F(t) = I + F_2(t)$.

**Remark 2**. A number of examples are found to show the time-varying bound for $F(t)$, such as aircraft control systems in which constantly weight decreasing due to fuel consumption, the switching operations of a power circuit board for voltage and current regulations, and the hard disk drives with rotational disks induced time-varying dynamic phenomena [6].

The control action to (1) is to design an observer-based output feedback control system, which processes the measured outputs $y(t)$ in order to determine the plant states and generate an appropriate control inputs $u(t)$ based on the estimated plant states. The following *observer dynamics* is developed for system (1),

$$\begin{aligned} \dot{\hat{x}}(t) &= A\hat{x}(t) + B_1 u(t) + B_2 w(t) + Le(t) \\ \hat{y}(t) &= C\hat{x}(t) \end{aligned} \tag{3}$$

where

http://dx.doi.org/10.5772/62697

$$e(t) = diag[\hat{y}(t)]\varsigma(t) - y(t),$$

$\hat{x}(t)$ is the observed state of $x(t)$ and the gain L is to be designed for the sake of stability. It should be noted that the usage of constant matrix $A$ in (3) instead of using time-varying $A(t)$ is due to the fact that *it is not possible or may be too expensive to build the time-varying plant matrix $A(t)$ for the time-varying observers* in a real analog circuit board that controls the system. On the contrary, we are able to establish a time-invariant observer with ease for constant system matrix $A$, $B_1$, and $B_2$ as stated in the Section 2. It is also seen that the observer (3) is Luenberger-like observer because of the use of observer gain L.

The time-varying vector-valued function $\varsigma(t) \in \mathbb{R}^p$ to be determined in the sequel is an additional degree of freedom for driving observer (3) to estimate the plant state $x(t)$. We should be aware that the intention of $\varsigma(t)$ is designed and meant to compensate time-varying effects of $F(t)$ to the system, that is, the effects of the time-varying functions will be adjusted by one such function $\varsigma(t)$. Therefore, in addition to input $u(t)$, $e(t)$ becomes an additional *driving force* to (3) such that $\hat{x}(t)$ tracks $x(t)$ is possible. If $F(t) = I$ and all elements of the vector $\varsigma(t)$ being equal to 1, then the system (1) with the observer (3) is a typical textbook example of Luenberger observer control system [21].

In order to facilitate the closed-loop system, the *error dynamics* can thus be found by manipulating (1) and (3) as follows

$$\dot{\tilde{x}}(t) = F(t)A\tilde{x}(t) + (I - F(t))A\hat{x}(t) + Le(t) \tag{4}$$

or, equivalently, by taking the advantages of polytopic bound of (S1)

$$\dot{\tilde{x}}(t) = (A + LC)\tilde{x}(t) + (I - F(t))Ax(t) + Ldiag[\epsilon(t)]\hat{y}(t) \tag{5}$$

where $\tilde{x}(t) = \hat{x}(t) - x(t)$ and $\varepsilon(t) = \varsigma(t) - 1$, in which $\mathbf{1}$ denotes the vector with all elements being equal to 1.

Once the observed state $\hat{x}$ is available, the control input $u$ is chosen to be a memoryless system of the form

$$u(t) = K\hat{x}(t), \tag{6}$$

where K is the static gain to be designed. The control purpose has twofold: to *achieve closed-loop stability* and to *attenuate the influence* of the exogenous input w on the penalty variable z, in the sense of rendering the $L_2$ gain of the corresponding closed-loop system less than a prescribed number $\gamma$, in the presence of time-varying plant. The problem of finding controllers achieving these goals can be formally stated in the following terms.

**Observer-based control via measured feedback**. Given a real number $\gamma>0$ and $\{A(t),\ B_1,\ B_2,\ C,\ D,\ D_2\}$ satisfying system properties (S1) and (S2). Find, if possible, two constant matrices $K$ and $L$ such that

**(O1)** the matrix

$$\begin{pmatrix} F(t)A+B_1K & B_1K \\ (I-F(t))A & A+LC \end{pmatrix} \tag{7}$$

has all eigenvalues in $C^-$,

**(O2)** the $L_2$-gain of the closed-loop system

$$\begin{aligned} &\dot{x}(t)=(F(t)A+B_1K)x(t)+B_1K\tilde{x}(t)+B_2w(t),\quad y(t)=Cx(t)\\ &\dot{\hat{x}}(t)=(A+B_1K)\hat{x}(t)+B_2w(t)+Le(t),\quad \hat{y}(t)=C\hat{x}(t)\\ &z(t)=Dx(t),\quad \text{with}\quad e(t)=diag[\hat{y}(t)]\varsigma(t)-y(t) \end{aligned} \tag{8}$$

is strictly less than $\gamma$, or equivalently, for each input $u(t)=K\hat{x}(t)\in L_2[0,\infty)$, the response $z(t)$ of (8) from initial state $(x(0),\ \tilde{x}(0))=(0,\ 0)$ is such that the following performance index is satisfied

$$\mathcal{J}_\infty=\int_0^\infty \|z(t)\|^2dt\le\gamma^2\int_0^\infty \|w(t)\|^2dt \tag{9}$$

for some $\gamma>0$ and every $w(t)\in L_2\ [0,\infty)$.

**Remark 3**. Here, we will be using the notion of quadratic stability with an $L_2$-gain measure which was introduced in [32]. This concept is a generalization of that of quadratic stabilization to handle $L_2$-gain performance constraint to time-varying system attenuation. To this end, the characterizations of robust performance based on quadratic stability will be given in terms of LMIs, where if LMIs can be found, then the computations by finite dimensional convex programming are efficient (see, for example, [32]).

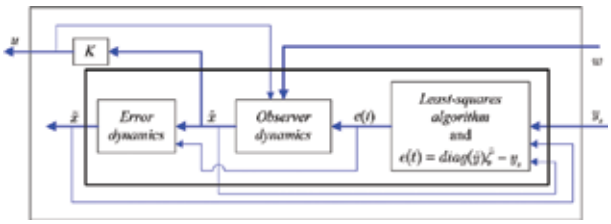


**Figure 1.** Overall control structure.

**Remark 4**. **Figure 2** shows the overall feedback control structure of (8) to be designed in the sequel, where the feedback loop, namely *observer–error dynamics*, serves as filtering process with $y(t)$ and $w(t)$ as inputs such that proper control inputs $u(t)$ and additional driving force of (3) $e(t)$ are produced.

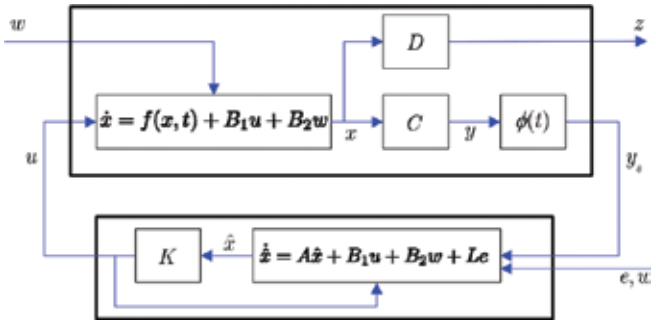


**Figure 2.** Observer–error dynamics.

## 3. Analyses and characterizations

Two issues will be addressed in this section. Firstly, the theorem states the sufficiency condition showing that the problem of observer-based control via measured feedback of time-varying system is solvable. Secondly, an identification process based on least-squares algorithms for $\varsigma(t)$ is derived to construct the feedback structure of the closed-loop system (8).

### 3.1. LMI characterizations

**Theorem 1**. Consider the time-varying system (1), observer dynamics (3), and error dynamics (4) satisfying system property (S1) and (S2). Then, (T1) implies (T2), where (T1) and (T2) are as follows.

**(T1)** There exist matrices $P1 \succ 0$, $P2 \succ 0$, $K$, and $L$ and positive scalars $\gamma$ and $\beta$ such that

$$\begin{pmatrix} \Pi_1(P_1,K) & \star \\ K^T B_1^T P_1 + P_2(I - F(t))A & \Pi_2(P_2,L) \end{pmatrix} \prec 0, \tag{10}$$

and matrices $P_3 \succ 0$ and $Q \succ 0$ with adaptive scheme of (t) satisfying

$$\dot{\epsilon}(t) = -P_3 \left( Q + \frac{1}{2}\beta^2 diag[\hat{y}(t)]^T diag[\hat{y}(t)] \right) \epsilon(t). \tag{11}$$

The matrices, $\Pi_1$ and $\Pi_2$, defined in (10) are

$$\Pi_1(P_1,K) = (F(t)A + B_1K)^T P_1 + P_1(F(t)A + B_1K) + \gamma^{-2} P_1 B_2 B_2^T P_1 + D^T D, \tag{12}$$

$$\mathcal{J}_\infty = \int_0^\infty \|z(t)\|^2 \, dt \le \gamma^2 \int_0^\infty \|w(t)\|^2 \, dt \tag{13}$$

**(T2)** (O1) and (O2) hold, that is, the problem of observer-based control via contaminated measured feedback is solvable.

**Proof**: the implication between (T1) and (T2) is shown in the Appendix.

**Remark 5**. It is shown in the Theorem 1 that if the matrix inequality (10) is satisfied and if $(t)$ is computationally adjusted according to (11), then the overall closed-loop system is not merely quadratically stabilizable, but the performance index (9) is fulfilled. It is highlighted that $(t)$ in (11) is exponentially approaching zero as $t \to \infty$ for any $\hat{y}(t)$. It is also noticed that there remains a problem, that is, to compute the observed states $\hat{x}(t)$ in (3), in addition to the input $u(t)$ and exogenous signal $w(t)$, the time-varying vector function $\varsigma(t)$ is needed in the computation. Therefore, the following modified least-squares algorithm is derived for recursive estimation of time-varying vector-valued function $\varsigma(t)$.

### 3.2. Modified least-squares algorithms

Prior to stating the modified least-squares scheme for computing $\varsigma(t)$, the following assumption is made

$$\varsigma(\alpha) = \varsigma(\beta), \;\; \alpha,\beta \in I_i, \;\; i = 0,1,2,\cdots, \tag{14}$$

where $Ii = \{t \mid t_i \le t < t_i + \Delta t\}$. This is to say that $\varsigma(t)$ is kept constant within the small time interval $\Delta t$, which, equivalently, is assumed that $\varsigma(t)$ is a piecewise continuous time-varying function. The problem in this section is to determine an adaptation law for the vector-valued function $\varsigma(t)$ in such a way that the $\tilde{x}(t)$ computed from the model (4) agree as closely as possible to zero in the sense of least squares. The following least-squares algorithms are developed by summing the index of each small time interval with cost function defined as follows

$$\mathcal{J} = \min_{\varsigma} \sum_i \mathcal{J}_i(\varsigma) = \min_{\varsigma} \sum_i \left\{ \frac{1}{2} \int_{t_i}^{t_i+\Delta t} \dot{\tilde{x}}^T \dot{\tilde{x}} \, d\tau \right\}. \tag{15}$$

To minimize the cost function $\mathfrak{I}$, each index $\mathfrak{I}_i$ should be minimized as well and the following conditions may be obtained for each time interval

http://dx.doi.org/10.5772/62697

$$\frac{\partial}{\partial \varsigma}\mathcal{J}_i = \int_{t_i}^{t} W^T(\tau)\left(F(\tau)A\tilde{x}(\tau) + (I - F(\tau))A\hat{x}(\tau) + W(\tau)\varsigma(\tau) - Ly(\tau)\right)d\tau = 0, \tag{16}$$

where $t \in I_i$ and

$$W(\tau) = Ldiag[\hat{y}(\tau)].$$

In view of (16), the *least-squares estimate* for $\varsigma(t)$ is given by

$$\hat{\varsigma}(t) = \Gamma(t)\int_{t_i}^{t} W^T(\tau)\left(Ly(\tau) - F(\tau)A\tilde{x}(\tau) - (I - F(\tau))A\hat{x}(\tau)\right)d\tau, \tag{17}$$

where $\Gamma(t)$ is called *covariance matrix* and is defined as follows

$$\Gamma(t) = \left(\int_{t_i}^{t} W^T(\tau)W(\tau)d\tau\right)^{-1}.$$

To assure positive definiteness and thus the invertibility, the covariance matrix will be further polished in the sequel. The covariance matrix plays an important role in the estimation of $\varsigma(t)$ and is worth noting that

$$\frac{d}{dt}\left(\Gamma^{-1}(t)\right) = W^T(t)W(t). \tag{18}$$

To find the least-squares estimator with recursive formulations, which parameters are updated continuously on the basis of available data, we differentiate (17) with respect to time and obtain

$$\frac{d}{dt}\hat{\varsigma}(t) = -\Gamma(t)W^T(t)W(t)\hat{\varsigma}(t) + f(t),\ \ \hat{\varsigma}(t_i) = \hat{\varsigma}_i, \tag{19}$$

where

$$f(t) = \Gamma(t)W^T(t)\left(Ly(t) - F(t)A\tilde{x}(t) - (I - F(t))A\hat{x}(t)\right), \tag{20}$$

for $t \in I_i,\ i = 0, 1, 2, \cdots$. The covariance matrix $\Gamma(t)$ acts in the $\hat{\varsigma}(t)$ update law as a time-varying, directional adaptation gain. We have to aware that by observing (18), which indicates positive

semi definite of $\frac{d}{dt}\Gamma - 1(t)$, implies that $\Gamma^{-1}(t)$ may go without bound and hence $\Gamma(t)$ will become very small in some directions and adaptation in those directions becomes very slow. Therefore, to avoid slowing adaptive propagation speed and to assure the positive definiteness of covariance matrix $\Gamma(t)$ such that invertibility exists, the following *covariance resetting propagation law* is developed. Within each time window, we modify (18) as follows,

$$\frac{d}{dt}\left(\Gamma^{-1}(t)\right) = gW^T(t)W(t),\ \Gamma(t_i) = k_0 I,\ t \in I_i, \tag{21}$$

and

$$\Gamma(t_r^+) = k_0 I \succ 0,\quad t_r = \{t | \lambda_{\min}(\Gamma(t)) \le k_1 < k_0,\ t \in I_i,\ i = 0,1,2,\cdots\}. \tag{22}$$

The scalar $g > 0$ is chosen such that the adaptation maintains suitable rate of propagation. The covariance resetting propagation is adjusted by (21), in which the initial condition is also reset. The condition (22) shows that the covariance matrix can also be reset within the time window if the covariance matrix is close to the singularity. That is, the covariance matrix is reset if its minimum eigenvalue is less than or equal to $k_1$, that is, $\lambda_{\min}(\Gamma(t)) \le k_1$. The following Lemma shows that the covariance matrix $\Gamma(t)$ is bounded and is positive definite based on the covariance resetting propagation law (21) and (22).

**Lemma 1**. Assuming that (21) and (22) hold. Then, $k_0 I \succcurlyeq \Gamma(t) \succcurlyeq k_1 I \succ 0$ and, thus, $k_0 \ge \| \Gamma(t) \| \ge k_1$ for $t \in I_i$, $i = 0, 1, 2, \cdots$.

**Proof**: At the resettings, the covariance matrix $\Gamma^{-1}(t)$ is reset at $t = t_r^+$, hence $\Gamma\left(t_r^+\right) = k_0 I$. Then, followed by $\frac{d}{dt}\Gamma^{-1}(t) = gW^T(t)W(t) \succcurlyeq 0$, we have $\Gamma^{-1}(t_1) - \Gamma^{-1}(t_2) \succcurlyeq 0$ for all $t_1 \ge t_2 > t_r$ between covariance resettings. The computation will progress until the next resetting time $t$, if it exists, on which $\lambda_{\min}(\Gamma(t)) \le k_1$. Hence, we may conclude that $k_0 I \succcurlyeq \Gamma(t) \succcurlyeq k_1 I \succ 0$, which says that $k_0 \ge \| \Gamma(t) \| \ge k_1$.

Before presenting the theorem for modified least-squares algorithms of $\hat{\varsigma}(t)$ showing that it is bounded, the following transition matrix Lemma for the solutions of (19) is essential.

**Lemma 2**. There exists a positive number $k$ such that the transition matrix, $\Phi(t, \tau)$, of (19) is bounded, that is, $\| \Phi(t, \tau) \| \le k < \infty$, for $t \in I_i$, $i = 0, 1, 2, \cdots$.

**Proof**: The proof is constructive. We first notice that the solution to (19) is given by

$$\hat{\varsigma}(t) = \Phi(t, t_i)\hat{\varsigma}_i + \int_{t_i}^{t} \Phi(t, \tau) f(\tau) d\tau,$$

where $\Phi(t, \tau)$ is the transition matrix of $\dot{\hat{\varsigma}}(t) = -\Gamma(t)W^T(t)W(t)\hat{\varsigma}(t)$ or the unique solution of

http://dx.doi.org/10.5772/62697

$$\dot{\Phi}(t,\tau) = -\Gamma(t)W^T(t)W(t)\Phi(t,\tau), \quad \Phi(\tau,\tau) = I. \tag{23}$$

A constructive method is suggested by letting a differential equation $\dot{\eta}(t) = -\eta(t)$, $\eta(t_i) = \eta_i$, where $\eta(t)$ is a vector of appropriate dimensions. We may conclude that $\eta(t)$, $\dot{\eta}(t) \in \mathsf{L}_2 \cap \mathsf{L}_\infty$..

Let $\pi(t) = \Phi(t, t_i)\eta(t)$ and Lyapunov candidate, $V_\pi = \pi^T(t)\Gamma^{-1}(t)\pi(t)$, where $\Gamma(t)$ is chosen as satisfying Lemma 1. Then, computing $\dot{V}\pi$ along solutions of $\dot{\pi}(t) = \dot{\Phi}(t, ti)\eta(t) + \Phi(t, ti)\dot{\eta}(t)$ between the covariance resettings is as follows,

$$\dot{V}_\pi = \pi^T(t)\left((-2+g)W^T(t)W(t) - \Gamma^{-1}(t)\right)\pi(t).$$

Without loss of generality, let $g = 2$. Then,

$$\dot{V}_\pi = \pi^T(t)\left(-\Gamma^{-1}(t)\right)\pi(t) = -V_\pi < 0. \tag{24}$$

At the point of resetting, that is, the point of discontinuity of $\Gamma(t)$, we obtain

$$V_\pi(t_r^+) - V_\pi(t_r) = \pi^T(t)\left(\Gamma^{-1}(t_r^+) - \Gamma^{-1}(t_r)\right)\pi(t) \le 0. \tag{25}$$

It follows from (24) and (25), we conclude that the Lyapunov candidate along the solution $\pi(t)$ has the property, $0 \le V_\pi(t) \le V_\pi(t_i)$. This shows that $\pi(t) \in \mathsf{L}_\infty$, which implies that $\| \Phi(t, t_i) \| \le k < \infty$ for some $k > 0$.

**Theorem 2**. Assuming that the problem of observer-based control via contaminated measured feedback is solvable. If there exist the identifier structure of least-squares algorithm (19) with covariance resetting propagation law (21) and (22), then $\hat{\varsigma}(t) \in \mathsf{L}_\infty$ for all $t \ge 0$.

**Proof**: To prove the claim is true, we need to show that $\| \hat{\varsigma}(t) \|_\infty = \sup_t \| \hat{\varsigma}(t) \| < \infty$ for $t \in I_i$, $i = 0, 1, 2, \cdots$. We have the solution to (19) is given by

$$\hat{\varsigma}(t) = \Phi(t,t_i)\hat{\varsigma}_i + \int_{t_i}^{t} \Phi(t,\tau)f(\tau)d\tau,$$

where $\Phi(t, \tau)$ is the transition matrix shown in (23). In view of Lemma 2, we obtain

$$\|\hat{\varsigma}(t)\|_\infty = \left\| \Phi(t,t_i)\hat{\varsigma}_i + \int_{t_i}^{t} \Phi(t,\tau)f(\tau)d\tau \right\|_\infty \le k\left( \|\hat{\varsigma}_i\|_\infty + \int_{t_i}^{t} \|f(\tau)\|_\infty d\tau \right).$$

The boundedness of $\int_{t_i}^{t} \| f(\tau) \|_\infty \, d\tau$ can be easily seen by observing (20), in which $\hat{\hat{x}}(t)$, $\tilde{x}(t)$, and $W(t) = Ldiag[\hat{\hat{y}}] = Ldiag[C\hat{\hat{x}}]$ followed by Theorem 1 have bounds and $\hat{\hat{x}}(t)$, $\tilde{x}(t)$, $W(t) \to 0$, as $t \to \infty$. The covariance matrix $\Gamma(t)$ satisfies (21) and, then, is bounded by Lemma 1. Followed by system property (S1), $F(t)$ is clearly bounded for all $t \geq 0$. The measured signal $y = Cx$, by Theorem 1, is 0 as $t \to \infty$. In summary, there exists a positive finite number $k_3$ such that

$$\int_{t_i}^{t} \|f(\tau)\|_\infty d\tau \leq k_3 \int_{t_i}^{t} d\tau \leq k_3 \Delta t.$$

Therefore,

$$\|\hat{\varsigma}(t)\|_\infty \leq k(\|\hat{\varsigma}_i\|_\infty + k_3 \Delta t) < \infty, \tag{26}$$

which indicates that $\hat{\hat{\varsigma}}(t) \in L_\infty$, for $t \in I_i$. As time evolves, for each small time interval, (26) always holds. Hence, we may extend $t \to \infty$. This completes the proof.

**Remark 6**. In this section, a modified least-squares algorithm is shown to find the estimated $\varsigma(t)$, which is intentionally designed to justify the effects of time-varying functions $F(t)$ produced in the plant (1). **Figure 3** depicts the complete structure of observer–error dynamics that has been shown in **Figure 2**, in which two filters, namely *observer dynamics* and *error dynamics*, and one lest squares algorithm construct the feedback control. The observer dynamics produces the estimated state of plant by filtering the signals $u(t)$, $w(t)$, and $e(t)$. It is worth noting that the signal $e(t)$ from least-squares algorithm plays an additional drive force to the observer dynamics. The error dynamics is to find the error state $\tilde{x}(t)$, which is then injected into the least-squares algorithms such that the time-varying function $\varsigma(t)$ is estimated.

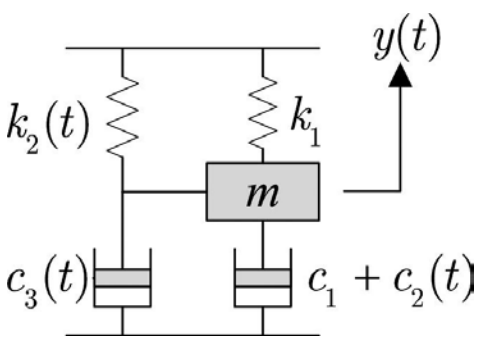


**Figure 3. M**ass-damper-spring system.

## 4. Control and observer gain synthesis

The synthesis of control and observer gains is addressed in Theorem 1. For the simplicity of expression, the time argument of matrix-valued function $F(t)$ will be dropped and denoted by $F$. A useful and important Lemma will be stated in advance for clarity:

**Lemma 3** (Elimination Lemma see [32]). Given $\mathsf{H}=\mathsf{H}^T \in \Re^{n\times n}$, $\mathsf{V}\in\Re^{n\times m}$, and $\mathsf{U}\in\Re^{n\times p}$ with Rank($\mathsf{V}$)<n and Rank($\mathsf{U}^T$)<n. There exists a matrix K such that

$$\mathcal{H}+\mathcal{V}K\mathcal{U}^T+\mathcal{U}K^T\mathcal{V}^T\prec 0$$

if and only if

$$\mathcal{V}_\perp^T\mathcal{H}\mathcal{V}_\perp\prec 0 \text{ and } \mathcal{U}_\perp^T\mathcal{H}\mathcal{U}_\perp\prec 0,$$

where $\mathsf{V}\perp$ and $\mathsf{U}\perp$ are orthogonal complement of $\mathsf{V}$ and $\mathsf{U}$, respectively, that is $\mathsf{V}_\perp^T\mathsf{V}=0$ and $[\mathsf{V}_\perp\ \mathsf{V}]$ is of maximum rank.

**Lemma 4**. Given a real number $\gamma>0$ and $\{A(t),\ B_1,\ B_2,\ C,\ D,\ D_2\}$ satisfying system properties (S1) and (S2), the following statements (Q1), (Q2), and (Q3) are equivalent.

**(Q1)** There exist matrices $P_1\succ 0$, $P_2\succ 0$, matrices $K$ and $L$, and positive scalars $\beta$ and $\delta$ such that the following inequality holds,

$$\begin{pmatrix}\Pi_1(P_1,K)+\delta^{-2}A^T(I-F)^T(I-F)A & P_1B_1K\\ K^TB_1^TP_1 & \Pi_2(P_2,L)+\delta^2P_2P_2\end{pmatrix}\prec 0. \tag{27}$$

**(Q2)** There exist matrices $P_1\succ 0$, $P_2\succ 0$, matrices $K$ and $L$, and positive scalars $\beta$ and $\delta$ such that the following inequality hold,

$$(B_1)_\perp^TP_1^{-1}\left(\Pi(P_1,K)+\delta^{-2}A^T(I-F)^T(I-F)A\right)P_1^{-1}(B_1)_\perp\prec 0, \tag{28}$$

$$\Pi_2(P_2,L)+\delta^2P_2P_2\prec 0, \tag{29}$$

**(Q3)** There exist matrices $X\succ 0$ and $P_2\succ 0$, matrix $W$ and $Y$, and the positive scalars $\gamma$, $\delta$ and $\beta$ such that the following two matrix inequalities hold,

$$\begin{pmatrix}XA^TF^T+FAX+W^TB_1^T+B_1W+\gamma^{-2}B_2B_2^T & X\\ X & -\left(D^TD+\delta^{-2}A^T(I-F)^T(I-F)A\right)^{-1}\end{pmatrix}\prec 0, \tag{30}$$

$$\begin{pmatrix} A^T P_2 + P_2 A + C^T Y^T + YC & Y & P_2 \\ Y^T & -\beta^2 I & 0 \\ P_2 & 0 & -\delta^{-2} I \end{pmatrix} \prec 0. \tag{31}$$

**Proof**: to prove (Q1) ⇔ (Q2). The inequality (27) may fit into Lemma 3 with

$$\mathcal{H} = \begin{pmatrix} \Pi_1(P_1) + \delta^{-2} A^T (I-F)^T (I-F) A & 0 \\ 0 & \Pi_2(P_2) + \delta^2 P_2 P_2 \end{pmatrix},$$

$$\mathcal{V} = \begin{pmatrix} P_1 B_1 \\ 0 \end{pmatrix}, \text{ and } \mathcal{U} = \begin{pmatrix} I \\ I \end{pmatrix}.$$

Next, the orthogonal complement of V and U is given by $\mathsf{V}_\perp$ and $\mathsf{U}_\perp$, respectively, which are

$$\mathcal{V}_\perp = \begin{pmatrix} P_1^{-1}(B_1)_\perp & 0 \\ 0 & I \end{pmatrix}, \text{ and } \mathcal{U}_\perp = \begin{pmatrix} I \\ -I \end{pmatrix},$$

which $(B_1)_\perp$ is defined as the orthogonal complement of $B_1$ and is such that $(B_1)_\perp^{\mathrm{T}} B_1$=0 and $[B_1 (B_1)_\perp]$ is of maximum rank. By applying Lemma 3, we may have the following inequalities,

$$\mathcal{V}_\perp^T \mathcal{H} \mathcal{V}_\perp = \begin{pmatrix} (B_1)_\perp^T P_1^{-1} \left(\Pi(P_1, K) + \delta^{-2} A^T (I-F)^T (I-F) A\right) P_1^{-1} (B_1)_\perp & 0 \\ 0 & \Pi_2(P_2, L) + \delta^2 P_2 P_2, \end{pmatrix} \prec 0, \tag{32}$$

and

$$\mathcal{U}_\perp^T \mathcal{H} \mathcal{U}_\perp = \Pi(P_1, K) + \delta^{-2} A^T (I-F)^T (I-F) + \Pi_2(P_2, L) + \delta^2 P_2 P_2 \prec 0. \tag{33}$$

It is seen that matrix inequalities (28) and (29) hold if and only if (32) is true. Given (32), (33) is also true. Therefore, by Lemma 3, (Q1) ⇔ (Q2).

To prove (Q2) ⇔ (Q3), let X = $P_1^{-1}$, we find the following *iff* condition for inequality (28),

$$\begin{aligned} & (B_1)_\perp^T P_1^{-1} \left(\Pi(P_1, K) + \delta^{-2} A^T (I-F)^T (I-F) A\right) P_1^{-1} (B_1)_\perp \prec 0 \\ \Leftrightarrow\ & (B_1)_\perp^T \left(XA^T F^T + FAX + W^T B_1^T + B_1 W + \gamma^{-2} B_2 B_2^T + X(D^T D + \delta^{-2} A^T (I-F)^T (I-F) A) X\right) (B_1)_\perp \prec 0, \\ \Leftrightarrow\ & XA^T F^T + FAX + W^T B_1^T + B_1 W + \gamma^{-2} B_2 B_2^T + X(D^T D + \delta^{-2} A^T (I-F)^T (I-F) A) X \prec 0, \\ \Leftrightarrow\ & \begin{pmatrix} XA^T F^T + FAX + W^T B_1^T + B_1 W + \gamma^{-2} B_2 B_2^T & X \\ X & -(D^T D + \delta^{-2} A^T (I-F)^T (I-F) A)^{-1} \end{pmatrix} \prec 0, \end{aligned} \tag{34}$$

http://dx.doi.org/10.5772/62697

where $W = KX$. It is noted that the last *iff* holds is due to Schur complement in that the positive definiteness of $D^T D + \delta^{-2} A^T (I-F)^T (I-F) A$ must ensure. As for the matrix inequality (29), let $Y = P_2 L$, we have

$$\begin{aligned} & \Pi_2(P_2, L) + \delta^2 P_2 P_2 \prec 0, \\ \Leftrightarrow\ & A^T P_2 + P_2 A + C^T Y^T + Y C + \beta^{-2} Y Y^T + \delta^2 P_2 P_2 \prec 0, \\ \Leftrightarrow\ & \begin{pmatrix} A^T P_2 + P_2 A + C^T Y^T + Y C & Y & P_2 \\ Y^T & -\beta^2 I & 0 \\ P_2 & 0 & -\delta^{-2} I \end{pmatrix} \prec 0. \end{aligned} \tag{35}$$

Again, the last *iff* of (35) is due to Schur complement and $\beta > 0$ and $\delta > 0$ ensure the inequality holds.

**Remark 7**. It is seen that $\delta$ is the only common scalar for matrix inequalities (34) and (35). In order to ease of computation and without loss of generality, we may assume that $\delta$ is a certain constant. The advantage of it, in addition to the ease of computation, is that the gains $K$ and $L$ are solely determined by (34) and (35), respectively. From rigorous point of view, we may not be able to say that the separation principle is completely valid for this case. But, loosely speaking, it fits by small modification.

**Lemma 5**. (Q1) implies (10).

**Proof**: let $(\pi_1, \pi_2) \neq (0, 0)$. Then

$$\begin{aligned} & \begin{pmatrix} \pi_1 \\ \pi_2 \end{pmatrix}^T \begin{pmatrix} \Pi_1(P_1, K) & \star \\ K^T B_1^T P_1 + P_2(I-F)A & \Pi_2(P_2, L) \end{pmatrix} \begin{pmatrix} \pi_1 \\ \pi_2 \end{pmatrix} \\ & = \pi_1^T (\Pi_1(P_1, K)) \pi_1 + \pi_2^T (\Pi_2(P_2, L)) \pi_2 + \pi_1^T \left( P_1 B_1 K + A^T (I-F)^T P_2 \right) \pi_2 + \pi_2^T \left( K^T B_1^T P_1 + P_2 (I-F) A \right) \pi_1 \\ & = \pi_1^T (\Pi_1(P_1, K)) \pi_1 + \pi_2^T (\Pi_2(P_2, L)) \pi_2 + \pi_1^T (P_1 B_1 K) \pi_2 + \pi_2^T \left( K^T B_1^T P_1 \right) \pi_1 \\ & \quad + \delta^{-2} \pi_1^T A^T (I-F)^T (I-F) A \pi_1 + \delta^2 \pi_2^T P_2 P_2 \pi_2 - \left( (I-F) A \pi_1 - \delta^2 P_2 \pi_2 \right)^T \delta^{-2} \left( (I-F) A \pi_1 - \delta^2 P_2 \pi_2 \right) \\ & \leq \pi_1^T (\Pi_1(P_1, K)) \pi_1 + \pi_2^T (\Pi_2(P_2, L)) \pi_2 + \pi_1^T (P_1 B_1 K) \pi_2 + \pi_2^T \left( K^T B_1^T P_1 \right) \pi_1 \\ & \quad + \delta^{-2} \pi_1^T A^T (I-F)^T (I-F) A \pi_1 + \delta^2 \pi_2^T P_2 P_2 \pi_2 \\ & = \begin{pmatrix} \pi_1 \\ \pi_2 \end{pmatrix}^T \begin{pmatrix} \Pi_1(P_1, K) + \delta^{-2} A^T (I-F)^T (I-F) A & P_1 B_1 K \\ K^T B_1^T P_1 & \Pi_2(P_2, L) + \delta^2 P_2 P_2 \end{pmatrix} \begin{pmatrix} \pi_1 \\ \pi_2 \end{pmatrix}. \end{aligned}$$

Thus, (Q1) implies (10). This completes the proof.

**Theorem 3**. Given a real number $\gamma > 0$ and $\{A(t),\ B_1,\ B_2,\ C,\ D,\ D_2\}$ satisfying system property (S1) and (S2). Then, (Q3) with scheme (11) implies (T2).

**Proof**: by Lemma 5, (Q1) implies matrix inequality (10). Moreover, by Lemma 4, we have (Q1) $\Leftrightarrow$ (Q3). Therefore, (Q3) with scheme (11) is equivalent to (T1). Moreover, by Theorem 1, the claim is true.

**Remark 8**. Theorem 3 states that the problems post in observer-based control via contaminated measured feedback, that is, (O1) and (O2), are solvable by proving that (T2) holds.

## 5. Illustrative application

In this application, a simple time-varying mass-damper-spring system is controlled to demonstrate that the time-varying effects appearing in the system matrix can be transferred to a force term in the observer structure. Thus, consider the system shown in **Figure 3** without sensor fault. $k_1$ and $c_1$ are linear spring and damping constant, respectively. $k_2(t)$, $c_2(t)$, and $c_3(t)$ are time-varying spring and viscous damping coefficients. The system is described by the following equation of motion

$$\begin{aligned} 0 &= -k_2(t)y(t) + c_3(t)\dot{y}(t) \\ m\ddot{y}(t) &= -k_1 y(t) - (c_1 + c_2(t))\dot{y}(t) + u(t), \end{aligned} \tag{36}$$

where time-varying functions are $c_2(t)=c_2(\sin\omega_2 t)$, $k_2(t)=\frac{k_1}{m}e^{-bt}(\cos\omega_1 t)$, $c_3(t)=-\frac{c_1}{m}e^{-bt}(\cos\omega_1 t)$, and the constants are $k_1 = k$ and $c_1=c_2 = c$. Define $x_1(t)=y(t)$ and $x_2(t)=\dot{y}(t)$, the state space representation of (36) is

$$\begin{aligned} \dot{x}(t) &= F(t)Ax(t) + B_1 u(t) \\ y(t) &= Cx(t), \end{aligned} \tag{37}$$

where

$$x(t) = \begin{pmatrix} x_1(t) \\ x_2(t) \end{pmatrix},\ F(t) = \begin{pmatrix} 1 & e^{-bt}\cos\omega_1 t \\ -\frac{c_2}{m}\sin\omega_2 t & 1 \end{pmatrix},$$
$$A = \begin{pmatrix} 0 & 1 \\ -\frac{k_1}{m} & -\frac{c_1}{m} \end{pmatrix},\ B_1 = \begin{pmatrix} 0 \\ \frac{1}{m} \end{pmatrix}, \text{ and } C = \begin{pmatrix} 1 & 0 \end{pmatrix}.$$

Here, we consider the parameters $m = 1$, $c = 1$, $k = 1$, $b = 0$, $\omega 1 = 1$, and $\omega_2$=10 (rad / sec). Thus, the set of vertices of polytope $\Psi_1$ associated with time-varying matrix $F(t)$ is

$$\mathbf{Co}\left\{\begin{pmatrix} 1 & 1 \\ 1 & 1 \end{pmatrix}, \begin{pmatrix} 1 & 1 \\ -1 & 1 \end{pmatrix}, \begin{pmatrix} 1 & -1 \\ 1 & 1 \end{pmatrix}, \begin{pmatrix} 1 & -1 \\ -1 & 1 \end{pmatrix}\right\}.$$

By applying linear matrix inequalities (30) and (31) of (Q3) in Lemma 4, the control and observer gain, $K$ and $L$ can be found by implementing Matlab Robust Control Toolbox. It is

also noted that the computation of two matrix inequalities can be separated by justifying $\delta = 0.05$. We thus find

$$K = \begin{pmatrix} -9.0322 & -10.2123 \end{pmatrix}, \; L = \begin{pmatrix} -7.0950 \\ -2.8926 \end{pmatrix}.$$

The control input is then computed by $u = K\hat{x}$, where the observed state $\hat{x}$ is from

$$\begin{aligned} \dot{\hat{x}}(t) &= (A + B_1 K)\hat{x}(t) + Le(t) \\ \hat{y}(t) &= C\hat{x}(t) \end{aligned} \tag{38}$$

with $e(t) = diag[\hat{y}(t)]\varsigma(t) - y(t)$, in which the time-varying vector-valued function $\varsigma(t)$ is estimated via the set of recursive formulations (19)–(22).

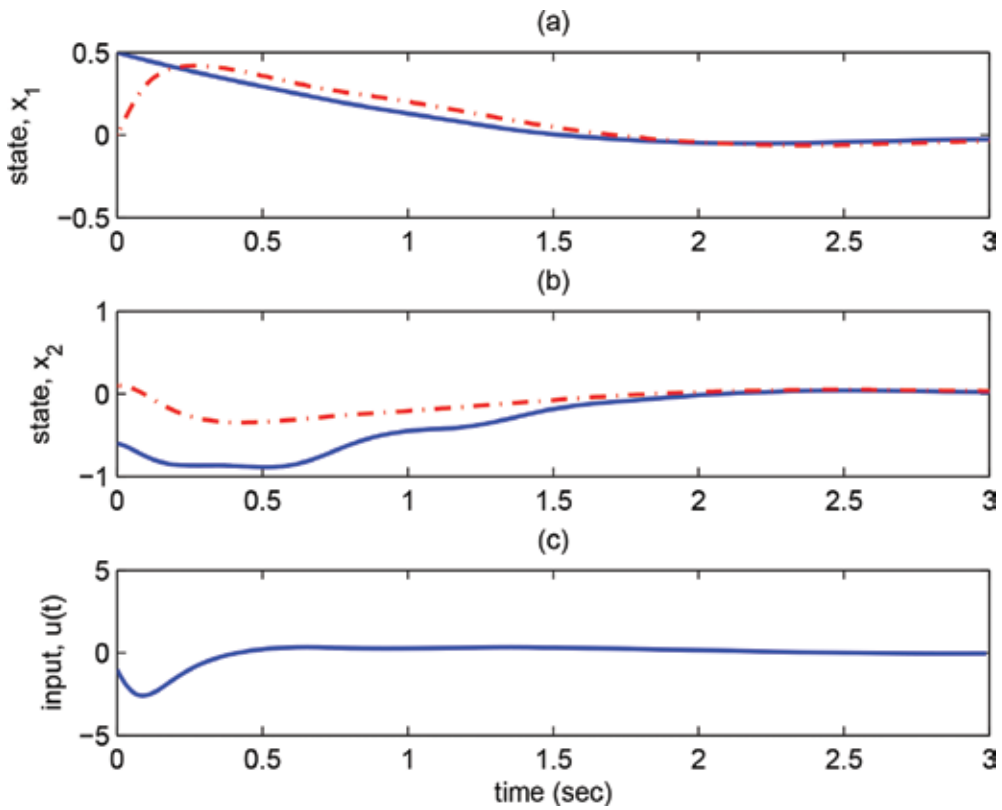


**Figure 4.** (a) shows plant state (solid line) $x_1$ and observer state (dash-dot line) $\hat{x}_1$. (b) is the plant state (solid line) $x_2$ and observer state (dash-dot line) $\hat{x}_2$. (c) gives the control input $u(t)$.

The implementation are coded in Matlab using the initial states: $x_1(0)=0.5$, $x_2(0)=-0.6$, $\hat{x}_1(0)=0.0$, $\hat{x}_2(0)=0.1$, $\hat{\varsigma}(0)=0.1$, $\Gamma(0)=k_0=2$, and $k_1=0.3$. The simulation results are depicted in **Figures 4** and **5**. **Figure 4(a)** and **(b)** shows that the observer states $\hat{x}$ cohere with the plant states $x$. It is, therefore, seen that the observer (38) being driven by time-varying term $e(t)$ can actually trace the plant (37). The control input $u(t)$ to the system is shown in **Figure 4**(c). The covariance resetting propagation law $\Gamma(t)$ and the estimated $\varsigma(t)$, that is, $\hat{\varsigma}(t)$ are shown in **Figure 5(a)** and **(b)**. The observer driving force $e(t)$ and 2-norm value of the time-varying matrix function $F(t)$ are depicted in **Figure 5(c)** and **(d)**. It is seen clearly that the $\Gamma(t)$ and $\hat{\varsigma}(t)$ are adjusted to accommodate the time-varying effects that driving the observer dynamics as the closed-loop system is approaching equilibrium point. The driving force to the observer dynamics $e(t)$ shows the same results. **Figure 5(c)** depicts that the time-varying matrix $F(t)$ is indeed varying with time.

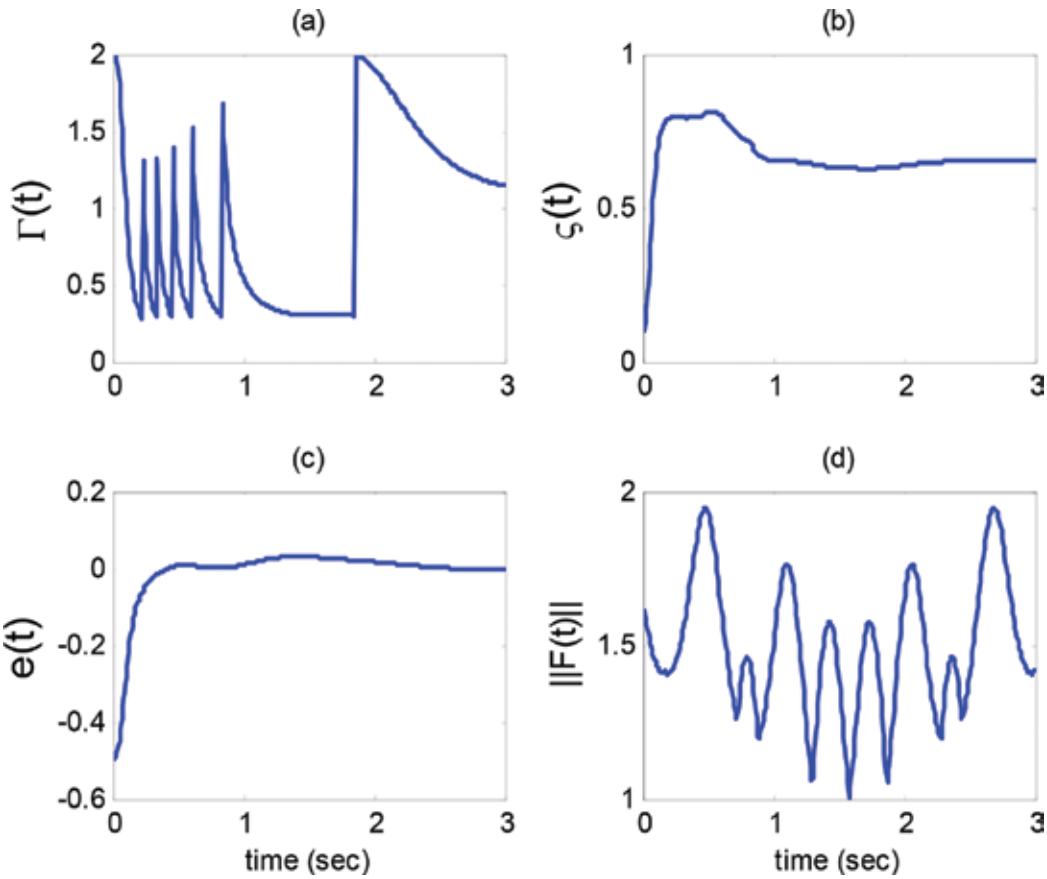


**Figure 5.** (a) is the values of $\Gamma(t)$. (b) demonstrates the least-squares estimated results of $\hat{\varsigma}(t)$. (c) is the driving force of the observer dynamics e(t). (d) computes the 2-norm value of time-varying matrix function $F(t)$ with $b = 0$.

http://dx.doi.org/10.5772/62697

## 6. Conclusion

This paper has developed the modified time-invariant observer control for a class of time-varying systems. The control scheme is suitable for the time-varying system that can be characterized by the multiplicative type of time-invariant and time-varying parts. The time-invariant observer is constructed directly from the time-invariant part of the system with additional adaptation forces that are prepared to account for time-varying effects coming from the measured output feeding into the modified observer. The derivation of adaptation forces is based on the least squares algorithms in which the minimization of the cost of error dynamics considers as the criteria. It is seen from the illustrative application that the closed-loop systems are showing exponentially stable with system states being asymptotically approached by the modified observer. Finally, the LMI process has been demonstrated for the synthesis of control and observer gains and their implementation on a mass-spring-damper system proves the effectiveness of the design.

## 7. Appendix

It is noted that in this appendix all time arguments of either vector-valued or matrix-valued time functions will be dropped for the simplicity of expression. They can be easily distinguished by their contents.

**Proof**: (T1) ⇒ (T2). We need to show that if the conditions (10) and (11) in (T1) hold, then (O1) and (O2), which are equivalent to (T2), hold. Let quadratic Lyapunov function be

$$V(x,\tilde{x},\epsilon) = x^T P_1 x + \tilde{x}^T P_2 \tilde{x} + \epsilon^T P_3^{-1} \epsilon,$$

with $P_1 \succ 0$, $P_2 \succ 0$, and $P_3 \succ 0$. Then, the performance index (9) can be written as

$$J_\infty = \int_0^\infty \|z\|^2 dt = \int_0^\infty \left[ z^T z + \frac{d}{dt} V(x,\tilde{x},\epsilon) \right] dt - V(x(\infty),\tilde{x}(\infty),\epsilon(\infty)), \tag{39}$$

for all states satisfying (1) and (3) with initial states $(x(0), \tilde{x}(0))=(0, 0)$, and $(0)=0$. In view of (8), the first integrand in (39) is

$$z^T z = x^T D^T D x \tag{40}$$

The second integrand in (39) is

$$\frac{d}{dt}V(x,\tilde{x},\epsilon) = \frac{d}{dt}\left(x^T P_1 x + \tilde{x}^T P_2 \tilde{x} + \epsilon^T P_3^{-1}\epsilon\right). \tag{41}$$

The right-hand side of equality (41) can be reorganized by using the closed-loop system (8), and thus, the first term is

$$\begin{aligned}
&\frac{d}{dt}x^T P_1 x \\
=&x^T\left((FA+B_1K)^T P_1 + P_1(FA+B_1K)\right)x \\
&+\tilde{x}^T(B_1K)^T P_1 x + x^T P_1 B_1 K\tilde{x} \\
&+w^T B_2^T P_1 x + x^T P_1 B_2 w
\end{aligned} \tag{42}$$

Completing the square of (42), we have

$$\begin{aligned}
&\frac{d}{dt}x^T P_1 x \\
=&x^T\left((FA+B_1K)^T P_1 + P_1(FA+B_1K)\right)x \\
&+\tilde{x}^T(B_1K)^T P_1 x + x^T P_1 B_1 K\tilde{x} \\
&+\gamma^2 w^T w + \gamma^{-2} x P_1 B_2^T B_2^T P_1 x \\
&-(w-\gamma^{-2}B_2^T P_1 x)^T\gamma^2(w-\gamma^{-2}B_2^T P_1 x).
\end{aligned} \tag{43}$$

Similarly, the second term of (41) is

$$\begin{aligned}
&\frac{d}{dt}\tilde{x}^T P_2 \tilde{x} \\
=&\tilde{x}^T\left((A+LC)^T P_2 + P_2(A+LC)\right)\tilde{x} \\
&+\hat{y}^T diag[\epsilon]^T L^T P_2\tilde{x} + \tilde{x}^T P_2 L diag[\epsilon]\hat{y} \\
&+x^T A^T(I-F)^T P_2\tilde{x} + \tilde{x}^T P_2(I-F)Ax.
\end{aligned} \tag{44}$$

Applying completing the square to (44), we obtain

$$\begin{aligned}
&\frac{d}{dt}\tilde{x}^T P_2 \tilde{x} \\
=&\tilde{x}^T\left((A+LC)^T P_2 + P_2(A+LC)\right)\tilde{x} \\
&+x^T A^T(I-F)^T P_2\tilde{x} + \tilde{x}^T P_2(I-F)Ax \\
&+\beta^2\hat{y}^T diag[\epsilon]^T diag[\epsilon]\hat{y} + \beta^{-2}\tilde{x}^T P_2 LL^T P_2\tilde{x} \\
&-(diag[\epsilon]\hat{y}-\beta^{-2}L^T P_2\tilde{x})^T\beta^2(diag[\epsilon]\hat{y}-\beta^{-2}L^T P_2\tilde{x}).
\end{aligned} \tag{45}$$

http://dx.doi.org/10.5772/62697

Substituting (40), (43), and (45) into (39), we have

$$\begin{aligned} J_\infty = \int_0^\infty \Bigg[ & \begin{pmatrix} x \\ \tilde{x} \end{pmatrix}^T \begin{pmatrix} \Pi_1(P_1,K) & \star \\ (P_1B_1K)^T + P_2(I-F)A & \Pi_2(P_2,L) \end{pmatrix} \begin{pmatrix} x \\ \tilde{x} \end{pmatrix} \\ & - (w-\gamma^{-2}B_2^TP_1x)^T\gamma^2(w-\gamma^{-2}B_2^TP_1x) \\ & - (diag[\epsilon]\hat{y}-\beta^{-2}L^TP_2\tilde{x})^T\beta^2(diag[\epsilon]\hat{y}-\beta^{-2}L^TP_2\tilde{x}) \\ & +\gamma^2w^Tw+\beta^2\hat{y}^Tdiag[\epsilon]^Tdiag[\epsilon]\hat{y}+\frac{d}{dt}(\epsilon^TP_3^{-1}\epsilon)\Bigg]dt \\ & - V(x(\infty),\tilde{x}(\infty),\epsilon(\infty)), \end{aligned} \tag{46}$$

where definition of Π1(P1) and Π2(P2) are defined as (12) and (13), respectively. Therefore, by eliminating the negative terms from (46), the following inequality is drawn,

$$\begin{aligned} J_\infty \le \int_0^\infty \Bigg[ & \begin{pmatrix} x \\ \tilde{x} \end{pmatrix}^T \begin{pmatrix} \Pi_1(P_1,K) & \star \\ (P_1B_1K)^T + P_2(I-F)A & \Pi_2(P_2,L) \end{pmatrix} \begin{pmatrix} x \\ \tilde{x} \end{pmatrix} \\ & +\gamma^2w^Tw+\beta^2\hat{y}^Tdiag[\epsilon]^Tdiag[\epsilon]\hat{y}+\frac{d}{dt}(\epsilon^TP_3^{-1}\epsilon)\Bigg]dt. \end{aligned} \tag{47}$$

Given that $diag[\,]\hat{y} = diag[\hat{y}]$, if (11) of (T1) holds, then it concludes that

$$\beta^2\hat{y}^Tdiag[\epsilon]^Tdiag[\epsilon]\hat{y}+\frac{d}{dt}(\epsilon^TP_3^{-1}\epsilon) = -\epsilon^T(2Q)\epsilon.$$

In view of (10) of (T1), we thus find that the inequality (47) is simply

$$J_\infty \le \int_0^\infty \left[\gamma^2w^Tw-\epsilon^T(2Q)\epsilon\right]dt \le \gamma^2\int_0^\infty w^Twdt. \tag{48}$$

Therefore, the inequality (48) satisfies the performance index (9), which completes the proof (O2).

To prove that (O1) holds, we use the inequality (10) in (T1) and get the equivalent inequality as follows,

$$\tilde{P}\tilde{A}+\tilde{A}^T\tilde{P} \prec -\tilde{P}\tilde{B}R^{-1}\tilde{B}^T\tilde{P}-\tilde{D}^T\tilde{D},$$

where

$$\tilde{P} = \begin{pmatrix} P_1 & 0 \\ 0 & P_2 \end{pmatrix}, \quad \tilde{A} = \begin{pmatrix} FA + B_1K & B_1K \\ (I-F)A & A + LC \end{pmatrix}, \quad \tilde{R} = \begin{pmatrix} \gamma^2 & 0 \\ 0 & \beta^2 \end{pmatrix},$$
$$\tilde{B} = \begin{pmatrix} B_2 & 0 \\ 0 & L \end{pmatrix}, \quad \tilde{D} = \begin{pmatrix} D & 0 \\ 0 & 0 \end{pmatrix}$$

It is concluded, by a standard Lyapunov stability argument, that $\tilde{A}$, that is (7), has all eigenvalues in $C^-$, which shows that (O1) holds. This completes the proof of Theorem 1.

## Author details

Chieh-Chuan Feng*

Address all correspondence to: ccfeng@isu.edu.tw

Department of Electrical Engineering, I-Shou University, Kaohsiung City, Taiwan

## References

[1] Amato F. Robust Control of Linear Systems Subject to Uncertain Time-Varying Parameters. Lecture Notes in Control and Information Sciences. Berlin Heidelberg: Springer-Verlag; 2006.

[2] Grewal MS, Andrews AP. Kalman Filtering: Theory and Practice Using MATLAB. New York, NY: John Wiley & Sons, Inc.; 2008.

[3] Simon D. Optimal State Estimation: Kalman, H∞, and Nonlinear Approaches. Hoboken, New Jersey: John Wiley & Sons, Inc.; 2006.

[4] Sontag ED. Mathematical Control Theory: Deterministic Finite Dimensional Systems. 2nd ed. New York: Springer; 1998.

[5] Chen BM, Lee TH, Venkatakrishnan V. Hard Disk Drive Servo Systems. Advances in Industrial Control. London: Springer-Verlag; 2002.

[6] Nie J, Conway R, Horowitz R. Optimal H∞ Control for Linear Periodically Time-Varying Systems in Hard Disk Drives. IEEE/ASME Transactions on Mechatronics. 2013;18(1):212–220.

[7] Phat VN. Global Stabilization for Linear Continuous Time-varying Systems. Applied Mathematics and Computation. 2006;175(2):1730–1743.

[8] Zhou K, Doyle JC. Essentials of Robust Control. Upper Saddle River, New Jersey: Prentice Hall; 1998.

[9] Syrmos VL, Abdallah CT, Dorato P, Grigoriadis K. Static Output Feedback-A Survey. Automatica. 1997;33(2):125–137.

[10] Huang D, Nguang SK. Robust H∞ Static Output Feedback Control of Fuzzy Systems: an ILMI Approach. IEEE Transactions on Systems, Man, and Cybernetics, Part B: Cybernetics. 2006;36(1):216–222.

[11] Rosinová D, Veselý V, Kućera V. A Necessary and Sufficient Condition for Static Output Feedback Stabilizability of Linear Discrete-time Systems. Kybernetika. 2003;39(4):447–459.

[12] Leibfritz F. An LMI-Based Algorithm for Designing Suboptimal Static H2/H∞ Output Feedback Controllers. SIAM Journal on Control and Optimization. 2000;39(6):1711–1735.

[13] Zhang J, Zhang C. Robustness of Discrete Periodically Time-varying Control Under LTI Unstructured Perturbations. IEEE Transactions on Automatic Control. 2000;45(7): 1370–1374.

[14] Zhang Y, Fidan B, Ioannou PA. Backstepping Control of Linear Time-Varying Systems with Known and Unknown Parameters. IEEE Transactions on Automatic Control. 2003;48(11):1908–1925.

[15] Astrom KJ, Wittenmark B. Adaptive Control. 2nd ed. Boston, MA: Addison-Wesley; 1994.

[16] Besançon G. Observer Design for Nonlinear Systems. A Loría FLL, Panteley E, editors. Lecture Notes in Control and Information Sciences, vol. 328. London: Springer; 2006.

[17] Besançon G. Nonlinear Observers and Applications. Lecture Notes in Control and Information Sciences. London: Springer; 2007.

[18] Spurgeon SK. Sliding Mode Observers: A Survey. International Journal of Systems Science. 2008;39(8):751–764.

[19] Luenberger DG. Observers for Multivariable Systems. IEEE Transactions on Automatic Control. 1966;11(2):190–197.

[20] Parr EA. Industrial Control Handbook. Jordan Hill, Oxford: Industrial Press; 1998.

[21] Franklin GF, Emami-Naeini A, Powell JD. Feedback Control of Dynamic Systems. 3rd ed. Boston, MA: Addison-Wesley; 1994.

[22] Feng CC. Fault-Tolerant Control and Adaptive Estimation Schemes for Sensors with Bounded Faults. In: IEEE International Conference on Control Applications; Singapore, 2007. p. 628–633.

[23] Feng CC. Robust Control for Systems with Bounded-Sensor Faults. Mathematical Problems in Engineering. 2012;2012, Article ID 471585.

[24] Sepe RB, Lang JH. Real-time observer-based (adaptive) control of a permanent-magnet synchronous motor without mechanical sensors. IEEE Transactions on Industry Applications. 1992;28(6):1345–1352.

[25] Swarnakar A, Marquez HJ, Chen T. A New Scheme on Robust Observer-Based Control Design for Interconnected Systems with Application to an Industrial Utility Boiler. IEEE Transactions on Control Systems Technology. 2008;16(3):539–547.

[26] Bellman RE. Stability Theory of Differential Equations. Dover books on Intermediate and Advanced Mathematics. New York, NY: Dover Publications; 1953.

[27] Amato F, Ariola M, Cosentino C. Finite-time control of linear time-varying systems via output feedback. In: Proceedings of the American Control Conference; Salt Lake City, 2005. p. 4722–4726.

[28] Callier FM, Desoer CA. Linear System Theory. London: Springer; 2012.

[29] Desoer C. Slowly Varying System $\dot{x}=A(t)x$. IEEE Transactions on Automatic Control. 1969;14(6):780–781.

[30] Green M, Limebeer DJN. Linear Robust Control. Englewood Cliffs, New Jersey: Prentice Hall; 1995.

[31] Rosenbrook HH. The Stability of Linear Time-dependent Control Systems. Journal of Electronics and Control. 1963;15(1):73–80.

[32] Boyd S, El Ghaoui L, Feron E, Balakrishnan V. Linear Matrix Inequalities in System and Control Theory. vol. 15 of Studies in Applied Mathematics. Philadelphia, PA: SIAM; 1994.

[33] Feng CC. Integral Sliding-Based Robust Control. In: Mueller A, editor. Recent Advances in Robust Control—Novel Approaches and Design Methods. Rijeka, Croatia: InTech; 2011.p. 165–186.

Chapter 2

# New Stabilization of Complex Networks with Non-delayed and Delayed Couplings over Random Exchanges

Guoliang Wang and Tingting Yan

Additional information is available at the end of the chapter

http://dx.doi.org/10.5772/62504

**Abstract**

In this chapter, the stabilization problem of complex dynamical network with non-delayed and delayed couplings is realized by a new kind of stochastic pinning controller being partially delay dependent, where the topologies related to couplings may be exchanged. The designed pinning controller is different from the traditional ones, whose non-delay and delay state terms occur asynchronously with a certain probability, respectively. Sufficient conditions for the stabilization of complex dynamical network over topology exchange are derived by the robust method and are presented with liner matrix inequities (LMIs). The switching between the non-delayed and delayed couplings is modeled by the related coupling matrices containing uncertainties. It has shown that the bound of such uncertainties play very important roles in the controller design. Moreover, when the bound is inaccessible, a kind of adaptive partially delay-dependent controller is proposed to deal with this general case, where another adaptive control problem in terms of unknown probability is considered too. Finally, some numerical simulations are used to demonstrate the correctness and effectiveness of our theoretical analysis.

**Keywords:** complex dynamical network, partially delay-dependent pinning controller, non-delayed and delayed couplings, robust method, adaptive control

## 1. Introduction

With the rapid development of science and technology, human beings have marched into the network era, and complex network has become a hot topic. Complex network is an important

method to describe and study complex systems, and all complex systems can be abstracted from practical background by different perspectives and become a complex network of interacting individuals, such as ecological network, food network, gene regulation network, social network, and distributed sensor network. Research on complex network has become a frontier subject with many subjects and challenges. Over the past few years, studies on complex network have received more and more attention from various fields of scientific research See [1–5]. The popularization of complex network has also caused a series of important problems about the network structures and studies of the network dynamic behaviors. Particularly, special attention has been paid to the studies of synchronization control problems of complex dynamical networks. As one of the significant dynamic behaviors of complex dynamical network, synchronization is widely used in neural network, public transit scheduling, laser system, secure communization system, information science, etc. [6–11]. So it is concerned by more and more scholars. In real networks, because of the complex dynamical network having a great many nodes, and every node has its dynamical behavior, it is hard for the complex dynamical network itself to make the states of the network to desired trajectory. Thus, the studies on the control strategy of complex dynamical network will be meaningful. So far, many control methods for complex dynamical network have been reported in refs. [12–17]. Pinning control such as in refs. [18–20] is widely welcomed for its advantages. It is easy to be realized and can save the cost effectively. The main idea of pinning control is to control a part of nodes in the complex networks to realize the whole network to the expected states and to reduce the number of the controllers effectively. When there exist some unknown parameters, the adaptive control method could be exploited, some of which was mentioned in refs. [21–23].

On the other hand, there are many factors that affect the stability of complex network, where time delay and network topology are two important factors. First, time delay is an objective phenomenon in nature and human society. In the process of transmission and response of complex network, it is inevitable to produce time delay, which is because of the physical limitations of the speed of transmission and the existence of network congestion, such as the existence of time delay in communication network and virus transmission. There are some typical time delay network systems such as circuit system [24], satellite communication system [25], and laser array system [26]. It is noticed that the majority of the studies on complex network have been performed on some absolute assumptions. For example, the stabilization referred to state feedback control is realized only by a non-delay or delay controller, which is relied on some absolute assumptions [18, 19, 27]. However, in many practical applications, these assumptions do not accord with the peculiarities of the real networks. Based on these facts, we may design a kind of controller that contains non-delay and delay states simultaneously. Second, the topology of the network plays an important role in determining the network characteristics and the synchronization control. The research of coupling delay also plays a significant role in complex networks. In most of the above papers, it is seen that the topologies are fixed. But in practical applications, the topological structure of the complex network is not constant and may be changed randomly. That is because of the influence of various stochastic factors. In this case, how to ensure the stabilization of networks by the proposed controller when the topologies related to couplings change is worth discussing.

http://dx.doi.org/10.5772/62504

Motivated by the above discussions, in this chapter, the stabilization problem of complex networks with non-delayed and delayed couplings over random exchanges is studied by exploiting the robust method to describe the topologies exchanging randomly. A kind of stochastic pinning controller being partially delay-dependent is developed, which contains non-delay and delay terms simultaneously but occur asynchronously. Here, the probability distributions are taken into account in the proposed controller design. The rest of this chapter is organized as follows: In Section 2, the model of complex dynamical networks with non-delayed and delayed couplings over random exchanges is established. In Section 3, the stabilization of the underlying complex networks is considered, which is realized by partially delay-dependent controller and adaptive controller respectively. A numerical example is demonstrated in Section 4; the conclusion of this chapter is given in Section 5.

**Notation**: $\mathbb{R}^n$ denotes the $n$ dimensional Euclidean space, $\mathbb{R}^{m\times n}$ is the set of all $m \times n$ real matrices. $E\{\cdot\}$ is the expectation operator with respect to some probability measure. diag$\{\cdots\}$ stands for a block-diagonal matrix. $I_N$ is an identity matrix being of $N$ dimensions. $\mathbb{S}=\mathbb{S}_\ell \cup \bar{\mathbb{S}}_\ell$, where $\mathbb{S}_l=\{1, 2, \ldots, l\}$, $\bar{\mathbb{S}}_\ell=\{l+1, l+2, \ldots, N\}$. $\lambda_{\max}(M)$ is the maximum eigenvalue of $M$, while $\sigma_{\max}(M)$ is the maximum singular value of $M$. $\|G\|$ denotes the 2-norm of matrix $G$. * stands for an ellipsis for the term induced by symmetry.

## 2. Model of complex networks with non-delayed and delayed couplings over random exchanges

As is known, time delay is ubiquitous in many network systems. When time delay exists in the interaction, it may affect the dynamic behavior and even destabilize the network system. Thus, time delay should be taken into consideration, which could accurately reflect some characteristics of networks. By investing the existing literatures, it is easy to find that most of the results on complex networks have been carried out under some implicit assumptions. That is the communication information of nodes is only related to $x(t)$ or $x(t-\tau)$. However, in many cases, this simplification is not satisfactory for the special nature of the networks. In fact, the information communication of nodes is not only related to $x(t)$ but also to $x(t-\tau)$. Unfortunately, this property has been ignored in many literatures that are about the complex systems with non-delayed and delayed couplings simultaneously. In this section, we will consider a general stabilization problem of complex systems with non-delayed and delayed couplings exchanging randomly.

Considering a kind of complex dynamical network consisting of $N$ nodes and every node is a $n$ -dimensional dynamical system, which is described as

$$\dot{x}_i(t) = f(x_i(t)) + c\sum_{j=1}^{N} a_{ij}x_j(t) + c\sum_{j=1}^{N} b_{ij}x_j(t-\tau), \quad i \in \mathbb{S} \tag{1}$$

where $x_i(t) = (x_{i1}(t), x_{i2}(t), \ldots, x_{in}(t))^T \in \mathbb{R}^n$ is the state vector of the $i$th node. $f : \mathbb{R}^n \to \mathbb{R}^n$ is a continuously differentiable function that describes the activity of an individual system.

$c > 0$ is the coupling strength among the nodes. $\tau > 0$ is the coupling delay. $A = (a_{ij}) \in \mathbb{R}^{N \times N}$ and $B = (b_{ij}) \in \mathbb{R}^{N \times N}$ stand for the configuration matrices of the complex dynamical network with the non-delayed and delayed couplings, respectively. $A$ and $B$ can be defined as follows: for $i \neq j$, if there exist non-delayed and delayed couplings between nodes $i$ and $j$, then $a_{ij} > 0$ and $b_{ij} > 0$; Otherwise, $a_{ij} = 0$ and $b_{ij} = 0$, respectively. Assuming both $A$ and $B$ are symmetric and also satisfy

$$a_{ii} = -\sum_{j=1, j\neq i}^{N} a_{ij}, b_{ii} = -\sum_{j=1, j\neq i}^{N} b_{ij}, i \in \mathbb{S}$$

Here, the topologies of the complex network are more general, whose related coupling matrices exchange each other randomly. That is, $A$ changes into $B$, while $B$ changes into $A$ simultaneously. In other words, matrices $A$ and $B$ exchange. In this case, we have the following complex network:

$$\dot{x}_i(t) = f(x_i(t)) + c\sum_{j=1}^{N} b_{ij}x_j(t) + c\sum_{j=1}^{N} a_{ij}x_j(t-\tau), \quad i \in \mathbb{S} \tag{2}$$

From these demonstrations, it is seen that the above two complex networks occur separately and randomly. To describe the above random switching between coupling matrices $A$ and $B$, a robust method will be exploited. That is

$$\dot{x}_i(t) = f(x_i(t)) + c\sum_{j=1}^{N} (a_{ij} + \Delta a_{ij})x_j(t) + c\sum_{j=1}^{N} (b_{ij} + \Delta b_{ij})x_j(t-\tau), \quad i \in \mathbb{S} \tag{3}$$

when $\Delta A = (\Delta a_{ij}) \in \mathbb{R}^{N \times N}$ and $\Delta B = (\Delta b_{ij}) \in \mathbb{R}^{N \times N}$. Especially, such uncertainties are selected to be $\Delta A = B - A$ and $\Delta B = A - B$, which is assumed to be

$$\|B - A\| \leq \delta^* \tag{4}$$

where $\delta^*$ is a given positive scalar.

Before giving the main results, a definition is needed.

**Definition 1.** The complex network (1) is asymptotically stable over topologies exchanging randomly, if the complex network (3) with condition (4) is asymptotically stable.

http://dx.doi.org/10.5772/62504

## 3. Stabilization of complex networks with couplings exchanging randomly

Based on the proposed model, this section focuses on the design of stochastic pinning controller. By investigating the existing references, it is found that most of the stabilization results of complex networks are achieved by either non-delay or delay controllers. However, from the above explanations, it is said that two such controllers may not describe the actual systems very well. Here, a kind of partially delay-dependent pinning controller containing both non-delay and delay states that take place with a certain probability is proposed to deal with the general case. Without loss of generality, it is assumed that the first $l$ nodes are selected to be added the desired pinning controller $u_i(t)$, which are described as

$$\begin{cases} u_i(t) = -c\alpha(t)k_i x_i(t) - c\big(1-\alpha(t)\big)k_{di}x_i(t-\tau), & i \in \mathbf{S}_\ell \\ u_i(t) = 0, & i \in \bar{\mathbf{S}}_\ell \end{cases} \tag{5}$$

where $k_i$ and $k_{di}$ are the non-delayed and delayed coupling control gains, respectively. $\alpha(t)$ is the Bernoulli stochastic variable and is described as follows:

$$\alpha(t) = \begin{cases} 1, & if\ x(t)\ is\ valid \\ 0, & if\ x(t-\tau)\ is\ valid \end{cases} \tag{6}$$

whose probabilities are expressed by

$$P_r\{\alpha(t)=1\} = \mathrm{E}\{\alpha(t)\} = \alpha^*, P_r\{\alpha(t)=0\} = 1-\alpha^*. \tag{7}$$

where $\alpha^* \in [0, 1]$. In addition, it is obtained that

$$\mathrm{E}\{\alpha(t)-\alpha^*\} = 0 \tag{8}$$

Substituting $u_i(t)$ into complex network (3), one has

$$\begin{cases} \dot{x}_i(t) = f(x_i(t)) + c\sum_{j=1}^{N}(a_{ij} + \Delta a_{ij})x_j(t) \\ \qquad\qquad + c\sum_{j=1}^{N}(b_{ij} + \Delta b_{ij})x_j(t-\tau) \\ \qquad - c\alpha(t)k_i x_i(t) - c(1-\alpha(t))k_{di}x_i(t-\tau), i \in S_\ell \\ \dot{x}_i(t) = f(x_i(t)) \\ \qquad\qquad + c\sum_{j=1}^{N}(a_{ij} + \Delta a_{ij})x_j(t) \\ \qquad\qquad + c\sum_{j=1}^{N}(b_{ij} + \Delta b_{ij})x_j(t-\tau), i \in \overline{S}_\ell \end{cases} \tag{9}$$

which is equivalent to

$$\begin{cases} \dot{x}_i(t) = f(x_i(t)) \\ \qquad\qquad + c\sum_{j=1}^{N}(a_{ij} + \Delta a_{ij})x_j(t) \\ \qquad\qquad + c\sum_{j=1}^{N}(b_{ij} + \Delta b_{ij})x_j(t-\tau) \\ \qquad - c(\alpha(t) - \alpha^*)k_i x_i(t) \\ \qquad\qquad + c(\alpha(t) - \alpha^*)k_{di}x_i(t-\tau) \\ \qquad - c\alpha^* k_i x_i(t) - c(1-\alpha^*)k_{di}x_i(t-\tau), i \in S_\ell \\ \dot{x}_i(t) = f(x_i(t)) \\ \qquad\qquad + c\sum_{j=1}^{N}(a_{ij} + \Delta a_{ij})x_j(t) \\ \qquad\qquad + c\sum_{j=1}^{N}(b_{ij} + \Delta b_{ij})x_j(t-\tau), i \in \overline{S}_\ell \end{cases} \tag{10}$$

**Assumption 1.** Supposing that there exists a positive definite diagonal matrix $P = \text{diag}\{p_1, p_2, \ldots, p_n\}$ and $\eta > 0$, such that

$$x_i^T(t)Pf(x(t)) \le \eta x_i^T(t)x_i(t), \forall x_i(t) \in \mathbb{R}^n, t \ge 0 \tag{11}$$

http://dx.doi.org/10.5772/62504

### 3.1 Stabilization realized by a partially delay-dependent pinning controller

**THEOREM 1.** Let Assumption 1 hold, for given scalars $\alpha^*$ and $\delta^*$, there exists a pinning controller (5) such that the complex network (9) is asymptotically stable over topology exchange (4), if there exist $Q > 0$, $k_i > 0$, and $k_{di} > 0$, $\forall\, i \in \mathrm{S}_\ell$, such that the following condition

$$\begin{bmatrix} 2\varphi I_N + 2c\tilde{A} + 2c\delta^* I_N + Q & c(\tilde{B} + \delta^* I_N) \\ * & -Q \end{bmatrix} < 0 \tag{12}$$

is satisfied, where

$$\varphi = \frac{\eta}{\min\limits_{1\le i\le n}(p_i)}$$

$$\tilde{A} = A - diag\{\underbrace{\alpha^* k_1, \alpha^* k_2, \ldots, \alpha^* k_l}_{l}, \underbrace{0, \ldots, 0}_{N-l}\},$$

$$\tilde{B} = B - diag\{\underbrace{(1-\alpha^*)k_{d1}, (1-\alpha^*)k_{d2}, \ldots, (1-\alpha^*)k_{dl}}_{l}, \underbrace{0, \ldots, 0}_{N-l}\}.$$

**Proof.** For complex network (9), we choose a Lyapunov function as follows:

$$V(x(t)) = \frac{1}{2}\sum_{i=1}^{N} x_i^T(t) P x_i(t) + \frac{1}{2}\sum_{j=1}^{n} p_j \int_{t-\tau}^{t} \tilde{x}_j^T(s) Q \tilde{x}_j(s) ds \tag{13}$$

where $\tilde{x}_j(t) = (x_{1j}(t),\ x_{2j}(t),\ \ldots,\ x_{Nj}(t))^T \in \mathbb{R}^N$, $j = 1, 2, \ldots, n$, and $Q$ is a positive definite of suitable dimensions matrix. Let L be the weak infinitesimal generator of stochastic process, it is defined as

$$\mathrm{L}V(x(t)) = \lim_{\Delta\to 0^+} \frac{\mathrm{E}\{V(x(t+\Delta))\} - V(x(t))}{\Delta} \tag{14}$$

Then, one has

$$
\begin{aligned}
\mathrm{L}V(x(t)) &= \sum_{i=1}^{N} x_i^T(t)P[f(x_i(t)) + c\sum_{j=1}^{N}(a_{ij}+\Delta a_{ij})x_j(t) + c\sum_{j=1}^{N}(b_{ij}+\Delta b_{ij})x_j(t-\tau)] \\
&\quad - c\alpha^*\sum_{i=1}^{l} k_i x_i^T(t)Px_i(t) - c(1-\alpha^*)\sum_{i=1}^{l} k_{di} x_i^T(t)Px_i(t-\tau) \\
&\quad + \frac{1}{2}\sum_{j=1}^{n} p_j[\tilde{x}_j^T(t)Q\tilde{x}_j(t) - \tilde{x}_j^T(t-\tau)Q\tilde{x}_j(t-\tau)] \\
&\le \eta\sum_{i=1}^{N} x_i^T(t)x_i(t) + c\sum_{i=1}^{N} x_i^T(t)P[\sum_{j=1}^{N}(a_{ij}+\Delta a_{ij})x_j(t) + \sum_{j=1}^{N}(b_{ij}+\Delta b_{ij})x_j(t-\tau)] \\
&\quad - c\alpha^*\sum_{i=1}^{l} k_i x_i^T(t)Px_i(t) - c(1-\alpha^*)\sum_{i=1}^{l} k_{di} x_i^T(t)Px_i(t-\tau) \\
&\quad + \frac{1}{2}\sum_{j=1}^{n} p_j[\tilde{x}_j^T(t)Q\tilde{x}_j(t) - \tilde{x}_j^T(t-\tau)Q\tilde{x}_j(t-\tau)] \\
&\le \frac{\eta}{\min\limits_{1\le i\le n}(p_i)}\sum_{i=1}^{N} x_i^T(t)Px_i(t) + c\sum_{i=1}^{N} x_i^T(t)P\sum_{j=1}^{N}(a_{ij}+\Delta a_{ij})x_j(t) \\
&\quad + c\sum_{i=1}^{N} x_i^T(t)P\sum_{j=1}^{N}(b_{ij}+\Delta b_{ij})x_j(t-\tau) \\
&\quad - c\alpha^*\sum_{i=1}^{l} k_i x_i^T(t)Px_i(t) - c(1-\alpha^*)\sum_{i=1}^{l} k_{di} x_i^T(t)Px_i(t-\tau) \\
&\quad + \frac{1}{2}\sum_{j=1}^{n} p_j[\tilde{x}_j^T(t)Q\tilde{x}_j(t) - \tilde{x}_j^T(t-\tau)Q\tilde{x}_j(t-\tau)] \\
&= \varphi\sum_{i=1}^{N} x_i^T(t)Px_i(t) + c\sum_{j=1}^{n} p_j\tilde{x}_j^T(t)\tilde{A}\tilde{x}_j(t) + c\sum_{j=1}^{n} p_j\tilde{x}_j^T(t)\tilde{B}\tilde{x}_j(t-\tau) \\
&\quad + c\sum_{j=1}^{n} p_j\tilde{x}_j^T(t)\Delta A\tilde{x}_j(t) + c\sum_{j=1}^{n} p_j\tilde{x}_j^T(t)\Delta B\tilde{x}_j(t-\tau) \\
&\quad + \frac{1}{2}\sum_{j=1}^{n} p_j\tilde{x}_j^T(t)Q\tilde{x}_j(t) - \frac{1}{2}\sum_{j=1}^{n} p_j\tilde{x}_j^T(t-\tau)Q\tilde{x}_j(t-\tau) \\
&\le \varphi\sum_{j=1}^{n} p_j\tilde{x}_j^T(t)\tilde{x}_j(t) + c\sum_{j=1}^{n} p_j\tilde{x}_j^T(t)\tilde{A}\tilde{x}_j(t) + c\sum_{j=1}^{n} p_j\tilde{x}_j^T(t)\tilde{B}\tilde{x}_j(t-\tau) \\
&\quad + c\delta^*\sum_{j=1}^{n} p_j\tilde{x}_j^T(t)\tilde{x}_j(t) + c\delta^*\sum_{j=1}^{n} p_j\tilde{x}_j^T(t)\tilde{x}_j(t-\tau) \\
&\quad + \frac{1}{2}\sum_{j=1}^{n} p_j\tilde{x}_j^T(t)Q\tilde{x}_j(t) - \frac{1}{2}\sum_{j=1}^{n} p_j\tilde{x}_j^T(t-\tau)Q\tilde{x}_j(t-\tau) \\
&\le \sum_{j=1}^{n} p_j\tilde{x}_j^T(t)(\varphi I_N + c\tilde{A} + c\delta^* I_N + \frac{1}{2}Q)\tilde{x}_j(t) \\
&\quad + c\sum_{j=1}^{n} p_j\tilde{x}_j^T(t)(\tilde{B} + \delta^* I_N)\tilde{x}_j(t-\tau) - \frac{1}{2}\sum_{j=1}^{n} p_j\tilde{x}_j^T(t-\tau)Q\tilde{x}_j(t-\tau)
\end{aligned}
\tag{15}
$$

http://dx.doi.org/10.5772/62504

$$= \frac{1}{2}\sum_{j=1}^{n} p_j \left[\tilde{x}_j^T(t) \quad \tilde{x}_j^T(t-\tau)\right] \Pi_1 \begin{bmatrix} \tilde{x}_j(t) \\ \tilde{x}_j(t-\tau) \end{bmatrix} < 0$$

where

$$\Pi_1 = \begin{bmatrix} 2\varphi I_N + 2c\tilde{A} + 2c\delta^* I_N + Q & c(\tilde{B} + \delta^* I_N) \\ * & -Q \end{bmatrix}$$

It is guaranteed by $\Pi_1 < 0$. By condition (12), it is known that $LV(x(t)) < 0$. This completes the proof.

**REMARK 1.** It is worth mentioning that for any given function $f(x_i(t))$, it is necessary to find suitable parameters $P$ and $\eta$. There, $P$ is related to $f(x_i(t))$, where $\eta$ can be obtained by the given matrix $P$. Moreover, Theorem 1 is also extended to other general cases that the coupling matrices $A$ and $B$ change to the other ones independently. Here, we only consider the special case that $A$ and $B$ exchanges each other.

Based on Theorem 1, it is claimed that $Q$ is selected with a general case. However, it may be selected to be some special cases. When $Q$ is chosen as the special case that $Q = c\sigma_{\max}(\tilde{B} + \delta^* I_N) I_N$, we will have the following corollary.

**COROLLARY 1.** Let Assumption 1 hold, for given scalars $\alpha^*$ and $\delta^* > 0$, there exists a pinning controller (5) such that the complex network (9) is asymptotically stable over topology exchange (4), if there exist $k_i > 0$, and $k_{di} > 0$, $\forall\, i \in S_\ell$, such that the following condition

$$\varphi I_N + c\tilde{A} + c\delta^* I_N + c\sigma_{max}(\tilde{B} + \delta^* I_N) I_N < 0 \tag{16}$$

is satisfied, where the other symbols are defined in Theorem 1.

**Proof.** Based on Theorem 1 and using the Schur complement lemma, one has

$$2\varphi I_N + 2c\tilde{A} + 2c\delta^* I_N + Q + c^2(\tilde{B} + \delta^* I_N) Q^{-1} (\tilde{B} + \delta^* I_N)^T < 0 \tag{17}$$

implying $\Pi_1 < 0$. By choosing $Q = c\sigma_{\max}(\tilde{B} + \delta^* I_N) I_N$, it is concluded that (17) is guaranteed by

$$2\varphi I_N + 2c\tilde{A} + 2c\delta^* I_N + 2c\sigma_{\max}(\tilde{B} + \delta^* I_N) I_N < 0 \tag{18}$$

This completes the proof.

When there is no topology exchange, we will have the following corollary directly.

**COROLLARY 2.** Let Assumption 1 hold, for given scalar $\alpha^*$, there exists a pinning controller (5) such that the complex network (9) is asymptotically stable over topology exchange (4), if there exist $Q > 0$, $k_i > 0$, and $k_{di} > 0$, $\forall\, i \in \mathrm{S}_\ell$, such that the following condition holds:

$$\begin{bmatrix} 2\varphi I_N + 2c\tilde{A} + Q & c\tilde{B} \\ * & -Q \end{bmatrix} < 0 \tag{19}$$

where $\varphi$, $\tilde{A}$, and $\tilde{B}$ are defined as those in (12).

It is seen that the expectation of $\alpha(t)$ in Theorem 1 plays a vital role in the control of the complex network, which needs to be given exactly. However, in practice, it may be very hard to get $\alpha^*$ exactly, and only its estimation $\tilde{\alpha}$ is available. For an uncertain $\alpha^*$ with its estimation $\tilde{\alpha}$, its admissible uncertainty $\Delta\alpha$ is defined as

$$\Delta\alpha = \alpha^* - \tilde{\alpha}, \tilde{\alpha} \in [0,1] \tag{20}$$

where $\Delta\alpha \in [-\mu, \mu]$ with $\mu \in [0, 1]$. Then, we have the following theorem.

**THEOREM 2.** Let Assumption 1 hold, for given scalars $\tilde{\alpha}$ and $\delta^* > 0$, there exists a pinning controller (5) satisfying condition (20) such that the complex network (9) is asymptotically stable over topology exchange (4), if there exist $Q > 0$, $W > 0$, $k_i > 0$, and $k_{di} > 0$, $\forall\, i \in \mathrm{S}_\ell$, such that the following conditions

$$\begin{bmatrix} 2\varphi I_N + 2c\bar{A} + 2c\mu K_1 + 2c\mu W_{11} + 2c\delta^* I_N + Q & c(\bar{B} - \mu K_2 + 2\mu W_{12} + \delta^* I_N) \\ * & 2c\mu W_{22} - Q \end{bmatrix} < 0 \tag{21}$$

$$\begin{bmatrix} -2K_1 - W_{11} & K_2 - W_{12} \\ * & -W_{22} \end{bmatrix} < 0 \tag{22}$$

hold, where

$$W = \begin{bmatrix} W_{11} & W_{12} \\ W_{21} & W_{22} \end{bmatrix},$$

$$K_1 = diag\{\underbrace{k_1, k_2, \ldots, k_l}_{l}, \underbrace{0, \cdots, 0}_{N-l}\},$$

http://dx.doi.org/10.5772/62504

$$K_2 = diag\{\underbrace{k_{d1}, k_{d2}, \ldots, k_{dl}}_{l}, \underbrace{0, \cdots, 0}_{N-l}\},$$

$$\bar{A} = A - diag\{\underbrace{\tilde{\alpha}k_1, \tilde{\alpha}k_2, \ldots, \tilde{\alpha}k_l}_{l}, \underbrace{0, \ldots, 0}_{N-l}\},$$

$$\bar{B} = B - diag\{\underbrace{(1-\tilde{\alpha})k_{d1}, (1-\tilde{\alpha})k_{d2}, \ldots, (1-\tilde{\alpha})k_{dl}}_{l}, \underbrace{0, \ldots, 0}_{N-l}\}$$

**Proof.** Based on the proof of Theorem 1, it is known that the stabilization of complex network (9) over random exchanges with (20) is guaranteed by (12), which is equivalent to

$$\begin{bmatrix} 2\varphi I_N + 2c\bar{A} - 2c\Delta\alpha K_1 + 2c\delta^* I_N + Q & c(\bar{B} + \Delta\alpha K_2 + \delta^* I_N) \\ * & -Q \end{bmatrix} < 0 \tag{23}$$

It could be rewritten as

$$\begin{bmatrix} 2\varphi I_N + 2c\bar{A} + 2c\delta^* I_N + Q & c(\bar{B} + \delta^* I_N) \\ * & -Q \end{bmatrix} + c\Delta\alpha \begin{bmatrix} -2K_1 & K_2 \\ * & 0 \end{bmatrix} < 0 \tag{24}$$

That is

$$\begin{bmatrix} 2\varphi I_N + 2c\bar{A} + 2c\delta^* I_N + Q & c(\bar{B} + \delta^* I_N) \\ * & -Q \end{bmatrix} + c(\Delta\alpha + \mu) \begin{bmatrix} -2K_1 & K_2 \\ * & 0 \end{bmatrix} - c(\Delta\alpha + \mu)W - c\mu \begin{bmatrix} -2K_1 & K_2 \\ * & 0 \end{bmatrix} + c(\Delta\alpha + \mu)W < 0 \tag{25}$$

which is implied by

$$\begin{bmatrix} 2\varphi I_N + 2c\bar{A} + 2c\delta^* I_N + Q & c(\bar{B} + \delta^* I_N) \\ * & -Q \end{bmatrix}$$
$$+c(\Delta\alpha + \mu)\begin{bmatrix} -2K_1 - W_{11} & K_2 - W_{12} \\ * & -W_{22} \end{bmatrix} - c\mu\begin{bmatrix} -2K_1 & K_2 \\ * & 0 \end{bmatrix} \tag{26}$$
$$+2c\mu\begin{bmatrix} W_{11} & W_{12} \\ * & W_{22} \end{bmatrix} < 0$$

Taking into account condition (22), it is further guaranteed by

$$\begin{bmatrix} 2\varphi I_N + 2c\bar{A} + 2c\delta^* I_N + Q & c(\bar{B} + \delta^* I_N) \\ * & -Q \end{bmatrix} - c\mu\begin{bmatrix} -2K_1 & K_2 \\ * & 0 \end{bmatrix}$$
$$+2c\mu\begin{bmatrix} W_{11} & W_{12} \\ * & W_{22} \end{bmatrix} < 0 \tag{27}$$

which is (21) actually. This completes the proof.

### 3.2 Stabilization realized by adaptive pinning controller

When $\alpha^*$ is unknown, how to stabilize a complex network through a pinning controller should also be taken into consideration. In this section, we will exploit the adaptive pinning control method to deal with this general case.

**THEOREM 3.** Let Assumption 1 hold, for given scalar $\delta^*$, if there exist $Q > 0$, $k_i > 0$, and $k_{di} > 0$, $\forall\, i \in \mathrm{S}_\ell$, such that the following condition

$$\begin{bmatrix} 2\varphi I_N + 2c\hat{A} + 2c\delta^* I_N + Q & c(\hat{B} + \delta^* I_N) \\ * & -Q \end{bmatrix} < 0 \tag{28}$$

holds with $\hat{A} = A - K_1$ and $\hat{B} = B - K_2$, then the complex network (9) is asymptotically stable over topology exchange (4) under the adaptive pinning controller

$$\begin{cases} u_i(t) = -ck_i x_i(t) - ck_{di} x_i(t-\tau) + v_i(t), i \in \mathrm{s}_\ell \\ u_i(t) = 0, \qquad\qquad\qquad\qquad\quad i \in \bar{\mathrm{s}}_\ell \end{cases} \tag{29}$$

where

$$v_i(t) = -c\hat{\alpha}(t)x_i(t)$$

http://dx.doi.org/10.5772/62504

and the updating law

$$\dot{\hat{\alpha}}(t)=\begin{cases}0, & \text{if } \hat{\alpha}(t)=1\\ \acute{o}c\sum_{i=1}^{l}x_i^T(t)Px_i(t), & \text{others}\end{cases} \tag{30}$$

where $\forall \acute{o}>0$ and $\hat{\alpha}_0\in[0,\ 1]$.

**Proof.** Here, the Lyapunov function is defined as

$$\begin{aligned}V(x(t))=&\frac{1}{2}\sum_{i=1}^{N}x_i^T(t)Px_i(t)\\&+\frac{1}{2}\sum_{j=1}^{n}p_j\int_{t-\tau}^{t}\tilde{x}_j^T(s)Q\tilde{x}_j(s)ds\\&+\frac{1}{2\acute{o}}\tilde{\alpha}(t)\tilde{\alpha}(t)\end{aligned} \tag{31}$$

where $\tilde{\alpha}(t)=\hat{\alpha}(t)-\alpha^*$, $\tilde{x}_j(t)$, and $Q$ are same as the ones in (13). Then, it is obtained

$$\begin{aligned}\mathrm{L}V(x(t))=&\sum_{i=1}^{N}x_i^T(t)P[f(x_i(t))+c\sum_{j=1}^{N}(a_{ij}+\Delta a_{ij})x_j(t)+c\sum_{j=1}^{N}(b_{ij}+\Delta b_{ij})x_j(t-\tau)]\\&-c\sum_{i=1}^{l}k_ix_i^T(t)Px_i(t)-c\sum_{i=1}^{l}k_{di}x_i^T(t)Px_i(t-\tau)+\sum_{i=1}^{l}x_i^T(t)Pv_i(t)\\&+\frac{1}{2}\sum_{j=1}^{n}p_j[\tilde{x}_j^T(t)Q\tilde{x}_j(t)-\tilde{x}_j^T(t-\tau)Q\tilde{x}_j(t-\tau)]+\frac{1}{\acute{o}}(\hat{\alpha}(t)-\alpha^*)\dot{\hat{\alpha}}(t)\\\le&\eta\sum_{i=1}^{N}x_i^T(t)x_i(t)+c\sum_{i=1}^{N}x_i^T(t)P[\sum_{j=1}^{N}(a_{ij}+\Delta a_{ij})x_j(t)+\sum_{j=1}^{N}(b_{ij}+\Delta b_{ij})x_j(t-\tau)]\\&-c\sum_{i=1}^{l}k_ix_i^T(t)Px_i(t)-c\sum_{i=1}^{l}k_{di}x_i^T(t)Px_i(t-\tau)+\sum_{i=1}^{l}x_i^T(t)Pv_i(t)\\&+\frac{1}{2}\sum_{j=1}^{n}p_j[\tilde{x}_j^T(t)Q\tilde{x}_j(t)-\tilde{x}_j^T(t-\tau)Q\tilde{x}_j(t-\tau)]+\frac{1}{\acute{o}}(\hat{\alpha}(t)-\alpha^*)\dot{\hat{\alpha}}(t)\\\le&\frac{\eta}{\min\limits_{1\le i\le n}(p_i)}\sum_{j=1}^{n}p_j\tilde{x}_j^T(t)\tilde{x}_j(t)+c\sum_{j=1}^{n}p_j\tilde{x}_j^T(t)A\tilde{x}_j(t)+c\sum_{j=1}^{n}p_j\tilde{x}_j^T(t)B\tilde{x}_j(t-\tau)\\&-c\sum_{j=1}^{n}p_j\tilde{x}_j^T(t)K_1\tilde{x}_j(t)-c\sum_{j=1}^{n}p_j\tilde{x}_j^T(t)K_2\tilde{x}_j(t-\tau)\\&+c\sum_{j=1}^{n}p_j\tilde{x}_j^T(t)\Delta A\tilde{x}_j(t)+c\sum_{j=1}^{n}p_j\tilde{x}_j^T(t)\Delta B\tilde{x}_j(t-\tau)+\sum_{i=1}^{l}x_i^T(t)Pv_i(t)\end{aligned} \tag{32}$$

$$
\begin{aligned}
&+\frac{1}{2}\sum_{j=1}^{n} p_j \tilde{x}_j^T(t) Q \tilde{x}_j(t) - \frac{1}{2}\sum_{j=1}^{n} p_j \tilde{x}_j^T(t-\tau) Q \tilde{x}_j(t-\tau) \\
&+\frac{1}{\acute{o}}(\hat{\alpha}(t)-\alpha^*)\dot{\hat{\alpha}}(t) \\
&\le \varphi \sum_{j=1}^{n} p_j \tilde{x}_j^T(t) \tilde{x}_j(t) + c\sum_{j=1}^{n} p_j \tilde{x}_j^T(t) \hat{A} \tilde{x}_j(t) \\
&+c\sum_{j=1}^{n} p_j \tilde{x}_j^T(t) \hat{B} \tilde{x}_j(t-\tau) \\
&+c\delta^* \sum_{j=1}^{n} p_j \tilde{x}_j^T(t) \tilde{x}_j(t) + c\delta^* \sum_{j=1}^{n} p_j \tilde{x}_j^T(t) \tilde{x}_j(t-\tau) \\
&+\sum_{i=1}^{l} x_i^T(t) P v_i(t) \\
&+\frac{1}{2}\sum_{j=1}^{n} p_j \tilde{x}_j^T(t) Q \tilde{x}_j(t) - \frac{1}{2}\sum_{j=1}^{n} p_j \tilde{x}_j^T(t-\tau) Q \tilde{x}_j(t-\tau) \\
&+\frac{1}{\acute{o}}(\hat{\alpha}(t)-\alpha^*)\dot{\hat{\alpha}}(t) \\
&\le \varphi \sum_{j=1}^{n} p_j \tilde{x}_j^T(t) \tilde{x}_j(t) + c\sum_{j=1}^{n} p_j \tilde{x}_j^T(t) \hat{A} \tilde{x}_j(t) \\
&+c\sum_{j=1}^{n} p_j \tilde{x}_j^T(t) \hat{B} \tilde{x}_j(t-\tau) \\
&+c\delta^* \sum_{j=1}^{n} p_j \tilde{x}_j^T(t) \tilde{x}_j(t) \\
&+c\delta^* \sum_{j=1}^{n} p_j \tilde{x}_j^T(t) \tilde{x}_j(t-\tau) \\
&+\frac{1}{2}\sum_{j=1}^{n} p_j \tilde{x}_j^T(t) Q \tilde{x}_j(t) \\
&-\frac{1}{2}\sum_{j=1}^{n} p_j \tilde{x}_j^T(t-\tau) Q \tilde{x}_j(t-\tau) \\
&=\frac{1}{2}\sum_{j=1}^{n} p_j \begin{bmatrix} \tilde{x}_j^T(t) & \tilde{x}_j^T(t-\tau) \end{bmatrix} \Pi_2 \begin{bmatrix} \tilde{x}_j(t) \\ \tilde{x}_j(t-\tau) \end{bmatrix} < 0
\end{aligned}
$$

where

$$
\Pi_2 = \begin{bmatrix} 2\varphi I_N + 2c\hat{A} + 2c\delta^* I_N + Q & c(\hat{B} + \delta^* I_N) \\ * & -Q \end{bmatrix}
$$

This completes the proof.

http://dx.doi.org/10.5772/62504

On the other hand, it is obtained that $\delta^*$ is also important to the control of the complex network. When it is unavailable, how to get the sufficient condition for the stabilization of complex network is an interesting problem to be discussed. In the next, such a problem will be solved by the following theorem.

**THEOREM 4.** Let Assumption 1 hold, for given scalar $\alpha^*$, if there exist $Q > 0$, $k_i > 0$, and $k_{di} > 0$, $\forall\, i \in \mathrm{S}_\ell$, such that the following condition

$$\begin{bmatrix} 2\varphi I_N + 2c\tilde{A} + Q & c\tilde{B} \\ * & -Q \end{bmatrix} < 0 \tag{33}$$

holds, then the complex network (9) is asymptotically stable over topology exchange (4) under the adaptive pinning controller

$$\begin{cases} u_i(t) = -c\alpha(t)k_i x_i(t) - c(1-\alpha(t))k_{di}x_i(t-\tau) + \varpi_i(t), & i \in \mathrm{s}_\ell \\ u_i(t) = 0, & i \in \bar{\mathrm{s}}_\ell \end{cases} \tag{34}$$

where

$$\varpi_i(t) = \begin{cases} 0, & if \ \sum_{i=1}^{l} x_i^T(t)Px_i(t) = 0 \\ \dfrac{-c\hat{\delta}x_i(t)[2\sum_{i=1}^{N} x_i^T(t)Px_i(t) + \sum_{i=1}^{N} x_i^T(t-\tau)Px_i(t-\tau)]}{\sum_{i=1}^{l} x_i^T(t)Px_i(t)}, & others \end{cases}$$

and the updating law

$$\dot{\hat{\delta}} = 2\xi c\sum_{i=1}^{N} x_i^T(t)Px_i(t) + \xi c\sum_{i=1}^{N} x_i^T(t-\tau)Px_i(t-\tau) \tag{35}$$

where $\xi$ is a positive constant and $\delta_0 \geq 0$.

**Proof.** For this case, we choose the Lyapunov function as

$$V(t) = \frac{1}{2}\sum_{i=1}^{N} x_i^T(t)Px_i(t) + \frac{1}{2}\sum_{j=1}^{n} p_j \int_{t-\tau}^{t} \tilde{x}_j^T(s)Q\tilde{x}_j(s)ds + \frac{1}{2\xi}\tilde{\delta}^2 \tag{36}$$

where $\tilde{\delta} = \hat{\delta} - \delta^*$. Then, it is obtained

$$
\begin{aligned}
&\mathrm{L}V(x(t)) \\
&=\sum_{i=1}^{N} x_i^T(t)P[f(x_i(t))+c\sum_{j=1}^{N}(a_{ij}+\Delta a_{ij})x_j(t) \\
&+c\sum_{j=1}^{N}(b_{ij}+\Delta b_{ij})x_j(t-\tau)] \\
&-c\alpha^*\sum_{i=1}^{l}k_i x_i^T(t)Px_i(t)-c(1-\alpha^*)\sum_{i=1}^{l}k_{di}x_i^T(t)Px_i(t-\tau) \\
&+\sum_{i=1}^{l}x_i^T(t)P\varpi_i(t) \\
&+\frac{1}{2}\sum_{j=1}^{n}p_j[\tilde{x}_j^T(t)Q\tilde{x}_j(t)-\tilde{x}_j^T(t-\tau)Q\tilde{x}_j(t-\tau)] \\
&+\frac{1}{\xi}(\hat{\delta}-\delta^*)\dot{\hat{\delta}} \\
&\le \eta\sum_{i=1}^{N}x_i^T(t)x_i(t)+c\sum_{i=1}^{N}x_i^T(t)P[\sum_{j=1}^{N}(a_{ij}+\Delta a_{ij})x_j(t) \\
&+\sum_{j=1}^{N}(b_{ij}+\Delta b_{ij})x_j(t-\tau)] \\
&-c\alpha^*\sum_{i=1}^{l}k_i x_i^T(t)Px_i(t)-c(1-\alpha^*)\sum_{i=1}^{l}k_{di}x_i^T(t)Px_i(t-\tau) \\
&+\sum_{i=1}^{l}x_i^T(t)P\varpi_i(t) \\
&+\frac{1}{2}\sum_{j=1}^{n}p_j[\tilde{x}_j^T(t)Q\tilde{x}_j(t)-\tilde{x}_j^T(t-\tau)Q\tilde{x}_j(t-\tau)] \\
&+\frac{1}{\xi}(\hat{\delta}-\delta^*)\dot{\hat{\delta}} \\
&\le \varphi\sum_{j=1}^{n}p_j\tilde{x}_j^T(t)\tilde{x}_j(t)+c\sum_{j=1}^{n}p_j\tilde{x}_j^T(t)\tilde{A}\tilde{x}_j(t) \\
&+c\sum_{j=1}^{n}p_j\tilde{x}_j^T(t)\tilde{B}\tilde{x}_j(t-\tau) \\
&+c\delta^*\sum_{j=1}^{n}p_j\tilde{x}_j^T(t)\tilde{x}_j(t)+c\delta^*\sum_{j=1}^{n}p_j\tilde{x}_j^T(t)\tilde{x}_j(t-\tau) \\
&+\sum_{i=1}^{l}x_i^T(t)P\varpi_i(t) \\
&+\frac{1}{2}\sum_{j=1}^{n}p_j\tilde{x}_j^T(t)Q\tilde{x}_j(t)-\frac{1}{2}\sum_{j=1}^{n}p_j\tilde{x}_j^T(t-\tau)Q\tilde{x}_j(t-\tau) \\
&+\frac{1}{\xi}(\hat{\delta}-\delta^*)\dot{\hat{\delta}}
\end{aligned}
\tag{37}
$$

http://dx.doi.org/10.5772/62504

$$
\begin{aligned}
&\le \varphi\sum_{j=1}^{n} p_j\tilde{x}_j^T(t)\tilde{x}_j(t) + c\sum_{j=1}^{n} p_j\tilde{x}_j^T(t)\tilde{A}\tilde{x}_j(t)\\
&+c\sum_{j=1}^{n} p_j\tilde{x}_j^T(t)\tilde{B}\tilde{x}_j(t-\tau)\\
&-c\delta^*\sum_{j=1}^{n} p_j\tilde{x}_j^T(t)\tilde{x}_j(t)\\
&+c\delta^*\sum_{j=1}^{n} p_j\tilde{x}_j^T(t)\tilde{x}_j(t-\tau)\\
&-c\delta^*\sum_{j=1}^{n} p_j\tilde{x}_j^T(t-\tau)\tilde{x}_j(t-\tau)\\
&+\frac{1}{2}\sum_{j=1}^{n} p_j\tilde{x}_j^T(t)Q\tilde{x}_j(t) - \frac{1}{2}\sum_{j=1}^{n} p_j\tilde{x}_j^T(t-\tau)Q\tilde{x}_j(t-\tau)\\
&\le \sum_{j=1}^{n} p_j\tilde{x}_j^T(t)(\varphi I_N + c\tilde{A} + \frac{1}{2}Q)\tilde{x}_j(t)\\
&+\sum_{j=1}^{n} p_j\tilde{x}_j^T(t)c\tilde{B}\tilde{x}_j(t-\tau)\\
&-\frac{1}{2}\sum_{j=1}^{n} p_j\tilde{x}_j^T(t-\tau)Q\tilde{x}_j(t-\tau)\\
&+c\delta^*\sum_{j=1}^{n} p_j[-\tilde{x}_j^T(t)\tilde{x}_j(t) + \tilde{x}_j^T(t)\tilde{x}_j(t-\tau)\\
&-\tilde{x}_j^T(t-\tau)\tilde{x}_j(t-\tau)]\\
&= \frac{1}{2}\sum_{j=1}^{n} p_j\begin{bmatrix}\tilde{x}_j^T(t) & \tilde{x}_j^T(t-\tau)\end{bmatrix}\Pi_2\begin{bmatrix}\tilde{x}_j(t)\\ \tilde{x}_j(t-\tau)\end{bmatrix}\\
&\quad + c\delta^*\sum_{j=1}^{n} p_j\begin{bmatrix}\tilde{x}_j^T(t) & \tilde{x}_j^T(t-\tau)\end{bmatrix}\begin{bmatrix}-I_N & \frac{1}{2}I_N\\ \frac{1}{2}I_N & -I_N\end{bmatrix}\begin{bmatrix}\tilde{x}_j(t)\\ \tilde{x}_j(t-\tau)\end{bmatrix}\\
&\le \frac{1}{2}\sum_{j=1}^{n} p_j\begin{bmatrix}\tilde{x}_j^T(t) & \tilde{x}_j^T(t-\tau)\end{bmatrix}\Pi_3\begin{bmatrix}\tilde{x}_j(t)\\ \tilde{x}_j(t-\tau)\end{bmatrix} < 0
\end{aligned}
$$

where

$$
\Pi_3 = \begin{bmatrix}2\varphi I_N + 2c\tilde{A} + Q & c\tilde{B}\\ c\tilde{B}^T & -Q\end{bmatrix}
$$

It is guaranteed by $\Pi_3 < 0$ which is equivalent to (33). This completes the proof.

## 4. Numerical example

In this section, a numerical example is used to verify the effectiveness of the proposed methods.

**Example 1.** Consider a dynamical network consisting of 10 nodes that are identical Chua's circuits. A single Chua's circuit is described by

$$\begin{cases} \dot{x}_1 = \vartheta(-x_1 + x_2 - \zeta(x_1)) \\ \dot{x}_2 = x_1 - x_2 + x_3 \\ \dot{x}_3 = -\omega x_2 \end{cases} \tag{38}$$

where $\vartheta = 10$, $\omega = 14.87$, $\zeta(x_1) = bx_1 + \frac{a-b}{2}(|x_1 + 1| - |x_1 - 1|)$, $a = -1.27$, and $b = -0.68$. It is known that the Chua's system has a chaotic attractor which is shown in **Figure 1**.

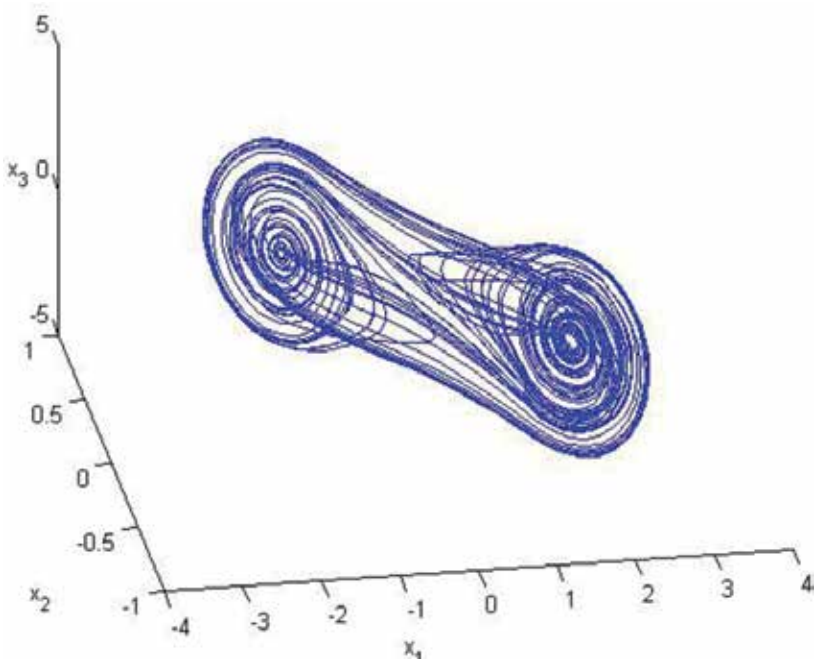


**Figure 1.** The chaotic attractor of Chua's circuit.

It is obvious that system (38) is also be rewritten as

$$\dot{x} = Hx + g(x) \tag{39}$$

where

http://dx.doi.org/10.5772/62504

$$x = \begin{bmatrix} x_1 & x_2 & x_3 \end{bmatrix}^T$$

$$H = \begin{bmatrix} -\vartheta & \vartheta & 0 \\ 1 & -1 & 1 \\ 0 & -\omega & 0 \end{bmatrix}$$

$$g(x) = \begin{bmatrix} -\vartheta\zeta(x_1) & 0 & 0 \end{bmatrix}^T$$

Without loss of generality, matrix $P$ here is selected as $P = \text{diag}\{1, \omega, 1\}$. Next, we will check whether there is a suitable $\eta$ satisfying condition (11) in Assumption 1. It is obtained that

$$\begin{aligned} x^T P(Hx + g(x)) &\le \frac{1}{2} x^T (PH + H^T P)x - \vartheta a x_1^2 \\ &= \frac{1}{2} x^T (\tilde{H} + \tilde{H}^T)x \\ &\le \frac{1}{2} \lambda_{max}(\tilde{H} + \tilde{H}^T) x^T x \\ &= \eta x^T x \end{aligned} \tag{40}$$

where $\widetilde{H} = PH + \text{diag}\{-\vartheta a, 0, 0\}$ and $\eta = \frac{1}{2}\lambda_{\max}\left(\widetilde{H} + \widetilde{H}^T\right) = 9.0620$. Thus, condition (11) is satisfied. Then, the resulting network closed by controller (4) is described as

$$\begin{cases} \dot{x}_{i1} = 10(-x_{i1} + x_{i2} - \zeta(x_{i1})) + c\sum_{j=1}^{N} a_{ij} x_{j1} + c\sum_{j=1}^{N} b_{ij} x_{j1}(t-\tau) + u_{i1} \\ \dot{x}_{i2} = x_{i1} - x_{i2} + x_{i3} + c\sum_{j=1}^{N} a_{ij} x_{j2} + c\sum_{j=1}^{N} b_{ij} x_{j2}(t-\tau) + u_{i2} \qquad i \in S_\ell \\ \dot{x}_{i3} = -14.87 x_{i2} + c\sum_{j=1}^{N} a_{ij} x_{j3} + c\sum_{j=1}^{N} b_{ij} x_{j3}(t-\tau) + u_{i3} \end{cases} \tag{41}$$

Without loss of generality, the coupling matrices $A$ and $B$ are expressed by small-world and scale-free networks, which are depicted in **Figures 2** and **3**, respectively.

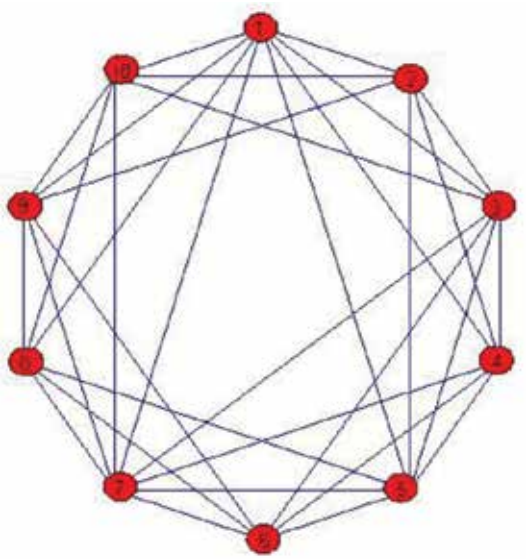

**Figure 2.** The simulation of coupling matrix $A$.

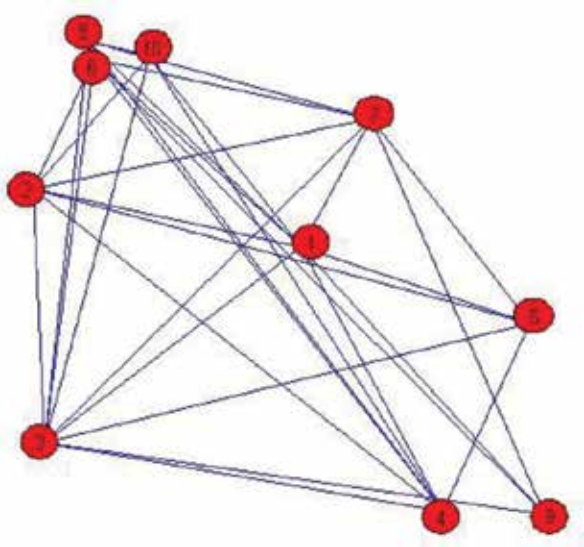

**Figure 3.** The simulation of coupling matrix $B$.

When such coupling matrices exchange randomly, under conditions such that $c = 50$, $\alpha^* = 0.85$, $\delta^* = 3.6$, and pinning fraction $= 0.8$, based on Theorem 1, we have the corresponding parameters computed as follows:

$k_i = 22.8791$, $k_{di} = 2.3840$, $i \in S_\ell$, and

http://dx.doi.org/10.5772/62504

$$Q = \begin{bmatrix} 1137.4 & -35.5 & -28.5 & -34.6 & -43.2 & -2.5 & -36.5 & -34.6 & -47.9 & -51.3 \\ * & 1074.4 & -34.8 & -35.9 & -41.1 & -9.1 & -9.7 & -4.9 & -54.9 & -53.3 \\ * & * & 1.1085 & -33.8 & -42.2 & -32.2 & -32.1 & -6.1 & -2.7 & -50.3 \\ * & * & * & 1075.2 & -45.4 & -40.3 & -47.0 & -4.8 & -3.5 & -3.2 \\ * & * & * & * & 1097.1 & -50.2 & -37.0 & -38.8 & -2.6 & -6.6 \\ * & * & * & * & * & 1075.5 & -36.3 & -39.2 & -54.0 & -0.8 \\ * & * & * & * & * & * & 1134.6 & -41.1 & -48.4 & -53.5 \\ * & * & * & * & * & * & * & 1074.8 & -54.7 & -51.9 \\ * & * & * & * & * & * & * & * & 156.6 & -78.4 \\ * & * & * & * & * & * & * & * & * & 148.1 \end{bmatrix}$$

Under the initial condition $x_i(t)=[0.1 \quad 0.1 \quad 0.2]^T$, where $i$ = 1, 2, …, 10 and $\tau$ = 0.005, we have the state response of the closed-loop network by the stochastic pinning controller (5) shown in **Figure 4** and is stable.

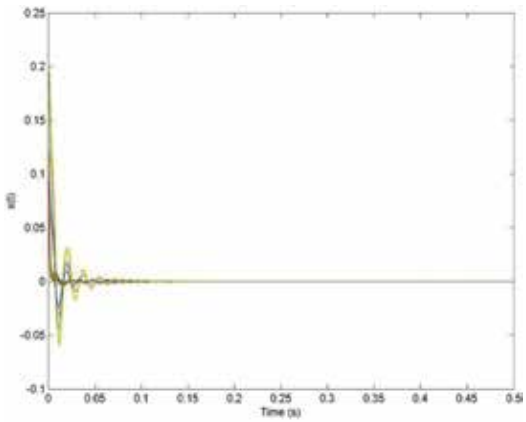


**Figure 4.** The state response of the complex network by controller (5).

Based on the results in this chapter, it is known that probability $\alpha^*$ plays important roles in the stabilization of complex networks, where non-delay and delay control gains $k_i$ and $k_{di}$ are very close to $\alpha^*$. Let $k_a=\sqrt{k_i^2+k_{di}^2}$, we have the relationship between parameters $\alpha^*$ and $k_i$, $k_{di}$ and $k_a$ given in **Table 1**, where the more detailed correlation between $\alpha^*$ and $k_i$, $k_{di}$ and $k_a$ is simulated in **Figure 5**. From **Table 1** and **Figure 5**, it is seen that both gains of $k_i$ and $k_{di}$ have effects in the stabilization of the underlying complex network. It is also found that there is not a phenomenon that larger $\alpha^*$ results in larger $k_{di}$ or smaller $k_i$. This property further demonstrates the necessity of considering the probability distribution of non-delay and delay states while the stabilization problem of delayed systems is considered. Particularly, it is seen that when $\alpha^*$ = 0, there are no solutions to $k_i$ and $k_{di}$. This is determined by condition (10), which is

actually determined by the inherent property of pinning control of complex network with delayed coupling.

| $\alpha^*$ | 0 | 0.02 | 0.1 | 0.3 | 0.5 | 0.7 | 0.8 | 0.85 | 0.9 | 1 |
|---|---|---|---|---|---|---|---|---|---|---|
| $k_i$ | – | 5108.5 | 1018.8 | 334.23 | 192.59 | 35.18 | 100.66 | 22.88 | 103.17 | 67.84 |
| $k_{di}$ | – | 22.91 | 25.56 | 34.07 | 45.33 | 5.67 | 86.89 | 2.38 | 204.64 | 4072.20 |
| $k_a$ | – | 5108.55 | 1019.12 | 335.96 | 197.86 | 35.64 | 132.98 | 23.00 | 229.17 | 4072.77 |

**Table 1.** The relations between $\alpha^*$ and $k_i$, $k_{di}$, $k_a$.

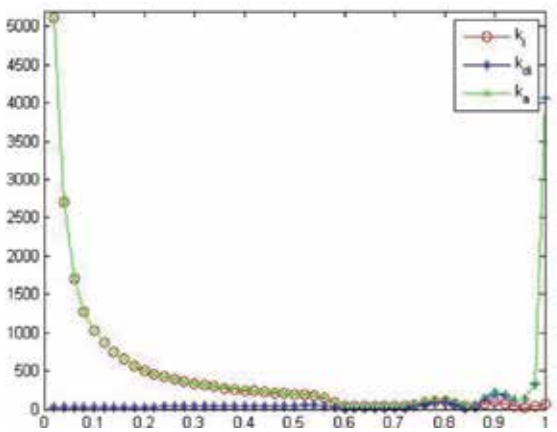


**Figure 5.** The simulation of correlation between $\alpha^*$ and $k_i$, $k_{di}$, $k_a$.

When probability $\alpha^*$ is uncertain and described as (20) such that $\tilde{\alpha} = 0.85$ and $\mu = 0.1$, by Theorem 2, one has the corresponding parameters computed as follows:

$k_i = 150.8308$, $k_{di} = 63.5059$, $i \in S_\ell$, and

$$Q = \begin{bmatrix} 2648.1 & 3.9 & 10.0 & 2.2 & -2.8 & 27.6 & -7.2 & 8.0 & -23.6 & -30.5 \\ * & 2540.4 & 17.9 & 19.4 & -2.6 & 9.7 & 23.7 & 20.3 & -21.4 & -29.0 \\ * & * & 2585.4 & 16.3 & 4.0 & 15.5 & 2.2 & 27.0 & -2.3 & -30.0 \\ * & * & * & 2542.1 & 5.4 & 0.3 & -2.9 & 29.5 & -0.4 & -6.8 \\ * & * & * & * & 2555.6 & -3.5 & -2.0 & -8.6 & -0.3 & 1.6 \\ * & * & * & * & * & 2548.0 & 19.2 & -7.0 & -22.3 & 0.8 \\ * & * & * & * & * & * & 2586.5 & -3.9 & -22.4 & -19.9 \\ * & * & * & * & * & * & * & 2538.5 & -21.3 & -27.8 \\ * & * & * & * & * & * & * & * & 118.3 & -55.8 \\ * & * & * & * & * & * & * & * & * & 0.1159 \end{bmatrix}$$

http://dx.doi.org/10.5772/62504

$$W_{11}=\begin{bmatrix}
813.9 & -10.19 & -10.86 & -10.07 & -9.55 & -2.78 & -9.14 & -10.63 & -7.00 & -6.26\\
* & 805.26 & -11.63 & -11.87 & -9.71 & -0.94 & -2.32 & -1.89 & -7.14 & -6.40\\
* & * & 810.49 & -11.34 & -10.21 & -11.38 & -10.06 & -2.69 & 0.19 & -6.32\\
* & * & * & 805.28 & -10.36 & -9.80 & -9.56 & -2.88 & 0.04 & 0.67\\
* & * & * & * & 813.78 & -9.40 & -9.63 & -8.92 & 0.04 & -0.15\\
* & * & * & * & * & 804.55 & -11.81 & -9.13 & -7.08 & -0.08\\
* & * & * & * & * & * & 820.49 & -9.54 & -7.09 & -7.30\\
* & * & * & * & * & * & * & 805.14 & -7.17 & -6.52\\
* & * & * & * & * & * & * & * & 7.17 & -2.97\\
* & * & * & * & * & * & * & * & * & 7.36
\end{bmatrix}$$

$$W_{12}=\begin{bmatrix}
101.76 & -4.67 & -4.64 & -4.71 & -4.72 & -4.70 & -4.69 & -4.69 & -4.18 & -4.18\\
* & 92.71 & -4.70 & -4.72 & -4.70 & -4.77 & -4.71 & -0.11 & -0.06 & -4.17\\
* & * & 101.91 & -4.68 & -4.73 & -4.74 & -4.76 & -4.71 & -4.06 & -4.18\\
* & * & * & 92.62 & -4.75 & -4.74 & -0.08 & -4.77 & 0.02 & -4.10\\
* & * & * & * & 83.40 & -0.11 & -4.74 & -0.09 & 0.01 & 0.02\\
* & * & * & * & * & 88.09 & -4.74 & -0.09 & -4.18 & 0.02\\
* & * & * & * & * & * & 92.76 & -4.68 & -4.16 & -0.05\\
* & * & * & * & * & * & * & 83.62 & -0.02 & -4.15\\
* & * & * & * & * & * & * & * & 1.39 & 0.01\\
* & * & * & * & * & * & * & * & * & 4.82
\end{bmatrix}$$

$$W_{22}=\begin{bmatrix}
209.59 & 0.33 & 1.05 & 0.23 & -0.36 & 2.42 & -0.62 & 0.64 & -1.96 & -2.52\\
* & 200.26 & 1.49 & 1.64 & -0.35 & 0.76 & 1.93 & 1.91 & -1.71 & -2.38\\
* & * & 204.41 & 1.37 & 0.23 & 1.28 & 0.12 & 2.36 & -0.23 & -2.48\\
* & * & * & 200.41 & 0.38 & -0.08 & -0.21 & 2.53 & -0.04 & -0.62\\
* & * & * & * & 201.24 & -0.20 & -0.28 & -0.69 & -0.02 & 0.14\\
* & * & * & * & * & 200.74 & 1.57 & -0.56 & -1.81 & 0.07\\
* & * & * & * & * & * & 204.31 & -0.48 & -1.83 & -1.55\\
* & * & * & * & * & * & * & 199.66 & -1.69 & -2.27\\
* & * & * & * & * & * & * & * & 8.06 & -3.82\\
* & * & * & * & * & * & * & * & * & 7.90
\end{bmatrix}.$$

When probability $\alpha^*$ is inaccessible, a kind of adaptive pinning control method may be exploited. Let the corresponding parameters $P$, $\eta$, and $\delta^*$ same to the above values, by Theorem 3, one could get the related parameters computed as follows: $k_i$ = 102.2258, $k_{di}$ = 22.3035, $i \in S_\ell$, and

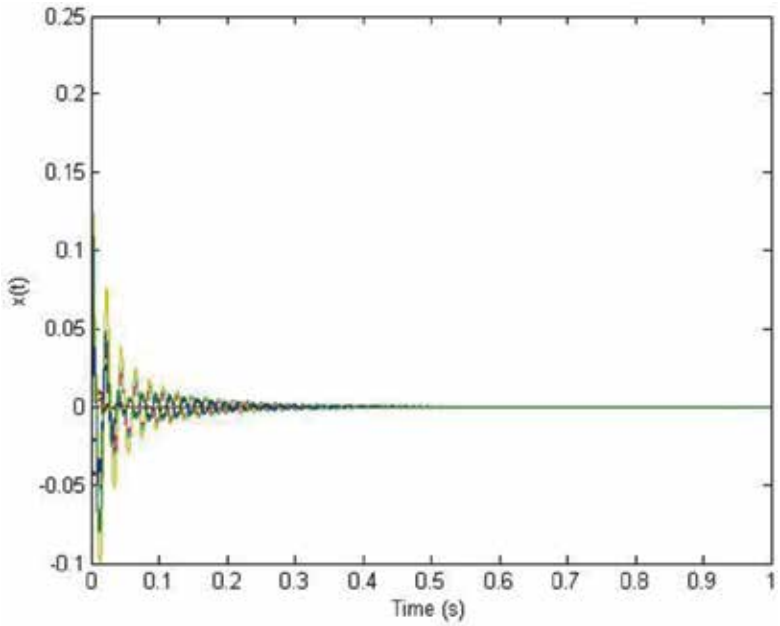


**Figure 6.** The state response of the complex network by controller (29).

$$Q = \begin{bmatrix} 5134.0 & -28.2 & 82.8 & 40.8 & -112.6 & -153.4 & -36.7 & 62.2 & -50.0 & -54.5 \\ * & 5437.0 & -82.4 & -61.7 & -100.9 & 2.1 & -84.6 & -87.9 & -49.7 & -51.8 \\ * & * & 5214.8 & 35.4 & -232.0 & -93.1 & 119.2 & 20.6 & -4.9 & -52.3 \\ * & * & * & 5516.0 & -173.6 & -12.1 & -303.0 & 24.9 & -5.2 & -2.3 \\ * & * & * & * & 5644.9 & -59.9 & -107.9 & -206.4 & -0.4 & 7.0 \\ * & * & * & * & * & 5431.7 & -195.1 & -196.0 & -47.2 & -0.6 \\ * & * & * & * & * & * & 5589.6 & -123.3 & -46.6 & -50.7 \\ * & * & * & * & * & * & * & 5101.7 & -50.8 & -50.5 \\ * & * & * & * & * & * & * & * & 143.9 & -66.4 \\ * & * & * & * & * & * & * & * & * & 133.0 \end{bmatrix}$$

where ó is selected to be ó = 5. Under the same initial condition and topologies having couplings exchanges, the simulations of the resulting complex network are given in **Figures 6** and **7**, where **Figure 6** is state response of the closed-loop system through the desired adaptive pinning controller with form (29) and updating law with form (30), and **Figure 7** is the curve of estimation $\alpha(t)$ with $\alpha_0$=0.2.

http://dx.doi.org/10.5772/62504

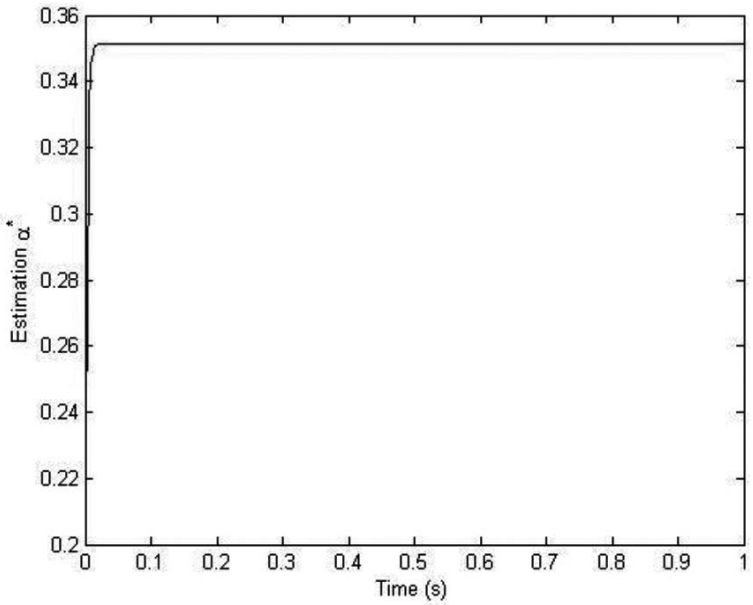


**Figure 7.** The curve of estimation of $\alpha^*$.

From these simulations, it is said that the desired partially delay-dependent controllers in terms of stochastic pinning controller (5) and adaptive controller (29) are both effective, where the resulting complex network is stable even if the coupling matrices experience random exchanges. On the other hand, when $\alpha$ is obtained exactly but $\delta^*$ is unavailable, using Theorem 4, we have the corresponding parameters obtained as follows: $k_i = 30.6104$, $k_{di} = 16.7135$, $i \in S_\ell$, and

$$Q = \begin{bmatrix} 1648.4 & -36.0 & -31.3 & -34.5 & -39.7 & 2.5 & -36.2 & -37.5 & -48.8 & -52.0 \\ * & 1573.4 & -35.6 & -33.0 & -38.4 & -5.7 & -6.0 & -1.5 & -53.0 & -52.1 \\ * & * & 1613.6 & -33.0 & -38.9 & -35.4 & -34.2 & 4.1 & -1.7 & -50.7 \\ * & * & * & 1574.9 & -41.5 & -40.3 & -42.6 & -0.5 & -2.0 & 5.0 \\ * & * & * & * & 1603.5 & -45.1 & -37.1 & -36.6 & 1.5 & 5.8 \\ * & * & * & * & * & 1576.6 & -34.3 & -44.8 & -43.6 & 0.3 \\ * & * & * & * & * & * & 1643.7 & -39.6 & -45.3 & -52.0 \\ * & * & * & * & * & * & * & 1578.1 & -52.8 & -48.6 \\ * & * & * & * & * & * & * & * & 334.8 & -75.6 \\ * & * & * & * & * & * & * & * & * & 308.0 \end{bmatrix}$$

where $\xi$ is selected to be $\xi = 1$.

## 5. Conclusion

In this chapter, the stabilization problem of complex dynamical network with non-delayed and delayed couplings exchanging randomly has been realized by a new kind of stochastic pinning controller being partially delay-dependent, where the switching between the non-delayed and delayed couplings is modeled by the related coupling matrices containing uncertainties. Different from the traditional pinning methods, the designed pinning controller contains non-delay and delay state terms simultaneously but occurs asynchronously with a certain probability, respectively. Sufficient conditions for the stabilization of complex dynamical network over topology exchange are derived by the robust method and presented with liner matrix inequities (LMIs). It has been shown that the probability distributions of non-delay and delay states in addition to the bound of such uncertainties play very important roles in the controller design. Moreover, when the probability is inaccessible, a kind of adaptive partially delay-dependent controller is proposed to deal with this general case, where another adaptive control problem in terms of unknown bound is also considered. Finally, the correctness and feasibility of the proposed method are verified by a numerical simulation.

## Author details

Guoliang Wang* and Tingting Yan

*Address all correspondence to: glwang985@163.com

School of Information and Control Engineering, Liaoning Shihua University, Liaoning, China

## References

[1] Strogatz S. Exploring complex networks. Nature. 2001;410(6825):268-276.

[2] Barabási A, Albert R. Emergence of scaling in random networks. Science. 1999;286(5439):509-512.

[3] Song C, Havlin S, Makse H. Self-similarity of complex networks. Nature. 2005;433(7024):392-395.

[4] Li Z, Duan Z, Chen G, Huang L. Consensus of multiagent systems and synchronization of complex networks: a unified viewpoint. IEEE Transactions on Circuits and Systems I: Regular Papers. 2010;57(1):213-224.

[5] Liu Y, Slotine J, Barabási A. Controllability of complex networks. Nature. 2011;473(7346):167-173.

[6] Liu Z, Chen Z, Yuan Z. Pinning control of weighted general complex dynamical networks with time delay. Physica A Statistical Mechanics and Its Applications. 2007;375(1):345-354.

[7] Ji D, Lee D, Koo J, Won S, Lee S, Ju H. Synchronization of neutral complex dynamical networks with coupling time-varying delays. Nonlinear Dynamics. 2011;65(4):349-358.

[8] Wang Y, Wang H, Xiao J, Guan Z. Synchronization of complex dynamical networks under recoverable attacks. Automatica. 2010;46(1):197-203.

[9] Liu J. Research on synchronization of complex networks with random nodes. Acta Physica Sinica. 2013;62(4):221-229.

[10] Li C, Yu W, Huang T. Impulsive synchronization schemes of stochastic complex networks with switching topology: average time approach. Neural Networks. 2014;54(6):85-94.

[11] Liu X, Chen T. Synchronization of complex networks via aperiodically intermittent pinning control. IEEE Transactions on Automatic Control. 2015;26(10):2396-2407.

[12] Zhou J, Wu Q, Xiang L. Pinning complex delayed dynamical networks by a single impulsive controller. IEEE Transactions on Circuits and Systems I: Regular Papers. 2011;58(12):2882-2893.

[13] Zhang W, Tang Y, Miao Q, Fang J. Synchronization of stochastic dynamical networks under impulsive control with time delays. IEEE Transactions on Neural Networks and Learning Systems. 2014;25(10):1758-1768.

[14] Cai S, Jia Q, Liu Z. Cluster synchronization for directed heterogeneous dynamical networks via decentralized adaptive intermittent pinning control. Nonlinear Dynamics. 2015;82(1-2):689-702.

[15] Hou H, Zhang Q, Zheng M. Cluster synchronization in nonlinear complex networks under sliding mode control. Nonlinear Dynamics. 2016; 83(1-2):739-749.

[16] Ma Q, Lu J. Cluster synchronization for directed complex dynamical networks via pinning control. Neurocomputing. 2013;101(3):354-360.

[17] Zhang W, Li C, Huang T, et al. Stability and synchronization of memristor-based coupling neural networks with time-varying delays via intermittent control. Neurocomputing. 2016;173:1066-1072.

[18] Feng J, Sun S, Xu C, Zhao Y, Wang J. The synchronization of general complex dynamical network via pinning control. Nonlinear Dynamics. 2012;67(2):1623-1633.

[19] Cheng R, Peng M, Yu W. Pinning synchronization of delayed complex dynamical networks with nonlinear coupling. Physica A: Statistical Mechanics and its Applications. 2014;413(11):426-431.

[20] Wu X, Lu H. Hybrid synchronization of the general delayed and non-delayed complex dynamical networks via pinning control. Neurocomputing. 2012;89(10):168-177.

[21] DeLellis P, Garofalo F. Novel decentralized adaptive strategies for the synchronization of complex networks. Automatica. 2009;45(5):1312-1318.

[22] Yu W, DeLellis P, Chen G, Bernardo M, Kurths J. Distributed adaptive control of synchronization in complex networks. IEEE Transactions on Automatic Control. 2012;57(8):2153-2158.

[23] Liang Y, Wang X, Eustace J. Adaptive synchronization in complex networks with non-delay and variable delay couplings via pinning control. Neurocomputing. 2014;123:292-298.

[24] Reddy D, Sen A, Johnston G. Experimental evidence of time-delay-induced death in coupled limit-cycle oscillators. Physical Review Letters. 2000;85(16):3381-3384.

[25] Lindsey W, Chen J. Mutual clock synchronization in global digital communication networks. European Transactions on Telecommunications. 1996;7(1):25-37.

[26] Kozyreff G, Vladimirov A, Mandel P. Global coupling with time delay in an array of semiconductor lasers. Physical Review Letters. 2000;85(18):3809-3812.

[27] Yu C, Qin J, Gao H. Cluster synchronization in directed networks of partial state coupled linear systems under pinning control. Automatica. 2014;50(9):2341-2349.

Chapter 3

# Event-Triggered Static Output Feedback Simultaneous $H_\infty$ Control for a Collection of Networked Control Systems

Sheng-Hsiung Yang and Jenq-Lang Wu

Additional information is available at the end of the chapter

http://dx.doi.org/10.5772/63020

**Abstract**

This chapter considers the design of event-triggered static output feedback simultaneous $H_\infty$ controllers for a collection of networked control systems (NCSs). It is shown that conventional point-to-point wiring delayed static output feedback simultaneous $H_\infty$ controllers can be obtained by solving linear matrix inequalities (LMIs) with a linear matrix equality (LME) constraint. Based on an obtained simultaneous $H_\infty$ controller, an $L_2$-gain event-triggered transmission policy is proposed for reducing the network usage. An illustrative example is presented to verify the obtained theoretical results.

**Keywords:** networked control systems, simultaneous stabilization, event-triggered, static output feedback, $H_\infty$ control.

## 1. Introduction

A networked control system (NCS) is a feedback control system with feedback loop closed through a communication network. As the signal in an NCS is exchanged via a network, the network-induced delay, packet dropout, and limited network bandwidth can degrade the control performance. Many results have been proposed for dealing with these issues [1–5]. In the early stages, the studies on NCSs were mainly based on periodic task models [4–6]. The number of data packets to be transmitted will be large as the sampling period is small. This leads to a conservative usage of network resources and possibly leads to a congested network traffic. Therefore, how to design networked feedback controllers to achieve desired performance with low network usage is an important issue in NCSs.

Recently, some sporadic task models have been presented in NCSs without degrading system performance. An important approach is the event-triggered scheme [7–26]. In [7], the state transmitting and the control signal updating events were triggered only if the error between the current measured state and the last transmitted state is larger than a threshold condition. In [8], event-triggered distributed NCSs with transmission delay were studied. Based on the designed event-triggered policy, an allowable upper bound of the transmission delay was derived. In [9], for distributed control systems, an implementation of event-triggering control policy in sensor-actuator network was introduced. In [10], the authors concerned with the design of event-triggered state feedback controllers for distributed NCSs with transmission delay and possible packet dropout. Under the proposed triggering policy, the tolerable packet delay and packet dropout were derived. In [11], an event-triggered control policy was developed for discrete-time control systems. In [12], under stochastic packet dropouts, an event-triggered control law for NCSs was calculated by the proposed algorithms. In [13], an event-triggered scheme was developed for uncertain NCSs under packet dropout. In [14], an event-based controller and a scheduler scheme were proposed for NCSs under limited bandwidth. The NCSs were modeled as discrete-time switched control systems. A sufficient condition for the existences of event-based controllers and schedulers was derived by the LMI optimization approach. Recently, the event-triggered scheme has been extended to $H_\infty$ control of NCSs for achieving the disturbance attenuation performance [15–21]. In [15] and [18], with considering transmission delays, event-triggered $H_\infty$ state feedback controllers for NCSs were proposed. Criterion for stability and criterion for co-designing both the controller gains and the trigger parameters were derived. In [16], an event-triggered state feedback control scheme was proposed for guaranteeing finite $L_2$-gain stability of a linear control system. In [17], an event-triggered state feedback $H_\infty$ controller for sampled-data control system was proposed. In [19], the design of event-triggered networked feedback controllers for discrete-time NCS was considered. In [20], based on Lyapunov-Krasovskii function, an event-triggered state feedback $H_\infty$ controller was derived for NCSs under time-varying delay and quantization.

All the results in [7–20] are derived in the assumption that the system states are available for measurement. For practical control systems, system states are often unavailable for direct measurement. In the literature, only few results have been proposed for output-based event-triggered NCSs [22–26]. In [22], a dynamic output feedback event-triggered controller for NCSs was proposed for guaranteeing the asymptotic stability. In [23] and [24], by the passivity theory approach, output-based event-triggered policies were derived for guaranteeing the satisfaction of $L_2$-gain requirements of dynamic output feedback NCSs in the presence of time-varying delays. The synthesis of controllers has not been discussed. In [25] and [26], under nonuniform sampling, new output-based event-triggered $H_\infty$ transmission policies were proposed of NCSs under time-varying transmission delays. Furthermore, the design of static output feedback $H_\infty$ controllers for NCSs was discussed. Conditions for the existence of $H_\infty$ controllers were presented in terms of bilinear matrix inequalities. A non-convex minimization problem must be solved to get a static output feedback $H_\infty$ controller.

http://dx.doi.org/10.5772/63020

On the other hand, few results have been proposed in the literature for simultaneous stabilization of NCSs. The consideration of simultaneous stabilization is important since it allows us to design highly reliable controllers that are able to accommodate possible element failures in control systems. As the signal transmitted through network, the solvability of simultaneous stabilization problem of NCSs is quite different to that of point-to-point wiring control systems. Only few results have been proposed for relevant issues [21, 27]. In [27], based on the average dwell time approach, the simultaneous stabilization for a collection of NCSs was considered. A sufficient condition for guaranteeing simultaneous stabilization was proposed. In [21], under the assumption that the network communication channel is ideal (no delay, no packet dropout, and no quantization error), we considered the design of state feedback event-triggered simultaneous $H_\infty$ transmission policies for a collection of NCSs. Under the proposed event-triggered transmission policies, the $L_2$-gain stability of all the closed-loop NCSs can be guaranteeing under low network usages.

It is known that static output feedback controllers are preferred in practical applications since their implementations are much easier than dynamic output feedback controllers. However, the design of static output feedback controllers is much more difficult than dynamic ones. In this chapter, we extend our previous work [21] to static output feedback case. Furthermore, we consider the network-induced time-varying delay that has not been considered in [21]. We develop an event-triggered static output feedback simultaneous $H_\infty$ transmission policy for a collection of continuous-time linear NCSs under time-varying delay. It is shown that, under mild assumptions, conventional point-to-point wiring delayed static output feedback simultaneous $H_\infty$ controllers can be obtained by solving LMIs with a LME constraint. Based on the obtained static output feedback simultaneous $H_\infty$ controllers, an event-triggered transmission policy was derived for reducing network usage. Different to the results presented in [25] and [26] that only considering the design of an event-triggered $H_\infty$ controller for a single system, this chapter considers the design of a fixed event-triggered $H_\infty$ controller that is able to $L_2$-stabilize a collection of NCSs simultaneously. By the proposed method, highly reliable NCSs that are able to accommodate possible element failures with low network usage can be designed. Even simplifying our results to the single system case, our method for designing static output feedback $H_\infty$ controllers is quite different from those in [25] and [26]. In [25] and [26], a non-convex minimization problem must be solved for getting a static output feedback $H_\infty$ controller. Moreover, the obtained controller can only guarantee uniform ultimate boundedness but not internal stability. In our approach, (simultaneous) static output feedback $H_\infty$ controllers are obtained by solving LMIs with a LME constraint. Moreover, internal stabilities of the closed-loop NCSs can be guaranteed.

## 2. Problem formulation and preliminaries

In this section, the problem to be solved is formulated and some preliminaries are given. For simplifying the expressions, we use the same notations $x$, $u$, $w$, and $z$ to denote the states, control inputs, exogenous inputs, and the controlled outputs of all considered systems.

### 2.1. Problem formulation

Consider a collect of continuous-time control systems:

$$\begin{aligned} \dot{x}(t) &= A_j x(t) + B_{1j} w(t) + B_{2j} u(t), \quad j = 1,2,...,N \\ z(t) &= C_{1j} x(t) + D_{11j} w(t) + D_{12j} u(t) \\ y(t) &= C_{2j} x(t) \end{aligned} \tag{1}$$

where $x(t) \in R^n$ is the system state, $u(t) \in R^m$ is the control input, $z(t) \in R^s$ is the controlled output, $y(t) \in R^l$ is the measured output, $w(t) \in R^r$ is the exogenous input, and $A_j$, $B_{1j}$, $B_{2j}$, $C_{1j}$, $D_{11j}$, $D_{12j}$, and $C_{2j}$ are constant matrices with appropriate dimensions. Here, for convenience, we assume $C_{2j}=C_2$, $j = 1,2,\ldots,N$. Suppose that $(A_j,B_{2j})$ are stabilizable and $(C_2,A_j)$ are detectable for each $j \in \{1, 2..., N\}$.Furthermore, assume that $\gamma^2 I - D_{11j}^T D_{11j} > 0$ for all $j \in \{1, 2..., N\}$.

In this chapter, we consider the case that the feedback loop of system (1) is closed through a real-time network, but not by the conventional point-to-point wiring. Suppose that the sensor node keeps measuring the output signal $y$, but not all the sampled data need to be sent to the controller node. The data transmission at the sensor node is not periodic. Let $t_i$ ($i = 1,2,\ldots$) be the time that the $i$-th transmission occurs at the sensor nodes. In this case, the controller node receives the networked feedback data $y(t_i)$ and updates the control signal at time $t_i + \tau_i$, $i = 1,2,\ldots$, where $\tau_i \in [\tau_{d\min}, \tau_{d\max}]$ is the transmission delay. That is,

$$u(t) = Fy(t_i), t_i + \tau_i \le t < t_{i+1} + \tau_{i+1}, i = 1,2,\ldots \tag{2}$$

where $F$ is the feedback gain to be designed later. With the same controller (2), the closed-loop systems are:

$$\begin{aligned} \dot{x}(t) &= A_j x(t) + B_{1j} w(t) + B_{2j} F C_2 x(t_i), \quad t_i + \tau_i \le t < t_{i+1} + \tau_{i+1}, j = 1,2,\ldots,N \\ z(t) &= C_{1j} x(t) + D_{11j} w(t) + D_{12j} F C_2 x(t_i) \end{aligned} \tag{3}$$

If the measured data is not critical for $L_2$-gain stability, it will not be sent for saving the network usage. In this case, the controller node does not update the control signal. If the measured data is critical, it will be sent through the network to the controller node, and the controller will update the control signal.

Our main goal is to design an event-triggered transmission rule to determine whether the currently measured data should be sent to the controller node, such that, under the transmis-

http://dx.doi.org/10.5772/63020

sion delay, all possible closed-loop systems in (3) are internally stable and satisfy, for a given constant $\gamma>0$ and for any $T>0$ and $w\in L_2[0,\ T]$,

$$\int_0^T z^T(t)z(t)\mathrm{d}t \le \gamma_0^2\int_0^T w^T(t)w(t)\mathrm{d}t, \text{for some}\,\gamma_0<\gamma \tag{4}$$

Note that, a practical control system may have several different dynamic modes since it may have several different operating points (please see e.g., the ship steering control problem considered in [28] ). On the other hand, for achieving higher reliability of a practical control system, we may want to design a controller to accommodate possible element failures. With considering possible element failures, a control system can have several different dynamic modes (see e.g., the reliable control problem for active suspension systems considered in [29]). The problem we considered has a practical importance owing to its high applicability in designing robust and/or reliable controllers.

### 2.2. Preliminaries

The following Lemmas will be used later.

***Lemma 1*** [30]: For any vectors $X,Y\in R^n$ and any positive definite matrix $G\in R^{n\times n}$, the following inequality holds:

$$2X^TY \le X^TGX + Y^TG^{-1}Y \ \blacksquare$$

***Lemma 2*** [31]: For any given matrices $\Pi<0$ and $\Phi=\Phi^T$, and any scalar $\lambda$, the following inequality holds:

$$\Phi\Pi\Phi \le -2\lambda\Phi - \lambda^2\Pi^{-1} \ \blacksquare$$

For convenience, define $x_t(s)=x(t+s),\ \ \forall\, s\in[-\tau_{\max},\ 0]$.

***Lemma 3*** (*Lyapunov–Krasovskii Theorem*) [32]: Consider a time-delay system:

$$\dot{x}(t) = Ax(t) + A_dx(t-\tau(t)),\ \forall t\ge 0 \tag{5}$$

with $\tau(t)\in[0,\ \tau_{\max}],\ \forall\, t\ge 0$. Suppose that $x(t)=\psi(t),\ \ \forall\, t\in[-\tau_{\max},\ 0]$. If there exists a function

$$V: C([-\tau_{\max},0],R^n)\to R$$

and a scalar $\varepsilon>0$, such that, for all $\varphi \in C([-\tau_{\max}, 0], R^n)$, $V(\varphi) \geq \varepsilon \| \varphi(0) \|^2$, and, along the solutions of (5),

$$\left. \frac{\mathrm{d}V(x_t)}{\mathrm{d}t} \right|_{x_t=\varphi} \leq -\varepsilon \|\varphi(0)\|^2,$$

then the system (5) is asymptotically stable. ■

## 3. Main results

We first consider the design of the event-triggered transmission policy under the assumption that we have a delayed simultaneous $H_\infty$ controller, and then show how to derive simultaneous $H_\infty$ controller under transmission delay.

### 3.1. Event-triggered transmission policy for NCSs under time-varying delay

Define the equivalent time-varying delay

$$\tau(t) = t - t_i,\ t_i + \tau_i \leq t < t_{i+1} + \tau_{i+1},\ i = 1,2,\ldots.$$

It is clear that

$$\tau(t) \in \left[\tau_{\min},\ \tau_{\max}\right] \forall t \geq 0, \text{and } \dot{\tau} = 1 \text{ almost everywhere} \tag{6}$$

where $\tau_{\min} \equiv \min_{i \in N}\{\tau_i\} = \tau_{d\min}$ and $\tau_{\max} \equiv \max_{i \in N}\{t_{i+1} - t_i + \tau_{i+1}\} = \max_{i \in N}\{t_{i+1} - t_i\} + \tau_{d\max}$. Then, the systems in (3) can be equivalently described as

$$\begin{aligned} \dot{x}(t) &= A_j x(t) + B_{1j} w(t) + B_{2j} F C_2 x(t - \tau(t)), \quad j = 1,2,\ldots,N \\ z(t) &= C_{1j} x(t) + D_{11j} w(t) + D_{12j} F C_2 x(t - \tau(t)) \end{aligned} \tag{7}$$

To derive an event-triggered transmission policy in the presence of transmission delay, assume that, for the systems in (1), we have a conventional delayed static output feedback simultaneous $H_\infty$ controller:

$$u(t) = Fy(t - \tau(t)) \tag{8}$$

http://dx.doi.org/10.5772/63020

which is such that all of the possible closed-loop systems in (7) are internally stable and satisfy the condition (4) for $\tau(t)\in[\tau_{\min},\ \tau_{\max}]$. How to get such a delayed static output feedback simultaneous $H_\infty$ controller will be discussed later.

Define the error signal:

$$e(t) = y(t) - y(t_i), t_i \le t < t_{i+1} \tag{9}$$

We have the following results.

***Theorem 1***: Consider the systems in (1). Suppose that the controller (8) is such that all the closed-loop systems in (7) are internally stable and satisfy the condition (4). If there exist matrices $P_j>0$, $Q_j>0$, $G_{1j}$, $G_{2j}$, $G_{3j}$, and $G_{4j}$, $j$=1,2,…,$N$, of appropriate dimensions, and scalars $\varepsilon_j>0$, $j$=1,2,…,$N$, satisfying the following LMIs:

$$\begin{bmatrix} \Phi_j & \Xi_j & G_{3j}^T & P_jB_{1j} + G_{4j}^T + C_{1j}^T D_{11j} & \tau_{\max} A_j^T Q_j & \tau_{\max} G_{1j} \\ * & \Sigma_j & -G_{3j}^T & -G_{4j}^T + C_2^T F^T D_{12j}^T D_{11j} & \tau_{\max} C_2^T F^T B_{2j}^T Q_j & \tau_{\max} G_{2j} \\ * & * & -\varepsilon_j I & 0 & 0 & \tau_{\max} G_{3j} \\ * & * & * & D_{11j}^T D_{11j} - r^2 I & \tau_{\max} B_{1j}^T Q_j & \tau_{\max} G_{4j} \\ * & * & * & * & -\tau_{\max} Q_j & 0 \\ * & * & * & * & * & -\tau_{\max} Q_j \end{bmatrix} < 0, \tag{10}$$

where

$$\Phi_j = A_j^T P_j + P_j A_j + C_{1j}^T C_{1j} + C_2^T C_2 + G_{1j} + G_{1j}^T$$

$$\Xi_j = P_j B_{2j} F C_2 + C_{1j}^T D_{12j} F C_2 - G_{1j} + G_{2j}^T$$

$$\Sigma_j = C_2^T F^T D_{12j}^T D_{12j} F C_2 - G_{2j} - G_{2j}^T$$

then all the networked closed-loop systems in (7) are internally stable and satisfy the condition (4) if the following condition holds:

$$\|e(t)\| < \min_{j\in\{1,2,\ldots,N\}} \frac{1}{\sqrt{\varepsilon_j}} \cdot \|y(t)\|, t_i \le t < t_{i+1} \tag{11}$$

***Proof:*** For the systems in (7), choose the candidate storage functions:

$$V_j(x(t)) = x^T(t)P_jx(t) + \int_{-\tau_{\max}}^{0}\int_{t+\sigma}^{t}\dot{x}^T(\theta)Q_j\dot{x}(\theta)d\theta d\sigma, j = 1,2,\ldots,N.$$

Define

$$\hat{\mathrm{H}}_{\mathrm{dj}}(\mathrm{x(t)},\mathrm{x(t_i)},\mathrm{e(t)},\mathrm{w(t)}) \equiv \dot{\mathrm{V}}_{\mathrm{j}}(\mathrm{x(t)}) + \mathrm{z^T(t)z(t)} - \gamma^2\mathrm{w^T(t)}$$
$$\mathrm{w(t)} + \mathrm{y^T(t)y(t)} - \varepsilon_{\mathrm{j}}\mathrm{e^T(t)e(t)},\ \mathrm{j} = 1,2,\ldots,\mathrm{N}$$

Along the solutions of the *j*-th system, we have

$$\hat{H}_{dj} = 2x^T(t)P_j\dot{x}(t) - \int_{t-\tau_{\max}}^{t}\dot{x}^T(\theta)Q_j\dot{x}(\theta)\mathrm{d}\theta + \tau_{\max}\dot{x}^T(t)Q_j\dot{x}(t) + z^T(t)z(t) - \gamma^2w^T(t)w(t)$$
$$+ y^T(t)y(t) - \varepsilon_j e^T(t)e(t) + 2\eta^T(t)G_j\left(x(t) - x(t_i) - \int_{t_i}^{t}\dot{x}(\theta)\mathrm{d}\theta\right)$$

where $\eta(t)=\left[x^T(t)\quad x^T(t_i)\quad e^T(t)\quad w^T(t)\right]^T$ and $G_j=\left[G_{1j}^T\quad G_{2j}^T\quad G_{3j}^T\quad G_{4j}^T\right]^T$. Then,

$$\hat{H}_{dj} = 2x^T(t)P_j\left(A_jx(t) + B_{1j}w(t) + B_{2j}FC_2x(t-\tau(t))\right) + x^T(t)C_{1j}^TC_{1j}x(t)$$

$$+2x^T(t)C_{1j}^TD_{12j}FC_2x(t-\tau(t)) + x^T(t-\tau(t))C_2^TF^TD_{12j}^TD_{12j}FC_2x(t-\tau(t))$$

$$+w^T(t)D_{11j}^TD_{11j}w(t) + 2x^T(t)C_{1j}^TD_{11j}w(t) + 2x^T(t-\tau(t))C_2^TF^TD_{12j}^TD_{11j}w(t)$$

$$-r^2w^T(t)w(t) - \int_{t-\tau_{\max}}^{t}\dot{x}^T(\theta)Q_j\dot{x}(\theta)\mathrm{d}\theta$$

$$+\tau_{\max}x^T(t)A_j^TQ_jA_jx(t) + \tau_{\max}w^T(t)B_{1j}^TQ_jB_{1j}w(t)$$

$$+\tau_{\max}x^T(t-\tau(t))C_2^TF^TB_{2j}^TQB_{2j}FC_2x(t-\tau(t))$$

$$+2\tau_{\max}x^T(t)A_j^TQ_jB_{1j}w(t) + 2\tau_{\max}x^T(t)A_j^TQ_jB_{2j}FC_2x(t-\tau(t))$$

$$+2\tau_{\max}x^T(t-\tau(t))C_2^TF^TB_{2j}^TQ_jB_{1j}w(t)$$

http://dx.doi.org/10.5772/63020

$$+x^T(t)C_2^TC_2x(t)-\varepsilon_j e^T(t)e(t)+2\eta^T(t)G_j\left(x(t)-x(t_i)-\int_{t_i}^{t}\dot{x}(\theta)\mathrm{d}\theta\right) \tag{12}$$

From the definition of $\tau_{max}$, it is clear that $\tau_{max}\geq t-t_i$ as $t\in[t_i+\tau_i,\ t_{i+1}+\tau_{i+1})$. As a result,

$$-\int_{t-\tau_{max}}^{t}\dot{x}^T(\theta)Q_j\dot{x}(\theta)\mathrm{d}\theta\leq-\int_{t_i}^{t}\dot{x}^T(\theta)Q_j\dot{x}(\theta)\mathrm{d}\theta. \tag{13}$$

By (12), (13), and the Jensen integral inequality [33], we can show that

$$\hat{H}_{dj}\leq\eta^T(t)\begin{bmatrix}\Phi_j & P_jB_{2j}FC_2+C_{1j}^TD_{12j}FC_2-G_{1j}+G_{2j}^T & G_{3j}^T & P_jB_{1j}+G_{4j}^T+C_{1j}^TD_{11j}\\ * & C_2^TF^TD_{12j}^TD_{12j}FC_2-G_{2j}-G_{2j}^T & -G_{3j}^T & -G_{4j}^T+C_2^TF^TD_{12j}^TD_{11j}\\ * & * & -\varepsilon_jI & 0\\ * & * & * & D_{11j}^TD_{11j}-r^2I\end{bmatrix}\eta(t)$$

$$+\tau_{max}x^T(t)A_j^TQ_jA_jx(t)+\tau_{max}w^T(t)B_{1j}^TQ_jB_{1j}w(t)$$

$$+\tau_{max}x^T(t-\tau(t))C_2^TF^TB_{2j}^TQ_jB_{2j}FC_2x(t-\tau(t))$$

$$+2\tau_{max}x^T(t)A_j^TQ_jB_{1j}w(t)+2\tau_{max}x^T(t)A_j^TQ_jB_{2j}FC_2x(t-\tau(t))$$

$$+2\tau_{max}x^T(t-\tau(t))C_2^TF^TB_{2j}^TQ_jB_{1j}w(t)+\tau_{max}\eta^T(t)G_jQ_j^{-1}G_j^T\eta(t) \tag{14}$$

Then, by Schur complement and after some manipulations, it can be proved that if (10) holds, we have

$$\hat{\mathrm{H}}_{\mathrm{dj}}(\mathrm{x}(\mathrm{t}),\mathrm{x}(\mathrm{t}_{\mathrm{i}}),\mathrm{e}(\mathrm{t}),\mathrm{w}(\mathrm{t}))<\text{ for all }\eta(\mathrm{t})\neq0$$

.

That is, under (11),

$$\dot{\mathrm{V}}_{\mathrm{j}}(\mathrm{x}(\mathrm{t}))+\mathrm{z}^{\mathrm{T}}(\mathrm{t})\mathrm{z}(\mathrm{t})-\gamma^2\mathrm{w}^{\mathrm{T}}(\mathrm{t})\mathrm{w}(\mathrm{t})<0,\ \eta(\mathrm{t})\neq0 \tag{15}$$

This shows that the *j*-th closed-loop system in (7) satisfies condition (4). To prove the internal stability, by letting $w(t)=0$ in (15) yields (note that *j* can be any number belonging to {1,2,…,*N*})

$$\dot{V}_j(x(t)) < -z^T(t)z(t) \le 0, \forall x(t) \ne 0.$$

That is, the *j*-th closed-loop system is internally stable. Note that *j* can be any number belonging to {1,2,…,*N*}. The above proof shows that all the closed-loop systems are internally stable and satisfy condition (4). ■

***Remark 1***: Note that condition (11) is checked at the sensor node but not the controller node. In practice, the transmission event is triggered by the condition

$$\|e(t)\| \ge \eta \cdot \min_{j\in\{1,2,\ldots,N\}} \frac{1}{\sqrt{\varepsilon_j}} \cdot \|y(t)\|$$

for some constant $0<\eta<1$. In general we set $\eta$ near to 1. ■

### 3.2. Synthesis of static output feedback delayed simultaneous $H_\infty$ controllers

In this subsection, we introduce how to derive a conventional delayed simultaneous static output feedback $H_\infty$ controller (8) such that all of the closed-loop systems (7) are internally stable and satisfy the condition (4). We have the following results.

***Lemma 4*:** Consider the systems in (1). For given positive scalars $\lambda$ and $\tau_{\max}$, if there exist matrices $S>0$, $Q>0$, $T_{1j}$, $T_{2j}$, $T_{3j}$, $j$=1,2,…,$N$, and matrices $M$ and $L$ of appropriate dimensions, satisfying the following LMIs and LME :

$$\begin{bmatrix} \Lambda_j & \zeta_j & B_{1j}+T_{3j}^T+SC_{1j}^TD_{11j} & \tau_{\max}SA_j^T & SC_{1j}^T & \tau_{\max}T_{1j} \\ * & -T_{2j}-T_{2j}^T & -T_{3j}^T+C_2^TL^TD_{12j}^TD_{11j} & \tau_{\max}C_2^TL^TB_{2j}^T & C_2^TL^TD_{12j}^T & \tau_{\max}T_{2j} \\ * & * & D_{11j}^TD_{11j}-r^2I & \tau_{\max}B_{1j}^T & 0 & \tau_{\max}T_{3j} \\ * & * & * & -\tau_{\max}Q^{-1} & 0 & 0 \\ * & * & * & * & -I & 0 \\ * & * & * & * & * & \tau_{\max}\left(-2\lambda S+\lambda^2Q^{-1}\right) \end{bmatrix} < 0 \qquad (16)$$

$$\mathrm{MC}_2 = \mathrm{C}_2\mathrm{S} \qquad (17)$$

where $\Lambda_j = SA_j^T + A_jS + T_{1j} + T_{1j}^T$ and $\zeta_j = B_{2j}L\ C_2 - T_{1j} + T_{2j}^T$, then the feedback law (8) with $F = L\ M^{-1}$ is a simultaneous $H_\infty$ controller for the systems in (1).

***Proof:*** Let $P = S^{-1}$. Choose a candidate storage function

http://dx.doi.org/10.5772/63020

$$V(x(t)) = x^T(t)Px(t) + \int_{-\tau_{\max}}^{0}\int_{t+\sigma}^{t}\dot{x}^T(\theta)Q\dot{x}(\theta)d\theta d\sigma$$

and define

$$H_{dj}(x(t),w(t)) \equiv \dot{V}(x(t)) + (C_{1j}x(t) + D_{11j}w(t) + D_{12j}u(t))^T(C_{1j}x(t) + D_{11j}w(t) + D_{12j}u(t)) \\ -\gamma^2 w^T(t)w(t), \quad j = 1,2,...,N.$$

Define

$$\mu(t) = \begin{bmatrix} x(t) \\ x(t-\tau(t)) \\ w(t) \end{bmatrix}, T_j = \begin{bmatrix} PT_{1j}P \\ PT_{2j}P \\ T_{3j}P \end{bmatrix}$$

Then, along the trajectories of the *j*-th system,

$$H_{dj} = 2x^T(t)P\dot{x}(t) + z^T(t)z(t) - \gamma^2 w^T(t)w(t) - \int_{t-\tau_{\max}}^{t}\dot{x}^T(\theta)Q\dot{x}(\theta)d\theta + \tau_{\max}\dot{x}^T(t)Q\dot{x}(t) \\ + 2\mu^T(t)T_j\left(x(t) - x(t-\tau(t)) - \int_{t-\tau(t)}^{t}\dot{x}(\theta)d\theta\right)$$

$$= 2x^T(t)P\left(A_jx(t) + B_{1j}w(t) + B_{2j}FC_2x(t-\tau(t))\right) + x^T(t)C_{1j}^TC_{1j}x(t)$$

$$+2x^T(t)C_{1j}^TD_{12j}FC_2x(t-\tau(t)) + x^T(t-\tau(t))C_2^TF^TD_{12j}^TD_{12j}FC_2x(t-\tau(t))$$

$$+w^T(t)D_{11j}^TD_{11j}w(t) + 2x^T(t)C_{1j}^TD_{11j}w(t) + 2x^T(t-\tau(t))C_{2j}^TF^TD_{12j}^TD_{11j}w(t)$$

$$-r^2w^T(t)w(t) - \int_{t-\tau_{\max}}^{t}\dot{x}^T(\theta)Q\dot{x}(\theta)d\theta + \tau_{\max}x^T(t)A_j^TQA_jx(t)$$

$$+\tau_{\max}w^T(t)B_{1j}^TQB_{1j}w(t) + \tau_{\max}x^T(t-\tau(t))C_2^TF^TB_{2j}^TQB_{2j}FC_2x(t-\tau(t))$$

$$+2\tau_{\max}x^T(t)A_j^TQB_{1j}w(t) + 2\tau_{\max}x^T(t)A_j^TQB_{2j}FC_2x(t-\tau(t))$$

$$+2\tau_{\max}x^T(t-\tau(t))C_2^TF^TB_{2j}^TQB_{1j}w(t)+2\mu^T(t)T_j\left(x(t)-x(t-\tau(t))-\int_{t-\tau(t)}^{t}\dot{x}(\theta)d\theta\right) \tag{18}$$

By Lemma 1 and the Jensen integral inequality [33], we can show that

$$-2\mu^T(t)T_j\int_{t-\tau(t)}^{t}\dot{x}(\theta)\mathrm{d}\theta\le\tau_{\max}\mu^T(t)T_jQ^{-1}T_j^T\mu(t)+\int_{t-\tau(t)}^{t}\dot{x}^T(\theta)Q\dot{x}(\theta)\mathrm{d}\theta \tag{19}$$

As a result,

$$H_{dj}\le 2x^T(t)P\left(A_jx(t)+B_{1j}w(t)+B_{2j}FC_2x(t-\tau(t))\right)+x^T(t)C_{1j}^TC_{1j}x(t)$$

$$+2x^T(t)C_{1j}^TD_{12j}FC_2x(t-\tau(t))+x^T(t-\tau(t))C_2^TF^TD_{12j}^TD_{12j}FC_2x(t-\tau(t))$$

$$+w^T(t)D_{11j}^TD_{11j}w(t)+2x^T(t)C_{1j}^TD_{11j}w(t)+2x^T(t-\tau(t))C_2^TF^TD_{12j}^TD_{11j}w(t)$$

$$-r^2w^T(t)w(t)-\int_{t-\tau(t)}^{t}\dot{x}^T(\theta)Q\dot{x}(\theta)\mathrm{d}\theta$$

$$+\tau_{\max}x^T(t)A_j^TQA_jx(t)+\tau_{\max}w^T(t)B_{1j}^TQB_{1j}w(t)$$

$$+\tau_{\max}x^T(t-\tau(t))C_2^TF^TB_{2j}^TQB_{2j}FC_2x(t-\tau(t))+2\tau_{\max}x^T(t)A_j^TQB_{1j}w(t)$$

$$+2\tau_{\max}x^T(t)A_j^TQB_{2j}FC_2x(t-\tau(t))+2\tau_{\max}x^T(t-\tau(t))C_2^TF^TB_{2j}^TQB_{1j}w(t)$$

$$+2\mu^T(t)T_jx(t)-2\mu^T(t)T_jx(t-\tau(t))+\tau_{\max}\mu^T(t)T_jQ^{-1}T_j^T\mu(t)+\int_{t-\tau(t)}^{t}\dot{x}^T(\theta)Q\dot{x}(\theta)\mathrm{d}\theta$$

$$=\mu^T(t)\begin{bmatrix}\Theta_j & PB_{2j}FC_2+C_{1j}^TD_{12j}FC_2-PT_{1j}P+PT_{2j}^TP & PB_{1j}+PT_{3j}^T+C_{1j}^TD_{11j}\\ * & C_2^TF^TD_{12j}^TD_{12j}FC_2-PT_{2j}P-PT_{2j}^TP & -PT_{3j}^T+C_2^TF^TD_{12j}^TD_{11j}\\ * & * & D_{11j}^TD_{11j}-r^2I\end{bmatrix}\mu(t)$$

$$+\tau_{\max}x^T(t)A_j^TQA_jx(t)+\tau_{\max}w^T(t)B_{1j}^TQB_{1j}w(t)$$

http://dx.doi.org/10.5772/63020

$$+\tau_{\max}x^T(t-\tau(t))C_2^TF^TB_{2j}^TQB_{2j}FC_2x(t-\tau(t))+2\tau_{\max}x^T(t)A_j^TQB_{1j}w(t)$$

$$+2\tau_{\max}x^T(t)A_j^TQB_{2j}FC_2x(t-\tau(t))+2\tau_{\max}x^T(t-\tau(t))C_2^TF^TB_{2j}^TQB_{1j}w(t)$$

$$+\tau_{\max}\mu^T(t)T_jQ^{-1}T_j^T\mu(t)$$

$$\equiv \mu^T(t)\Omega_j\mu(t)$$

where

$$\Theta_j = PA_j + A_j^TP + C_{1j}^TC_{1j} + PT_{1j}P + PT_{1j}^TP$$

and

$$\Omega_j=\begin{bmatrix}\Theta_j & PB_{2j}FC_2+C_{1j}^TD_{12j}FC_2-PT_{1j}P+PT_{2j}^TP & PB_{1j}+PT_{3j}^T+C_{1j}^TD_{11j}\\ * & C_2^TF^TD_{12j}^TD_{12j}FC_2-PT_{2j}P-PT_{2j}^TP & -PT_{3j}^T+C_2^TF^TD_{12j}^TD_{11j}\\ * & * & D_{11j}^TD_{11j}-r^2I\end{bmatrix}$$
$$+\begin{bmatrix}\tau_{\max}A_j^TQA_j & \tau_{\max}A_j^TQB_{2j}FC_2 & \tau_{\max}A_j^TQB_{1j}\\ * & \tau_{\max}C_2^TF^TB_{2j}^TQB_{2j}FC_2 & \tau_{\max}C_2^TF^TB_{2j}^TQB_{1j}\\ * & * & \tau_{\max}B_{1j}^TQB_{1j}\end{bmatrix}+\tau_{\max}T_jQ^{-1}T_j^T$$

By noting (17) and the Schur complement, we know that $\Omega_j<0$ if $\hat{\Omega}_j<0$, where

$$\hat{\Omega}_j=\begin{bmatrix}\Psi_j & \delta_j & PB_{1j}+PT_{3j}^T+C_{1j}^TD_{11j} & \tau_{\max}A_j^T & C_{1j}^T & \tau_{\max}PT_{1j}P\\ * & -PT_{2j}P-PT_{2j}^TP & -PT_{3j}^T+C_2^TF^TD_{12j}^TD_{11j} & \tau_{\max}C_2^TF^TB_{2j}^T & C_2^TF^TD_{12j}^T & \tau_{\max}PT_{2j}P\\ * & * & D_{11j}^TD_{11j}-r^2I & \tau_{\max}B_{1j}^T & 0 & \tau_{\max}T_{3j}P\\ * & * & * & -\tau_{\max}Q^{-1} & 0 & 0\\ * & * & * & * & -I & 0\\ * & * & * & * & * & -\tau_{\max}Q\end{bmatrix}$$

with

$$\Psi_j = PA_j + A_j^T P + PT_{1j}P + PT_{1j}^T P$$
$$\delta_j = PB_{2j}FC_2 - PT_{1j}P + PT_{2j}^T P$$

Moreover, $\hat{\Omega}_j < 0$ if and only if $\tilde{\Omega}_j < 0$, where $\tilde{\Omega}_j$ is the matrix obtained by pre- and post-multiplying $\hat{\Omega}_j$ by $diag\{S \quad S \quad I \quad I \quad I \quad S\}$:

$$\tilde{\Omega}_j = \begin{bmatrix} S\Psi_j S & S\delta_j S & B_{1j} + T_{3j}^T + SC_{1j}^T D_{11j} & \tau_{\max} SA_j^T & SC_{1j}^T & \tau_{\max} T_{1j} \\ * & -T_{2j} - T_{2j}^T & -T_{3j}^T + SC_2^T F^T D_{12j}^T D_{11j} & \tau_{\max} SC_2^T F^T B_{2j}^T & SC_2^T F^T D_{12j}^T & \tau_{\max} T_{2j} \\ * & * & D_{11j}^T D_{11j} - r^2 I & \tau_{\max} B_{1j}^T & 0 & \tau_{\max} T_{3j} \\ * & * & * & -\tau_{\max} Q^{-1} & 0 & 0 \\ * & * & * & * & -I & 0 \\ * & * & * & * & * & -\tau_{\max} SQS \end{bmatrix}$$

By Lemma 2, it follows that $\tilde{\Omega}_j < 0$ (and then $\Omega_j < 0$) if (16) and (17) hold. This proves that the feedback law (8) with $F = L\ M^{-1}$ is a simultaneous static output feedback $H_\infty$ controller for all the systems in (1). ■

## 4. An illustrative example

Suppose that a control system operates at three different operating points. The dynamics at these operating points are different. Suppose that it behaves in the following three possible modes:

$$\begin{aligned} \dot{x}(t) &= A_j x(t) + B_{1j} w(t) + B_{2j} u(t) \\ z(t) &= C_{1j} x(t) + D_{11j} w(t) + D_{12j} u(t),\ j = 1,2,3 \\ y(t) &= C_2 x(t) \end{aligned} \tag{20}$$

where

$$A_1 = \begin{bmatrix} 0.211 & -1.471 & -0.361 \\ -0.585 & -1.683 & 0.729 \\ -1.811 & 0.64 & -2.287 \end{bmatrix},\ B_{11} = \begin{bmatrix} 0.696 \\ 0.385 \\ 0.176 \end{bmatrix},\ B_{21} = \begin{bmatrix} -1.824 \\ -1.182 \\ 2.564 \end{bmatrix},$$
$$C_{11} = \begin{bmatrix} 0.686 & -0.421 & -2.211 \end{bmatrix},\ D_{111} = 1.164,\ D_{121} = 0.665$$
$$C_2 = \begin{bmatrix} 0.657 & 0.265 & -1.288 \\ -0.439 & 0.336 & -0.246 \end{bmatrix},$$

http://dx.doi.org/10.5772/63020

$$A_2 = \begin{bmatrix} -0.406 & -1.525 & 0.321 \\ 0.625 & -1.145 & 1.239 \\ -4.185 & 1.212 & -1.431 \end{bmatrix}, B_{12} = \begin{bmatrix} -0.559 \\ 0.47 \\ -0.679 \end{bmatrix}, B_{22} = \begin{bmatrix} -0.591 \\ 1.521 \\ 2.351 \end{bmatrix},$$
$$C_{12} = \begin{bmatrix} -0.829 & 0.451 & 2.395 \end{bmatrix}, D_{112} = -1.523, D_{122} = -0.414,$$
$$C_2 = \begin{bmatrix} 0.657 & 0.265 & -1.288 \\ -0.439 & 0.336 & -0.246 \end{bmatrix},$$

$$A_3 = \begin{bmatrix} -0.121 & -1.235 & 0.261 \\ 0.625 & -0.733 & 0.639 \\ -2.106 & 0.55 & 1.147 \end{bmatrix}, B_{13} = \begin{bmatrix} 0.509 \\ 0.585 \\ -0.776 \end{bmatrix}, B_{23} = \begin{bmatrix} -0.824 \\ 1.202 \\ 3.514 \end{bmatrix},$$
$$C_{13} = \begin{bmatrix} 0.686 & -0.421 & -2.211 \end{bmatrix}, D_{113} = 1.164, D_{123} = 0.569,$$
$$C_2 = \begin{bmatrix} 0.657 & 0.265 & -1.288 \\ -0.439 & 0.336 & -0.246 \end{bmatrix}.$$

We want to design a static output feedback event-triggered $H_\infty$ controller that is able to $L_2$-stabilize the system at all the three possible operating points with $\gamma$=7. Suppose that the minimal and maximal transmission delays are $\tau_{d\min}$=0.1ms and $\tau_{d\max}$=0.45ms, respectively. We first need to derive a conventional simultaneous static output feedback $H_\infty$ controller for all the modes in (20) and then, based on the obtained controller, we can obtain an event-triggered transmission policy.

Given $\lambda$=0.6 and $\tau_{\max}$=0.1 $s$, by solving (16) and (17) we can get a simultaneous $H_\infty$ controller

$$u(t) = Fy(t - \tau(t)) = \begin{bmatrix} 0.885 & -1.559 \end{bmatrix} y(t - \tau(t))$$

With this controller, by solving (10) we can get solutions:

$$\mathrm{P}_1 = \begin{bmatrix} 112.141 & -30.286 & -9.24 \\ -30.286 & 113.675 & 14.086 \\ -9.24 & 14.086 & 47.207 \end{bmatrix} > 0 \quad \mathrm{P}_2 = \begin{bmatrix} 60.909 & -1.957 & 8.043 \\ -1.957 & 42.793 & -1.25 \\ 8.043 & -1.25 & 71.935 \end{bmatrix} > 0$$

$$\mathrm{P}_3 = \begin{bmatrix} 129.678 & -14.921 & -18.771 \\ -14.921 & 63.544 & -18.135 \\ -18.771 & -18.135 & 40.175 \end{bmatrix} > 0 \quad \mathrm{Q}_1 = \begin{bmatrix} 297.0174 & -97.1611 & 42.8020 \\ -97.1611 & 345.4888 & 58.5580 \\ 42.8020 & 58.5580 & 134.3278 \end{bmatrix} > 0$$

$$Q_2 = \begin{bmatrix} 157.5111 & 14.4987 & 6.6046 \\ 14.4987 & 120.8614 & 11.6833 \\ 6.6046 & 11.6833 & 117.3282 \end{bmatrix} > 0 \quad Q_3 = \begin{bmatrix} 282.727 & -17.226 & -12.768 \\ -17.226 & 61.7053 & -10.87 \\ -12.768 & -10.87 & 103.349 \end{bmatrix} > 0$$

$$G_{11} = \begin{bmatrix} -217.2794 & 119.9043 & 11.8195 \\ 39.8052 & 12.3064 & -28.9204 \\ 46.2486 & -53.3922 & -72.2522 \end{bmatrix} \quad G_{21} = \begin{bmatrix} 217.253 & -42.004 & 10.029 \\ 19.619 & 73.242 & 0.249 \\ -88.031 & 31.144 & 156.995 \end{bmatrix}$$

$$G_{31} = \begin{bmatrix} -9.24 & 14.086 & 47.207 \\ 60.91 & -1.957 & 42.793 \end{bmatrix} \quad G_{41} = \begin{bmatrix} -40.504 & 9.752 & 16.069 \end{bmatrix}$$

$$G_{12} = \begin{bmatrix} -134.794 & 35.386 & 65.797 \\ 73.976 & -46.104 & -60.232 \\ 118.174 & -34.092 & -46.002 \end{bmatrix} \quad G_{22} = \begin{bmatrix} 170.595 & -39.806 & -49.551 \\ -7.746 & 56.83 & 17.2 \\ -21.124 & 16.814 & 140.097 \end{bmatrix}$$

$$G_{32} = \begin{bmatrix} -9.2402 & 14.0864 & 47.2070 \\ 60.9096 & -1.9572 & 42.7932 \end{bmatrix} \quad G_{42} = \begin{bmatrix} -7.001 & -8.089 & 21.297 \end{bmatrix}$$

$$G_{13} = \begin{bmatrix} -150.599 & 38.683 & -6.694 \\ 69.354 & -43.986 & -33.385 \\ 126.071 & -47.435 & -130.298 \end{bmatrix} \quad G_{23} = \begin{bmatrix} 258.559 & -32.327 & -49.367 \\ -40.332 & 58.951 & 15.119 \\ -142.399 & 35.247 & 141.214 \end{bmatrix}$$

$$G_{33} = \begin{bmatrix} -9.24 & 14.086 & 47.207 \\ 60.91 & -1.957 & 42.793 \end{bmatrix} \quad G_{43} = \begin{bmatrix} -78.396 & 1.269 & 45.971 \end{bmatrix}$$

$$\varepsilon_1 = 38.2561,\ \varepsilon_2 = 72.7127, \text{ and } \varepsilon_3 = 72.8613$$

According to Theorem 1 and Remark 1, the event-triggered policy is (let $\eta$=0.99):

$$\left\|e(t)\right\| \geq \eta \cdot \min_{j\in\{1,2,3\}} \frac{1}{\sqrt{\varepsilon_j}} \cdot \left\|y(t)\right\| = 0.1116\left\|y(t)\right\| \tag{21}$$

http://dx.doi.org/10.5772/63020

With the triggering condition (21), the sensor node can determine whether the currently measured data must be transmitted. If the currently measured data is such that condition (21) is violated, it will be discarded for reducing network usage. If the measured data is such that condition (21) holds, it will be sent to the controller node for updating the control signal.

By simulation, for guaranteeing the simultaneous $L_2$–gain stability, the number of transmission events at the sensor node of the first system is 64 in the first 10 s. The average inter-transmitting time is 0.1563 s. The number of transmission events at the sensor node of the second system is 585. The average inter-transmitting time is 0.0171 s. The number of transmission events at the sensor node of the third system is 595. The average inter-transmitting time is 0.0168 s. **Figures 1–3** are the responses of the event-triggered and non-event-triggered closed-loop systems under the same initial condition $x(0)=[1\ \ -1\ \ 1]^T$ and the same exogenous disturbance $w(t)=(3\sin(8t)+2\cos(5t))\times e^{-0.5t}$ (shown in **Figure 4**). It is clear that the proposed event-triggered policy guarantees simultaneous $L_2$–gain stability under low network usages. Moreover, it can be seen that the responses of closed-loop systems controlled by the event-triggered controller and the non-event-triggered controller are almost the same. That is, the obtained event-triggered controller, in a very low network usage rate, can perform almost the same control performance as the conventional non-event-triggered controller. A low network usage rate will in general lead to a good quality of network service.

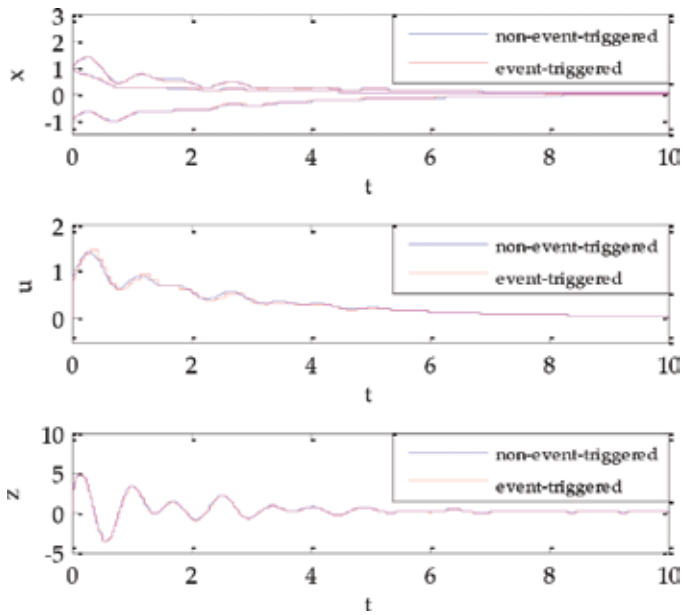


**Figure 1.** Responses of the first closed-loop NCS.

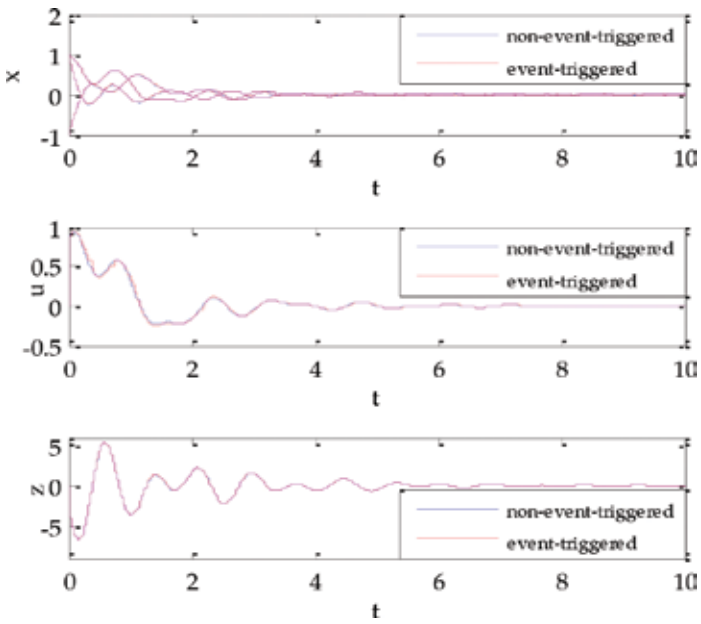


**Figure 2.** Responses of the second closed-loop NCS.

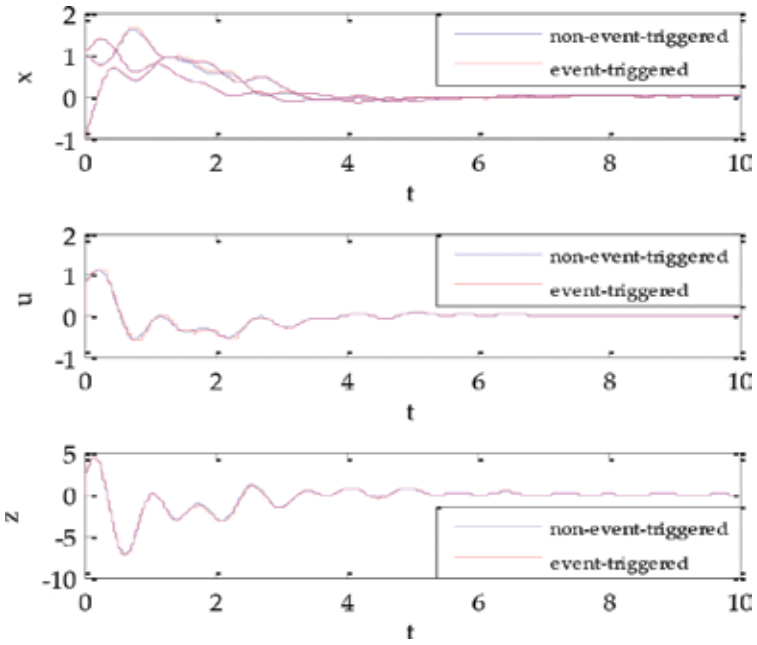


**Figure 3.** Responses of the third closed-loop NCS.

http://dx.doi.org/10.5772/63020

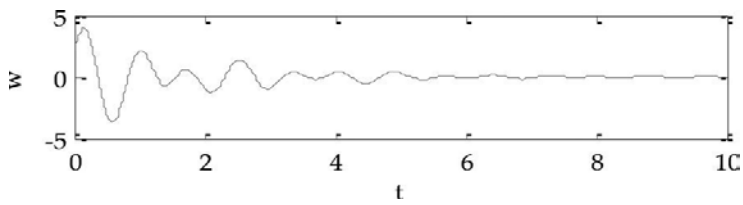


**Figure 4.** Disturbance input.

## 5. Conclusions

In this chapter, we develop an event-triggered static output feedback simultaneous $H_\infty$ transmission policy for NCSs under time-varying transmission delay. With the proposed method, we do not need to switch controllers or event-triggered policies for an NCS with several different operating points. Moreover, the reliability of NCSs can be improved as possible element failures can be accommodated. The implementation of the obtained event-triggered simultaneous $H_\infty$ controller is easy as it is in the static output feedback framework. One weakness of our result is that the conditions for the existence of static output feedback simultaneous $H_\infty$ controllers are represented in terms of LMIs with a LME constraint. Standard LMI tools cannot be directly applied to find the solutions. Possible issues for further study include finding less conservative event-triggered transmission policies, considering the possibility of packet dropouts, and relaxing the continuous monitoring requirement at the sensor node by replacing the event-triggered scheme with a self-triggered one.

## Acknowledgements

This work was supported by the National Science Council of the Republic of China under Grant NSC 101-2221-E-019-037.

**Nomenclatures**

$R^n$ real vector of dimension $n$.

$R^{n\times m}$ real $n\times m$ matrix.

$\|\cdot\|$ the Euclidean vector norm.

$M^T$ (resp., $M^{-1}$) the transpose (resp., inverse) of matrix $M$.

$M>0$ (resp., $M\geq 0$) the matrix $M$ is positive definite (resp., positive semidefinite).

$M = \begin{bmatrix} A & B \\ * & C \end{bmatrix}$ the symbol * denotes the symmetric terms in a symmetric matrix

$I$ the identity matrix of appropriate dimension.

diag$\{\cdots\}$ the block diagonal matrix.

min $z(\cdot)$ the minimum value of $z(\cdot)$.

## Author details

Sheng-Hsiung Yang and Jenq-Lang Wu*

*Address all correspondence to: D97530001@mail.ntou.edu.tw and wujl@mail.ntou.edu.tw

Department of Electrical Engineering, National Taiwan Ocean University, Keelung, Taiwan, R.O.C

## References

[1] Zhang L, Gao H, Kaynak O. Network-induced constraints in networked control systems—a survey. IEEE Transactions on Industrial Informatics. 2013;9:403–416. DOI: 10.1109/TII.2012.2219540

[2] Orihuela L, Gomez-Estern F, Rodriguez Rubio F. Scheduled communication in sensor networks. IEEE Transactions on Control Systems Technology. 2014;22:801–808. DOI: 10.1109/TCST.2013.2262999

[3] Li Z, Alsaadi F, Hayat T, Gao H. New results on stability analysis and stabilisation of networked control system. IET Control Theory and Applications. 2014;8:1707–1715. DOI: 10.1049/iet-cta.2014.0189

[4] Walsh GC, Ye H, Bushnell LG. Stability analysis of networked control systems. IEEE Transactions on Control Systems Technology. 2002;10:438–446. DOI: 10.1109/87.998034

[5] Nesic D, Teel AR. Input-output stability properties of networked control systems. IEEE Transactions on Automatic Control. 2004;49:1650–1667. DOI: 10.1109/TAC.2004.835360

[6] Carnevale D, Teel A R, Nesic D. Further results on stability of networked control systems: a Lyapunov approach. In: Proceedings of the IEEE American Control Conference (ACC '07); 9–13 July 2007; New York. New York: IEEE; 2008. p. 1741–1746

[7] Tabuada P. Event-triggered real-time scheduling of stabilizing control tasks. IEEE Transactions on Control System Technology. 2007;52:1680–1685. DOI: 10.1109/TAC.2007.904277

[8] Wang X, Lemmon M D. Asymptotic stability in distributed event-triggered networked control systems with delays. In: Proceedings of the IEEE American Control Conference (ACC '10); 30 June–2 July 2010; Baltimore. New York: IEEE; 2011. p. 1362–1367

[9] Mazo M, Tabuada P. On event-triggered and self-triggered control over sensor/actuator networks. In: Proceedings of the IEEE Conference on Decision and Control (CDC '08); 9–11 December 2008; Cancun. New York: IEEE; 2009. p. 435–440

[10] Wang X, Lemmon MD. Event-triggering in distributed networked control systems. IEEE Transactions on Automatic Control. 2011;56:586–601. DOI: 10.1109/TAC.2010.2057951

[11] Eqtami A, Dimarogonas D V, Kyriakopoulos K J. Event-triggered control for discrete-time systems. In: Proceedings of the IEEE American Control Conference (ACC '10); 30 June–2 July 2010; Baltimore. New York: IEEE; 2011. p. 4719–4724

[12] Quevedo DE, Gupta V, Ma W, Yüksel S. Stochastic stability of event-triggered anytime control. IEEE Transactions on Automatic Control. 2014;59:3373–3379. DOI: 10.1109/TAC.2014.2351952

[13] Qu FL, Guan ZH, He DX, Chi M. Event-triggered control for networked control systems with quantization and packet losses. Journal of the Franklin Institute. 2015;352:974–986. DOI: 10.1016/j.jfranklin.2014.10.004

[14] Al-Areqi S, Gorges D, Liu S. Event-based networked control and scheduling codesign with guaranteed performance. Automatica. 2015;57:128–134. DOI: 10.1016/j.automatica.2015.04.003

[15] Yue D, Tian E, Han QL. A delay system method for designing event-triggered controllers of networked control systems. IEEE Transactions on Automatic Control. 2013;58:475–481. DOI: 10.1109/TAC.2012.2206694

[16] Wang X, Lemmon MD. Self-triggered feedback control systems with finite-gain $L_2$ stability. IEEE Transactions on Automatic Control. 2009;54:452–467. DOI: 10.1109/TAC.2009.2012973

[17] Peng C, Han QL. A novel event-triggered transmission scheme and $L_2$ control co-design for sampled-data control systems. IEEE Transactions on Automatic Control. 2013;58:2620–2626. DOI: 10.1109/TAC.2013.2256015

[18] Hu S, Yue D. $L_2$-gain analysis of event-triggered networked control systems: a discontinuous Lyapunov functional approach. International Journal of Robust and Nonlinear Control. 2013;23:1277–1300. DOI: 10.1002/rnc.2815

[19] Wu W, Reimann S, Görges D, Liu S. Event-triggered control for discrete-time linear systems subject to bounded disturbance. International Journal of Robust and Nonlinear Control. 2016;26:1902-1918. DOI: 10.1002/rnc.3388

[20] Yan H, Yan S, Zhang H, Shi H. $L_2$ control design of event-triggered networked control systems with quantizations. Journal of the Franklin Institute. 2015;352:332–345. DOI: 10.1016/j.jfranklin.2014.10.008

[21] Yang SH, Wu JL. Design of event-triggered simultaneous $H_\infty$ controllers for a collection of networked control systems. In: Proceedings of the IEEE Annual Conference on Society of Instrument and Control Engineers (SICE '14); 9–12 September 2014; Sapporo. New York: IEEE; 2015. p. 68–72

[22] Zhang XM, Han QL. Event-triggered dynamic output feedback control for networked control systems. IET Control Theory and Applications. 2014;8:226–234. DOI: 10.1049/iet-cta.2013.0253

[23] Yu H, Antsaklis P J. Event-triggered output feedback control for networked control systems using passivity: time-varying networked induced delays. In: Proceedings of the IEEE Conference on Decision and Control (CDC '11); 12–15 December 2011; Orlando. New York: IEEE; 2012. p. 205–210

[24] Yu H, Antsaklis PJ. Event-triggered output feedback control for networked control systems using passivity: achieving $L_2$ stability in the presence of communication delays and signal quantization. Automatica. 2013;49:30–38. DOI: 10.1016/j.automatica.2012.09.005

[25] Peng C, Han QL. Output-based event-triggered $H_\infty$ control for sampled-data control systems with nonuniform sampling. In: Proceedings of the IEEE American Control Conference (ACC '13); 17–19 June 2013; Washington. New York: IEEE; 2014. p. 1727–1732

[26] Peng C, Zhang J. Event-triggered output-feedback $H_\infty$ control for networked control systems with time-varying sampling. IET Control Theory and Applications. 2015;9:1384–1391. DOI: 10.1049/iet-cta.2014.0876

[27] Dai S L, Lin H, Ge S S, Li X. Simultaneous stability of a collection of networked control systems with uncertain delays. In: Proceedings of the International Conference on Control, Automation, Robotics and Vision (ICARCV '08); 17–20 December 2008; Hanoi. New York: IEEE; 2009. p. 35–40

[28] Schmitendorf, W E, Hollot, C V. Simultaneous stabilization via linear state feedback control. In: Proceedings of the IEEE Conference on Decision and Control (CDC 1988); 7–9 December 1988; Austin. New York: IEEE; 1989. p. 1781–1786

[29] Wu JL. A simultaneous mixed $LQR/H_\infty$ control approach to the design of reliable active suspension controllers. Asian Journal of Control. 2015;17(6):1–13. DOI: 10.1002/asjc.1058

[30] Yu M, Wang L, Chu T, Hao F. An LMI approach to networked control systems with data packet dropout and transmission delays. In: Proceedings of the IEEE Conference

on Decision and Control (CDC '04); 14–17 December 2004; Bahamas. New York: IEEE; 2005. p. 3545–3550

[31] Gassara H, Hajjaji AE, Chaabane M. Robust control of nonlinear time-delay systems via Takagi-Sugeno fuzzy models. In: Mueller A, editor. Recent Advances in Robust Control—Novel Approaches and Design Methods. Rijeka: InTech; 2011. p. 21–38. DOI: 10.5772/16645

[32] Hespanha JP, Naghshtabrizi P, Xu Y. A survey of recent results in networked control systems. Proceedings of the IEEE. 2007;95:138–162. DOI: 10.1109/JPROC.2006.887288

[33] Zhu XL, Yang GH. Jensen integral inequality approach to stability analysis of continuous-time systems with time-varying delay. IET Control Theory and Applications. 2008;2:524–534. DOI: 10.1049/iet-cta:20070298

Chapter 4

# Sliding Mode Speed and Position Control of Induction Motor Drive in Cascade Connection

Grzegorz Tarchała and Teresa Orłowska-Kowalska

Additional information is available at the end of the chapter

http://dx.doi.org/10.5772/63407

**Abstract**

This chapter deals with sliding mode application in control of an induction motor (IM) torque, speed, and position. Classical, direct approaches to control mentioned variables are described. Their drawbacks are presented and analyzed. Direct control structures are then compared with the proposed cascade sliding mode control structures. These structures allow to control all of the IM variables effectively, simultaneously ensuring supervision of all remaining variables. All of the analyzed structures are illustrated with block diagrams, as well as with simulation and experimental test results.

**Keywords:** induction motor, sliding mode control, torque control, speed control, position control

## 1. Introduction

Sliding mode control (SMC) is a commonly recognized robust control method. It is known to be independent on external disturbances [load torque in case of the induction motor (IM)] and internal changes (e.g., variation of motor parameters, due to heating). It can be successfully applied in control of all IM variables like flux, torque, speed and position [1]. However, it suffers from some characteristic negative features, such as steady-state and dynamical errors, chattering and variable switching frequency.

Over the several past decades, researchers tried to eliminate or reduce the disadvantages of the sliding mode applied to the IM control. The steady-state speed control error has been eliminated using the sliding surface with an additional integral part in reference [2]. Integral

part in the switching function has also been used to eliminate the dynamical and steady-state errors in the torque control [3].

Most of the papers focused on reducing the most negative feature of the SMC, i.e. chattering (large oscillations of controlled variables). Position control with adaptive continuous approximation of the sign function is proposed in reference [4]. Load torque estimator was introduced in reference [5] to reduce level of the discontinuous part of the control signal. One of the effective solutions to reduce the chattering is the application of higher-order sliding modes. They were introduced for all of the IM variables: torque in reference [6], speed (in a speed-sensorless approach) in reference [7] and position in reference [8]. The IM drive control, supplied from a current source inverter with the second-order SMC is introduced in reference [9]. Integral SMC of stator current components is shown in references [10–12] to reduce the chattering.

One of the chattering sources is a discretization caused by digital implementations of the drives' control structures; therefore, the discrete SMC methods have been proposed. The IM position discrete control is proposed in references [13] and [14]. The discrete SMC of the IM speed is introduced in reference [15].

Another drawback of the SMC in a direct approach (when the control algorithm defines the transistors' control signals directly) is a variable switching frequency. In order to eliminate this phenomenon, a voltage modulator can be applied. The classical direct torque control (DTC), SMC and space vector modulation (SVM) were combined in references [16] and [17]. Similarly, the indirect field-oriented control (IFOC) method and SMC were combined in reference [18].

In the past years, there have also been the attempts to extend the robustness of the IM control over the reaching phase, not only the sliding phase. The proposed approaches can be divided into two groups. In the first one, the switching line (or a surface) is designed to include the starting point: for speed control in reference [2] and for the position control in reference [19]. The second group consists of the methods with time-varying switching lines. They have been applied mainly in the position control [20], but also for the speed control [21].

In this chapter, a comparative analysis of the SMC of all IM state variables is presented. Direct approaches that define the transistor control signals directly are described and illustrated with simulation and experimental results. The cascade connection of sliding mode controllers is proposed for speed and position regulation, presented in a unified manner. The equivalent signal-based control is used to lower the level of the chattering in regulated variables.

This chapter consists of nine numerated sections. The following section presents the mathematical model of IM. Next three sections show the control of IM variables: torque, speed and position, respectively. Sections related to the speed and position control are divided into two subsections that include the direct and the cascade control. After short conclusions section, there is an appendix with experimental setup description and tables with tested IM parameters and base values, necessary to obtain the normalized unit system.

http://dx.doi.org/10.5772/63407

## 2. Mathematical model of induction motor drive

SMC algorithms are strictly based on the mathematical model of the controlled object, which is the IM in this research. This model will be shown in this section—it is created with commonly known simplifying assumptions [22]. It is written with normalized [per unit (p.u.)] units, in an arbitrary frame, rotating with the angular velocity $\omega_k$. Base values, required to the p.u. system transformation, are shown in the appendix.

Stator and rotor voltage equations:

$$\mathbf{u_s} = r_s \mathbf{i_s} + T_N \frac{\mathrm{d}}{\mathrm{d}t} \boldsymbol{\psi}_\mathbf{s} + j\omega_k \boldsymbol{\psi}_\mathbf{s}, \tag{1}$$

$$\mathbf{u_r} = r_r \mathbf{i_r} + T_N \frac{\mathrm{d}}{\mathrm{d}t} \boldsymbol{\psi}_\mathbf{r} + j\left(\omega_k - \omega_m\right) \boldsymbol{\psi}_\mathbf{r}, \tag{2}$$

where $\mathbf{u_s} = u_{s\alpha} + ju_{s\beta}$, $\mathbf{u_r} = u_{r\alpha} + ju_{r\beta}$ are stator and rotor voltage vectors, $\mathbf{i_s} = i_{s\alpha} + ji_{s\beta}$, $\mathbf{i_r} = i_{r\alpha} + ji_{r\beta}$ are stator and rotor current vectors, $\boldsymbol{\psi}_\mathbf{s} = \psi_{s\alpha} + j\psi_{s\beta}$, $\boldsymbol{\psi}_\mathbf{r} = \psi_{r\alpha} + j\psi_{r\beta}$ are stator and rotor flux vectors, $r_s$, $r_r$ are stator and rotor winding resistances, $T_\mathrm{N} = 1/(2\pi f_{sN})$ is nominal time constant, appearing after the per unit system is introduced, $f_{sN}$ is nominal frequency of the motor and $\omega_m$ is mechanical velocity.

Flux equations:

$$\boldsymbol{\psi}_\mathbf{s} = l_s \mathbf{i_s} + l_m \mathbf{i_r} \tag{3}$$

$$\boldsymbol{\psi}_\mathbf{r} = l_r \mathbf{i_r} + l_m \mathbf{i_s}, \tag{4}$$

where $l_s = l_m + l_{s\sigma}$, $l_r = l_m + l_{r\sigma}$ are stator and rotor winding inductances, $l_m$ is magnetizing inductance and $l_{s\sigma}$, $l_{r\sigma}$ are stator and rotor leakage inductances.

Electromagnetic torque and the motion equation are as follows:

$$m_e = \mathrm{Im}\left(\boldsymbol{\psi}_\mathbf{s}^* \mathbf{i_s}\right) = \psi_{s\alpha} i_{s\beta} - \psi_{s\beta} i_{s\alpha}, \tag{5}$$

$$\frac{\mathrm{d}\omega_m}{\mathrm{d}t} = \frac{1}{T_M}\left(m_e - m_o\right), \tag{6}$$

where $m_e$ is electromagnetic torque, $m_o$ is load torque and $T_M$ is mechanical time constant of the drive.

It is assumed that the IM is supplied by an ideal voltage source inverter (VSI), which can be described by the following matrix equation:

$$\mathbf{u_s} = \begin{bmatrix} u_{s\alpha} \\ u_{s\beta} \end{bmatrix} = \frac{u_{DC}}{3}\mathbf{Tk}, \quad \mathbf{T} = \begin{bmatrix} 1 & -1/2 & -1/2 \\ 0 & \sqrt{3}/2 & -\sqrt{3}/2 \end{bmatrix}, \tag{7}$$

where $\mathbf{k} = [k_A, k_B, k_C]^T$ is the control signals' vector of the VSI transistors and $u_{DC}$ is the DC-bus voltage.

## 3. Sliding mode direct torque control

In order to create a cascade connection of sliding mode controllers (for example torque and speed controllers), it is necessary to design first the sliding mode DTC. This method of control utilizes the IM mathematical model and its equations, shown in the previous chapter.

The first step in the designing is to define the so-called switching functions. The classical approach is first taken into account [1]:

$$\mathbf{s} = \begin{bmatrix} s_1 & s_2 & s_3 \end{bmatrix}^T, \tag{8}$$

where the components of **s** vector allow to control the motor torque, stator flux amplitude and to ensure the three-phase balance of the system, respectively:

$$s_1 = \alpha_1 \left( m_e^{ref} - m_e \right), \tag{9}$$

$$s_2 = \alpha_2 \left( (\psi_s^{ref})^2 - \psi_s^2 \right), \tag{10}$$

$$s_3 = \alpha_3 \int \left( k_A + k_B + k_C \right) \mathrm{d}t, \tag{11}$$

where $\alpha_1$, $\alpha_2$, $\alpha_3$ are control parameters, that need to be chosen.

The goal of the sliding mode controller will be to force the switching functions from Eqs. (9) to (11) to zero, which means that the real values will follow the reference ones. This goal can be achieved using the classical sliding-mode control formula, expressed as:

http://dx.doi.org/10.5772/63407

$$\begin{aligned} \mathbf{k} &= -\text{sign}(\mathbf{s}^*)^{\text{T}}, \\ \mathbf{s}^* &= \mathbf{s}^{\text{T}}\mathbf{D}, \end{aligned} \tag{12}$$

where the **D** matrix comes from the division of the switching function derivative into:

$$\dot{\mathbf{s}} = \mathbf{f} + \mathbf{D}\mathbf{k} \tag{13}$$

and can be calculated as follows:

$$\mathbf{D} = \begin{bmatrix} & \mathbf{D}_1 & \\ \alpha_3 & \alpha_3 & \alpha_3 \end{bmatrix}, \tag{14}$$

$$\mathbf{D}_1 = \frac{1}{T_N}\begin{bmatrix} \alpha_1\left(-i_{s\beta} + \frac{1}{x_s\sigma}\psi_{s\beta}\right) & \alpha_1\left(i_{s\alpha} - \frac{1}{x_s\sigma}\psi_{s\alpha}\right) \\ -2\alpha_2\psi_{s\alpha} & -2\alpha_2\psi_{s\beta} \end{bmatrix}\mathbf{T}. \tag{15}$$

In order to check the usefulness of the proposed control algorithm and to verify the stability of the proposed control system, the Lyapunov function method is applied. A positive defined Lyapunov function is proposed as follows:

$$L = \frac{1}{2}\mathbf{s}^{\text{T}}\mathbf{s} = \frac{1}{2}\left(s_1^2 + s_s^2 + \ldots + s_n^2\right) > 0. \tag{16}$$

Its derivative can be calculated as:

$$\begin{aligned} \dot{L} &= \mathbf{s}^{\text{T}}\dot{\mathbf{s}} = \\ &= \mathbf{s}^{\text{T}}\left(\mathbf{f} - \mathbf{D}\,\text{sign}(\mathbf{s}^*)^{\text{T}}\right) = \\ &= \mathbf{s}^{\text{T}}\mathbf{f} - \mathbf{I}\left|\mathbf{s}^{\text{T}}\mathbf{D}\right|^{\text{T}}, \end{aligned} \tag{17}$$

where $|\mathbf{s}^*| = [\,|s_1^*| \quad |s_2^*| \quad |s_3^*|\,]$, $\mathbf{I} = [1 \quad 1 \quad 1]$.

The stability inequality [negative value of Eq. (17)] is defined as:

$$|\mathbf{f}| < |\mathbf{D}|\mathbf{I}^{\text{T}}. \tag{18}$$

If the control parameters $\alpha_1$, $\alpha_2$, $\alpha_3$, included in the **D** matrix in Eq. (14) are high enough to fulfill the condition [Eq. (18)], the system is stable and the real values follow their reference values.

Full SM-DTC block diagram is shown in **Figure 1**. The control structure defines the control signals $k_A$, $k_B$, $k_C$ directly, to control the switches of the VSI without any voltage modulator. The input values are the reference values of stator flux amplitude and electromagnetic torque. If the speed exceeds the nominal value, the amplitude of the flux must be weakened in order to ensure the constant power operation of the induction machine.

It is also necessary to provide the measurement of the DC-bus voltage [this value is present in the **T** matrix in Eq. (14)] and stator phase currents (transformed to the stationary $\alpha$-$\beta$ frame from two-phase currents, when the three-phase symmetry is assumed). The control structure also needs estimated values, such as stator flux vector components (or its magnitude and angle) and electromagnetic torque (the hat "∧" indicates the estimated value). They must be determined by a proper estimator—this problem will not be addressed in this chapter. If the estimator requires the stator voltage vector knowledge, its components can be transformed from measured signals or calculated using the Eq. (7), taking into account the inverter dead-time [23].

The block diagram, shown in **Figure 1**, also emphasizes the digital implementation of the SM-DTC, together with the measurement delays ($\tau_d$ for current and voltage measurement and $\tau_{d\omega}$ for speed measurement). Nowadays, the continuous algorithms are realized in a discrete form using the digital signal processors (DSPs). The influence of the digital implementation will be shown in the following part of the chapter.

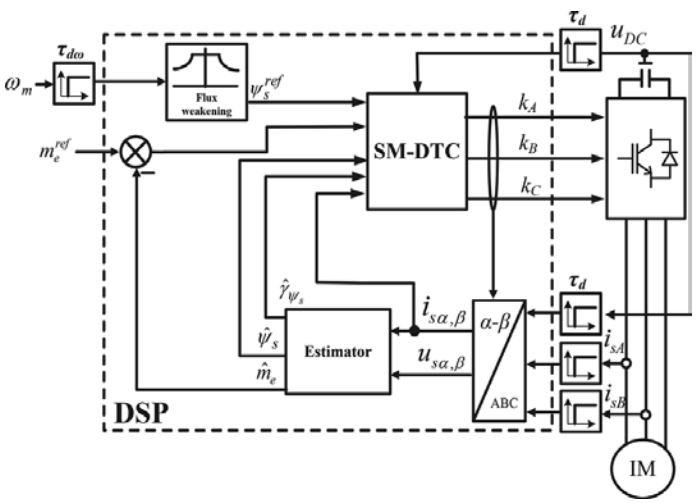


**Figure 1.** Block diagram of the SM-DTC (digital realization).

**Figure 2** shows a comparative study of performance of the SM-DTC structure for three different cases: ideal simulation study (**Figure 2a**), simulation study with the DSP discretization taken into account (**Figure 2b**) and experimental results (**Figure 2c**).

http://dx.doi.org/10.5772/63407

**Figure 2a** shows the ideal operation of the SM-DTC and proves its perfect dynamical features. The torque and stator flux amplitudes follow their reference values almost immediately and without any oscillations. The speed is a result of the motor and load torque difference [according to Eq. (6)] and therefore is changing in a triangular way. Three-phase currents are smooth and sinusoidal—their frequency is changed automatically by the control structure.

Unfortunately, one of the negative properties of the SMC structures is the phenomenon called chattering [24]. There are many sources of the chattering—one of them is the discretization, connected with limited sampling rate of modern processors [25]. In order to check the influence of this phenomenon, special simulation model has been built. Suitable results are shown in **Figure 2b**. Large chattering (sometimes called the discretization chattering) can be seen in the controlled variables. It is also visible in phase currents. Due to the moment of inertia of the drive system, speed signal is still smooth.

Simulation test results have been validated using an experimental setup (see Appendix). Obtained results illustrate the same situation in a very similar way—the chattering can be seen in torque, flux and currents. The level of the obtained oscillations is even higher than during the simulation tests—it causes mechanical stress, dangerous for the drive, and acoustic noise.

One of the efficient solutions to avoid the chattering, visible in **Figure 2**, is to use the continuous approximation of the sign function. One of them is a saturation function:

$$\mathbf{d} = -0.5\left(\mathrm{sat}(\mathbf{s}^*, \varepsilon_{me})^{\mathrm{T}} + 1\right), \tag{19}$$

where $\varepsilon_{me}$ is positive control parameter to be chosen and column vector $\mathbf{d} = [d_A, d_B, d_C]^{\mathrm{T}}$ is duty cycles' vector and the saturation function:

$$\mathrm{sat}(s) = \begin{cases} s/\varepsilon & \text{if } |s| \le \varepsilon \\ \mathrm{sign}(s) & \text{if } |s| > \varepsilon \end{cases}. \tag{20}$$

In this case, the control structure defines not the transistor control signals directly, but the duty cycle functions for each phase (relation of the switching-on time to the whole sampling period). Specific form of the Eq. (19) is imposed by the duty cycle feature—its values can vary between 0 and 1 (0% and 100%).

Effects of the saturation function usage are shown in **Figure 3a**. It can be seen that the oscillations level is greatly reduced. However, a significant and changing in time, regulation error can be seen in the electromagnetic torque transient. It can be eliminated using simple modification of the switching function [Eq. (9)], to obtain the following formula [3]:

$$s_1 = \alpha_1\left(m_e^{ref} - m_e\right) + K_I \int \left(m_e^{ref} - m_e\right) \mathrm{d}t \tag{21}$$

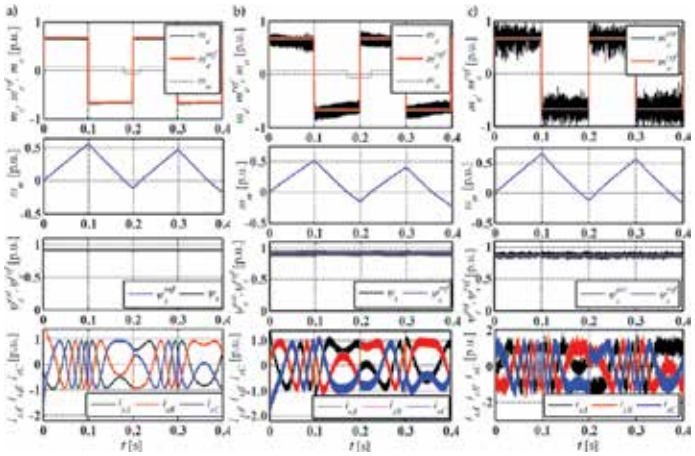

**Figure 2.** Performance of the SM-DTC for induction motor: (a) simulation study: ideal case, digital implementation is not taken into account, (b) simulation study: digital implementation taken into account, (c) experimental study; first row: reference and real (estimated) torque, second row: speed, third row: reference and real (estimated) stator flux, fourth row: phase currents.

where $K_I$ is positive control parameter.

Results of the integral part introduction in the switching function are shown in **Figure 3b** and **3c** for simulation and experimental tests, respectively. The torque and stator flux are controlled perfectly, without any steady-state or dynamical errors. Additionally, the chattering phenomenon is reduced considerably—level of the oscillations in regulated signals is acceptable now.

Sliding mode DTC structure with the modified switching function, shown in this section, will be used to create the cascade speed and position control structures, shown in the following sections.

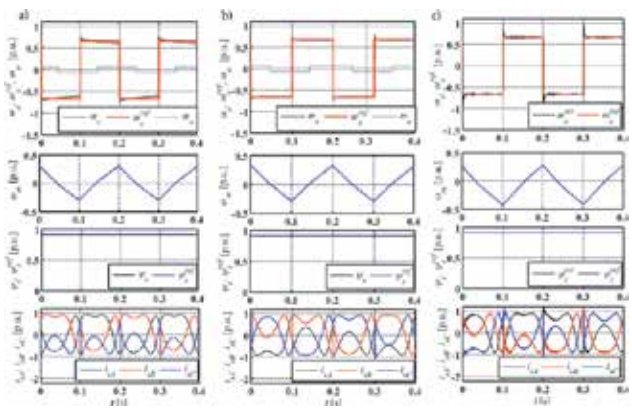

**Figure 3.** Performance of the SM-DTC for induction motor: (a) simulation study: saturation function used instead of the sign function, (b) simulation study: integral part added in the torque switching function, (c) experimental study; first row: reference and real (estimated) torque, second row: speed, third row: reference and real (estimated) stator flux, fourth row: phase currents.

http://dx.doi.org/10.5772/63407

## 4. Sliding mode speed control

### 4.1. Direct sliding mode speed control

The direct IM speed control can be realized very similarly to the DTC. The most significant difference is another switching function that can be expressed as in [1]:

$$s_1 = s_\omega = \alpha_1 \left( \omega_m^{ref} - \omega_m - T_{c\omega} \dot{\omega}_m \right), \tag{22}$$

where $T_{c\omega}$ is time constant that defines the required dynamics of the speed.

When the switching function is zero, the controlled object acts as first-order inertia with time constant $T_{c\omega}$. Settling time of the system (95%) is equal to:

$$T_s = 3T_{c\omega}. \tag{23}$$

In this case, the same control algorithm [Eq. (12)] can be applied to regulate motor speed; however, the $\mathbf{D_1}$ matrix in Eq. (14) must be slightly modified (the additional term $T_{c\omega}/T_M$ appears):

$$\mathbf{D_1} = \frac{1}{T_N} \begin{bmatrix} \alpha_1 \frac{T_{c\omega}}{T_M} \left( -i_{s\beta} + \frac{1}{x_s \sigma} \psi_{s\beta} \right) & \alpha_1 \frac{T_{c\omega}}{T_M} \left( i_{s\alpha} - \frac{1}{x_s \sigma} \psi_{s\alpha} \right) \\ -2\alpha_2 \psi_{s\alpha} & -2\alpha_2 \psi_{s\beta} \end{bmatrix} \mathbf{T}. \tag{24}$$

The condition of the system stability remains the same as in Eq. (18).

The block diagram of the direct sliding mode speed control is shown in **Figure 4**. It is almost identical as the one shown in **Figure 1**; however, the speed switching function $s_\omega$ is provided instead of the torque regulation error. For the clarity of the block diagram, the digital realization and measurement delays will not be presented in the following figures.

**Figure 5a** shows the performance of the direct SM speed control structure in the ideal simulation case. The reverses of the speed are presented—the speed follows the reference value with the requested dynamics, which is indicated by the $\omega_m^{ref,dyn}$ signal. Even in this ideal case, the steady-state error exists—it is shown in the second row of **Figure 5a**. Additionally, electromagnetic torque of the motor is not controlled and supervised. Therefore, it exceeds the maximum value, set at the level 1.0 (it is about 150% of the nominal torque in p.u., see Appendix). If the digital realization of the control structure and measurement delays are taken into account, the steady-state speed error increases significantly—it can be seen in **Figure 5b**. Moreover, the torque and stator flux oscillation levels are much higher, similarly to the DTC

algorithm, shown in the previous section. If the saturation function is applied (**Figure 5c**), the regulation error becomes even larger; however, the chattering level is reduced. This simulation study is verified using the experimental tests (**Figure 5d**)—and both of them give almost the same results.

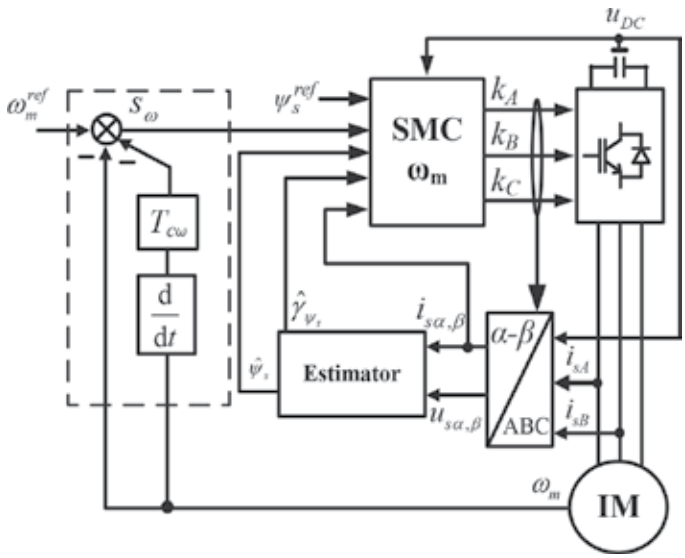


**Figure 4.** Block diagram of the direct SM speed control.

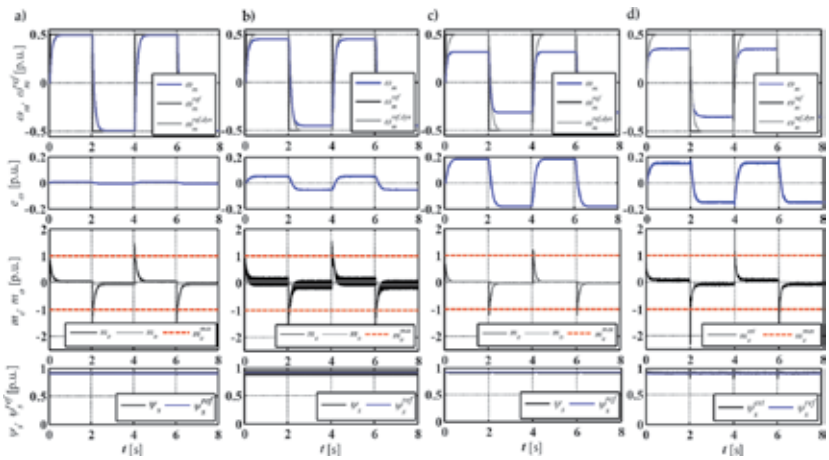


**Figure 5.** Performance of the SM direct speed control: (a) simulation study: control in the ideal case, (b) simulation study: speed control in case of the digital implementation and measurement delays taken into account, (c) simulation study: saturation function used instead of the sign function, (d) experimental tests results for saturation function usage; first row: reference and real speed, second row: speed control error, third row: load, electromagnetic and maximum torque, fourth row: reference and real amplitude of stator flux.

http://dx.doi.org/10.5772/63407

In both the previously mentioned cases, direct SM torque and speed control, the torque becomes higher than the acceptable level and can be dangerous for the drive and its mechanical elements. This drawback can be eliminated reducing the desired dynamics, defined by $T_{c\omega}$ or applying the cascade structure of the SM controllers. The second solution will be now described.

### 4.2. Cascade sliding mode speed control

In order to create the cascade connection of SM speed and torque regulators, the torque control loop has to be simplified to the first-order inertial element, described by the following transfer function:

$$\frac{m_e(p)}{m_e^{ref}(p)} = \frac{1}{T_{me}p+1}, \tag{25}$$

where $p$ is Laplace operator, $T_{me}$ is replacement time constant of the torque control circuit.

The control signals' vector becomes a scalar quantity $\mathbf{k}=[m_e^{ref}]$ and the switching functions' vector $\mathbf{s}=[s_\omega]$ likewise. In this case, the derivative of the switching function can be divided into:

$$\dot{s}_\omega = f_{1\omega} + f_{2\omega} + d_\omega m_e^{ref}, \tag{26}$$

where:

$$f_{1\omega} = \dot{\omega}_m^{ref} + \frac{T_{c\omega} - T_{me}}{T_M T_{me}} m_e, \tag{27}$$

$$f_{2\omega} = \frac{T_{c\omega}}{T_M}\dot{m}_o + \frac{1}{T_M} m_o, \tag{28}$$

$$d_\omega = -\frac{T_{c\omega}}{T_M T_{me}}. \tag{29}$$

In the above equations, $f_{1\omega}$ is the part that can be calculated from available variables, $f_{2\omega}$ depends on the unknown variables and $d_\omega$ stands next to the reference torque.

If the equivalent signal-based control method is applied, then the reference torque signal consists of two parts [26]:

$$m_e^{ref} = m_e^{ref,eq} + m_e^{ref,d}, \tag{30}$$

$$m_e^{ref,eq} = -\frac{1}{d_\omega} f_{1\omega}, \tag{31}$$

$$m_e^{ref,d} = -\frac{\Gamma_\omega^d}{d_\omega} \text{sign}(s_\omega), \tag{32}$$

where $\Gamma_\omega^d$ is a control parameter.

Continuous control signal part $m_e^{ref,eq}$ is calculated from available signals, and is designed to force the switching function to zero in presence of no load torque and motor parameters changes. The discontinuous part must be included in the SM control system, in order to compensate external disturbances, such as the load torque present in $f_{2\omega}$ and the inaccuracy of the simplification from Eq. (25). The switching function derivative becomes:

$$\dot{L} = s_\omega \dot{s}_\omega = s_\omega f_{2\omega} - \Gamma_\omega^d |s_\omega|, \tag{33}$$

while its negative value is ensured if:

$$\Gamma_\omega^d > |f_{2\omega}|. \tag{34}$$

Thus, if the control parameter is chosen properly, the stability of the proposed control system can be guaranteed. The block diagram of the cascade control structure described here is shown in **Figure 6**. Unlike the direct control from **Figure 4**, the speed controller output signal is the reference torque, and it consists of two parts. Furthermore, this signal can be limited at desired value. The reference torque is the input of the SM-DTC structure, described in the previous chapter.

Performance of the cascade SM speed control in presence of the passive load torque is shown in **Figure 7**. The obtained results are shown for the speed reverses. It can be seen that the speed follows the reference signal with required dynamics in all cases. First subfigure shows the relay control—the equivalent signal from Eq. (31) is not taken into account in this case and the control parameter is equal to $\Gamma_{me}^d = m_e^{max}$. Performance of the control structure is presented during simulation tests—despite the ideal conditions, some small dynamic and steady-state error appears. Due to the enormous mechanical vibrations, it is impossible to conduct the experimental tests. Therefore, the equivalent signal was taken into account and its performance is shown in **Figure 7b** and **7c** for simulation and experimental tests, respectively. The results are

http://dx.doi.org/10.5772/63407

almost the same. Electromagnetic torque has acceptable oscillations and is limited on a maximum value. Stator flux amplitude is kept constant at nominal value.

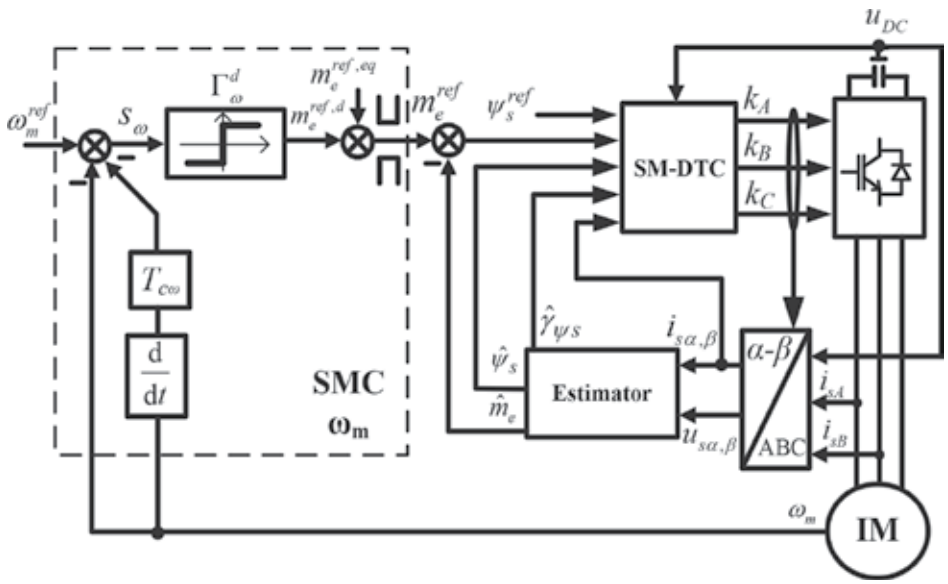


**Figure 6.** Block diagram of the SM speed control in cascade connection.

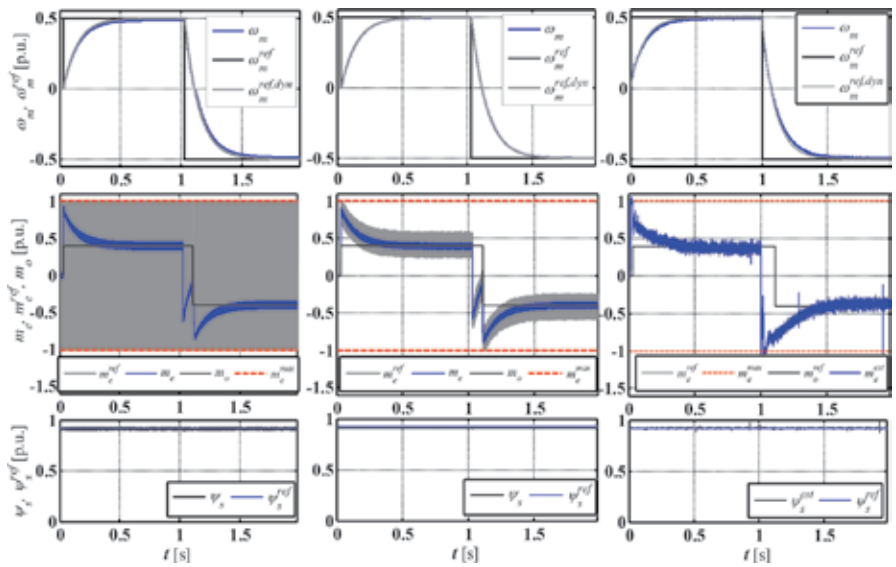


**Figure 7.** Performance of the SM cascade speed control: (a) simulation study: relay control, (b) simulation study: equivalent control, (c) experimental study: equivalent signal-based control; first row: reference and real speed, second row: load, electromagnetic and maximum torques, third row: reference and real amplitude of stator flux.

## 5. Sliding mode position control

### 5.1. Direct sliding mode position control

By the analogy to the torque and speed control, presented in previous sections, IM shaft position control can be designed using the direct approach [1]. The control algorithm [Eq. (12)] and the $\mathbf{D_1}$ matrix [Eq. (24)] remain the same as for the direct speed control, $T_{c\omega}$ is only replaced by $T_{c\theta}$. Switching function for the position control becomes:

$$s_1 = s_\theta = \alpha_1 \left( \theta_m^{ref} - \theta_m - T_\theta \dot{\theta}_m - T_{c\theta} \ddot{\theta}_m \right) \tag{35}$$

where $T_\theta$, $T_{c\theta}$ are time constants that can be selected according to the required settling time (5%) of the position control $T_{s\theta}$, using the following rule [27]:

$$T_\theta = 2T_{cr},\ T_{c\theta} = T_{cr}^2,\ T_{cr} = \frac{2T_{s\theta}}{9}. \tag{36}$$

The block diagram of the SM direct position control is presented in **Figure 8**. Performance of the SM direct position control during experimental tests is shown in **Figure 9**. It can be seen that the shaft position has the desired dynamics and tracks the reference value without almost any error. Unfortunately, the chattering visible in the torque is entirely unacceptable. Therefore, the saturation function is applied (**Figure 9b**)—the level of the undesired oscillations is greatly reduced. In both cases, similarly to the direct speed control, the electromagnetic torque is not supervised in this type of the control. Simultaneously, the speed does not exceed the accepted value, which is 120% of the nominal value in this research. The flux is kept constant (not shown in the figure).

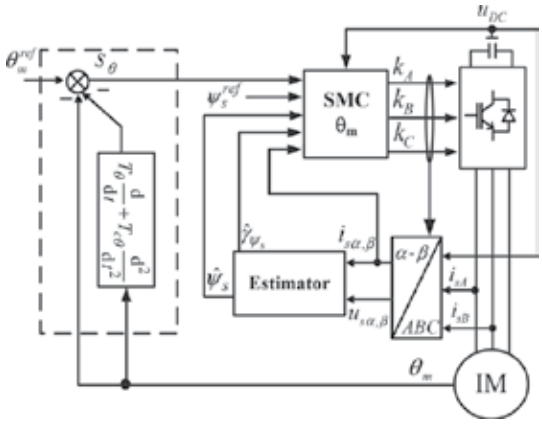


**Figure 8.** Block diagram of the direct SM position control.

http://dx.doi.org/10.5772/63407

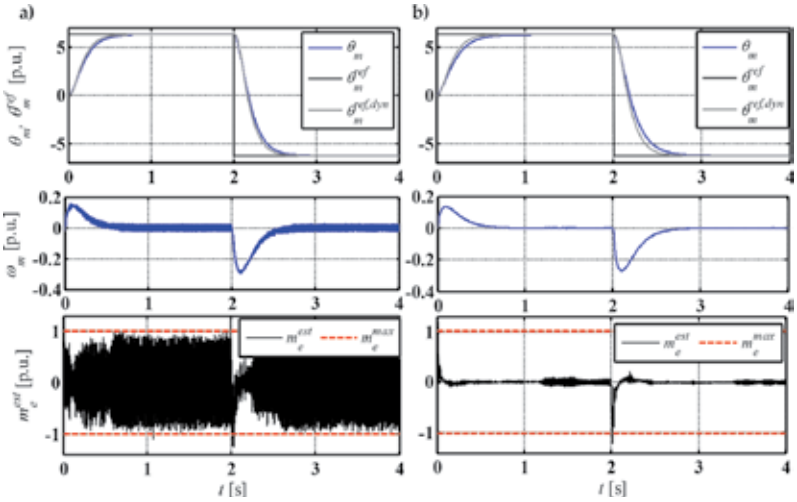


**Figure 9.** Experimental performance of the SM direct position control: (a) with sign function, (b) with saturation function.

### 5.2. Cascade sliding mode position control

According to the previous section, the cascade position control structure will now be analyzed. It is based on the assumption that the SM speed control works perfectly and ensures zero value of the speed switching function from Eq. (22). In such situation, the speed control loop can be described by the following transfer function:

$$\frac{\omega_m(p)}{\omega_m^{ref}(p)} = \frac{1}{T_{c\omega}p+1} \tag{37}$$

Similarly, as for the speed control, the control signals vector and switching functions' vector become scalars, $\mathbf{k}=[\omega_m^{ref}]$, $\mathbf{s}=[s_\theta]$, respectively. In this case, the switching function derivative becomes:

$$\dot{s}_\theta = f_{1\theta} + f_{2\theta} + d_\theta \omega_m^{ref}, \tag{38}$$

$$f_{1\theta} = \dot{\theta}_m^{ref} - \frac{1}{T_N}\left(\omega_m - \frac{T_\theta}{T_\omega}\right) - \frac{T_{c\omega}}{T_M T_N}\dot{m}_e, \tag{39}$$

$$f_{2\theta} = \frac{T_{c\theta}}{T_M T_N}\dot{m}_o, \tag{40}$$

$$d_\theta = -\frac{T_\theta}{T_N T_{c\omega}}. \tag{41}$$

By analogy to equation (30), the reference speed control signal is as follows:

$$\omega_m^{ref} = \omega_m^{ref,eq} + \omega_m^{ref,d}, \tag{42}$$

$$\omega_m^{ref,\,eq} = -\frac{1}{d_\theta} f_{1\theta}, \tag{43}$$

$$\omega_m^{ref,\,d} = -\frac{\Gamma_\theta^d}{d_\theta} \mathrm{sign}(s_\theta), \tag{44}$$

where $\Gamma_\theta^d$ is a control parameter.

According to the methodology shown in previous sections, the position control system is stable if:

$$\Gamma_\theta^d > |f_{2\theta}|. \tag{45}$$

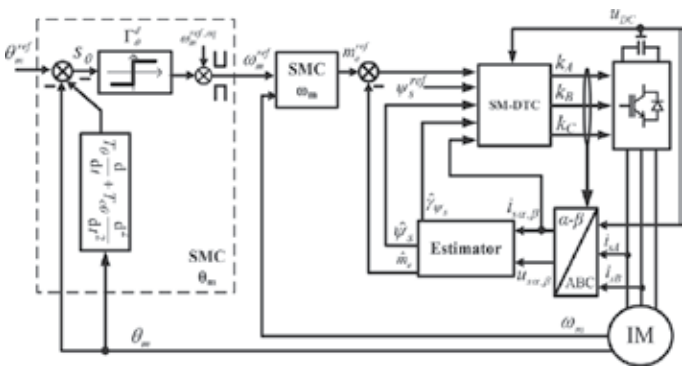


**Figure 10.** Block diagram of the cascade SM position control.

The block diagram of the proposed cascade position control structure is shown in the **Figure 10**. Performance of the control structure for nominal load operation is shown in **Figure 11**. First, the simulation study for the ideal case is shown (**Figure 11a**), the sign function is used in the control algorithm directly. It can be seen that the position follows the reference signal with required dynamics. Due to the torque constraint introduced, some small dynamical

http://dx.doi.org/10.5772/63407

error of the position control is visible. In order to decrease the level of the chattering of torque and speed, visible especially when the digital operation is taken into account (**Figure 11b**), the saturation function is applied in **Figure 11c**. The oscillations level is reduced successfully, while the position dynamic error is maintained. **Figure 11d** shows the experimental results—because of the digital realization of the control structure and additional, parasitic dynamics (measurement delays), the controlled variables are characterized by larger chattering; however, its level is acceptable. The position dynamic error is slightly higher than in case of the simulation tests.

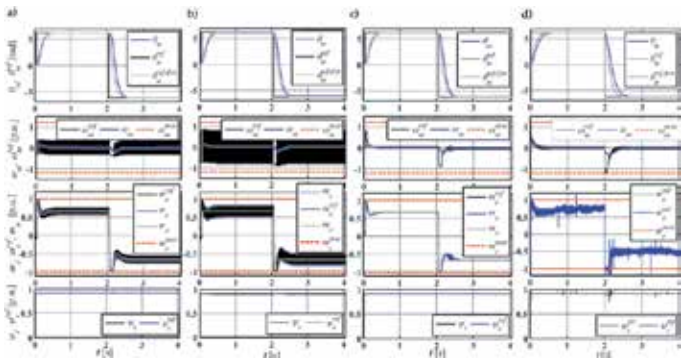

**Figure 11.** Performance of the SM equivalent control signal-based position control in a cascade structure: (a) simulation study: ideal case, (b) simulation study: digital operation and delays taken into account, (c) simulation study: saturation function used instead of the sign function in cascade control, (d) experimental results with saturation function used in cascade control; first row: reference and real position, second row: reference, real and maximum speed; third row: reference, real (estimated), load and maximum torque; fourth row: reference and real (estimated) stator flux amplitude.

## 6. Conclusions

This chapter deals with the SMC of the most important IM variables: torque, speed and position of the shaft, simultaneously ensuring constant value of the stator flux amplitude.

First part of the chapter is connected with the sliding mode DTC for IM. It is proved that the classical DT-SMC approach gives undesirable torque chattering. In order to reduce the chattering, the saturation function is used instead of the sign function. However, the saturation function introduces large steady-state control error. An integral part in the torque switching function is successfully used to eliminate this error. Such designed torque control is then used in the cascade speed and position IM control.

Next part of the chapter is the IM speed control. It is shown that the sliding mode speed control in its classical, direct approach is characterized by a large steady-state error and chattering. It is proved using a specially prepared simulation model and experimental setup. Additionally, the torque value is not constrained in this direct speed control structure. Therefore, the cascade connection of speed and torque regulators is introduced. The equivalent signal-based control method is applied to reduce the chattering. This solution allows to supervise the value of the electromagnetic torque, while reducing the control error effectively.

The last part of the chapter shows the position control of the drive. Conclusions that come from the SM position control analysis are analogical to the ones from the speed control. Direct position control does not ensure the torque and speed supervision, that is solved by the cascade control structure. Simultaneously, the chattering can be reduced using the continuous approximation of the sign function and the equivalent signal-based approach.

All of these control concepts are illustrated using simulation and experimental study. Special attention has been paid to create a simulation model that allows to take the digital realization of modern DSP control applications and measurement delays into account.

## Acknowledgements

This work has been financed by the National Science Centre (Poland) under project number 2015/17/B/ST7/03846.

## Appendices

Experimental tests were realized using the DSP dSpace 1103 with sampling time equal to 100 μs (10 kHz). The DSP controlled the transistors of the classical two-level VSI, which supplied the 3 kW tested motor. 6 kW DC motor was used to generate the load torque.

**Tables 1–3** include rated values of the tested IM, its parameters and base values, necessary to make the transition from physical units to the p.u. system, respectively.

| Name | Symbol | SI units | | Normalized units [p.u.] |
|---|---|---|---|---|
| Voltage | $U_N$ | 400Δ/680Y | [V] | 0.707 |
| Current | $N_N$ | 7.0Δ/4.0Y | [A] | 0.707 |
| Power | $P_N$ | 3000 | [W] | 0.62 |
| Torque | $M_N$ | 20.46 | [Nm] | 0.67 |
| Rotational frequency | $n_N$ | 1400 | [rpm] | 0.933 |
| Frequency | $f_{SN}$ | 50 | [Hz] | 1 |
| Stator flux | $\Psi_{sN}$ | 1.65 | [Wb] | 0.91 |
| Rotor flux | $\Psi_{rN}$ | 1.55 | [Wb] | 0.86 |
| Pole pairs | $p_b$ | 2 | [-] | 2 |
| Power factor | $\cos\varphi$ | 0.80 | [-] | 0.80 |
| Efficiency | $\eta$ | 0.778 | [-] | 0.778 |

**Table 1.** Rated parameters of the tested induction motor.

| Name | Symbol | SI units ([]) | | Normalized units [p.u.] |
|---|---|---|---|---|
| Stator resistance | $R_s$, $r_s$ | 7.073 | [Ω] | 0.707 |
| Rotor resistance | $R_r$, $r_r$ | 7.372 | [Ω] | 0.737 |
| Main inductance | $L_m$, $l_m$ | 597.8 | [mH] | 1.87 |
| Stator leakage inductance | $L_{s\sigma}$, $l_{s\sigma}$ | 31.2 | [mH] | 0.098 |
| Rotor leakage inductance | $L_{r\sigma}$, $l_{r\sigma}$ | 21.2 | [mH] | 0.066 |

**Table 2.** Equivalent circuit parameters of the tested induction motor.

| Name | Expression | Value | Units |
|---|---|---|---|
| Power | $S_b = 3/2U_bI_b$ | 4800 | [VA] |
| Torque | $M_b = p_bS_b/\Omega_b$ | 30.55 | [Nm] |
| Speed | $N_b = 60f_{sN}/p_b$ | 1500 | [rpm] |
| Stator voltage | $U_{sb} = \sqrt{2}U_{sN}$ | 565.7 | [V] |
| Stator current | $I_{sb} = \sqrt{2}I_{sN}$ | 5.657 | [A] |
| Frequency | $f_{sb} = f_{sN}$ | 50 | [Hz] |
| Angular velocity | $\Omega_b = 2\pi f_{sN}$ | 100π | [rad/s] |
| Flux | $\Psi_b = U_b/\Omega_b$ | 1.80 | [Wb] |
| Inductance | $L_b = \Psi_b/I_b$ | 0.318 | [H] |
| Impedance | $Z_b = U_b/I_b$ | 100 | [Ω] |

**Table 3.** Calculation of per unit system base values.

## Author details

Grzegorz Tarchała and Teresa Orłowska-Kowalska

*Address all correspondence to: grzegorz.tarchala@pwr.edu.pl

Department of Electrical Machines, Drives and Measurements, Wrocław University of Technology, Wrocław, Poland

## References

[1] Utkin VI. Sliding mode control design principles and applications to electric drives. IEEE Trans Ind Electron. 1993;40(1):23-36.

[2] Shyu KK, Shieh HJ. A new switching surface sliding-mode speed control for induction motor drive systems. IEEE Trans Power Electron. 1996;11(4):660-7.

[3] Orłowska-Kowalska T, Tarchała G. Integral sliding mode direct torque control of the induction motor drives. 39th Annual Conference of the IEEE Industrial Electronics Society (IECON), November 10-13, 2013, Vienna, 2013, p. 8482-7.

[4] Dunnigan MW, Wade S, Williams BW, Yu X. Position control of a vector controlled induction machine using Slotine's sliding mode control approach. IEE Proc-Electr Power Appl. 1998;145(3):231-8.

[5] Wang WJ, Chen JY. A new sliding mode position controller with adaptive load torque estimator for an induction motor. IEEE Trans Energy Convers. 1999;14(3):413-8.

[6] Zhang Z, Zhu J, Tang R, Bai B, Zhang H. Second order sliding mode control of flux and torque for induction motor. Asia-Pacific Power and Energy Engineering Conference (APPEEC), March 28-31, 2010, Chengdu, 2010, p. 1-4.

[7] Rashed M, Goh KB, Dunnigan MW, MacConnell P, Stronach A, Williams BW. Sensorless second-order sliding-mode speed control of a voltage-fed induction-motor drive using nonlinear state feedback. IEE Proc-Electr Power Appl. 2005;152(5):1127-36.

[8] Bartolini G, Marchesoni M, Pisu P, Usai E. Chattering reduction and robust position control in induction motor with second-order VSS. Int J Syst Sci. 1998;29(1):1-12.

[9] Ferrara A, Rubagotti M. A sub-optimal second order sliding mode controller for current-fed induction motors. American Control Conference, June 10-12; St Louis, MO: IEEE; 2009, p. 59-64.

[10] Comanescu M, Batzel T. A novel speed estimator for induction motor based on integral sliding mode current control. IEEE Power & Energy Society General Meeting, 2008, p. 371-6.

[11] Comanescu M, Xu L, Batzel TD. Decoupled current control of sensorless induction-motor drives by integral sliding mode. IEEE Trans Ind Electron. 2008;55(11):3836-45.

[12] Comanescu M. An induction-motor speed estimator based on integral sliding-mode current control. IEEE Trans Ind Electron. 2009;56(9):3414-23.

[13] Veselic B, Perunicic-Drazenovic B, Milosavljevic C. High-performance position control of induction motor using discrete-time sliding-mode control. IEEE Trans Ind Electron. 2008;55(11):3809-17.

[14] Veselic B, Perunicic-Drazenovic B, Milosavljevic C. Improved discrete-time sliding-mode position control using euler velocity estimation. IEEE Trans Ind Electron. 2010;57(11):3840-7.

[15] Castillo-Toledo B, Di Gennaro S, Loukianov AG, Rivera J. Discrete time sliding mode control with application to induction motors. Automatica. 2008;44(12):3036-45.

http://dx.doi.org/10.5772/63407

[16] Lascu C, Boldea I, Blaabjerg F. Variable-structure direct torque control: A class of fast and robust controllers for induction machine drives. IEEE Trans Ind Electron. 2004;51(4):785-92.

[17] Lascu C, Trzynadlowski AM. Combining the principles of sliding mode, direct torque control, and space-vector modulation in a high-performance sensorless AC drive. IEEE Trans Ind Appl. 2004;40(1):170-7.

[18] Derdiyok A, Guven MK, Inanc N, Rehman H, Xu LY. A DSP-based indirect field oriented induction machine control by using chattering-free sliding mode. IEEE National Aerospace and Electronics Conference: Engineering Tomorrow. Dayton, Ohio, USA 2000:568-73.

[19] Wai RJ. Adaptive sliding-mode control for induction servomotor drive. IEE Proc-Electr Power Appl. 2000;147(6):553-62.

[20] Betin F, Capolino G-A. Sliding mode control for an induction machine submitted to large variations of mechanical configuration. Int J Adapt Control Signal Process. 2007;21(8-9):745-63.

[21] Tarchała G, Orłowska-Kowalska T. Application of a time-varying switching line in the cascade sliding-mode speed control of the induction motor drive. IEEE 23rd International Symposium on Industrial Electronics (ISIE), June 1-4, 2014, Istanbul, 2014, p. 1310-5.

[22] Kaźmierkowski MP, Tunia H. Automatic Control of Converter-Fed Drives. Elsevier Science; 1994.

[23] Holtz J, Quan JT. Drift- and parameter-compensated flux estimator for persistent zero-stator-frequency operation of sensorless-controlled induction motors. IEEE Trans Ind Appl. 2003;39(4):1052-60.

[24] Levant A. Chattering analysis. IEEE Trans Automat Control. 2010;55(6):1380-9.

[25] Utkin V, Lee H. Chattering problem in sliding mode control systems. International Workshop on Variable Structure Systems. Alghero, Sardinia, Italy 2006:346-50.

[26] Orłowska-Kowalska T, Tarchała G. Unified approach to the sliding-mode control and state estimation - application to the induction motor drive. Bull Pol Acad Sci-Tech Sci. 2013;61(4):837-46.

[27] Dodds SJ. Settling time formulae for the design of control systems with linear closed loop dynamics. 3rd Annual Conference Advances in Computing and Technology: The School of Computing and Technology, University of East London, UK; 2008, p. 31-9.

Chapter 5

# Robust Adaptive Repetitive and Iterative Learning Control for Rotary Systems Subject to Spatially Periodic Uncertainties

Cheng-Lun Chen

Additional information is available at the end of the chapter

http://dx.doi.org/10.5772/63082

**Abstract**

This book chapter reviews and summarizes the recent progress in the design of spatial-based robust adaptive repetitive and iterative learning control. In particular, the collection of methods aims at rotary systems that are subject to spatially periodic uncertainties and based on nonlinear control paradigm, e.g., adaptive feedback linearization and adaptive backstepping. We will elaborate on the design procedure (applicable to generic *n*th-order systems) of each method and the corresponding stability and convergence theorems.

**Keywords:** rotary system, disturbance rejection, robust adaptive control, repetitive control, iterative learning control

## 1. Introduction

Rotary systems play important roles in various industry applications, e.g., packaging, printing, assembly, fabrication, semiconductor, and robotics. A conspicuous characteristic of such systems is the utilization of actuators, e.g., electric motor, to control the angular position, velocity, or acceleration of the system load. Depending on the occasion of application, simple or complicated motion control algorithm may be used. The increasing complexity in architecture and the high-performance requirement of recent rotary systems have posed a major challenge on conceiving and synthesizing a desirable control algorithm.

Nonlinearities and uncertainties are common issues when designing a control algorithm for a rotary system. Nonlinearities are either intrinsic properties of the system or actuator and sensor

dynamics being nonlinear. Uncertainties mainly come from structured/unstructured uncertainties (also known as parametric uncertainty/unmodeled dynamics) and disturbances. For tackling nonlinearities, conventional techniques, e.g., feedback linearization and backstepping, are to employ feedback to cancel all or part of the nonlinear terms. On the contrary, design techniques for conducting disturbance rejection or attenuation in control systems may be roughly categorized with respect to whether or not the techniques generate the disturbance by an exosystem. Representative techniques that resort to the exosystem of the disturbance are internal model design [1,2], which originates from the internal model principle [3], and observer-based design [4,5]. Establishing a suitable mathematical description of the disturbance is an essential step for internal model design techniques. An internal model design for systems in an extended output feedback form and subject to unknown sinusoidal disturbances was addressed in [1]. For observer-based design techniques, an observer is usually employed to estimate the states of the unknown exosystem. Chen [5] showed that the design of the observer can be separated from the controller design. For techniques that do not resort to the exosystem of the disturbance, disturbance observer [6,7] or optimization-based control approaches [8,9] have been shown to work well. In [6], integral phase shift and half-period integration operator were used together to estimate the periodic disturbances. Another type of disturbance observers was introduced in [7]. The proposed disturbance observer may estimate lumped disturbances that comprise unmodeled dynamics and disturbances. However, the performance of the disturbance observer is very sensitive to the adaptation rate of the estimated disturbance components. If the output error of the disturbance observer does not converge sufficiently fast, instability or performance degradation is inevitable.

With measurement of the system states not available, a common technique is to establish a state observer that provides estimates of the states. Unlike state observer for linear systems, no state observer is applicable to general nonlinear systems. Most state observers for nonlinear systems are suited for systems transformable to a specific representation, e.g., normal form [10] or adaptive observer form [11]. One class of observers, known as adaptive state observers, are those having their own update laws adapt the estimated parameters [11,12] or the observer gain [10] to minimize the observer error, i.e., the error between the real states and the estimated states. Marine et al. [11] and Vargas and Hemerly [12] presented a state estimator design for systems subject to bounded disturbances. Bullinger and Allgöwer [10] proposed a high-gain observer design for nonlinear systems, which adapts the observer gain instead of the estimated system parameters. The uncertainties under consideration are nonlinearities of the system. However, the observer error converges to zero only when persistent excitation exists or the disturbance magnitude goes to zero. Moreover, the update law for the observer might have an unexpected interaction with that of the control law. The other type of state observers, e.g., K-filters [13,14] and MT-filters [15,16], does not estimate the system states directly. Specifically, the update law for adapting estimated system parameters (which include both observer and system parameters) is determined from the control law to ensure desired stability and convergence property.

Temporal-based motion control algorithms of various class have been in progress lately. Adaptive control is suited for systems susceptible to uncertain but constant parameters.

http://dx.doi.org/10.5772/63082

Moreover, repetitive and iterative learning control [17–21] is capable of dealing with systems affected by periodic disturbances or in need of tracking periodic commands. Lately, adaptive control has been adopted to adapt the period of the repetitive controller [22,23]. Adaptive and iterative learning control has consolidated and been studied by researchers (see [17] and references therein). The integration immediately gains benefits, such as perfect tracking over finite time, dealing with time-varying parameters, and nonresetting of initial condition. As indicated by Chen and Chiu [19] and Chen and Yang [24], most temporal-based control algorithms for rotary systems of variable speed do not explore the characteristics of most uncertainties being spatially periodic. Analyzing and synthesizing such control system in time domain will mistakenly admit those spatially periodic disturbances/parameters as nonperiodic/time-varying ones. This often results in a design either with complicated time-varying feature or with degraded performance.

Spatial-based control algorithms have been studied by researchers recently. The initial step is to reformulate the given system model into the one in spatial domain. Because the reformulation renders those spatial uncertainties stationary in spatial domain, position-invariant control design can be performed to achieve the desired performance regardless of the operating speed. A spatial-based repetitive controller synthesizes its kernel (i.e., $e^{-Ls}$ with positive feedback) and operates in accordance with spatial coordinate, e.g., angular displacement. Therefore, its ability for spatially periodic disturbances or references rejection/tracking will not deteriorate as the system operates at variable speed. A regular repetitive controller is composed of repetitive (i.e., a kernel) and nonrepetitive (e.g., a stabilizing controller) parts. With the kernel synthesized with respect to spatial coordinate and given a time-domain system, designing the nonrepetitive portion that interfaces with the repetitive kernel properly poses a challenge. For spatially periodic disturbance rejection, Nakano et al. [18] reformulated a given linear time-invariant (LTI) system in an angular position domain. The resulting nonlinear system was linearized around an operating speed. Coprime factorization is then used to synthesize a stabilizing controller with repetitive kernel for the acquired linear model. A more sophisticated design based on linearization and robust control was proposed by Chen et al. [25]. Design approaches for linearized systems are straightforward. However, the overall system might lack the stability of operating at a variable speed or coping with large velocity fluctuation. For tracking of spatially periodic references, Mahawan and Luo [26] have validated the idea of operating the repetitive kernel in angular domain and the stabilizing controller in time domain. Doing so does not require reformulation of the open-loop system. For experimental verification, however, the approach involves solving an optimization problem to synchronize the hardware (time) and software (angular position) interruptions. To further limit the applicability, the mapping between time and angular position has to be known *a priori*. The problem formulation made by Nakano and Mahawan assumed the simplest scenario, i.e., the open-loop system is LTI without nonlinearity and modeling uncertainty. Chen and Chiu [19] reported that a class of nonlinear models can be reformulated into a quasi-linear parameter varying (quasi-LPV) system. An LPV gain-scheduling controller was synthesized subsequently to address unmodeled dynamics, actuator saturation, and spatially periodic disturbances. The approach could lead to conservative design if the number of varying parameters rises, the parametric space is nonconvex, or the modeling uncertainties

are significant. The restraint and conservatism of modeling uncertainties was relieved by Chen and Yang [24] by formulating a spatial-based repetitive control system with the adoption of adaptive feedback linearization. However, this method is only applicable to systems with measurement of all states available in real time.

The design of spatial-based repetitive control has been sophisticated enough to cope with a class of uncertain nonlinear systems. On the contrary, existing spatial-based iterative learning controls [27,28] are still primitive and aim at only linear systems. It is not apparent whether those methods can be generalized to be applicable for nonlinear and high-order systems. Knowing that spatial uncertainties in rotary systems may be tackled as periodic disturbances or periodic parameters [29–31], treating the uncertainties as disturbances seem to be more prevalent in literatures.

This book chapter reviews and summarizes the recent progress in the design of spatial-based robust adaptive repetitive and iterative learning control. In particular, the collection of methods aims at rotary systems that are subject to spatially periodic uncertainties and based on nonlinear control paradigm, e.g., adaptive feedback linearization and adaptive backstepping. We will elaborate on the design procedure (applicable to generic $n$th-order systems) of each method and the corresponding stability and convergence theorems. The outline of the chapter is as follows.

Section 2 presents a spatial-based robust repetitive control design that builds on the design paradigm of feedback linearization. This design basically evolves from the work of Chen and Yang [24]. The proposed design resolves the major shortcoming in their design, i.e., which requires full-state feedback, by the incorporation of a K-filter-type state observer. The system is allowed to operate at varying speed, and the open-loop nonlinear time-invariant (NTI) plant model identified for controller design is assumed to have both unknown parameters and unmodeled dynamics. To attain robust stabilization and high-performance tracking, we propose a two-degrees-of-freedom control configuration. The controller consists of two modules, one aiming at robust stabilization and the other tracking performance. One control module applies adaptive feedback linearization with projected parametric adaptation to stabilize the system and account for parametric uncertainty. Adaptive control plays the role of tuning the estimated parameters, which differs from those methods (e.g., [22,23]), where it was for tuning the period of the repetitive kernel. The other control module comprises a spatial low-order and attenuated repetitive controller combined with a loop-shaping filter and is integrated with the adaptively controlled system. The overall system may operate in variable speed and is robust to model uncertainties and capable of rejecting spatially periodic and nonperiodic disturbances. The stability of the design can be proven under bounded disturbance and uncertainties.

Section 3 presents another spatial-based robust repetitive control design that resorts to the design paradigm of backstepping. This design basically builds on the work of Yang and Chen [32]. The method has been extended to a category of nonlinear systems (instead of just LTI systems). Furthermore, the main deficiency of requiring full-state feedback in Yang and Chen's design is resolved by incorporating a K-filter-type state observer. To achieve robust stabilization and high-performance tracking, a two-module control configuration is constructed. One

http://dx.doi.org/10.5772/63082

of the module using adaptive backstepping with projected parametric adaptation to robustly stabilize the system. The other module incorporates a spatial-based low-order and attenuated repetitive controller cascaded with a loop-shaping filter to improve the tracking performance. The overall system incorporating the state observer can be proven to be stable under bounded disturbance and system uncertainties.

Section 4 introduces a spatial-based iterative learning control design that is suited for a generic class of nonlinear rotary systems with parameters being unknown and spatially periodic. Fundamentally, this design borrows the feature of parametric adaptation in adaptive control and integrates it with iterative learning. Note that the theoretical success of the integration is not immediate because the stability and tracking performance of the overall system is in need of further justification. Control input and periodic parametric tuning law are specified by establishing a sensible Lyapunov-Krasovskii functional (LKF) and rendering its derivative negative semidefinite. The synthesis of the control input and parametric tuning law and stability/convergence analysis established for this design is distinct from that in [17]. Moreover, unlike a typical adaptive control, the proposed periodic parametric tuning law can cope with unknown parameters of stationary or arbitrarily fast variation.

Section 5 concludes the chapter and points out issues and future research directions relevant to spatial-based robust adaptive repetitive and iterative learning control.

## 2. Spatial-based output feedback linearization robust adaptive repetitive control (OFLRARC)

Consider the state-variable model of an $n$th-order single-input single-output NTI system with model uncertainties and output disturbance, i.e.,

$$\begin{aligned}\dot{x}(t) &= \left[f_t\left(x(t),\phi_f\right)+\Delta f_t\left(x(t),\phi_f\right)\right]+\left[g_t\left(x(t),\phi_g\right)+\Delta g_t\left(x(t),\phi_g\right)\right]u(t)\\ y &= \Psi x(t)+d_y(t)=x_1(t)+d_y(t)\end{aligned} \tag{1}$$

where $x(t)=[x_1(t) \quad \cdots \quad x_n(t)]^T$, $\Psi=[1 \quad 0 \quad \cdots \quad 0]$, $u(t)$, and $y(t)$ correspond to the control input and measured output angular velocity of the system, respectively.

**Assumption 2.1**

(1) $d_y(t)$ is a class of bounded signals with (dominant) spatially periodic and band-limited (or nonperiodic) components.

Here, band-limited disturbances are signals with Fourier transform or power spectral density being zero above a certain finite frequency. The number of distinctive spatial frequencies and the spectrum distribution are the only available information of the disturbances.

(2) $f_t(x(t),\ \phi_f)$ and $g_t(x(t),\ \phi_g)$ are known vector-valued functions with unknown but bounded system parameters, i.e., $\phi_f=[\phi_{f1} \quad \cdots \quad \phi_{fk}]$ and $\phi_g=[\phi_{g1} \quad \cdots \quad \phi_{gl}]$.

(3) $\Delta f_t(x(t),\ \phi_f)$ and $\Delta g_t(x(t),\ \phi_g)$ represent unmodeled dynamics, which are also assumed to be bounded.

Consider an alternate variable $\theta = \lambda(t)$, i.e., the angular displacement, instead of time $t$ as the independent variable. Because $\lambda(t) = \int_0^t \omega(\tau)d\tau + \lambda(0)$ where $\omega(t)$ is the angular velocity, the following condition

$$\omega(t) = \frac{d\theta}{dt} > 0,\ \forall\ t > 0 \tag{2}$$

will ensure that $\lambda(t)$ is strictly monotonic, so that $t = \lambda^{-1}(\theta)$ exists. Hence, all the time-domain variables can be transformed into their counterparts in the $\theta$-domain, i.e.,

$$\hat{x}(\theta) = x(\lambda^{-1}(\theta)),\ \hat{y}(\theta) = y(\lambda^{-1}(\theta)),\ \hat{u}(\theta) = u(\lambda^{-1}(\theta)),\ \hat{d}(\theta) = d(\lambda^{-1}(\theta)),\ \hat{\omega}(\theta) = \omega(\lambda^{-1}(\theta))$$

where we denote $\hat{\bullet}$ as the $\theta$-domain representation of $\bullet$. Note that, in practice, (2) can usually be satisfied for most rotational motion system where the rotary component rotates only in one direction. Because

$$dx(t)/dt = d\theta/dt \cdot d\hat{x}(\theta)/d\theta = \hat{\omega}(\theta) \cdot d\hat{x}(\theta)/d\theta$$

(1) can be rewritten as

$$\begin{aligned} \hat{\omega}(\theta)\frac{d\hat{x}(\theta)}{d\theta} &= \left[ f_t\left(\hat{x}(\theta), \phi_f\right) + \Delta f_t\left(\hat{x}(\theta), \phi_f\right)\right] + \left[ g_t\left(\hat{x}(\theta), \phi_g\right) + \Delta g_t\left(\hat{x}(\theta), \phi_g\right)\right]\hat{u}(\theta) \\ \hat{y}(\theta) &= \Psi\hat{x}(\theta) + \hat{d}_y(\theta) = \hat{x}_1(\theta) + \hat{d}_y(\theta). \end{aligned} \tag{3}$$

Equation (3) is an nonlinear position-invariant (NPI; as opposed to the definition of time-invariant) system with the $\theta$ as the independent variable. Note that we define the Laplace transform of a signal $\hat{g}(\theta)$ in the angular displacement domain as $\hat{G}(\tilde{s}) = \int_0^\infty \hat{g}(\theta)e^{-\tilde{s}\theta}d\theta$.

This definition will be useful for describing the linear portion of the overall control system.

Drop the $\theta$ notation and rewrite (3) in the form

$$\hat{\dot{x}} = f(\hat{x}, \phi_f) + g(\hat{x}, \phi_g)\hat{u} + \hat{d}_s,\ \hat{y} = h(\hat{x}) + \hat{d}_y = \hat{\omega} + \hat{d}_y \tag{4}$$

http://dx.doi.org/10.5772/63082

where terms involving unstructured uncertainty are merged into $\hat{d}_s=\Delta f(\hat{x},\ \phi_f)+\Delta g(\hat{x},\ \phi_g)\hat{u}$ with $\Delta f(\hat{x},\ \phi_f)=\Delta f_t(\hat{x},\ \phi_f)/\hat{x}_1$, $\Delta g(\hat{x},\ \phi_g)=\Delta g_t(\hat{x},\ \phi_f)/\hat{x}_1$. In addition, we have

$$f(\hat{x},\phi_f)=f_t(\hat{x},\phi_f)/\hat{x}_1,\ g(\hat{x},\phi_g)=g_t\left(\hat{x},\phi_g\right)/\hat{x}_1,\ h(\hat{x})=\hat{\omega}=\hat{x}_1$$

The state variables have been specified such that the angular velocity $\hat{\omega}$ is equal to $\hat{x}_1$, i.e., the undisturbed output $h(\hat{x})$. To proceed, we will adopt the definitions and notations given in [24] for Lie derivative, relative degree, diffeomorphism.

It can be verified that (4) has the same relative degree in $D_0=\{\hat{x}\in\mathbb{R}^n \mid \hat{x}_1\neq 0\}$ as the NTI model in (1). If (4) has relative degree $r$, the following nonlinear coordinate transformation can be defined as

$$\hat{z}=T(\hat{x})=\left[\psi_1(\hat{x})\ \ \cdots\ \ \psi_{n-r}(\hat{x})\ \middle|\ h(\hat{x})\ \ \cdots\ \ L_f^{r-1}h(\hat{x})\right]^T\triangleq\begin{bmatrix}\hat{z}_2\\ \hat{z}_1\end{bmatrix}$$

where $\psi_1$ to $\psi_{n-r}$ are chosen such that $T(\hat{x})$ is a diffeomorphism on $D_0\subset D$ and

$$L_g\psi_i(\hat{x})=0,\ 1\le i\le n-r$$

$\forall\ \hat{x}\in D_0$. With respect to the new coordinates, i.e., $\hat{z}_1$ and $\hat{z}_2$, (4) can be transformed into the so-called normal form, i.e.,

$$\begin{aligned}\dot{\hat{z}}_2&=L_f\psi(\hat{x})\big|_{\hat{x}=T^{-1}(\hat{z})}+\hat{d}_{so}\triangleq\Psi(\hat{z}_1,\hat{z}_2)\\ \dot{\hat{z}}_1&=A_c\hat{z}_1+B_c\left[L_gL_f^{r-1}h(\hat{x})\big|_{\hat{x}=T^{-1}(\hat{z})}\right]\left[\hat{u}+\frac{L_f^rh(\hat{x})}{L_gL_f^{r-1}h(\hat{x})}\bigg|_{\hat{x}=T^{-1}(\hat{z})}\right]+\hat{d}_{si},\ \hat{y}=C_c\hat{z}_1+\hat{d}_y\end{aligned}\tag{5}$$

where $\hat{d}_{so}$ and $\hat{d}_{si}=[\hat{d}_{si_1}\ \cdots\ \hat{d}_{si_r}]^T$ come from $\hat{d}_s$ going through the indicated coordinate transformation. $\hat{z}_1=[\hat{z}_{11}\ \cdots\ \hat{z}_{1r}]^T\in\mathbb{R}^r$, $\hat{z}_2\in\mathbb{R}^{n-r}$, and $(A_c,\ B_c,\ C_c)$ is a canonical form representation of a chain of $r$ integrators. The first equation in (5) is the internal dynamics and not affected by the control $\hat{u}$. By setting $\hat{z}_1=0$, we obtain $\dot{\hat{z}}_2=\Psi(0,\ \hat{z}_2)$, which is the zero dynamics of (4) or (5). The system is called minimum phase if the zero dynamics has an asymptotically stable equilibrium point in the domain of interest. To allow us to present the proposed algorithm and stability analysis in a simpler context, we will make the following assumptions for the subsequent derivation.

**Assumption 2.2**

(1) $f(\hat{x}(\theta),\ \phi_f)$ and $g(\hat{x}(\theta),\ \phi_g)$ are linearly related to those unknown system parameters, i.e.,

$$f\left(\hat{x}(\theta),\phi_f\right)=\phi_{f1}f_1\left(\hat{x}(\theta)\right)+\ldots+\phi_{fk}f_k\left(\hat{x}(\theta)\right),\ g\left(\hat{x}(\theta),\phi_g\right)=\phi_{g1}g_1\left(\hat{x}(\theta)\right)+\ldots+\phi_{gl}g_l\left(\hat{x}(\theta)\right) \tag{6}$$

(2) (4) is exponentially minimum phase, i.e., the zero dynamics is exponentially stable;

(3) The output disturbance is sufficiently smooth [i.e., $\hat{\hat{d}}_y$, ⋯, $\hat{d}_y^{(r)}$ exists];

(4) $\hat{d}_{si_1}^{(r-1)}$, $\hat{d}_{si_2}^{(r-2)}$, ⋯, $\hat{\hat{d}}_{si_{r-1}}$ exist, i.e., the transformed unstructured uncertainty is sufficiently smooth; and

(5) The reference command $\hat{y}_m$ and its first $r$ derivates are known and bounded. Moreover, $\hat{y}_m^{(r)}$ is piecewise continuous.

With Assumption 2, the design of a nonlinear state observer may focus on the external dynamics of (5), i.e.,

$$\dot{\hat{z}}_1=A_c\hat{z}_1+B_c\left[L_gL_f^{r-1}h(\hat{x})\Big|_{\hat{x}=T^{-1}(\hat{z})}\right]\left[\hat{u}+\frac{L_f^rh(\hat{x})}{L_gL_f^{r-1}h(\hat{x})}\Bigg|_{\hat{x}=T^{-1}(\hat{z})}\right]+\hat{d}_{si} \tag{7}$$

**2.1 State observer design**

In this section, we show how to establish a state observer for the transformed NPI system (5). Because $f(\hat{x})$ and $g(\hat{x})$ are assumed to be linearly related to system parameters, $L_gL_f^{r-1}h(\hat{x})$ and $L_gL_f^{r-1}h(\hat{x})$ can be expressed as

$$L_f^rh(\hat{x})=\Theta^TW_f\left(\hat{x}\right),\ L_gL_f^{r-1}h(\hat{x})=\Theta^TW_g\left(\hat{x}\right)$$

where $W_f(\hat{x})$ and $W_g(\hat{x})$ are two nonlinear functions, and

$$\Theta=\left[\phi_{f1}\ \ \cdots\ \ \phi_{fk}\ \ \phi_{g1}\ \ \cdots\ \ \phi_{gl}\ \ \cdots\right]^T=\left[\phi_1\ \ \cdots\ \ \phi_\ell\right]^T\in\mathbb{R}^\ell.$$

where $\ell$ denotes the number of unknown parameters. Hence, (7) can be rewritten as

$$\dot{\hat{z}}_1=A_c\hat{z}_1+B_c\left[\Theta^TW_g\left(\hat{x}\right)\hat{u}+\Theta^TW_f\left(\hat{x}\right)\right]+\hat{d}_{si} \tag{8}$$

http://dx.doi.org/10.5772/63082

Equation (8) can be further written in the form

$$\dot{\hat{z}}_1 = A_0\hat{z}_1 + \bar{k}\,\hat{z}_{11} + B_c\left[\Theta^T W_g(\hat{x})\hat{u} + \Theta^T W_f(\hat{x})\right] + \hat{d}_{si}, \tag{9}$$

where $A_0 = \begin{bmatrix} -k_1 & I_{(r-1)\times(r-1)} \\ \vdots & \\ -k_r & 0_{1\times(r-1)} \end{bmatrix}$ and $\bar{k} = [k_1 \quad \cdots \quad k_r]^T$.

By properly choosing $\bar{k}$, the matrix $A_0$ can be made Hurwitz. Next, we adopt the following observer structure:

$$\dot{\bar{z}}_1 = A_0\bar{z}_1 + \bar{k}\hat{y} + B_c\left[\Theta^T \bar{W}_g(\hat{y})\hat{u} + \Theta^T \bar{W}_f(\hat{y})\right] \tag{10}$$

where $\bar{z}_1 = [\bar{z}_{11} \quad \cdots \quad \bar{z}_{1r}]^T$ is the estimate of $\hat{z}_1$ and $\overline{W}_f(\hat{y})$ and $\overline{W}_g(\hat{y})$ are nonlinear functions with the same structure as $W_f(\hat{x})$ and $W_g(\hat{x})$, except that each entry of $\hat{x}$ is replaced by $\hat{y}$. Equation (10) can be further expressed as

$$\dot{\bar{z}}_1 = A_0\bar{z}_1 + \bar{k}\hat{y} + F(\hat{y},\hat{u})^T\Theta \text{ with } F(\hat{y},\hat{u})^T = \begin{bmatrix} 0_{(r-1)\times\ell} \\ \bar{W}_f^T(\hat{y}) + \bar{W}_g^T(\hat{y})\hat{u} \end{bmatrix} \in \mathbb{R}^{r\times\ell} \tag{11}$$

Define the state estimated error as $\varepsilon \triangleq [\varepsilon_{\hat{z}_{11}} \quad \cdots \quad \varepsilon_{\hat{z}_{1r}}]^T \triangleq \hat{z}_1 - \bar{z}_1$. The dynamics of the estimated error can be obtained by subtracting (10) from (9), i.e.,

$$\dot{\varepsilon} = A_0\varepsilon + \Delta \quad \Delta = -\bar{k}\hat{d}_y + B_c\Theta^T\left[W_g(\hat{x}) - \bar{W}_g(\hat{y})\right]\hat{u} + B_c\Theta^T\left[W_f(\hat{x}) - \bar{W}_f(\hat{y})\right] + \hat{d}_{si}. \tag{12}$$

Here, we further assume that

**Assumption 2.3**

(9) $W_g(\hat{x}) - \overline{W}_g(\hat{y})$ and $W_f(\hat{x}) - \overline{W}_f(\hat{y})$ are bounded to ensure the boundness of the estimated error. To see this, note that the solution of (12) may be viewed as sum of zero input response $\varepsilon_u$ and zero state response $\varepsilon_s$, i.e., $\varepsilon = \varepsilon_u + \varepsilon_s$. The zero input response $\dot{\varepsilon}_u = A_0\varepsilon_u$ will decay to zero exponentially, as $A_0$ is Hurwitz, and the zero state response $\varepsilon_s$ will be bounded due to the bounded disturbance $\hat{d}_y$, $W_g(\hat{x}) - \overline{W}_g(\hat{y})$, and $W_f(\hat{x}) - \overline{W}_f(\hat{y})$.

Equation (10) or (11) cannot be readily implemented due to the unknown parametric vector $\Theta$, but it motivates the subsequent mathematical manipulation. Define the state estimate as $\bar{z}_1 \triangleq \xi + \Omega^T\Theta$ such that $\xi = [\xi_{11} \quad \cdots \quad \xi_{1r}]^T \in \mathbb{R}^r$ and $\Omega^T \in \mathbb{R}^{r\times\ell}$ and employ the following two K-filters:

$$\dot{\xi} = A_0\xi + \overline{k}\hat{y},\ \dot{\Omega}^T = A_0\Omega^T + F(\hat{y},\hat{u})^T. \tag{13}$$

It can be easily verified that (13) is equivalent to (11). Hence, (13) may replace the role of (11) for providing the state estimate. With $\Omega^T \triangleq [v_1 \ \cdots \ v_\ell]$, the second equation of (13) may be further decomposed into

$$\dot{v}_j = A_0 v_j + e_r\sigma_j,\ j = 1,2,\cdots,\ell \tag{14}$$

where $e_r = [0 \ \cdots \ 0 \ \ 1] \in \mathbb{R}^r$ and $\sigma_j = w_{1j} + w_{2j}\hat{u}$ with $w_{1j}$ and $w_{2j}$ are the $j^{th}$ columns of $\overline{W}_f^T(\hat{y})$ and $\overline{W}_g^T(\hat{y})$, respectively. Equation (13) is still not applicable due to $\Theta$. However, with the definition of the state estimated error $\varepsilon$, the state estimate, the first equation of (13), and (14), we acquire the following relationship that is not available from (11):

$$\begin{aligned}\hat{z}_{11} &= \overline{z}_{11} + \varepsilon_{\hat{z}_{11}} = \xi_{11} + \sum_{j=1}^{\ell} v_{j,1}\phi_j + \varepsilon_{\hat{z}_{11}},\ \cdots,\ \hat{z}_{1r} \\ &= \overline{z}_{1r} + \varepsilon_{\hat{z}_{1r}} = \xi_{1r} + \sum_{j=1}^{\ell} v_{j,r}\phi_j + \varepsilon_{\hat{z}_{1r}}\end{aligned} \tag{15}$$

where $\bullet_{j,i}$ denotes the i$^{th}$ row of $\bullet_j$. Equation (15) will be used in the subsequent design.

### 2.2 Output feedback robust adaptive repetitive control system

In this section, we show how to incorporate the state observer established in the previous section into an output feedback adaptive repetitive control system. The control configuration consists of two layers. The first layer is the adaptive feedback linearization, which tackles system nonlinearity and parametric uncertainty. The second layer is a repetitive control module of a repetitive controller and a loop-shaping filter. This layer not only enhances the ability of the overall system for rejection of disturbance, sensitivity reduction to model uncertainty, and state estimated error but also improves the robustness of the parametric adaptation. Although inclusion of the state observer relieves the design of the need of full-state feedback, it actually introduces extra dynamics into the system. Hence, the stability of the resulting system needs to be further justified.

Suppose that (4) has relative degree $r$. To perform input/output feedback linearization, differentiate the output $\hat{y}$ until the control input $\hat{u}$ appears to obtain

$$\hat{y}^{(r)} = \hat{z}_{11}^{(r)} + \hat{d}_y^{(r)} = \dot{\hat{z}}_{1r} + \hat{d}_y^{(r)} = \dot{\overline{z}}_{1r} + \dot{\varepsilon}_{\hat{z}_{1r}} + \hat{d}_y^{(r)} \tag{16}$$

Substituting the $r^{th}$ state equation of (10) into (16), we have

http://dx.doi.org/10.5772/63082

$$\hat{y}^{(r)} = \dot{\bar{z}}_{1r} + \dot{\varepsilon}_{\hat{z}_{1r}} + \hat{d}_y^{(r)} = -k_r \bar{z}_{11} + k_r \hat{y} + \Theta^T \bar{W}_f(\hat{y}) + \Theta^T \bar{W}_g(\hat{y})\hat{u} + \dot{\varepsilon}_{\hat{z}_{1r}} + \hat{d}_y^{(r)} z \tag{17}$$

To put the previously developed state observer into use, we substitute the first equation of (15) into (17) and arrive at

$$\hat{y}^{(r)} = -k_r \left( \xi_{11} + \sum_{j=1}^{\ell} v_{j,1} \phi_j \right) + k_r \hat{y} + \Theta^T \bar{W}_f(\hat{y}) + \Theta^T \bar{W}_g(\hat{y})\hat{u} + \dot{\varepsilon}_{\hat{z}_{1r}} + \hat{d}_y^{(r)} \tag{18}$$

Define the estimated parametric vector of $\Theta$ as

$$\tilde{\Theta} = \begin{bmatrix} \tilde{\phi}_{f1} & \cdots & \tilde{\phi}_{fk} & \tilde{\phi}_{g1} & \cdots & \tilde{\phi}_{gl} & \cdots \end{bmatrix}^T = \begin{bmatrix} \tilde{\phi}_1 & \cdots & \tilde{\phi}_\ell \end{bmatrix}^T \in \mathbb{R}^\ell.$$

The control law using the estimated system parameters and states is

$$\hat{u} = \frac{1}{\tilde{\Theta}^T \bar{W}_g(\hat{y})} \left( -\tilde{\Theta}^T \bar{W}_f(\hat{y}) + k_r \left( \xi_{11} + \sum_{j=1}^{\ell} v_{j,1} \tilde{\phi}_j \right) - k_r \hat{y} + \tilde{\tilde{v}}_d + \hat{u}_{\hat{R}} \right), \tag{19}$$

where we introduce two designable inputs, $\tilde{\tilde{v}}_d$ and $\hat{u}_{\hat{R}}$. Specify $\tilde{\tilde{v}}_d$, the estimate of $\hat{v}_d$, as

$$\tilde{\tilde{v}}_d = \hat{y}_m^{(r)} + \alpha_1 (\hat{y}_m^{(r-1)} - \tilde{\tilde{y}}^{(r-1)}) + \cdots + \alpha_{r-1} (\dot{\hat{y}}_m - \dot{\tilde{\hat{y}}}) + \alpha_r (\hat{y}_m - \hat{y}), \tag{20}$$

where $\hat{y}_m$ is a prespecified reference trajectory, $\tilde{\tilde{y}}^{(k)}$ denotes the estimate of $\hat{y}^{(k)}$, and $\alpha_i$'s are adjustable parameters. Substituting (19) back into (18) and defining the tracking error $\hat{e} \triangleq \hat{y} - \hat{y}_m$, we arrive at the following error equation:

$$\begin{aligned} &\hat{e}^{(r)} + \alpha_1 \hat{e}^{(r-1)} + \cdots + \alpha_{r-1} \dot{\hat{e}} + \alpha_r \hat{e} = \Phi^T W + \hat{u}_{\hat{R}} + \hat{d}_y^{(r)} + \dot{\varepsilon}_{\hat{z}_{1r}} \\ &+ \alpha_1 \left( \hat{d}_y + \varepsilon_{\hat{z}_{11}} \right)^{(r-1)} + \cdots + \alpha_{r-1} \left( \dot{\hat{d}}_y + \dot{\varepsilon}_{\hat{z}_{11}} \right), \end{aligned} \tag{21}$$

where $\Phi = \Theta - \tilde{\Theta}$ and $W$ is a function of $\xi$, $v$, and $\tilde{\Theta}$. If we denote $M(\tilde{s}) = 1 / (\tilde{s}^r + \alpha_1 \tilde{s}^{r-1} + \cdots + \alpha_r)$, (21) implies that

$$\frac{1}{M(\tilde{s})}\hat{E}(\tilde{s}) = \Phi^T W + \hat{U}_{\hat{R}}(\tilde{s}) + \left(\tilde{s}^r + \alpha_1\tilde{s}^{r-1} + \cdots + \alpha_{r-1}\tilde{s}\right)\hat{d}_y + \left(\alpha_1\tilde{s}^{r-1} + \cdots + \alpha_{r-1}\tilde{s}\right)\varepsilon_{\hat{z}_{11}} + \tilde{s}\varepsilon_{\hat{z}_{1r}}. \tag{22}$$

Neglecting the details of $\Phi^T W$, we can view (21) or (22) as a linear system (with the output $\hat{e}$) subject to five inputs. We propose adding another control loop between $\hat{E}(\tilde{s})$ and $\hat{U}_{\hat{R}}(\tilde{s})$. This control loop provides an additional degree-of-freedom for reducing the effect of the unstructured uncertainty, the state estimated error, and the output disturbance. The tracking error $\hat{E}(\tilde{s})$ and the control input $\hat{U}_{\hat{R}}(\tilde{s})$ is related by

$$\hat{U}_{\hat{R}}(\tilde{s}) = -\hat{R}(\tilde{s})\hat{C}(\tilde{s})\hat{E}(\tilde{s}),\ \hat{R}(\tilde{s}) = \prod_{i=1}^{k}\frac{\tilde{s}^2 + 2\zeta_i\omega_{ni}\tilde{s} + \omega_{ni}^2}{\tilde{s}^2 + 2\xi_i\omega_{ni}\tilde{s} + \omega_{ni}^2}\ \text{(low-order repetitive controller)} \tag{23}$$

where $k$ is the number of periodic frequencies, $\omega_{ni}$ is the $i$th disturbance frequency in rad/rev, and $\xi_i$ and $\zeta_i$ are damping ratios with $0<\xi_i<\zeta_i<1$. The gain of $\hat{R}(\tilde{s})$ at those periodic frequencies may be varied by adjusting the values of $\xi_i$ and $\zeta_i$. Furthermore, $\hat{C}(\tilde{s})$ is a controller that should ensure the stability of the overall system. Substitute (23) back into (22), we obtain

$$\left[1/M(\tilde{s}) + \hat{R}(\tilde{s})\hat{C}(\tilde{s})\right]\hat{E}(\tilde{s}) = \Phi^T W + \left(\tilde{s}^r + \alpha_1\tilde{s}^{r-1} + \cdots + \alpha_{r-1}\tilde{s}\right)\hat{d}_y + \left(\alpha_1\tilde{s}^{r-1} + \cdots + \alpha_{r-1}\tilde{s}\right)\varepsilon_{\hat{z}_{11}} + \tilde{s}\varepsilon_{\hat{z}_{1r}} \tag{24}$$

Define

$$\bar{M}(\tilde{s}) \triangleq \left[1/M(\tilde{s}) + \hat{R}(\tilde{s})\hat{C}(\tilde{s})\right]^{-1}, \tag{25}$$

Equation (24) becomes

$$\hat{e} = \bar{M}(\tilde{s})\Phi^T W + \hat{d}_{\bar{M}},\ \hat{d}_{\bar{M}} = \bar{M}(\tilde{s})\left[\left(\tilde{s}^r + \alpha_1\tilde{s}^{r-1} + \cdots + \alpha_{r-1}\tilde{s}\right)\hat{d}_y + \left(\alpha_1\tilde{s}^{r-1} + \cdots + \alpha_{r-1}\tilde{s}\right)\varepsilon_{\hat{z}_{11}} + \tilde{s}\varepsilon_{\hat{z}_{1r}}\right] \tag{26}$$

where

$$\hat{d}_{\bar{M}} = \bar{M}(\tilde{s})\left[\left(\tilde{s}^r + \alpha_1\tilde{s}^{r-1} + \cdots + \alpha_{r-1}\tilde{s}\right)\hat{d}_y + \left(\alpha_1\tilde{s}^{r-1} + \cdots + \alpha_{r-1}\tilde{s}\right)\varepsilon_{\hat{z}_{11}} + \tilde{s}\varepsilon_{\hat{z}_{1r}}\right]$$

http://dx.doi.org/10.5772/63082

Because $\hat{e}, \dot{\hat{e}}, \cdots, \hat{e}^{(r-1)}$ cannot be measured directly, the so-called augmented error scheme will be used. The augmented error is defined as

$$\hat{e}_1 = \hat{e} + \left(\Phi^T \bar{M}(\tilde{s})W - \bar{M}(\tilde{s})\Phi^T W\right). \tag{27}$$

Substituting (26) into (27), we obtain

$$\hat{e}_1 = \Phi^T \bar{\varsigma} + \hat{d}_{\bar{M}}, \tag{28}$$

where $\bar{\varsigma} = \overline{M}(\tilde{s})W$. The parametric adaptation law to be used is modified from the normalized gradient method proposed in [33], i.e.,

$$\dot{\tilde{\Theta}} = -\dot{\Phi} = \begin{cases} \dfrac{\rho \hat{e}_1 \bar{\varsigma}}{1 + \bar{\varsigma}^T \bar{\varsigma}} & \text{if } |\hat{e}_1| > \hat{d}_{\bar{M}_0} \text{ and } \tilde{\Theta} \in w^0, \\ P_R\left(\dfrac{\rho \hat{e}_1 \bar{\varsigma}}{1 + \bar{\varsigma}^T \bar{\varsigma}}\right) & \text{if } |\hat{e}_1| > \hat{d}_{\bar{M}_0}, \tilde{\Theta} \in \partial w, \text{ and } \hat{e}_1 \bar{\varsigma}^T \tilde{\Theta}_{perp} > 0, \\ 0 & \text{if } |\hat{e}_1| \le \hat{d}_{\bar{M}_0}, \end{cases} \tag{29}$$

where $w$ is the allowable parametric variation set (compact and convex) with its interior and boundary denoted by $w^0$ and $\partial w$, respectively, $\hat{d}_{\bar{M}_0}$ is an upper bound for the magnitude of $\hat{d}_{\bar{M}}$, and $\rho$ is an adjustable adaptation rate that affects the convergence property. If the magnitude of $\hat{e}_1$ is small and dominated by the magnitude of $\hat{d}_{\bar{M}}$, the adaptation law is disabled to prevent the parameters from being adjusted based on the disturbance. If $\hat{e}_1$ is greater than $\hat{d}_{\bar{M}}$ magnitude-wise, two scenarios need to be considered. If the current estimated parametric vector locates within the allowable parametric set, regular adaptation law is applied. If the current estimated parametric vector is on the boundary of the allowable parametric set, the projected adaptation law is employed to stop the parametric vector from leaving the variation set.

In the following, we present stability theorem for the proposed spatial-based OFLRARC system. The theorem extends the results in the literature [33,34] to take into account the addition of the repetitive control module. It will be seen that the overall OFLRARC system will stay stable and the tracking error will be bounded as long as a stable and proper loop-shaping filter stabilizes a certain feedback system.

**Theorem 2.1** The error equation (28) with the parametric update law (29) leads to $\Phi \in L_\infty$, $\dot{\Phi} \in L_2 \cap L_\infty$, and $\| \Phi^T \bar{\varsigma}(\theta) \|_2 \le \gamma(1 + \| \bar{\varsigma} \|_{TL_\infty})$ for all $\theta$.

Proof: Follow the same steps for proof of Theorem 3.1 in [24].

**Theorem 2.2** Consider an exponentially minimum-phase nonlinear system with parameter uncertainty and subject to output disturbance as given by (4), which is augmented with a state observer (or K-filters) described by (13) [35]. Specify the control laws as (19), (20), and (23). Let Assumptions (1) to (9) be satisfied. Assume that $\hat{y}_m, \hat{\dot{y}}_m, \cdots, \hat{y}_m^{(r-1)}$ (where $r$ is the relative degree) and $\hat{d}_{\bar{M}}$ are bounded with an upper bound $\hat{d}_{\bar{M}_0}$, $f$, $g$, $h$, $L_f^k h$, $L_g L_f h$ are Lipschitz continuous functions, and $W$ has bounded derivative with respect to $\xi$, $v$, and $\widetilde{\Theta}$. In addition, assume that a stable and proper controller $\hat{C}(\tilde{s})$ is specified such that the feedback system shown in **Figure.1** is stable. Then, the parametric adaptation law given by (29) yields the bounded tracking error, i.e., $|\hat{y}(\theta)-\hat{y}_m(\theta)| < \hat{d}_{\bar{M}_0}$ as $\theta \to \infty$.

Proof: Follow the same steps for proof of Theorem 3.2 in [24] with some differences.

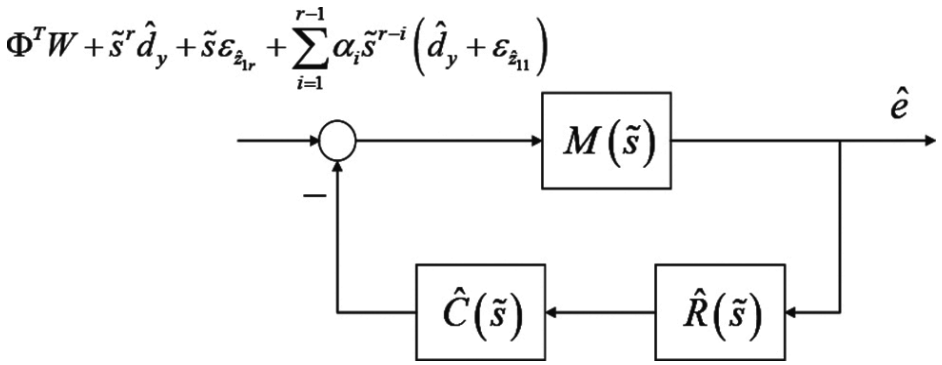


**Figure 1.** Repetitive controller and stabilizing compensator.

## 3.Spatial-based output feedback backstepping robust adaptive repetitive control (OFBRARC)

Consider the same NPI model (3), which is transformed from the NTI model (1), under the same set of assumptions (Assumptions 2.1 and 2.2). The NPI model will be used for the subsequent design and discussion.

### 3.1 Nonlinear state observer

Drop the $\theta$ notation and note that (3) can be expressed as a standard nonlinear system:

$$\dot{\hat{y}} = \dot{\hat{\xi}}_{11} + \left(-k_1 v_{01} + v_{02}\right) b_0 + \dot{\Xi}_1^T a + \dot{\varepsilon}_{\hat{x}_1} + \dot{\hat{d}}_y, \ \dot{v}_{02} = -k_2 v_{01} + \sigma \hat{u}. \tag{30}$$

http://dx.doi.org/10.5772/63082

where terms involving unstructured uncertainty are merged into $\hat{d}_s = \Delta f(\hat{x},\ \phi_f) + \Delta g(\hat{x},\ \phi_g)\hat{u}$ with

$$\Delta f\left(\hat{x}, \phi_f\right) = \frac{\Delta f_t(\hat{x}, \phi_f)}{\hat{x}_1}, \Delta g\left(\hat{x}, \phi_g\right) = \frac{\Delta g_t(\hat{x}, \phi_g)}{\hat{x}_1}$$

In addition, we have

$$f(\hat{x}, \phi_f) = \frac{f_t(\hat{x}, \phi_f)}{\hat{x}_1}, g(\hat{x}, \phi_g) = \frac{g_t\left(\hat{x}, \phi_g\right)}{\hat{x}_1}, h(\hat{x}) = \hat{\omega} = \hat{x}_1$$

The state variables have been specified such that the angular velocity $\hat{\omega}$ is equal to $\hat{x}_1$, i.e., the undisturbed output $h(\hat{x})$. It is not difficult to verify that (30) has the same relative degree in $D_0 = \{\hat{x} \in \mathbb{R}^n \mid \hat{x}_1 \neq 0\}$ as the NTI model in (1). If (30) has relative degree $r$, we can use the same nonlinear coordinate transformation defined previously. With respect to the new coordinates, i.e., $\hat{z}_1$ and $\hat{z}_2$, (30) can be transformed into the so-called normal form, i.e., (5). With zero dynamics being assumed to be asymptotically stable, we may focus on designing a nonlinear state observer for external dynamics of (5), i.e., (7).

Because $f(\hat{x})$ and $g(\hat{x})$ are linearly related to system parameters, $L_g L_f^{r-1} h(\hat{x})$ and $L_g L_f^{r-1} h(\hat{x})$ can be written as $L_f^r h(\hat{x}) = \Theta^T W_f(\hat{x})$ and $L_g L_f^{r-1} h(\hat{x}) = \Theta^T W_g(\hat{x})$, where $W_f(\hat{x})$ and $W_g(\hat{x})$ are two nonlinear functions, and $\Theta = [\phi_{f1} \ \cdots \ \phi_{fk} \ \phi_{g1} \ \cdots \ \phi_{gl} \ \cdots]^T = [\phi_1 \ \cdots \ \phi_\ell]^T \in \mathbb{R}^\ell$, where $\ell$ is the number of unknown parameters. Next, we adopt the following observer structure: $\dot{\bar{z}}_1 = A_0 \bar{z}_1 + \bar{k} y + F(y, u)^T \Theta$, where $\bar{z}_1 = [\bar{z}_{11} \ \cdots \ \bar{z}_{1r}]^T$ is the estimate of $z_1$ and $\overline{W}_f(y)$ and $\overline{W}_g(y)$ are nonlinear functions with the same structure as $W_f(x)$ and $W_g(x)$, except that each entry of $x$ is replaced by $y$. Furthermore, $A_0 = \begin{bmatrix} -k_1 & I_{(r-1)\times(r-1)} \\ \vdots & \\ -k_r & 0_{1\times(r-1)} \end{bmatrix}$, $\bar{k} = [k_1 \ \cdots \ k_r]^T$, and $F(y, u)^T = \begin{bmatrix} 0_{(r-1)\times\ell} \\ \overline{W}_f^T(y) + \overline{W}_g^T(y)u \end{bmatrix} \in \mathbb{R}^{r\times\ell}$.

By properly choosing $\bar{k}$, the matrix $A_0$ can be made Hurwitz. Define the state estimated error as $\varepsilon \triangleq [\varepsilon_{z_{11}} \ \cdots \ \varepsilon_{z_{1r}}]^T \triangleq z_1 - \bar{z}_1$. The dynamics of the estimated error can be obtained as $\dot{\varepsilon} = A_0 \varepsilon + \Delta$, where $\Delta = -\bar{k} d_y + B_c \Theta^T [W_g(x) - \overline{W}_g(y)] u + B_c \Theta^T [W_f(x) - \overline{W}_f(y)] + d_{si}$. To proceed, the role of the state observer is replaced by $\bar{z}_1 \triangleq \xi + \Omega^T \Theta$ and the following two K-filters:

$$\dot{\xi} = A_0 \xi + \bar{k} y, \ \dot{\Omega}^T = A_0 \Omega^T + F(y,u)^T \tag{31}$$

such that $\xi=[\xi_{11} \quad \cdots \quad \xi_{1r}]^T \in \mathbb{R}^r$ and $\Omega^T \triangleq [v_1 \quad \cdots \quad v_\ell] \in \mathbb{R}^{r\times\ell}$. Decompose the second equation of (31) into $\dot{v}_j = A_0 v_j + e_r \sigma_j$, $j=1, 2, \cdots, \ell$, where $e_r=[0 \quad \cdots \quad 0 \quad 1] \in \mathbb{R}^r$ and $\sigma_j = w_{1j} + w_{2j} u$ with $w_{1j}$ and $w_{2j}$ are the $j^{th}$ columns of $\overline{W}_f^T(y)$ and $\overline{W}_g^T(y)$, respectively. With the definition of the state estimated error $\varepsilon$, the state estimate $\bar{z}_1$, and (31), we acquire the following set of equations that will be used in the subsequent design:

$$z_{1k} = \overline{z}_{1k} + \varepsilon_{z_{1k}} = \xi_{1k} + \sum_{j=1}^{\ell} v_{j,k}\phi_j + \varepsilon_{z_{1k}},\ k = 1,...,r \tag{32}$$

where $\bullet_{j,i}$ denotes the $i^{\text{th}}$ row of $\bullet_j$.

### 3.2 Spatial domain output feedback adaptive control system

To apply adaptive backstepping method, we first rewrite the derivative of output $\hat{y}$ as

$$\dot{\hat{y}} = \dot{\hat{z}}_{11} + \dot{\hat{d}}_y = \hat{z}_{12} + \hat{d}_{si_1} + \dot{\hat{d}}_y = \overline{z}_{12} + \varepsilon_{\hat{z}_{12}} + \hat{d}_{si_1} + \dot{\hat{d}}_y \tag{33}$$

With the second equation in (32), (33) can be written as

$$\dot{\hat{y}} = \overline{z}_{12} + \varepsilon_{\hat{z}_{12}} + \hat{d}_{si_1} + \dot{\hat{d}}_y = \xi_{12} + v_{\ell,2}\phi_\ell + \overline{\omega}^T\Theta + \varepsilon_{\hat{z}_{12}} + \hat{d}_{si_1} + \dot{\hat{d}}_y$$

where $\overline{\omega}^T=[v_{1,2} \quad \cdots \quad v_{\ell-1,2} \quad 0]$.

In view of designing output feedback backstepping with K-filters, we need to find a set of K-filter parameters, i.e., $v_{\ell,2}, \cdots, v_{1,2}$, separated from $\hat{u}$ by the same number of integrators between $\hat{z}_{12}$ and $\hat{u}$. From (31), we see that $v_{\ell,2}, \cdots, v_{1,2}$ are all candidates if $w_{2j}$ are not zero. In the subsequent derivation, we assume that $v_{\ell,2}$ is selected. Therefore, the system incorporated the K-filters can be represented by

$$\begin{aligned} &\dot{\hat{y}} = \xi_{12} + v_{\ell,2}\phi_\ell + \overline{\omega}^T\Theta + \varepsilon_{\hat{z}_{12}} + \hat{d}_{si_1} + \dot{\hat{d}}_y,\ \dot{v}_{\ell,i} = v_{\ell,i+1} - \\ &k_i v_{\ell,1},\ i = 2,\cdots,r-1,\ \dot{v}_{\ell,r} = -k_r v_{\ell,1} + w_{1\ell} + w_{2\ell}\hat{u} \end{aligned} \tag{34}$$

To apply adaptive backstepping to (34), a new set of coordinates will be introduced

$$z_1 = \hat{y} - \hat{y}_m,\ z_i = v_{\ell,i} - \alpha_{i-1},\ i = 2,\cdots,r \tag{35}$$

http://dx.doi.org/10.5772/63082

where $\hat{y}_m$ is the prespecified reference output, and $\alpha_{i-1}$ is the virtual input to be used for stabilizing each state equation. For simplicity, we define $\partial\alpha_0/\partial\hat{y} \triangleq -1$ for subsequent derivations.

**Step 1:** $i=1$With (35), the first state equation in (34) can be expressed as

$$\dot{z}_1 = \xi_{12} + z_2\phi_\ell + \alpha_1\phi_\ell + \bar{\omega}^T\Theta + \varepsilon_{\hat{z}_{12}} + \hat{d}_{si_1} + \dot{\hat{d}}_y - \dot{\hat{y}}_m \tag{36}$$

Consider a Lyapunov function $V_1=(1/2)z_1^2$ and calculate its derivative

$$\dot{V}_1 = z_1\dot{z}_1 = z_1\left(\xi_{12} + z_2\phi_\ell + \alpha_1\phi_\ell + \bar{\omega}^T\Theta + \varepsilon_{\hat{z}_{12}} + \hat{d}_{si_1} + \dot{\hat{d}}_y - \dot{\hat{y}}_m\right) \tag{37}$$

Define the estimates of $\phi_i$ as $\tilde{\varphi}_i$ and $\Phi=[\Phi_1 \ \cdots \ \Phi_\ell]=\Theta-\tilde{\Theta}$, where $\tilde{\Theta}=[\tilde{\varphi}_{f1} \ \cdots \ \tilde{\varphi}_{fk} \ \tilde{\varphi}_{g1} \ \cdots \ \tilde{\varphi}_{gl} \ \cdots]^T=[\tilde{\varphi}_1 \ \cdots \ \tilde{\varphi}_\ell]^T \in \mathbb{R}^\ell$. Note that $\Theta$ is the "true" parameter vector, whereas $\tilde{\Theta}$ is the estimated parameter vector. Design the virtual input $\alpha_1$ as $\alpha_1=\bar{\alpha}_1/\tilde{\varphi}_\ell$ and specify

$$\bar{\alpha}_1 = \frac{1}{z_1}\left(-z_1\xi_{12} - z_1z_2\tilde{\phi}_\ell - z_1\bar{\omega}\tilde{\Theta} + z_1\dot{\hat{y}}_m - c_1z_1^2 - d_1z_1^2 - g_1z_1^2\right) \tag{38}$$

where $c_i$, $d_i$, $g_i$ are variables. Therefore, (37) becomes

$$\dot{V}_1 = -c_1z_1^2 - d_1z_1^2 - g_1z_1^2 + \tau_1\Phi + z_1\left(\varepsilon_{\hat{z}_{12}} + \hat{d}_{si_1} + \dot{\hat{d}}_y\right) \tag{39}$$

where $\tau_1\Phi = z_1z_2\Phi_\ell + \alpha_1\Phi_\ell + z_1\bar{\omega}^T\Phi$.

**Step 2:** $i=2, \cdots, r-1$With respect to the new set of coordinates (35), the second equation of (34) can be rewritten as

$$\begin{aligned}\dot{z}_i = z_{i+1} + \alpha_i - k_iv_{\ell,1} - \Bigg[&\frac{\partial\alpha_{i-1}}{\partial\hat{y}}\left(\xi_{12} + v_{\ell,2}\phi_\ell + \bar{\omega}^T\Theta + \varepsilon_{\hat{z}_{12}} + \hat{d}_{si_1} + \dot{\hat{d}}_y\right) + \\ &\frac{\partial\alpha_{i-1}}{\partial\xi}\left(A_0\xi + \bar{k}\hat{y}\right) + \frac{\partial\alpha_{i-1}}{\partial\tilde{\Theta}}\dot{\tilde{\Theta}} \\ &\sum_{j=1}^{\ell}\frac{\partial\alpha_{i-1}}{\partial v_j}\left(A_0v_j + e_r\sigma_j\right) + \sum_{j=1}^{i-1}\frac{\partial\alpha_{i-1}}{\partial\hat{y}_m^{(j-1)}}\hat{y}_m^{(j)}\Bigg]\end{aligned}$$

Consider a Lyapunov function $V_i = \sum_{j=1}^{i-1} V_j + \frac{1}{2} z_i^2$. Specify

$$\alpha_i = \frac{1}{z_i}\Bigg\{ -z_i z_{i+1} + z_i k_i v_{\ell,1} + z_i \Bigg[ \frac{\partial \alpha_{i-1}}{\partial \hat{y}} \left( \xi_{12} + v_{\ell,2} \tilde{\phi}_\ell + \bar{\omega}^T \tilde{\Theta} \right) + \frac{\partial \alpha_{i-1}}{\partial \xi} \left( A_0 \xi + \bar{k} \hat{y} \right) + \frac{\partial \alpha_{i-1}}{\partial \tilde{\Theta}} \dot{\tilde{\Theta}} \sum_{j=1}^{\ell} \frac{\partial \alpha_{i-1}}{\partial v_j} \left( A_0 v_j + e_r \sigma_j \right) + \sum_{j=1}^{i-1} \frac{\partial \alpha_{i-1}}{\partial \hat{y}_m^{(j)}} \hat{y}_m^{(j)} \Bigg] - c_i z_i^2 - d_i \left( \frac{\partial \alpha_{i-1}}{\partial \hat{y}} \right)^2 z_i^2 - g_i \left( \frac{\partial \alpha_{i-1}}{\partial \hat{y}} \right)^2 z_i^2 \Bigg\}$$

The derivative of $V_i$ becomes

$$\dot{V}_i = -\sum_{j=1}^{i-1} \left( c_j z_j^2 + d_j \left( \frac{\partial \alpha_{j-1}}{\partial \hat{y}} \right)^2 z_j^2 + g_j \left( \frac{\partial \alpha_{j-1}}{\partial \hat{y}} \right)^2 z_j^2 \right) + \tau_i \Phi - \sum_{j=1}^{i-1} z_j \frac{\partial \alpha_{j-1}}{\partial \hat{y}} \left( \varepsilon_{\hat{z}_{12}} + \hat{d}_{si_1} + \dot{\hat{d}}_y \right)$$

where $\tau_i \Phi = \tau_1 \Phi - \sum_{j=2}^{i-1} \frac{\partial \alpha_{j-1}}{\partial y} \left( z_j v_{\ell,1} \Phi_\ell + z_j \bar{\omega}^T \Phi \right)$.

**Step 3:**

With respect to the new set of coordinates (35), the third equation of (34) can be written as

$$\dot{z}_r = -k_r v_{\ell,1} + w_{1\ell} + w_{2\ell} \hat{u} - \Bigg[ \frac{\partial \alpha_{r-1}}{\partial \hat{y}} \left( \xi_{12} + v_{\ell,2} \phi_\ell + \bar{\omega}^T \Theta + \varepsilon_{\hat{z}_{12}} + \hat{d}_{si_1} + \dot{\hat{d}}_y \right) + \frac{\partial \alpha_{r-1}}{\partial \xi} \left( A_0 \xi + \bar{k} \hat{y} \right) + \frac{\partial \alpha_{r-1}}{\partial \tilde{\Theta}} \dot{\tilde{\Theta}} \sum_{j=1}^{\ell} \frac{\partial \alpha_{r-1}}{\partial v_j} \left( A_0 v_j + e_r \sigma_j \right) + \sum_{j=1}^{r-1} \frac{\partial \alpha_{r-1}}{\partial \hat{y}_m^{(j-1)}} \hat{y}_m^{(j)} \Bigg]$$

The overall Lyapunov function may now be chosen as

$$V_r = \sum_{j=1}^{r-1} V_j + \frac{1}{2} z_r^2 + \frac{1}{2} \Phi^T \Gamma^{-1} \Phi + \sum_{j=1}^{r} \frac{1}{4 d_j} \varepsilon^T P \varepsilon \tag{40}$$

where $\Gamma$ is a symmetric positive definite matrix, i.e., $\Gamma = \Gamma^T > 0$. With the definition of state estimated error $\varepsilon$, we can obtain that

http://dx.doi.org/10.5772/63082

$$\dot{V}_r = \sum_{j=1}^{r-1}\dot{V}_j + z_r\left\{\begin{array}{l} -k_r v_{\ell,1} + w_{1\ell} + w_{2\ell}\hat{u} \\ -\left[\dfrac{\partial \alpha_{r-1}}{\partial \hat{y}}\left(\xi_{12} + v_{\ell,2}\phi_\ell + \bar{\omega}^T\Theta + \varepsilon_{\hat{z}_{12}} + \hat{d}_{si_1} + \dot{\hat{d}}_y\right) + \dfrac{\partial \alpha_{r-1}}{\partial \xi}\left(A_0\xi + \bar{k}\hat{y}\right)\right. \\ \left. + \dfrac{\partial \alpha_{r-1}}{\partial \tilde{\Theta}}\dot{\tilde{\Theta}}\sum_{j=1}^{\ell}\dfrac{\partial \alpha_{r-1}}{\partial v_j}\left(A_0 v_j + e_r\sigma_j\right) + \sum_{j=1}^{r-1}\dfrac{\partial \alpha_{r-1}}{\partial \hat{y}_m^{(j-1)}}\hat{y}_m^{(j)}\right]\end{array}\right\}$$
$$+\dot{\Phi}^T\Gamma^{-1}\Phi - \sum_{j=1}^{r}\frac{1}{4d_j}\varepsilon^T\varepsilon + \sum_{j=1}^{r}\frac{1}{4d_j}\left(\varepsilon^T P\Delta + \Delta^T P\varepsilon\right)$$

Specify the control input as

$$\hat{u} = \frac{1}{z_r w_{2\ell}}\left\{ z_r k_r v_{\ell,1} - z_r w_{1\ell} + z_r\left[\frac{\partial \alpha_{r-1}}{\partial \hat{y}}\left(\xi_{12} + v_{\ell,2}\tilde{\phi}_\ell + \bar{\omega}^T\tilde{\Theta}\right) + \frac{\partial \alpha_{r-1}}{\partial \xi}\left(A_0\xi + \bar{k}\hat{y}\right) + \frac{\partial \alpha_{r-1}}{\partial \tilde{\Theta}}\dot{\tilde{\Theta}}\right.\right.$$
$$\left.\left.\sum_{j=1}^{\ell}\frac{\partial \alpha_{r-1}}{\partial v_j}\left(A_0 v_j + e_r\sigma_j\right) + \sum_{j=1}^{r-1}\frac{\partial \alpha_{r-1}}{\partial \hat{y}_m^{(j-1)}}\hat{y}_m^{(j)}\right] - c_r z_r^2 - d_r\left(\frac{\partial \alpha_{r-1}}{\partial \hat{y}}\right)^2 z_r^2 - g_r\left(\frac{\partial \alpha_{r-1}}{\partial \hat{y}}\right)^2 z_r^2 + z_r\hat{u}_{\hat{R}}\right\} \tag{41}$$

where $\hat{u}_{\hat{R}}$ is an addition input that will be used to target on rejection of uncertainties.

Substituting (41) into $\dot{V}_r$ and writing $\tau_r\Phi = \tau_{r-1}\Phi - \frac{\partial \alpha_{r-1}}{\partial \hat{y}}\left(z_r v_{\ell,1}\Phi_\ell + z_r\bar{\omega}^T\Phi\right)$, we arrive at

$$\dot{V}_r = -\sum_{j=1}^{r}\left(c_j z_j^2 + d_j\left(\frac{\partial \alpha_{j-1}}{\partial \hat{y}}\right)^2 z_j^2 + g_j\left(\frac{\partial \alpha_{j-1}}{\partial \hat{y}}\right)^2 z_j^2\right) + \left(\tau_r + \dot{\Phi}^T\Gamma^{-1}\right)\Phi + z_r\hat{u}_{\hat{R}}$$
$$-\sum_{j=1}^{r} z_j\frac{\partial \alpha_{j-1}}{\partial \hat{y}}\left(\varepsilon_{\hat{z}_{12}} + \hat{d}_{si_1} + \dot{\hat{d}}_y\right) - \sum_{j=1}^{r}\frac{1}{4d_j}\varepsilon^T\varepsilon + \sum_{j=1}^{r}\frac{1}{4d_j}\left(\varepsilon^T P\Delta + \Delta^T P\varepsilon\right) \tag{42}$$

From (42), we may specify the parameter update law to cancel the term $\left(\tau_r + \dot{\Phi}^T\,\Gamma^{-1}\right)\Phi$. To guarantee that the estimated parameters will always lie within allowable region $w$, a projected parametric update law will be specified as

$$\dot{\tilde{\Theta}} = \left\{\begin{array}{ll} \Gamma\tau_r^T & \text{if } \tilde{\Theta} \in w^0, \\ P_R(\Gamma\tau_r^T) & \text{if } \hat{\Theta} \in \partial w \text{ and } \tau_r\Gamma\tilde{\Theta}_{perp} > 0, \end{array}\right. \tag{43}$$

where $w$ is the allowable parametric set. It is compact and convex with its interior and boundary denoted by $w^0$ and $\partial w$, respectively. If the current estimated parametric vector locates within the allowable parametric set, the regular update law is used. If the current estimated parametric vector is on the boundary of the allowable parametric set, the projected

update law denoted by $P_R(.)$ is employed to stop the parametric vector from leaving the set. With (43), add and subtract terms $\sum_{j=1}^{r} \frac{1}{4g_j} | \hat{d}_{si_1} + \hat{\hat{d}}_y |^2$ to (42), we have

$$\begin{aligned}
\dot{V}_i \le & -\sum_{j=1}^{r} c_j z_j^2 - \sum_{j=1}^{r} d_j \left( \frac{\partial \alpha_{j-1}}{\partial \hat{y}} z_j + \frac{1}{2d_j} \varepsilon_{\hat{z}_{12}} \right)^2 \\
& - \sum_{j=1}^{r} g_j \left( \frac{\partial \alpha_{j-1}}{\partial \hat{y}} z_j + \frac{1}{2g_j} \left| \hat{d}_{si_1} + \dot{\hat{d}}_y \right| \right)^2 \\
& + \sum_{j=1}^{r} \frac{1}{4g_j} \left| \hat{d}_{si_1} + \dot{\hat{d}}_y \right|^2 + \sum_{j=1}^{r} \frac{1}{4d_i} \left( \varepsilon^T P \Delta + \Delta^T P \varepsilon \right) \\
& - \sum_{j=1}^{r} \frac{1}{4d_j} \left( \varepsilon_{\hat{z}11}^2 + \varepsilon_{\hat{z}13}^2 + \cdots + \varepsilon_{\hat{z}1r}^2 \right) + z_r \hat{u}_{\hat{R}}
\end{aligned} \tag{44}$$

The tracking error $Z_1(\tilde{s})$ and the control input $\hat{U}_{\hat{R}}(\tilde{s})$ are related by

$$\hat{U}_{\hat{R}}(\tilde{s}) = -\hat{R}(\tilde{s}) \hat{C}(\tilde{s}) Z_1(\tilde{s}) \tag{45}$$

where we have chosen $\hat{R}(\tilde{s})$ as a low-order and attenuated-type internal model filter, i.e.,

$$\hat{R}(\tilde{s}) = \prod_{i=1}^{k} \frac{\tilde{s}^2 + 2\zeta_i \omega_{ni} \tilde{s} + \omega_{ni}^2}{\tilde{s}^2 + 2\xi_i \omega_{ni} \tilde{s} + \omega_{ni}^2} \tag{46}$$

where $k$ is the number of periodic frequencies, $\omega_{ni}$ is the $i$th disturbance frequency in rad/rev, and $\xi_i$ and $\zeta_i$ are damping ratios satisfying $0<\xi_i<\zeta_i<1$. The gain of $\hat{R}(\tilde{s})$ at those periodic frequencies can be varied by adjusting the values of $\xi_i$ and $\zeta_i$.

**Theorem 3.1**

Consider the control law of (41) and (45) employed to a nonlinear system with unmodeled dynamics, parametric uncertainty, and output disturbance given by (30). Suppose that $\hat{y}_m$, $\hat{\hat{y}}_m$, $\cdots$, $\hat{y}_m^{(r)}$ (where $r$ is the relative degree) and $\hat{d}_y$, $\hat{\hat{d}}_y$, $\cdots$, $\hat{d}_y^{(r)}$ are known and bounded, $\hat{d}_{si_1}^{(r-1)}$, $\hat{d}_{si_2}^{(r-2)}$, $\cdots$, $\hat{\hat{d}}_{si_{r-1}}$ are sufficiently smooth, $f$, $g$, $h$, $L_f^r h$, $L_g L_f^{r-1} h$ are Lipschitz continuous functions, and at least one column of $\overline{W}(\hat{y})$ is bounded away from zero. Moreover, suppose that a loop-shaping filter $\hat{C}(\tilde{s})$ is specified to stabilized the feedback system. Then, the parametric update law given by (43) yields the bounded tracking error.

Proof: Refer to [36].

http://dx.doi.org/10.5772/63082

## 4. Spatial-based adaptive iterative learning control of nonlinear rotary systems with spatially periodic parametric variation

Consider an NTI system described by

$$\dot{x}(t) = f_t\left(x, \varphi_f(\theta)\right) + B_c g_t\left(x, \varphi_g(\theta)\right)u(t),\ y(t) = \Psi x(t) \tag{47}$$

where

$$x(t) = \left[x_1(t) \quad \cdots \quad x_n(t)\right]^T,\ \Psi = \left[0 \quad \cdots \quad 0 \quad 1\right],\ B_c = \left[0 \quad \cdots \quad 0 \quad 1\right]^T$$

$y(t)$ is the system output, $u(t)$ is the control input, and $\varphi_f(\theta)$=$[\varphi_1(\theta) \quad \cdots \quad \varphi_p(\theta)]$ and $\varphi_g(\theta)$ are system parameters that are periodic with respect to angular position $\theta$ (i.e., spatially periodic). Using the aforementioned change of coordinate, we may transform (47) in the time domain into

$$\hat{\omega}(\theta)\dot{\hat{x}}(\theta) = f_t\left(\hat{x}, \varphi_f(\theta)\right) + B_c g_t\left(\hat{x}, \varphi_g(\theta)\right)\hat{u}(\theta),\ \hat{y}(\theta) = \Psi\hat{x}(\theta) \tag{48}$$

in the $\theta$-domain. If $\hat{\omega}(\theta)$ equals one of the state variables, (48) is an NPI system in the $\theta$-domain.

**Remark 4.1.** As mentioned previously, uncertainties for rotary systems may be treated as periodic disturbances or periodic parameters. Periodic parametric variation is, in fact, a sensible and practical assumption.

### 4.1 Definitions and assumptions

In this section, we list and present the definitions and assumptions to be used in the subsequent sections.

**Definition 4.1**. (Lie derivative) The Lie derivative is defined as

$$L_f^0 h(x) = h(x),\ L_f h(x) = \frac{\partial h}{\partial x} f(x), L_f^2 h(x) = L_f L_f h(x) = \frac{\partial\left(L_f h\right)}{\partial x} f(x), L_g L_f h(x) = \frac{\partial\left(L_f h\right)}{\partial x} g(x), \ldots$$

**Definition 4.2**. (Diffeomorphism) A diffeomorphism is considered as a mapping $T(.): D \subset R^n \to R^n$ being continuously differentiable on $D$ and has a continuously differentiable inverse $T^{-1}(.)$.

**Definition 4.3**. (Adaptation rate) Instead of constant adaptation rate in regular adaptive control, a varying adaptation rate will be used. Consider a matrix $\Gamma(\theta,\ \varphi_c)$ defined by

$$\Gamma(\theta,\varphi_c)=\begin{cases}0, & \theta=0\\ \alpha(\theta), & 0<\theta<\varphi_c\\ \beta, & \varphi_c\le\theta\end{cases} \tag{49}$$

where $\varphi_c$ is the lowest common multiple of the parametric periods, $\beta=diag\{\beta_1 \ \cdots \ \beta_\ell\}$ with nonzero positive constant $\beta_i$, and $\alpha(\theta)=diag\{\alpha_1(\theta) \ \cdots \ \alpha_\ell(\theta)\}$ with $\alpha_i(\theta)$ a strictly increasing function, $\alpha_i(0)=0$, and $\alpha_i(\varphi_c)=\beta_i$.

**Assumption 4.1**. The desired trajectory (or reference command signal) $y_m$ is sufficiently smooth or $y_m^{(n)}$, $y_m^{(n-1)}$, $\cdots$, $\dot{y}_m$ exists.

**Assumption 4.2.** For a $\theta$-domain NPI system described by

$$\hat{\dot{x}}(\theta)=f\left(\hat{x}(\theta),\varphi_f(\theta)\right)+B_c g\left(\hat{x}(\theta),\varphi_g(\theta)\right)\hat{u}(\theta),\ \hat{y}(\theta)=\Psi\hat{x}(\theta)$$

the nonlinear functions $f(\hat{x}(\theta))$ and $g(\hat{x}(\theta))$ are assumed to linearly relate to the system parameters $\varphi_f$ and $\varphi_g$, i.e.,

$$f\left(\hat{x}(\theta),\varphi_f(\theta)\right)=\sum_{i=1}^{p}\varphi_i(\theta)f_i\left(\hat{x}(\theta)\right),\ g\left(\hat{x}(\theta),\varphi_g(\theta)\right)=\varphi_g(\theta)g\left(\hat{x}(\theta)\right)$$

**Remark 4.2**. Assumption 1 may be satisfied by considering a reference trajectory without sudden change of slope. Assumption 2 may be satisfied by many systems, e.g., LTI and NTI systems.

### 4.2 Spatial-based adaptive iterative learning control

For tidy presentation, the $\theta$ notation will be dropped from most of the equations in the sequel. Rewrite (48) as

$$\hat{\dot{x}}=f\left(\hat{x},\varphi_f\right)+B_c g\left(\hat{x},\varphi_g\right)\hat{u},\ \hat{y}=\hat{\omega}=\Psi\hat{x} \tag{50}$$

where the output $\hat{y}$ is equal to the angular velocity $\hat{\omega}$, which is set to be the first state of the system. Also note that

$$f\left(\hat{x},\varphi_f\right)=f_t\left(\hat{x},\varphi_f\right)/\hat{x}_1 \text{ and } g\left(\hat{x},\varphi_g\right)=g_t\left(\hat{x},\varphi_g\right)/\hat{x}_1$$

http://dx.doi.org/10.5772/63082

The system (50) is valid within the set $D_0=\{\hat{x}\in R \mid \hat{x}_1\neq 0\}$. Within this set, a diffeomorphism $T(\hat{x}): D_0\subset D$ (as defined previously) exists and may be described by

$$\hat{z}=T(\hat{x})=\begin{bmatrix} L_f^0 h(\hat{x}) & L_f h(\hat{x}) & \cdots & L_f^{n-1}h(\hat{x})\end{bmatrix}^T \tag{51}$$

where $\hat{z}=[\hat{z}_1 \quad \cdots \quad \hat{z}_n]^T$. Using (51), we may transform (50) into

$$\dot{\hat{z}}=A_c\hat{z}+B_c\left[L_f^n h(\hat{x})+L_g L_f^{n-1}h(\hat{x})\hat{u}\right]_{\hat{x}=T^{-1}(\hat{z})},\ \hat{y}=\hat{z}_1 \tag{52}$$

where

$$A_c=\begin{bmatrix} 0 & I_{(n-1)\times(n-1)} \\ 0 & 0_{1\times(n-1)}\end{bmatrix}$$

According to Assumption 3.2, we may rewrite (52) as

$$\dot{\hat{z}}=A_c\hat{z}+B_c\left[\rho(\hat{z})+\Theta^T W_f(\hat{z})+\varphi_g W_g(\hat{z})\hat{u}\right],\ \hat{y}=\hat{z}_1 \tag{53}$$

where $\Theta=[\varphi_1 \quad \cdots \quad \varphi_p \quad \varphi_g \quad \cdots]^T$ is the actual parametric vector, $\varphi_g$ is a parameter mapped via the diffeomorphism, $W_f(\hat{z})$ is a vector of nonlinear terms, and $\rho(\hat{z})$ and $W_g(\hat{z})$ are two nonlinear functions.

Consider a reference trajectory $y_m(t)$ satisfying Assumption 3.1, which may be transformed into its counterpart in the $\theta$-domain, i.e., $\hat{y}_m(\theta)=y_m(\lambda^{-1}(\theta))=y_m(t)$. Define another state or coordinate transformation:

$$\hat{z}_{1r}=\hat{y}_m(\theta),\ \hat{z}_{2r}=\dot{\hat{y}}_m(\theta),\cdots,\ \hat{z}_{nr}=\hat{y}_m^{(n-1)}(\theta).$$

We may form a state space model, which produces the reference trajectory, as

$$\dot{\hat{z}}_r=A_c\hat{z}_r+B_c\hat{y}_m^{(n)} \tag{54}$$

where $\hat{z}_r=[\hat{z}_{1r} \quad \cdots \quad \hat{z}_{nr}]^T$. Define the tracking error as $\hat{e}=\hat{z}-\hat{z}_r$. Then, the error dynamics can be obtained using the first equation of (53) and (54), i.e.,

$$\dot{\hat{e}} = A\hat{e} + B_c\left[\Theta^T W_f + \rho + \sigma - \hat{y}_m^{(n)} + \varphi_g W_g \hat{u}\right] \tag{55}$$

where $\sigma = c\hat{e}$ with $c = [c_1 \quad \cdots \quad c_{n-1} \quad 1]$, and

$$A = \begin{bmatrix} 0_{(n-1)\times 1} & I_{(n-1)\times(n-1)} \\ & c \end{bmatrix}$$

Next, specify an LKF as

$$V = \sigma^2/2\varphi_g + 1/2\int_{\theta-\varphi_c}^{\theta} \Phi^T(\tau)\beta^{-1}\Phi(\tau)d\tau \tag{56}$$

where $\Phi = \bar{\Theta} - \tilde{\bar{\Theta}}$ and $\bar{\Theta}$ is a vector of parameters (to be defined later). $\tilde{\bar{\Theta}}$ is the estimate of $\bar{\Theta}$. The objective for the following steps is to establish a suitable control input and parametric update law rendering the derivative of the LKF negative semidefinite. Calculating the derivative of $V$, we obtain

$$\dot{V} = V_1 + V_2\ ,\ V_1 = \frac{\sigma}{\varphi_g}c\dot{\hat{e}} - \frac{\sigma^2}{2\varphi_g^2}\dot{\varphi}_g,\ V_2 = 1/2\left[\Phi^T(\theta)\beta^{-1}\Phi(\theta) - \Phi^T(\theta-\varphi_c)\beta^{-1}\Phi(\theta-\varphi_c)\right]. \tag{57}$$

Substituting the error dynamics (55) into $V_1$ and recalling that $\sigma = c\hat{e}$, we have

$$V_1 = \sigma\left[\frac{1}{\varphi_g}\left(\bar{c}\hat{e} + \rho - \hat{y}_m^{(n)}\right) + \frac{\Theta^T}{\varphi_g}W_f - \frac{\dot{\varphi}_g}{\varphi_g}\frac{\sigma^2}{2} + W_g\hat{u}\right]. \tag{58}$$

where $\bar{c} = [0 \quad c_1 \quad \cdots \quad c_{n-1}]$. Hence, we may specify $\hat{u}$ as

$$\hat{u} = -1/W_g\left(k\sigma + \tilde{\bar{\Theta}}^T W\right), \tag{59}$$

where $k$ is a positive variable, $\tilde{\bar{\Theta}}$ is the corresponding estimate of

$$\bar{\Theta} = \begin{bmatrix} \frac{1}{\varphi_g} & \frac{\Theta^T}{\varphi_g} & \frac{\dot{\varphi}_g}{\varphi_g} \end{bmatrix}^T, \text{ and } W = \begin{bmatrix} \left(\bar{c}\hat{e} + \rho - \hat{y}_m^{(n)}\right) & W_f & -\frac{\sigma^2}{2} \end{bmatrix}^T.$$

http://dx.doi.org/10.5772/63082

This will simplify $V_1$, i.e.,

$$V_1 = -k\sigma^2 + \sigma\Phi^T W \tag{60}$$

Using the periodicity of $\bar{\Theta}(\theta)=\bar{\Theta}(\theta-\varphi_c)$, we may rewrite $V_2$ as

$$V_2 = 1/2\left[\left(\bar{\Theta}-\tilde{\bar{\Theta}}\right)^T \beta^{-1}\left(\bar{\Theta}-\tilde{\bar{\Theta}}\right)-\left(\bar{\Theta}-\tilde{\bar{\Theta}}(\theta-\varphi_c)\right)^T \beta^{-1}\left(\bar{\Theta}-\tilde{\bar{\Theta}}(\theta-\varphi_c)\right)\right]. \tag{61}$$

According to the following algebraic relationship,

$$(a-b)^T \beta(a-b)-(a-c)^T \beta(a-c) = 1/2(c-b)^T \beta\left[2(a-b)+(b-c)\right]$$

where *a*, *b*, and *c* are vectors, (61) implies that

$$V_2 = 1/2\left(\tilde{\bar{\Theta}}(\theta-\varphi_c)-\tilde{\bar{\Theta}}\right)^T \beta^{-1}\left[2\left(\bar{\Theta}-\tilde{\bar{\Theta}}\right)+\left(\tilde{\bar{\Theta}}-\tilde{\bar{\Theta}}(\theta-\varphi_c)\right)\right] \tag{62}$$

Therefore, we may specify a periodic parametric update law as

$$\dot{\tilde{\bar{\Theta}}}(\theta) = \dot{\tilde{\bar{\Theta}}}(\theta-\varphi_c)+\Gamma(\theta,\varphi_c)W\sigma;\ \tilde{\bar{\Theta}}(\theta)=0 \text{ if } -\varphi_c \le \theta \le 0 \tag{63}$$

Recall that $\Gamma(\theta,\ \varphi_c)$ is the adaptation rate as defined in (49). For $\varphi_c \le \theta$, $V_2$ becomes

$$V_2 = -\sigma\Phi^T W - 1/2\,\sigma^T W^T \beta W\sigma \tag{64}$$

With (60) and (64), we conclude that

$$\dot{V} = -k\sigma^2 - 1/2\,\sigma^T W^T \beta W\sigma \le -k\sigma^2 \tag{65}$$

The objective is achieved. The main results are summarized in the following theorem.

**Theorem 4.1** Consider a spatial-based nonlinear system (50) with spatially periodic parameters satisfying Assumption 3.2. The error dynamics described by (55) exists under Assumption 3.1. Assume that the control input is determined by (59) along with the periodic parametric adaptation law (63). Then, the tracking error $\hat{e}$ will converge to 0 with the performance characteristics described by

$$\int_{\theta-\varphi_c}^{\theta} \|\hat{e}\|^2 \, d\tau \to 0, \, as \, \theta \to \infty$$

**Proof:** Refer to [37].

## 5. Conclusion

Adaptive fuzzy control (AFC) has been investigated for coping with nonlinearities and uncertainties of unknown structures [38–40]. The major distinctions between AFC techniques and the ones described in Sections 2 and 3 are (a) time-based (AFC) versus spatial-based design (OFLRARC/OFBRARC) and (b) less information assumed on the nonlinearities/uncertainties (AFC) versus more information on the nonlinearities/uncertainties (OFLRARC/OFBRARC). Because, in spatial-based design, a nonlinear coordinate transformation is conducted to change the independent variable from time to angular displacement, the systems under consideration in AFC and OFLRARC/OFBRARC are distinct. Next, AFC design techniques claim being able to tackle systems with a more generic class of nonlinearities/uncertainties, which relies on incorporating a fuzzy system to approximate those nonlinearities/uncertainties. It is not clear how to determine the required structure complexity of the fuzzy system (e.g., number of membership functions) to achieve desired control performance with reasonable control effort. Generally speaking, known characteristics of the uncertainties or disturbances should be incorporated as much as possible into the control design to improve performance, avoid conservativeness, and produce sensible control input. Therefore, instead of assuming the disturbances to be of generic type (as done by AFC), the methods presented in this chapter aim at a category of disturbances prevalent in rotary systems and explore the spatially periodic nature of the disturbances to design a specific control module and integrate into the overall control system.

## Acknowledgements

The author gratefully acknowledges the support from the Ministry of Science and Technology, R.O.C. under grant MOST104-2221-E-005-043.

## Author details

Cheng-Lun Chen

Address all correspondence to: chenc@dragon.nchu.edu.tw

National Chung Hsing University, Taiwan, R.O.C

http://dx.doi.org/10.5772/63082

## References

[1] Ding Z. Adaptive disturbance rejection of nonlinear systems in an extended output feedback form. Control Theory & Applications, IET. 2007;1(1):298–303.

[2] Priscoli FD, Marconi L, Isidori A. A new approach to adaptive nonlinear regulation. SIAM Journal on Control and Optimization. 2006;45(3):829–55.

[3] Francis BA, Wonham WM. The internal model principle of control theory. Automatica. 1976;12(5):457–65.

[4] Kravaris C, Sotiropoulos V, Georgiou C, Kazantzis N, Xiao M, Krener AJ. Nonlinear observer design for state and disturbance estimation. Systems & Control Letters. 2007;56(11):730–5.

[5] Chen W-H. Disturbance observer based control for nonlinear systems. Mechatronics, IEEE/ASME Transactions on. 2004;9(4):706–10.

[6] Ding Z. Asymptotic rejection of asymmetric periodic disturbances in output-feedback nonlinear systems. Automatica. 2007;43(3):555–61.

[7] Liu ZL, Svoboda J. A new control scheme for nonlinear systems with disturbances. Control Systems Technology, IEEE Transactions on. 2006;14(1):176–81.

[8] Tang G-Y, Gao D-X. Approximation design of optimal controllers for nonlinear systems with sinusoidal disturbances. Nonlinear Analysis: Theory, Methods & Applications. 2007;66(2):403–14.

[9] Teoh J, Du C, Xie L, Wang Y. Nonlinear least-squares optimisation of sensitivity function for disturbance attenuation on hard disk drives. Control Theory & Applications, IET. 2007;1(5):1364–9.

[10] Bullinger E, Allgöwer F, editors. An adaptive high-gain observer for nonlinear systems. In Decision and Control, Proceedings of the 36th IEEE Conference on; 1997; San Diego. California: IEEE.

[11] Marine R, Santosuosso GL, Tomei P. Robust adaptive observers for nonlinear systems with bounded disturbances. Automatic Control, IEEE Transactions on. 2001;46(6):967–72.

[12] Vargas JAR, Hemerly E, editors. Nonlinear adaptive observer design for uncertain dynamical systems. IEEE Conference on Decision and Control; 2000: Citeseer.

[13] Kanellakopoulos I, Kokotovic P, Morse A, editors. Adaptive output-feedback control of a class of nonlinear systems. Decision and Control, Proceedings of the 30th IEEE Conference on; 1991: IEEE.

[14] Yang Z-J, Kunitoshi K, Kanae S, Wada K. Adaptive robust output-feedback control of a magnetic levitation system by K-filter approach. Industrial Electronics, IEEE Transactions on. 2008;55(1):390–9.

[15] Marino R, Tomei P. Global adaptive observers for nonlinear systems via filtered transformations. Automatic Control, IEEE Transactions on. 1992;37(8):1239–45.

[16] Marino R, Tomei P. Global adaptive output-feedback control of nonlinear systems. I. Linear parameterization. Automatic Control, IEEE Transactions on. 1993;38(1):17–32.

[17] Chi R, Hou Z, Sui S, Yu L, Yao W. A new adaptive iterative learning control motivated by discrete-time adaptive control. International Journal of Innovative Computing, Information and Control. 2008;4(6):1267–74.

[18] Nakano M, She J-H, Mastuo Y, Hino T. Elimination of position-dependent disturbances in constant-speed-rotation control systems. Control Engineering Practice. 1996;4(9): 1241–8.

[19] Chen C-L, Chiu GT-C. Spatially periodic disturbance rejection with spatially sampled robust repetitive control. Journal of Dynamic Systems, Measurement, and Control. 2008;130(2):021002.

[20] Moore KL. Iterative Learning Control for Deterministic Systems. Springer Science & Business Media; 2012.

[21] Xu J-X, Tan Y. Linear and Nonlinear Iterative Learning Control. New York: Springer; 2003.

[22] De Wit CC, Praly L. Adaptive eccentricity compensation. Control Systems Technology, IEEE Transactions on. 2000;8(5):757–66.

[23] Tsao T-C, Bentsman J. Rejection of unknown periodic load disturbances in continuous steel casting process using learning repetitive control approach. Control Systems Technology, IEEE Transactions on. 1996;4(3):259–65.

[24] Chen CL, Yang YH. Position-dependent disturbance rejection using spatial-based adaptive feedback linearization repetitive control. International Journal of Robust and Nonlinear Control. 2009;19(12):1337–63.

[25] Chen C-L, Chiu GT-C, Allebach J. Robust spatial-sampling controller design for banding reduction in electrophotographic process. Journal of Imaging Science and Technology. 2006;50(6):530–6.

[26] Mahawan B, Luo Z-H. Repetitive control of tracking systems with time-varying periodic references. International Journal of Control. 2000;73(1):1–10.

[27] Ahn H, Chen Y, Dou H. State-periodic adaptive cogging and friction compensation of permanent magnetic linear motors. Magnetics, IEEE Transactions on. 2005;41(1):90–8.

http://dx.doi.org/10.5772/63082

[28] Moore KL, Ghosh M, Chen YQ. Spatial-based iterative learning control for motion control applications. Meccanica. 2007;42(2):167–75.

[29] Fardad M, Jovanović MR, Bamieh B. Frequency analysis and norms of distributed spatially periodic systems. Automatic Control, IEEE Transactions on. 2008;53(10):2266–79.

[30] Al-Shyyab A, Kahraman A. Non-linear dynamic analysis of a multi-mesh gear train using multi-term harmonic balance method: period-one motions. Journal of Sound and Vibration. 2005;284(1):151–72.

[31] Young T, Wu M. Dynamic stability of disks with periodically varying spin rates subjected to stationary in-plane edge loads. Journal of Applied Mechanics. 2004;71(4): 450–8.

[32] Yang Y-H, Chen C-L, editors. Spatially periodic disturbance rejection using spatial-based output feedback adaptive backstepping repetitive control. American Control Conference; 2008: IEEE.

[33] Sastry SS, Isidori A. Adaptive control of linearizable systems. Automatic Control, IEEE Transactions on. 1989;34(11):1123–31.

[34] Peterson BB, Narendra KS. Bounded error adaptive control. Automatic Control, IEEE Transactions on. 1982;27(6):1161–8.

[35] Khalil HK, Grizzle J. Nonlinear Systems: Prentice-Hall, New Jersey; 1996.

[36] Yang Y-H, Chen C-L. Spatial domain adaptive control of nonlinear rotary systems subject to spatially periodic disturbances. Journal of Applied Mathematics. 2012;2012.

[37] Yang Y-H, Chen C-L, editors. Spatial-based adaptive iterative learning control of nonlinear rotary systems with spatially periodic parametric variation. Asian Control Conference, ASCC 7th; 2009: IEEE.

[38] Tong S-C, He X-L, Zhang H-G. A combined backstepping and small-gain approach to robust adaptive fuzzy output feedback control. Fuzzy Systems, IEEE Transactions on. 2009;17(5):1059–69.

[39] Tong S, Li Y. Observer-based fuzzy adaptive control for strict-feedback nonlinear systems. Fuzzy Sets and Systems. 2009;160(12):1749–64.

[40] Shaocheng T, Changying L, Yongming L. Fuzzy adaptive observer backstepping control for MIMO nonlinear systems. Fuzzy Sets and Systems. 2009;160(19):2755–75.

Chapter 6

# Sequential Optimization Model for Marine Oil Spill Control

Kufre Bassey

Additional information is available at the end of the chapter

http://dx.doi.org/10.5772/63050

**Abstract**

This chapter gives credence to the introduction of optimal control theory into oil spill modeling and develops an optimization process that will aid in the effective decision-making in marine oil spill management. The purpose of the optimal control theory is to determine the control policy that will optimize (maximize or minimize) a specific performance criterion, subject to the constraints imposed by the physical nature of the problem. A fundamental theorem of the calculus of variations is applied to problems with unconstrained states and controls, whereas a consideration of the effect of control constraints leads to the application of Markovian decision processes. The optimization objectives are expressed as value function or reward to be optimized, whereas the optimization models are formulated to adequately describe the marine oil spill control, starting from the transportation process. These models consist of conservation relations needed to specify the dynamic state of the process given by the chemical compositions and movements of crude oil in water.

**Keywords:** decision theory, marine oil spill, optimal control, sequential optimization, Markov processes

## 1. Introduction

The degradation of aquatic ecosystem is generally agreed to be undesirable. Historically, most evaluations of the ecological effects of petroleum contamination have related impacts to effects on the supply of products and services of importance to human cultures. According to Xu and Pang [1], most of the environmental and pollution control laws were legislated to protect ecological objectives and public health. Here, a substance is considered to be a pollutant if it is perceived to have adverse effects on wildlife or human well-being. In recent years, a number

of substances appear to pose such threats. Among them is crude oil spillage, which first came to public attention with the *Torrey Canyon* disaster in 1967.

The risk of crude oil spillage to the sea presents a major threat to the marine ecology compared with other sources of pollution in the oceans. Before now, it was earlier reported that oil spillage impacts negatively on wildlife and their environments in various ways, which include the alteration of the ecological conditions, and can result into alterations of the environmental physical and chemical composition, destruction of nutritional capita of the marine biomass, changes in the biological equilibrium of the habitat, and as a threat to human health [2]. The same can also be said about Nigeria, where oil spillage is a major environmental problem and its coastal zone is rated as one of the most polluted spots on the planet in the year 2006 [3]. For instance, from 1976 to 2007, over 1,896,960 barrels of oil were sunk into the Nigerian coastal waters resulting in a serious pollution of drinkable water and destruction of resort centers, properties, and lives along the coastal zone. This was seen to be a major contributor to the regional crisis in the Nigeria Niger-Delta region.

As a case in point, after a spill in the ocean, oil in water body, regardless of whether it originated as surface or subsurface spill, forms a thin film called oil slick as it spreads in water. The oil slick movement is governed by the advection and blustery diffusion as a result of water current and wind action. The slick always spreads over the water surface due to gravitational, inertia, gluey, and interfacial strain force equilibrium. The oil composition also changes from the early time of the spill. Thus, the water-soluble components of the oil dissolve in the water column, whereas the immiscible components emulsified and disperse in the water column as small droplets and light (low molecular weight) fractions evaporate (for example, see [4]).

In essence, the frequency of accidental oil spills in aquatic environments has presented a growing global concern and awareness of the risks of oil spills and the damage they do to the environment. However, it is widely known that oil exploration is a necessity in our industrial society and a major sustainer of our lifestyle, as most of the energy used in Canada and the United States, for instance, is for transportation that runs on oil and petroleum products. Thus, in as much as the industry uses oil and petroleum derivatives for the manufacturing of vital products, such as plastics, fertilizers, and chemical feedstock, the drifts in energy usage are not likely to decrease much in the near future. In what follows, it is a global belief that the production and consumption of oil and petroleum products might continue to increase worldwide while the threat of oil pollution is also likely to increase accordingly.

Consequently, a fundamental problem in environmental research in recent time has been identified in the literature to how to properly assess and control the spatial structure of pollution fields at various scales, and several studies showed that mathematical models were the only available tools for rapid computations and determinations of spilled oil fate and for the simulation of the various clean-up operations.

http://dx.doi.org/10.5772/63050

## 2. Methodological model

Now, consider the introduction of an optimal control theory into spill modeling to develop an optimization process that will aid effective decision-making in marine oil spill management. The purpose of the optimal control theory is to determine the control policy that will optimize (maximize or minimize) a specific performance criterion subject to the constraints imposed by the physical nature of the problem. A fundamental theorem of the calculus of variations is applied to problems with unconstrained states and controls, whereas a consideration of the effect of control constraints leads to the application of Markovian decision processes.

The optimization objectives are expressed as a performance index (value function or reward) to be optimized, whereas the optimization models are formulated to adequately describe the marine oil spill control starting from the transportation process. These models consist of conservation relations needed to specify the dynamic state of the process given by the chemical compositions and movements of crude oil in water.

### 2.1. Mathematical preliminaries and definition of terms

In our basic optimal control problem, $u(t)$ is used for the control and $x(t)$ is used for the state variables. The state variable satisfies a differential equation that depends on the control variable:

$$x'(t) = g\left(t, x(t), u(t)\right) \tag{1}$$

where $x'(t)$ is the state differential defining the performance index. This implies that, as a control function changes, the solution to the differential equation will also change. In other words, one can view the control-to-state relationship as a map $u(t) \mapsto x = x(u)$ [we wrote $x(u)$ just to remind us of the dependence on $u$]. Our basic optimal control problem therefore consisted of finding, in mathematical terms, a piecewise continuous control $u(t)$ and the associated state variable $x(t)$ to optimize a given objective function. That is to say,

$$\max_{u} \int_{t_0}^{t_1} f\left(t, x(t), u(t)\right) dt \tag{2}$$

$$\begin{aligned} & x'(t) = g\left(t, x(t), u(t)\right) \\ \textit{Subject to} \quad & \\ & x(t_0) = 0 \quad \textit{and} \quad x(t_1)\ \textit{free} \end{aligned} \tag{3}$$

Such a maximizing control is called an optimal control. By "$x(t_1)$ free", it means that the value of $x(t_1)$ is unrestricted. Here, the functions $f$ and $g$ are continuously differentiable functions in

all arguments. Thus, whereas the control(s) is piecewise continuous, the associated states are piecewise differentiable. This implies that, depending on the scale of the spatial resolution (like the case of oil spill), an introduction of space variables could alter the basic model from ordinary differential equations (with just time as the underlying variable) to partial differential equations (PDEs). Let us focus our attention to the consideration of optimal control of PDEs. Our solution to the control problem will then depend on the existence of an optimal control in the PDE.

The general idea of the optimal control of PDEs here starts with a PDE with a state solution $x$ and control $u$. Set ∂ to denote a partial differential operator with appropriate initial and boundary conditions:

$$\partial x = f\left(x,u\right)\text{in}\,\Omega\times\left[0,T\right] \tag{4}$$

This implies that we are considering a problem with space $x$ and time $t$ within a territorial boundary, $\Omega\times[0,\ T]$. The objective functional in this problem represents the goal of the problem, and we seek to find an optimal control $u^*$ in an appropriate control set such that

$$J\left(u^*\right)=\min_u J\left(u\right) \tag{5}$$

When the control cost is considered, with an objective functional

$$J\left(u\right)=\int_0^T\int_\Omega g\left(x,t,x\left(t\right),u\left(x,t\right)\right)dxdt \tag{6}$$

To consider the properties of the functional, it is important to note the following fundamentals:

**i.** A functional $J$ is "a rule of correspondence that assigns to each function, say $x(t)$, constrained in a certain set of functions, say $X$, a unique real number. The set of functions is called the domain of the functional, and the set of real numbers associated with the functions in the domain is called the range of the functional" [5].

**ii.** Let $\delta(J)$ be the first variation of the functional; thus, $\delta(J)$ is the part of the increment of $\Delta J$, which is linear in the variation $\delta(x)$ such that

$$\Delta J\left(x,\delta\left(x\right)\right)=\delta\left(J\right)\left[x,\delta\left(x\right)\right]+g\left(x,\delta\left(x\right)\right)\left\|\delta\left(x\right)\right\| \tag{7}$$

where $\delta(J)$ is also linear in $\delta(x)$. Suppose that $\lim_{\|\delta(x)\|\to 0} g(x,\ \delta(x))=0$; then, $J$ is said to be differentiable on $x$, whereas $\delta(J)$ is the first variation of $J$ evaluated for $x(t)$ [5].

http://dx.doi.org/10.5772/63050

**iii.** A functional $J$ with domain $X$ has a relative optimum at $x^*$ if there is an $\varepsilon>0$, such that, for all functions $x \in X$, which satisfy that $\| x-x^* \| < \varepsilon$, the increment of $J$ has the same sign. In other words, $J(x^*)$ is a relative minimum if $\Delta J = J(x)-J(x^*) \geq 0$ and a relative maximum if $\Delta J = J(x)-J(x^*) \leq 0$. Hence, $J$ is said to be a functional of the function $x(t)$ if and only if it first satisfies the scalar commutative property $J(\alpha x)=\alpha J(x)$ for all $x \in X$ and for all real numbers $\alpha$ such that $\alpha x \in X$.

**iv.** A rule of correspondence that assigns to each function $x(t) \in X$, defined for $t \in [t_0, T]$, a real number is called the norm of a function, where the norm of $x$ is given as $\| x \|$. If $x$ and $x+\delta(x)$ are both functions for which the functional $J$ is defined, then the increment of the functional $\Delta J$ is defined as

$$\Delta J = J\left(x+\delta\left(x\right)\right) - J\left(x\right) \tag{8}$$

**v.** A differential equation whose solutions are the functions for which a given functional is stationary is known as an Euler-Lagrange equation (Euler's equation or Lagrange's equation).

**Fundamental theorem of variational calculus [5]:** This theorem states that "if $x^*$ is optimum, then it is a necessary condition that the first variation of $J$ must vanish on $x$. That is to say, $\delta(J)[x^*, \delta(x)]=0$ for all admissible $\delta(x)$".

### 2.2. Model conceptualization

The fundamental principle upon which the pollutant fate and transport models are based is the law of conservation of mass [6]:

$$\begin{cases} \dfrac{\partial h}{\partial t} + \bar{\nabla}\left(h\bar{v}\right) - \bar{\nabla}\left(D\bar{\nabla}h\right) = R_h \\ \dfrac{\partial \mathbf{C}}{\partial t} + \vec{\nabla}\left(\mathbf{C}\vec{\mathbf{u}}\right) - \vec{\nabla}\left(\vec{E}\vec{\nabla}\mathbf{C}\right) = \mathbf{R} \end{cases} \tag{9}$$

where

$h$ = oil slick thickness,

$\mathbf{C}$ = oil concentration,

$\bar{v}$ = oil slick drifting velocity,

$D$ = oil fluid velocity,

$\vec{E}$ = dispersion-diffusion coefficient,

$\vec{\nabla}$ = computational slick spreading function,

$R_h$ and $\mathbf{R}$ = physical chemical kinetic terms,

$\vec{\mathbf{u}}$ = grid size,

$\overline{\nabla}$ = Cartesian coordinate, and

$t$ = time.

Eq. (9) can be modified as

$$\frac{\partial \gamma_i}{\partial i} dxdydz,$$

where $dxdydz$ denotes the differential volume of the state variable assuming a net chemical contaminant flux in each axial direction such that $\gamma_i$ = contaminant movement in each axial direction ($i = x, y, z$) and $dx, dy, dz$ = differential distances in the $x$, $y$, and $z$ directions.

The fluidity of oil in water contains the advection due to current and wind as well as the dispersive instability due to weathering processes. Thus, if we set

$$\gamma = \omega q - d\nabla q \tag{10}$$

where

$\gamma$ = movement of contaminant vector,

$\omega$ = contaminant discharge vector,

$q$ = contaminant molar concentration,

$d$ = dispersion tensor, and

$\nabla$ = gradient operator (Laplacian).

With minor mathematical regularities, Eq. (10) will become

$$-\nabla\left(\omega q - d\nabla q\right) = \frac{\partial \tau}{\partial t} + m \tag{11}$$

where

$\tau$ = total concentration of contaminant in the system,

$m$ = decay rate of contaminant, and

$t$ = time.

A two-dimensional differential representation of Eq. (11) is given as

http://dx.doi.org/10.5772/63050

$$\begin{aligned}\frac{\partial \tau}{\partial t} &= \left[ c\frac{\partial v_x}{\partial x} + v_x\frac{\partial q}{\partial x} + \frac{\partial v_x}{\partial x}\frac{\partial q}{\partial x} + v_x\frac{\partial^2 q}{\partial x^2} - q\frac{\partial v_y}{\partial y} - v_y\frac{\partial q}{\partial y} + \frac{\partial v_y}{\partial y}\frac{\partial q}{\partial y} + v_y\frac{\partial^2 q}{\partial y^2}\right] - m \\ &= \frac{\partial\left(q.v_x\right)}{\partial x} + \frac{\partial\left[v_x\dfrac{\partial q}{\partial x}\right]}{\partial x} - \frac{\partial\left(q.v_y\right)}{\partial y} + \frac{\partial\left[v_y\dfrac{\partial q}{\partial y}\right]}{\partial y} - m,\end{aligned} \tag{12}$$

so that we have $v_x$ and $v_y$, which represented the fluid velocities in the $x$ and $y$ directions. By applying the principle of the conservation of mass, the steady-state equation of spill transportation is given as

$$\begin{aligned}\frac{2VST}{dxdylb} &= \frac{\partial h_x}{\partial x}\frac{\partial p^2}{\partial x} + h_x\frac{\partial^2 p^2}{\partial x^2} + \frac{\partial h_y}{\partial y}\frac{\partial p^2}{\partial y} + h_y\frac{\partial^2 p^2}{\partial y^2} \\ &= \frac{\partial}{\partial x}\left[h_x\frac{\partial p^2}{\partial x}\right] + \left[h_y\frac{\partial p^2}{\partial y}\right]\end{aligned} \tag{13}$$

where

$h$ = oil penetrability trajectory,

$p$ = oil stress,

$V$ = oil viscidness,

$S$ = source of oil mass fluidity,

$T$ = temperature,

$b$ = molecular weight of oil, and

$l$ = a fixed length of the $z$ direction.

According to Refs. [5–7], "the transport and fate of the spilled oil is governed by the advection due to current and wind, horizontal spreading of the surface slick due to turbulent diffusion, gravitational force, force of inertia, viscous and surface tension forces, emulsification, mass transfer of heat, and changes in the physiochemical properties of oil due to weathering processes (evaporation, dispersion, dissolution, oxidation, etc.)". Thus, Eq. (13) can be transformed to

$$\frac{\partial q(x,t)}{\partial t} = -h_x\frac{\partial}{\partial x}q(x,t) + D\frac{\partial^2}{\partial x^2}q(x,t) + R + S \tag{14}$$

where $q=\{q_e, q_d, q_p\}$ denotes the oil spill concentration in emulsified, dissolved, and particulate phases, respectively, at state $x$ and time $t$; $h$ is the fluid velocity; $D$ is the spreading function, and $R$ and $S$ denote the environmental factors and the spill source term, respectively.

### 2.3. Optimality problem

When hydrocarbons enter an aquatic environment, their concentrations tend to decrease with time due to the evaporation, oxidation, and other weathering processes. This could be described as a death process and could be modeled as a first-order reaction [7]. Having known this, the optimal control problem can then be formulated by setting $R$ in Eq. (14) to be

$$R=-kC(x,t) \tag{15}$$

so that $k$ denotes a kinetic constant of the environmental factors that influenced the concentration of oil in water. Here, it is assumed that the source term is not known so that' $S=0$.

Then, Eq. (14) can be expressed as

$$\frac{\partial q(x,t)}{\partial t}=-\nabla\left(Vq(x,t)\right)+\nabla\cdot\left(D\nabla q(x,t)\right)-kq(x,t) \tag{16}$$

which is called "oil spill dynamical (or transport) problem". To solve this problem, a mechanism for controlling the system in marine environment can be set up as follows:

Let $\Omega$ be an open, connected subset of $\mathbb{R}^n$, where $\mathbb{R}^n$i is the Euclidean $n$-dimensional space. We defined the spatial boundary of the problem as $\Omega$. The unit variable is $t$ and is contained in the interval $[0,\ T]$, where $T<\infty$. Let $x$ be the space variable associated with $\Omega$, and let $\partial$ be a partial differential operator with appropriate initial and boundary conditions, where $\partial\Omega$ is the differential boundary of $\Omega$; then,

$$\begin{aligned} &q_t(x,t)-\alpha\Delta q(x,t)=q(x,t)\left(1-q(x,t)\right)-u(x,t)q(x,t) \quad in \quad \Omega\times[0,T] \\ &q(x,0)=q_0(x)\geq 0 \quad on \quad \Omega, t=0 \quad (seabed\ boundary) \\ &q(x,t)=0 \quad on \quad \partial\Omega\times[0,T] \quad (sea-side\ boundary) \end{aligned} \tag{17}$$

where $\partial\Omega\times[0,\ T]$ mathematically defined an operation with a PDE operator $\partial$ in the spatial boundary of the problem $\Omega$ within a specified upper and lower horizons $[0,\ T]$.

Eq. (17) is defined as the state equation with a logistic growth $q(1-q)$ and a constant diffusion coefficient $\alpha$ due to weathering processes. The symbol $\Delta$ represents the Laplacian. The state $q(x,\ t)$ denotes the volume or concentration of the crude oil and $u(x,\ t)$ is the control that entered the problem over the volumetric domain. The zero boundary conditions imply the limitation of the slick at the surrounding environment.

http://dx.doi.org/10.5772/63050

The reward or value objective functional can be obtained as

$$J(u) = \int_0^T \int_\Omega e^{-\theta t}\left(\xi u(x,t) q(x,t) - A u(x,t)^2\right) dx dt \tag{18}$$

Here, $\xi$ denotes the price of spilled oil, so that $\xi uq$ represents the reward from the control amount $uq$. Note that a quadratic cost for the clean-up effort with a weighted coefficient $A$, where $A$ is assumed to be a positive constant, is applied. The term $e^{-\theta t}$ is introduced to denote a discounted value of the accrued future costs with $0 \le \theta < 1$. By setting $\xi = 1$ (for convenience), an optimal control $u^*$ is needed to optimize a control strategy focusing on the actual detected spill point, such that application of any control on a no-spill region (look-alike) would be minimized [i.e., $u^*(x, t) = 0$] and the value of all future earnings would be maximized. In other words, we seek for $u^*$ such that

$$J(u^*) = \max_{u \in U} J(u) \tag{19}$$

where $U$ denotes a set of allowable control, and the maximization is over all measurable controls with $0 \le u(x, t) \le m < 1$ a.e. Under this set-up, it follows that, within the context of optimal control, the state solution satisfies $q(x, t) \ge 0$ on $\Omega \times (0, T)$ by the maximum principle for parabolic equations.

**Lemma 1 [8]:** Let $U$ be a convex set and $J$ be strictly convex on $U$. Then, there exists at most one $u^* \in U$ such that $J$ has a minimum at $u^*$. This implies that, by the maximum principle for parabolic equations, the necessary conditions for optimality are satisfied whenever the state solution satisfies $q(x, t) \ge 0$ on $\Omega \times (0, T)$.

## 3. Necessary optimality conditions

Consider the following conservation relations [8]:

$$\dot{x}_t = f(x_t, u_t) x_{t=0} \Rightarrow x(0) \tag{20}$$

where $x_t$ is the composition and concentration of the pollutant at time $t$, $u_t$ denotes controls that enter on the boundary of the problem at time $t$, $f$ is a set of nonlinear functions representing the conservation relation, and $x_{t=0}$ denotes the initial condition of $x$. Every change in the control function changes the solution to Eq.(20). Thus, for a given objective functional to be maximized, a piecewise continuous control policy $u_t$ and the state variable $x_t$ have to be obtained. The principle technique is to determine the necessary conditions that define an optimal control

policy $u(t)$ that would cause the system to follow a path $x(t)$, such that the performance functional

$$J(u) = \int_0^T F(x,u,t)dt \tag{21}$$

would be optimized.

Consider also the Lagrangian

$$L = F(x,u,t) + \lambda'\left(f(\cdot) - \dot{x}\right) \tag{22}$$

where $\lambda$ denotes the dynamic Lagrange multipliers or costate variables with its derivative given as $\lambda'$. For more simplification, an augmented functional with the same optimum of (21) could further be derived as

$$J = \int_0^T L(x,\dot{x},u,\lambda,t)dt \tag{23}$$

,

and by introducing the variations $\delta(x)$, $\delta(\dot{x})$, $\delta(u)$, $\delta(\lambda)$, $\delta(T)$, the first variation of the functional would be

$$\begin{aligned}\delta J = &\int_0^T \left[\frac{\partial L}{\partial x} - \frac{d}{dt}\frac{\partial L}{\partial \dot{x}}\right]'\delta(x)dt + \left[\frac{\partial L}{\partial \dot{x}}(T)\right]'\delta(x_T) \\ &+ \left[L(T) - \left(\frac{\partial L}{\partial \dot{x}}(T)\right)'\dot{x}(T)\right]\delta(T) \\ &+ \int_0^T \left(\frac{\partial L}{\partial \lambda}\right)'\delta(\lambda)dt + \int_0^T \left(\frac{\partial L}{\partial u}\right)'\delta(u)dt\end{aligned} \tag{24}$$

Noticed that, by the fundamental theorem of variational calculus, for $x(t)$ to be an optimum of the functional $J$, it is necessary that $\delta J = 0$. Because the controls and states are unbounded, the variations $\delta(x)$, $\delta(\lambda)$, and $\delta(u)$ are free and unconstrained. Thus, the following are the necessary conditions for optimality:

(i) *Existence and uniqueness: Euler-Lagrange equations*

Because the variation $\delta(x)$ was not bounded (i.e., it was free), we have

http://dx.doi.org/10.5772/63050

$$\frac{\partial L}{\partial x} - \frac{d}{dt}\frac{\partial L}{\partial \dot{x}} = 0 \tag{25}$$

Using Eq. (22), obtain

$$\frac{\partial L}{\partial \dot{x}} = -\lambda. \tag{26}$$

The Euler-Lagrange equations could be transformed as

$$\dot{\lambda} = \frac{\partial L}{\partial x}, \tag{27}$$

and by the definition of the Lagrangian, Eq. (27) becomes

$$\dot{\lambda} = \left(\frac{\partial f}{\partial x}\right)' \lambda - \frac{\partial F}{\partial x} \tag{28}$$

Eq. (28) shows that the Euler-Lagrange equations are the equations that specify the dynamic Lagrange multipliers.

(ii) *Constraints relations*

Because the variation$\delta(\lambda)$ is free, we have

$$\frac{\partial L}{\partial \lambda} = 0 \tag{29}$$

which is equivalent to (20). This implies that, along the optimal trajectory, the state differential equations must hold.

(iii) *Optimal control*

Also, because the variation $\delta(u)$ is free, it follows that the optimal control policy must be consistent with

$$\frac{\partial L}{\partial u} = 0 \tag{30}$$

or

$$\frac{\partial F}{\partial u}+\left(\frac{\partial f}{\partial u}\right)'\lambda=0\ ,\ \text{and} \tag{31}$$

(iv) *Transversality boundary conditions*

$$-\lambda'(T)\delta(T)+\left[F(T)+\lambda'(T)f(T)\right]\delta(T)=0 \tag{32}$$

The necessary conditions (i) to (iv) could be simplified further by introducing an Hamiltonian

$$H=F(x,u,t)+\lambda' f(x,u,t) \tag{33}$$

Such that

**i.** *Euler's equation*:

$$\dot{\lambda}=-\frac{\partial H}{\partial x} \tag{34}$$

**ii.** *Constraints relations*:

$$\dot{x}=f(\cdot)=\frac{\partial H}{\partial \lambda} \tag{35}$$

**iii.** *Optimal control*:

$$\frac{\partial H}{\partial u}=0,\text{and} \tag{36}$$

**iv.** *Boundary conditions*:

$$-\lambda'(T)\delta(x_T)+H(T)\delta(T)=0 \tag{37}$$

Furthermore, with the assumption that all the necessary conditions for optimality exist and sufficient for a unique optimal control, a sequential decision processes for optimal response strategy can be developed.

http://dx.doi.org/10.5772/63050

## 4. Sequential optimization processes

Sequential decision processes are mathematical abstractions of situations in which decisions must be made in several stages while incurring a certain cost at each stage. The philosophy here is to establish a sequential decision policy to be used as a combating technique strategy in oil spill control.

First, consider $x_t$ at time $t \in [0, T]$, where $T$ specifies the time horizon for the situation. For a control $u_t$ defined on $[0, T]$, the state equation given in Eq. (38) assumes a sudden rate of variation in the system. Thus, $x_t \in \mathbb{R}^n$ denotes the state of oil spill in waters, whereas $\dot{x}_t \in \mathbb{R}^n$ represents the vector of first-order time derivatives of $x_t$ and $u_t \in U \subset \mathbb{R}^m$ denotes the control vector. With the assumption that the initial value $x_0$ and the control trajectory over the time interval $0 \le t \le T$ are known, the optimization problem over the control trajectory is given as

$$\min_u \int_0^T f\left(x(t), u(t), t\right) dt \tag{38}$$

$$\textit{subject to} \quad \dot{x}(t) = g\left(x(t), u(t), t\right) \tag{39}$$

where $g$ is a given function of $u$, $t$a, and possibly $x$. This model establishes a sequential decision path for optimal policy to be used in the application of oil spill combating technique.

By introducing a value function $V$, we have

$$\begin{aligned} V(0, x_0) &:= \min_u \int_0^T f\left(t, x(t), u(t)\right) dt \\ \textit{subject to} \quad \dot{x}(t) &= g\left(t, x(t), u(t)\right), \end{aligned} \tag{40}$$

and by fixing $\Delta t > 0$, we get

$$V(0, x_0) = \min_u \left\{ \int_0^{\Delta t} f\left(t, x(t), u(t)\right) dt + \int_{\Delta t}^T f\left(t, x(t), u(t)\right) dt. \right. \tag{41}$$

Also, with the application of the principle of optimality,[1] we have

[1] See [9] for detailed discussion on principle of optimality.

$$V(0,x_0)=\min_u\left\{\int_0^{\Delta t} f(t,x(t),u(t))dt+V(\Delta t,x(\Delta t))\right. \tag{42}$$

Discretizing via Taylor series expansion, we get

$$V(0,x_0)=\min_u\left\{f(t_0,x_0,u)\Delta t+V(t_0,x_0)+V_t(t_0,x_0)\Delta t+V_x(x_0,t_0)\Delta x+\cdots\right. \tag{43}$$

where $\Delta x=x(t_0+\Delta t)-x(t_0)$. Thus, letting $\Delta t\to 0$ and dividing by $\Delta t$, we have

$$-V_t(x,t)=\min_u\left\{f(t,x,u)+V_x(x,t)g(t,x,u)\right. \tag{44}$$

with boundary condition

$$V(T,x_T)=0. \tag{45}$$

**Theorem 1 [8]:** Let $[t_0,\ t_1]$ denotes the range of time in which a sequence of control is applied. Then, for any processes, $t_0\le\tau_1\le\tau_2\le t_1$:

$$V(\tau_1,x(\tau_1))\le V(\tau_2,x(\tau_2)) \tag{46}$$

and for any $t$, such that $t_0\le t\le t_1$, the set$\Lambda_{t,x(t)}$ is not empty, as the restriction of the control to the time interval is feasible for $x(t)$.

***Proof:***

Let $u^*$ be any optimal control in $\Lambda_{\tau_2,x(\tau_2)}$, where $u^*$ is defined on $[\tau_1,\ \vec{\tau}_1]$ and is given by

$$u^*(\xi)=\begin{cases}u(\xi), & if\ \tau_1\le\xi\le\tau_2\\ \vec{u}(\xi), & if\ \tau_2\le\xi\le\vec{\tau}_1\end{cases} \tag{47}$$

Then, $u^*\in\Lambda_{\tau_1,x(\tau_1)}$. Hence,

$$V(\tau_1,x(\tau_1))\le\phi_1(\vec{\tau}_1,x^*(\vec{\tau}_1)) \tag{48}$$

http://dx.doi.org/10.5772/63050

where $\phi_1(\cdot)$ is a value function defined on $[\tau_1, \vec{\tau}_1]$. Because $u^*$ was any optimal control in $\Lambda_{\tau_2, x(\tau_2)}$, taking the infimum over the controls in $\Lambda_{\tau_2, x(\tau_2)}$ gives

$$V\left(\tau_1, x(\tau_1)\right) \leq V\left(\tau_2, x(\tau_2)\right) \tag{49}$$

This implies that, if $u^*$ is any optimal control for the sequential optimization process, the value function $V$ evaluated along the state and control trajectories will be a nondecreasing function of time.

Theorem 1 summarizes the expected future utility at any node of the decision tree on the assumption that an optimal policy will be imminent. The implication is that a continuous selection of a sequence of control at different assessment point will optimize the performance index of the control strategy. This, however, requires a decision rule, and the next section contained further explanation on this.

### 4.1. Decision rule

A successful sequential decision requires a decision rule that will prescribe a procedure for action selection in each state at a specified decision epoch. This is a known strategy in the field of operation research. More so, the problems of decision-making under uncertainty are best modeled as Markov decision processes (MDP) [8]. When a rule depends on the previous states of the system or actions through the current state or action only, it is said to be Markovian but deterministic if it chooses an action with certainty [8]. Thus, a deterministic decision rule that depends on the past history of the system is known as "history dependent". In general, MDP can be expressed as a process that

- allowed the decision maker to select an action whenever the system state changes and model the progression in continuous time and
- allowed the time spent in a certain state to follow a known probability distribution.

It follows a time-homogeneous, finite state, and finite action semi-MDP (SMDP) defined as

**i.** $P(x_{t+1} \mid u_t, x_t)$, $t = \{0, 1, 2, \cdots, T\}$, $T \leq \infty$ transition probability;

**ii.** $P(r_t \mid u_t, x_t)$ reward probability; and

**iii.** $P(u_t \mid x_t) = \pi(u_t \mid x_t)$ policy

This implies that, although the system state may change several times between decision epochs, the decision rule remains that only the state at a decision epoch is relevant to the decision maker. Consider the stochastic process $x_0, x_1, x_2, \ldots,$ where $x_t$ or $x(t)$ (which may be used interchangeably). Note that we are considering an optimal control of a discrete-time Markov process with a finite time horizon $T$, where the Markov process $x$ takes values in some measurable space $\Omega$. In what follows, assuming that we have a sequence of control $u_0, u_1, u_2, \ldots,$

where $u_n$ is the action taken by the decision maker at time $t = 0, 1, \cdots, n$, take values in some assessable space $U$ of allowable control. The decision rule is described by considering a class of randomized history-dependent strategies consisting of a sequence of functions

$$d_n = \left(d_0, d_1, \cdots, d_{T-1}\right), \tag{50}$$

and also by considering the following sequence of events:

- an initial state $x_0$ is obtained;
- having known $x_0$, the response official (the controller) selects a control $u_0 \in U$;
- a state $x_1$ is attained according to a known probability measure $P(x_1 \mid x_0, u_0)$; and
- knowing $x_1$, the response official selects a control $u_1 \in U$.

The basic problem therefore is to find a policy $\pi = (d_0, d_1)$ consisting of $d_0$ and $d_1$ that will minimize the objective functional $J(x_0) = \int f[x_1, d_1(x_1)]P(x_1 \mid x_0, d_0(x_0))$, which is given as $P(u_t \mid x_t) = \pi(u_t \mid x_t)$. Hence, we set $\mu_t^{\pi}: H_t^d \to R^1$ to denote the total expected reward obtained by using Eq. (50) at decision epochs $t, t+1, \cdots, T-1$. With an assumption that the history at decision epoch $t$ is $h_t^d \in H_t^d$, the decision rule follows $\mu_t^{\pi}$ for $t < T$ such that

$$\mu_t^{\pi}\left(h_t^d\right) = E_{h_t}^{\pi}\left[\sum_{k=t}^{T-1} r_k\left(x_k, u_k\right) + r_k\left(x_T\right)\right] \tag{51}$$

In particular, if the SMD processes (i) to (iii) are stationary, then, for a given rule $\pi$ and an initial state $x$, the future rewards can be estimated. Let $V^{\pi}(x)$ be the value function; then, the expected discounted return could be measured as

$$V^{\pi}\left(x\right) = E\left[\sum_{t=0}^{\infty} \theta^t rt \mid x_0 = x; \pi\right] \tag{52}$$

However, the entire cast of players involved in oil spill control (the contingency planners, response officials, government agencies, pipeline operators, tanker owners, etc.) shares keen interest in being able to anticipate oil spill response costs for planning purposes according to Arapostathis et al. [9]. This means that the type of decision and/or action chosen at a given point in time is a function of the clean-up cost. In other words, the clean-up/response cost is a key indicator for the optimal control. Thus, to set a pace for rapid response, it is important to introduce cost concepts into the control paradigm as discussed in the next section.

http://dx.doi.org/10.5772/63050

## 5. Optimal costs model

Considered the following synthesis: the system starts in state $x_0$ and the response team takes a permitted action $u_t(x_0)$, resulting in an output (reward) $r_t$. This decision determines the cost to incur. Now, defining a cost function that assigned a cost to each sequence of controls as

$$C\left(x_0, u_{0:T-1}\right) = \sum_{t=0}^{T-1} \beta\left(t, x_t, u_t\right) + \omega\left(x_T\right) \tag{53}$$

where $\beta(t, x, u)$ is the cost associated with taking action $u$ at time $t$ in state $x$ and $\omega(x_T)$ is the cost related to actions taken up to time $T$; the optimal control problem is to find the sequence $u_{0:T-1}$, that minimizes Eq. (53). Thus, we introduce the optimal cost functional:

$$C\left(t, x_t\right) = \min_{u_{t:T-1}} \left( \sum_{k=t}^{T-1} \beta\left(k, x_k, u_k\right) + \omega\left(x_T\right) \right) \tag{54}$$

which solves the optimal problem from an intermediate time $t$ until the fixed end time $T$, starting at an arbitrary state $x_t$. Here, the minimum of Eq. (53) is denoted by $C(0, x_0)$. Hence, a procedure to compute $C(t, x)$ from $C(t+1, x)$ for all $x$ recursively using dynamic programming is given as follows:

Set

$$C\left(T, x\right) = \omega\left(x\right)$$

So that

$$\begin{aligned} C\left(t, x_t\right) &= \min_{u_{t:T-1}} \left\{ \sum_{k=t}^{T-1} \beta\left(k, x_k, u_k\right) + \omega\left(x_T\right) \right\} \\ &= \min_{u_t} \left\{ \beta\left(t, x_t, u_t\right) + \min_{u_{t+1:T-1}} \left[ \sum_{k=t+1}^{T-1} \beta\left(k, x_k, u_k\right) + \omega\left(x_T\right) \right] \right\} \\ &= \min_{u_t} \left\{ \beta\left(t, x_t, u_t\right) + C\left(t+1, x_{t+1}\right) \right\} \\ &= \min_{u_t} \left\{ \beta\left(t, x_t, u_t\right) + C\left(t+1, x_t + f\left(t, x_t, u_t\right)\right) \right\} \end{aligned} \tag{55}$$

It could be seen that the reduction to a sequence of minimizations over $u_t$ from the minimization over the whole path $u_{0:T-1}$ is due to the Markovian nature of the problem: the future depends on the past and the past depends on the future only through the present. Thus, it could be seen that, in the last line of Eq. (55), the minimization is done for each $x_t$ separately and also explicitly depends on time. The procedure for the dynamic programming is illustrated as follows:

**Step 1:** Initialization: $C(T,\ x)=\omega(x)$

**Step 2:** Backwards: For $t=T-1,\ \cdots,\ 0$ and for all $x$, compute

$$u_t^*(x)=\arg\min_u\left\{\beta(t,x,u)+C(t+1,x+f(t,x,u))\right\}$$
$$C(t,x)=\beta\left(t,u_t^*(x)\right)+C\left(t+1,x+f\left(t,x,u_t^*(x)\right)\right)$$

**Step 3:** Forwards: For $t=0,\ \cdots,\ T-1$, compute

$$x_{t+1}^*=x_t^*+f\left(t,x_t^*,u_t^*\left(x_t^*\right)\right),\qquad x_0^*=x_0$$

**Lemma 2:** Let $\pi^*\rightarrow\left[u_0^*,\ u_1^*,\ \cdots,\ u_{T-1}^*\right]$ be an optimal control policy for the control problem and assume that, when using $\pi^*$, a given state $x_i$ occurs at time $i$, $(i\geq t)$ a.e. Suppose that the state is at stage $x_i$ at time $i$, and we wish to minimize the cost functional from time $i$ to $T$:

$$E\left[\omega(x_T)+\sum_{t=i}^{T-1}\beta\left(x_t,u_t(x_t)\right)\right] \tag{56}$$

Then, $\left[u_i^*,\ u_{i+1}^*,\ \cdots,\ u_{T-1}^*\right]$ is the optimal path for this problem and $u_t^*$ is the optimal control.

***Proof:*** Define $C^*(t,\ x)=\omega(x)$ as the optimal cost-to-go:

$$\min_u\left[g(x,u)+\nabla_t C^*(t,x)+\nabla_x C^*(t,x)'f(x,u)\right]=0 \tag{57}$$

where $C^*(T,\ x)=\omega(x)$. We can say that $\nabla_x C^*(T,\ x)=\nabla\omega(x)$. If we define $\nabla_x C^*\left(t,\ x_t^*\right)=\lambda_t$, then, by introducing the Hamiltonian, $H(x,\ u,\ \lambda)=g(x,\ u)+\lambda' f(x,\ u)$, where $\lambda_t=-\nabla_x H\left(x_t^*,\ u_t^*,\ \lambda_t\right)$; it follows from the optimality principle that

http://dx.doi.org/10.5772/63050

$$u_t^* = \arg\min_u \left[ g\left(x_t^*, u\right) + \lambda_t' f\left(x_t^*, u\right) \right] \quad \forall t \in \left[0, T\right] \tag{58}$$

**Theorem 2**: *Let* $\min_u \left[ g(x,\ u) + \nabla_t V(t,\ x) + \nabla_x V(t,\ x)' f(x,\ u) \right] = 0 \quad \forall\, t,\ x$ (59)

with the condition that $V(T,\ x) = \omega(x) \quad \forall\, x$

Suppose that $u_t^*$ attains the minimum in Eq. (59) for all $t$ and $x$. Let $\left(x_t^* \mid t \in [0,\ T]\right)$ be the oil trajectory obtained from the known quantity of spill at the initial state denoted by $x_0$, when the control trajectory, $u_t^* \to V\left(t,\ x_t^*\right)$, is used and $\dot{x}_t = f\left(x_t^*,\ u^*\left(t,\ x_t^*\right)\right) \quad \forall\, t \in [0,\ T]$. Then,

$$V\left(t,x\right) = C^*\left(t,x\right) \quad \forall t,x \tag{60}$$

and $\left\{u_t^* \mid t \in [0,\ T]\right\}$ is optimal control [7].

## 6. Conclusion

This chapter presents the mathematical abstractions of optimal control process where decisions must be made in several stages following an optimal control path to minimize the apparent toxicological effect of oil spill clean-up technique by determining the control measure that will cause a process to satisfy the physical constraints and at the same time optimizing some performance criteria for all future earnings from marine biota. Hence, in the future, if the optimal policy is followed, the recursive method for the sequential optimization will converge to optimal costs control and value function, which optimizes the probable future value at any node of the decision tree.

## Author details

Kufre Bassey

Address all correspondence to: kjbassey@gmail.com

Statistics Department, Central Bank of Nigeria, Abuja, Nigeria

## References

[1] Xu X, Pang S: Briefing of activities relating to the studies on environmental behaviour and economic toxicity of toxic organics. Journal of Environmental Science, 1992; 4(4): 3–9.

[2] Bassey K, Chigbu P: On optimal control theory of marine oil spill management: A Markovian decision approach. European Journal of Operational Research, 2012; 217(2): 470–478.

[3] Brown J: Nigeria Niger Delta bears brunt after 50 years of oil spills. The Independent, UK, October 20, 2006.

[4] Yapa P: State-of-the-art review of modelling transport and fate of oil spills. Journal of Hydraulic Engineering. 1996; 122(11): 594–600.

[5] Bassey K: On optimality of marine oil spill pollution control. International Journal of Operations Research and Optimization, 2011; 2(2): 215–238.

[6] Tkalich P, Huda M, Gin K: A multiphase oil spill model. Journal of Hydraulic Research. 2003; 4(2): 115–125.

[7] Chigbu P, Bassey K: Numerical modelling of spilled oil transport in marine environment. Pacific Journal of Science and Technology. 2010; 10(2):565–571.

[8] Bassey K. Methodological model for optimal control of marine oil spill [Ph.D. thesis]. University of Nigeria; 2014.

[9] Arapostathis A, Borkar V, Fernandez-Gaucherand E, Ghosh M, Marcus S: Discrete-time controlled Markov processes with average cost criterion: A survey. SIAM Journal on Control and Optimization. 1993; 31: 282–344.

Chapter 7

# Graphical Method for Robust Stability Analysis for Time Delay Systems: A Case of Study

Gerardo Romero, David Lara, Irma Pérez and Esmeralda Lopez

Additional information is available at the end of the chapter

http://dx.doi.org/10.5772/63158

**Abstract**

This chapter presents a tool for analysis of robust stability, consisting of a graphical method based on the construction of the value set of the characteristic equation of an interval plant that is obtained when the transfer function of the mathematical model is connected with a feedback controller. The main contribution presented here is the inclusion of the time delay in the mathematical model. The robust stability margin of the closed-loop system is calculated using the zero exclusion principle. This methodology converts the original analytic robust stability problem into a simplified problem consisting on a graphic examination; it is only necessary to observe if the value-set graph on the complex plane does not include the zero. A case of study of an internal combustion engine is treated, considering interval uncertainty and the time delay, which has been neglected in previous publications due to the increase in complexity of the analysis when this late is considered.

**Keywords:** robust stability, robustness margin, polynomials of Kharitonov, value set, interval uncertainty

## 1. Introduction

The automatic control systems that are applied on the industrial process or on any production plant are previously analyzed, before they can be physically implemented. This analysis consists of obtaining some properties of interest such as qualitative and quantitative that are very helpful to achieve good performance in the closed-loop control system. The analysis is realized with the intention to predict the behavior that the control system will have when this is implemented. However, most of the time, this prediction lacks precision such that analysis is strongly based

on the mathematical model of the physical process, and this does not represent in an exact way its dynamic behavior. This problem has been of great interest for scientific researchers in the last years, because it is desirable to get the best results when the control system is implemented but depends on these properties. A way of solving this problem is through the consideration of uncertainty on the mathematical model of the physical process. This uncertainty can be dynamic (see references [1–3]) or parametric (see references [4–6]). This chapter describes the qualitative property analysis of robust stability of a system. A case of study of an internal combustion engine is analyzed considering parametric uncertainty in the mathematical model. This case of study process is taken from references [5, 7], where conditions are obtained to verify the robust stability of the control system.

It is important to mention that in these research works several simplifications of the mathematical model were made, which may affect the real behavior of the system; one simplification performed by the authors is the cancellation of time delay in a part of the mathematical model, which has an influence that affects the stability property. The main contribution presented here is the consideration of the time delay on the mathematical model of an internal combustion engine, which is taken into account to obtain the property of robust stability. The methodology used is based on the application of the value-set concept to the particular case of the internal combustion engine (see reference [5]); to be more precise, it consists of the characterization of the value set of the resulting characteristic equation of the closed-loop system when the controller is connected. This controller assigns the poles in a position previously defined. Using this characteristic and applying the zero exclusion principle [8], it is possible to obtain robust stability conditions through a visual inspection of a graphic in the complex plane.

This chapter is organized as follows: Section 2 presents the elements used to verify the robust stability, Section 3 provides an abstract regarding obtaining the mathematical model of the internal combustion motor, in Section 4 the problem statement is set, in Section 5 the robust stability tools are used in simulation to verify robustness margin, and finally in Section 6 the conclusions of this work are presented.

## 2. Preliminary

In this section, we give the value-set concept, which is widely used to verify robust stability (see references [5, 9, 10]). The methodology that will be used consists of obtaining the value set for the characteristic equation, which results from the interval plants including time delay that are defined using the following definition:

**Definition 1.** A transfer function type interval plant is composed in the following manner:

$$g(s,\boldsymbol{q},\boldsymbol{r}) = \frac{n(s,\boldsymbol{q})}{d(s,\boldsymbol{r})} = \frac{\sum_{i=0}^{m}\left[q_i^-, q_i^+\right]s^i}{s^n + \sum_{i=0}^{n-1}\left[r_i^-, r_i^+\right]s^i} \forall \boldsymbol{q} \in \mathcal{Q}, \boldsymbol{r} \in \mathcal{R} \tag{1}$$

http://dx.doi.org/10.5772/63158

Now, if the interval plant includes the time delay, then it can be denoted by the following expression:

$$\mathrm{g}\left(s,\boldsymbol{q},\boldsymbol{r},e^{-\tau s}\right)=\mathrm{g}\left(s,\boldsymbol{q},\boldsymbol{r}\right)e^{-\tau s}\tau\in\left[0,\tau_{\max}\right] \tag{2}$$

Notice that $m < n$, then g($s$,$\boldsymbol{q}$, $\boldsymbol{r}$) is a set of strictly proper rational functions, $\boldsymbol{Q}$ and $\boldsymbol{R}$ are sets that represent the parametric uncertainty and are defined as follows:

$$\mathcal{R}\triangleq\left\{\boldsymbol{r}=\left[r_1\cdots r_{n-1}\right]^T:r_i^-\le r_i\le r_i^+\right\}$$
$$\mathcal{Q}\triangleq\left\{\boldsymbol{q}=\left[q_1\cdots q_{n-1}\right]^T:q_i^-\le q_i\le q_i^+\right\}$$

These kinds of sets are called as boxes. Equation (2) represents a type of systems known as interval plants. Both the numerator and the denominator of the transfer function have coefficients of uncertain values, which reside in a closed interval. The main interest in the study of this chapter is the robust stability analysis of feedback control systems, as the one depicted in **Figure 1**, whose main process is represented by an interval plant, with time delay and negative unitary gain feedback. The characteristic equation of this feedback system can be expressed in terms of the numerator, denominator, and time delay as follows:

$$\mathrm{p}(s,\boldsymbol{q},\boldsymbol{r},e^{-\tau s})=\mathrm{d}(s,\boldsymbol{r})+\mathrm{n}(s,\boldsymbol{q})e^{-\tau s} \tag{3}$$

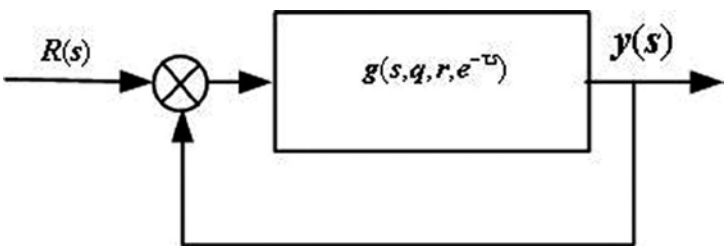


**Figure 1.** Uncertain interval plant with time delay in negative feedback.

The term quasi-polynomial is used to describe these types of functions. Note that the above characteristic Eq. (3) is not a single equation but rather a family of an infinite number of characteristic equations. Then, this whole family must be considered if robust stability verification is carried out. This family is defined as follows:

$$P_\tau\triangleq\left\{\mathrm{p}\left(s,\boldsymbol{q},\boldsymbol{r},e^{-\tau s}\right)=\boldsymbol{q}\in\mathcal{Q};\boldsymbol{r}\in\mathcal{R};\tau\in\left[0,\tau_{\max}\right]\right\} \tag{4}$$

The robust stability property is guaranteed if and only if the following equation is satisfied:

$$\mathrm{p}(s, \boldsymbol{q}, \boldsymbol{r}, e^{-\tau s}) \neq 0 \ \forall s \in \mathbb{C}_{+} \tag{5}$$

where $\mathbb{C}_{+}$ is used to denote the set of complex numbers with real part positive or equal to zero. From Eq. (3), it can be comprehended that the robust stability property of the dynamic system is very hard to verify using analytical methods, because this equation contains an endless number of equations. The goal of this work is to show a simple method to validate the robust stability property of time delay systems. The contribution of this work is based on the value-set characterization of the family of characteristic equations $P_{\tau}$. The value set is defined here as follows:

**Definition 2**. The value set, denoted as $V_{\tau}(\omega)$, of the characteristic equation of an interval polynomial with time delay is the set of complex numbers obtained by substituting $s = j\omega$ in the polynomial:

$$V_{\tau}(\omega) \triangleq \{\, p\,(s, \boldsymbol{q}, \boldsymbol{r}\, e^{-\tau s}) : s = j\omega, \omega \in \mathbb{R}, \boldsymbol{q} \in \boldsymbol{Q}; \boldsymbol{r} \in \boldsymbol{\mathcal{R}}; \tau \in [0, \tau_{max}] \,\} \tag{6}$$

where **Q** and **R** represent the set containing all possible values of the uncertainty of the parameters $q_i$ and $r_i$ expressed in a vector form as elements of the vector $q$ and $r$. It is clear that the value set of $P_{\tau}$ is a set of complex numbers plotted on the complex plane for values of $q_i$, $r_i$, $\omega$, and $\tau$ inside the defined boundaries. An important result that is applied in this chapter is the characterization of the value set for a characteristic equation as the one considered in the previous definition; this result is represented in references [11] and [12] with the following lemma:

**Lemma 1**. For each frequency $\omega$, the value set $V_{\tau}(\omega)$ is formed by octagons, where each one changes their geometry in function of the time delay $\tau$. The coordinates in the complex plane of the vertices or corners of each octagon are given by the following formulas:

$$\upsilon_{i+1} = d_{i+1}(j\omega) + n_k(j\omega)e^{-j\omega\tau} \tag{7}$$

$$\upsilon_{i+5} = d_{i+1}(j\omega) + n_h(j\omega)e^{-j\omega\tau} \tag{8}$$

where

$$i = 0,1,2,3,$$

$$k = (\gamma + i) \bmod_4 + 1$$

http://dx.doi.org/10.5772/63158

$$h = (\gamma + i + 1) \bmod_4 + 1$$

The term $\bmod_4$ represents the whole module base four operation, for example, $\bmod_4 (3)$. $\gamma$ can take integer values 0, 1, 2, and 3 depending on $\omega\tau$, see reference [9]:

$$\gamma \triangleq \begin{cases} 0 \; 2n\pi \le \omega\tau \le \dfrac{\pi}{2} + 2n\pi \\ 1 \; \dfrac{\pi}{2} + 2n\pi \le \omega\tau \le +2n\pi \\ 2 \; \pi + 2n\pi \le \omega\tau \le \dfrac{3\pi}{2} + 2n\pi \\ 3 \; \dfrac{3\pi}{2} + 2n\pi \le \omega\tau \le 2\pi + 2n\pi \end{cases}$$

The corresponding Kharitonov polynomials for the numerator and denominator of the interval plant are denoted by $n_i(s)$ y $d_i(s)$, respectively.

An example of a particular value set for fixed frequency and time delay is presented in **Figure 2**.

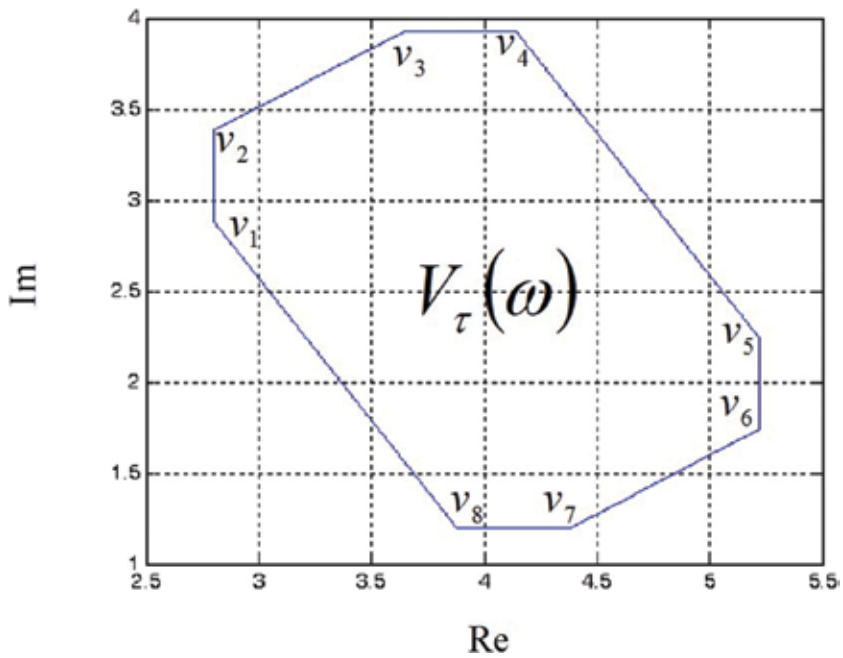


**Figure 2.** Value set for a fixed frequency and time delay.

From the definition given for the value set, one can conclude that it includes all the values that the infinite family $P_\tau$ can take when it is evaluated in $s = j\omega$. Then, if the complex plane origin is contained in the value set $V_\tau(\omega)$, this means that $P_\tau$ has roots located over the imaginary axis $j\omega$ for some values of $\omega \in \mathbb{R}$. This, in fact, causes instability in the time delay feedback system. Consequently, the value-set technique can be used as an instrument that serves to validate the robust stability property. A question that arises in this point is how to show that $P_\tau$ does not have roots on the right half plane when a sweep over $j\omega$ is done. The answer to this question is sustained in the following result known as the zero exclusion principle, see references [5, 11, 12]. This result will be applied to verify robust stability property.

**Theorem 1:** Suppose that $p(s, q, r, e^{-\tau s})$ has at least one member stable for $\tau = 0$, then $p(s, q, r, e^{-\tau s})$ is robustly stable only if the value set satisfies:

$$0 \notin V_T(\omega) \forall \omega \geq 0 \tag{9}$$

**Proof:** See reference [8]

From the previous theorem, the robust stability problem is transformed into a problem where it only needs to verify that the value-set plot just avoids the zero of the complex plane.

## 3. Case of study mathematical model

In this section, the internal combustion motor is modeled. The idle mode operation condition is considered, which means the vehicle engine is running without accelerating; this is because the original objective is to reduce the fuel consumption when the vehicle is on and stopped, such as waiting for the green of the traffic light when circulating in the city. This fuel economy can be achieved increasing the air ratio of the fuel mixture, but this action causes instability in engine operation, resulting in a variation in the angular speed of the motor shaft. The mathematical model was compiled from article [7] and it is divided into three parts for better comprehension: (a) manifold chamber, (b) internal combustion chamber, and (c) rotational motion system.

### 3.1. Manifold chamber

The rate of chance of the pressure in the manifold chamber is affected by the current chamber pressure, the opening position of the throttle valve $d(t)$, which controls the incoming air mass flow in a proportional way, and the outgoing flow that is proportional to the motor angular velocity $n(t)$. The output of the chamber is the relative air pressure $p(t)$. Then, the equation that gives the relationship between these two inputs and the output is given as the first-order differential equation as follows:

$$\dot{p}(t) + k_2 p(t) = k_1 d(t) - k_3 n(t) \tag{10}$$

where $k_1$, $k_2$, $y$ $k_3$ are the respective proportionality constants. Applying the Laplace transform to previous equation, the following transfer function corresponding to the manifold chamber is obtained:

$$p(s) = \frac{1}{s + k_2}[k_1 d(s) - k_3 n(s)] \tag{11}$$

### 3.2. Internal combustion chamber

The combustion chamber produces the necessary torque to move the motor shaft. The torque generation subsystem can be modeled in a simple way having as inputs the spark advance (forward position of the rotor) $a(t)$, the relative air pressure on the chamber $p(t)$, the motor angular velocity $n(t)$, and the fuel flow $f(t)$. These variables contribute to the torque generation in a linear form. There is a time delay $\tau_d$ called *induction-to-power-stroke delay*, which affects the fuel control and the chamber pressure variables; this delay $\tau_d$ depends on the motor speed and the number of cylinders activated independently (denoted by $n_c$) as given by the following formula:

$$\tau_d = \frac{120}{n_c n(t)} \tag{12}$$

Thus, the Laplace transform of the engine torque delivery $T_e(s)$ generated for the combustion block is represented by the following equation:

$$T_e(s) = e^{-\tau_d s}\left[k_4 p(s) + k_5 n(s) + k_f f(s)\right] + k_6 a(s) \tag{13}$$

Most of the time the delay is neglected, but when parameter uncertainty is considered, this has an influence on the control system stability, which is the reason this has been taken into account for analysis in this work.

### 3.3. Shaft rotational dynamics

Finally, the equations that represent the rotational can be obtained using Newton's second law for rotational movement as follows:

$$J\dot{n}(t) = T_e(t) - T_L(t) - k_7 n(t) \tag{14}$$

where $J$ represents the rotational inertia, $T_L$ is the torque of external load including its disturbances, and $k_7$ is an attenuation constant of the viscous friction that depends on the tempera-

ture, type of lubricant, and the gear that the motor uses. Therefore, the Laplace transform of the engine speed $n(s)$ can be described as follows:

$$n(s) = \frac{1}{Js + k_7}\left[T_e(t) - T_L(s)\right] \tag{15}$$

Then, considering the transfer functions for each subsystem, the complete block diagram representing the mathematical model of the internal combustion motor can be obtained and implemented in Simulink MATLAB, for numerical simulation as shown in **Figure 3**.

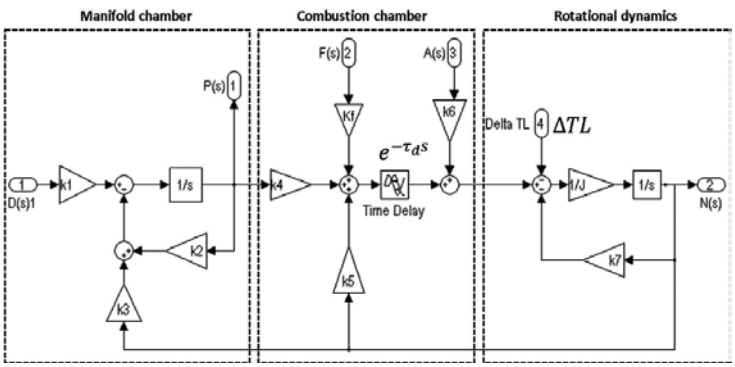


**Figure 3.** System block diagram in Simulink MATLAB.

The interest in this case of study is the relation between the variables $d(s)$ and $n(s)$ taking into account the time delay; then using block diagram algebra, the corresponding transfer function is given as follows:

$$g(s) = \frac{k_1 k_4 e^{-\tau_d s}}{Js^2 + (k_2 J + k_7)s + k_2 k_7 + [k_3 k_4 - k_2 k_5 - k_5 s]e^{-\tau_d s}} \tag{16}$$

The previous transfer function will be considered as the mathematical model of the internal combustion motor.

## 4. Problem statement

It is important to mention that the engine mathematical model is expressed in terms of the parameters $k_i$ and $J$. These parameters depend on the motor operating point; therefore, they cannot be considered as constant in the transfer function and they will be considered as uncertain terms that change depending on the operation point, but around the nominal parameters. The nominal values considered here are the same values as [7]: $k_1$ = 3.4329, $k_2$ =

http://dx.doi.org/10.5772/63158

0.1627, $k_3$ = 0.1139, $k_4$ =0.2539, $k_5$ = 1.7993, $k_7$ =1.8201, and the inertia $J$ = 1. Making a change on the variables, the transfer function on the mathematical model can be simplified as follows:

$$g(s) = \frac{a_1 e^{-\tau_d s}}{s^2 + a_2 s + a_3 + (a_4 s + a_5) e^{-\tau_d s}} \tag{17}$$

where the uncertain parameters are the ones included in $a_i$, the inertia $J$ will be considered as a fixed number and equal to 1. Comparing the transfer functions (16) and (17), it can be observed that the new nominal parameters take the following values: $a_1$ = 0.8716, $a_2$ = 1.9828, $a_3$ = 0.2961, $a_4$ = 1.7993, $a_5$ = –0.2638.

A controller can be connected in the closed-loop system, as shown in **Figure 4**, with two objectives: the first one to regulate the angular speed and the second to improve the performance of the process. This controller is given by the following function:

$$c(s) = \frac{50.0194s + 26.3065}{s^2 + 9.8165s + 33.1664} \tag{18}$$

which assigns the system poles of the feedback control, considering a unitary feedback [13], at the following position: {−1, −2, −3, −4} on the complex plane. The controller was designed with the nominal parameters and time delay equal to zero. The characteristic equation of the closed-loop control system considering the uncertain parameters and the time delay has the following structure:

$$p\left(s, q, r, e^{-T_d s}\right) = d(s, r) + n(s, q) e^{-\tau_d s}$$

where

$$\begin{aligned} d(s,r) &= s^4 + (a_2 + 9.82)s^3 + a_3 + 9.82a_2 + \\ &33.17)s^2 + (9.82a_3 + 33.17a_2)s + 33.17a_3 \end{aligned} \tag{19}$$

$$\begin{aligned} n(s,q) &= -a_4 s^3 + (a_5 - 9.82a_4)s^2 + (9.82a_5 - \\ &33.17a_4 + 50.02a_1)s + 33.17a_5 + 26.31a_1 \end{aligned} \tag{20}$$

The problem considered in this work is to determine the property of robust stability of the internal combustion motor when uncertainty is included in the new nominal parameters $a_i$. This property is directly related to the characteristic equation.

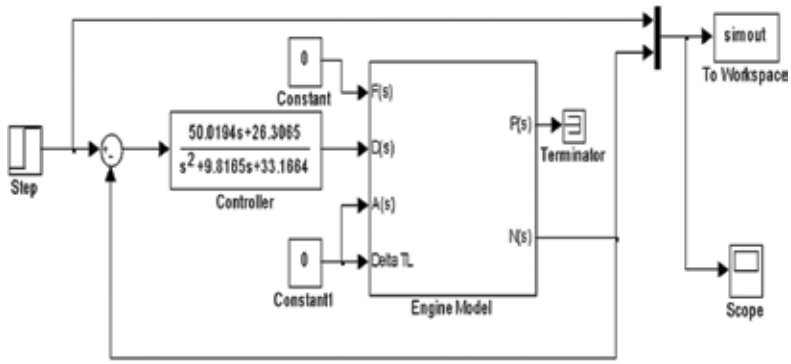


**Figure 4.** Control for angular velocity of the internal combustion motor.

## 5. Robust stability verification

First, the characteristic equation is considered without uncertainty, taking into account the nominal parameters and the time delay, which means:

$$p\left(s,q,e^{-T_d s}\right)=s^4+r_1s^3+r_2s^2+r_3s+r_4+\left(q_1s^3+q_2s^2+q_3s+q_4\right)e^{-\tau_d s}$$

where $r_1 = 11.80$, $r_2 = 52.93$, $r_3 = 68.67$, $r_4 = 9.82$, $q_1 = -1.80$, $q_2 = -17.93$, $q_3 = -18.67$, $q_4 = 14.18$.

Using Lemma 1, the corresponding value set for $\omega \in [0, .5]$ y $\tau_d \in [0, 9.9]$ is obtained, which is represented on the graphic shown in **Figure 5**.

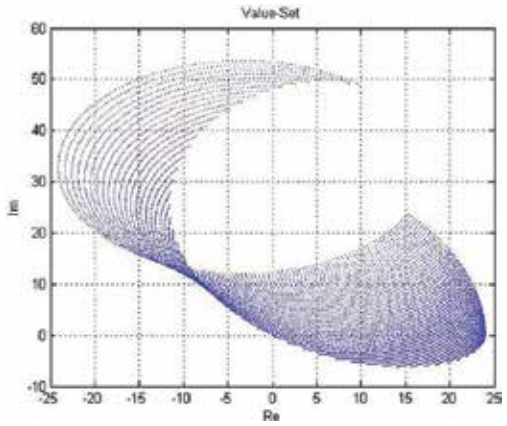


**Figure 5.** Value set without uncertainty in the parameters.

http://dx.doi.org/10.5772/63158

From the previous graphic, it can be appreciated that the value set does not reach the zero of the complex plain, but is very close; thus, it can be determined that the maximum delay the control system supports to preserve the stability is 9.9 s. Several numerical simulations can be run for different time delay limits to appreciate more clearly if the value set reaches the origin, for instance, considering the time delays $\tau_1$=2.5, $\tau_2$=9.9, $\tau_3$=13, which correspond to the stable, oscillatory, and unstable system responses, respectively, as shown in **Figures 6–8**, respectively.

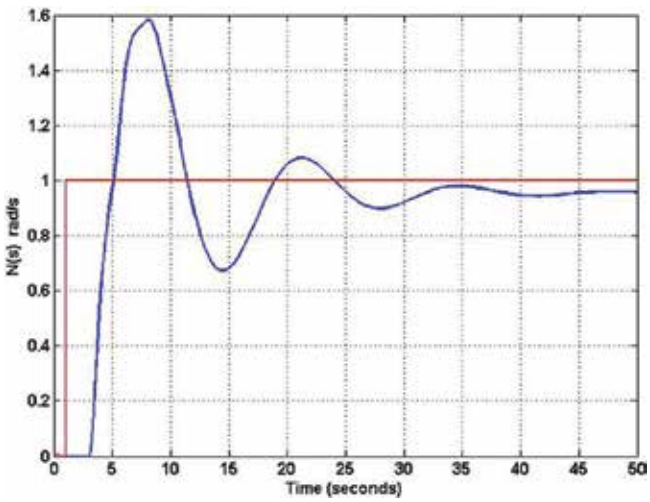


**Figure 6.** Transient response for stable behavior.

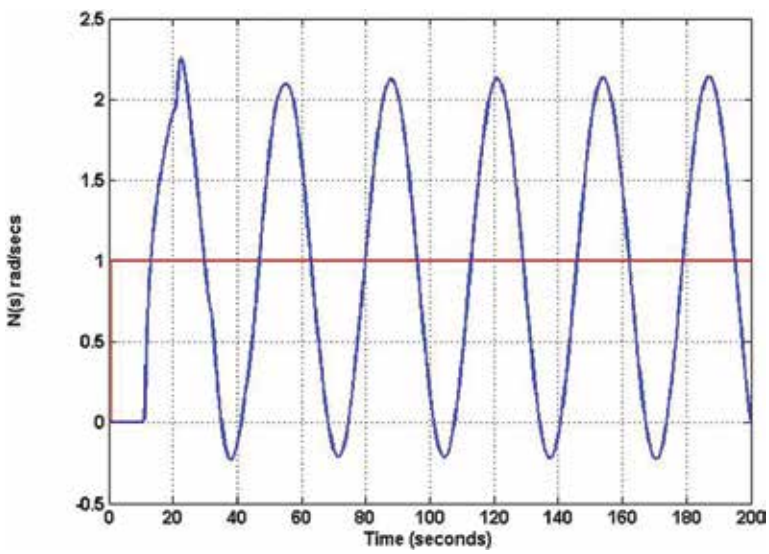


**Figure 7.** Transient response for oscillatory behavior.

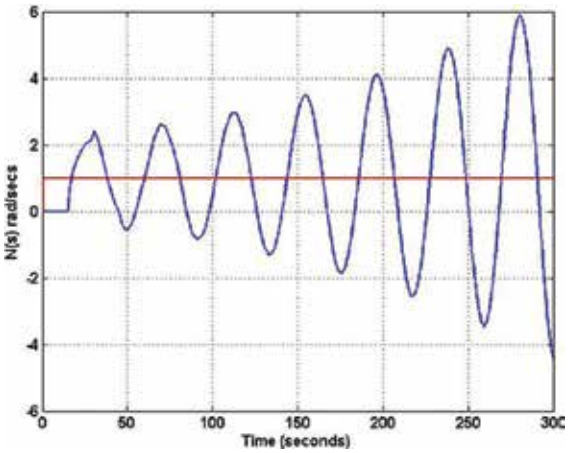


**Figure 8.** Transient response for unstable behavior.

Finally, considering an uncertainty of 10% in each of the parameters, the following characteristic equation is obtained, where an overestimation was made to obtain interval polynomials with time delay:

$$p\left(s,q,r,e^{-T_d s}\right) = s^4 + r_1 s^3 + r_2 s^2 + r_3 s + r_4 + \left(q_1 s^3 + q_2 s^2 + q_3 s + q_4\right) e^{-\tau_d s}$$

where $r_1$ = [11.60,11.99],, $r_2$ = [50.95, 54.90], $r_3$ = [61.80,75.53], $r_4$ = [8.84,10.80], $q_1$ = −1.98, −1.62], $q_2$ = [−19.72, −16.13], $q_3$ = −29.25, −8.08], $q_4$ = [11.01,17.35].

Once again, using the lemma, the value set of the characteristic equation is obtained now with uncertainty in the coefficients; This can be appreciated in the graphic of the **figure 9**.

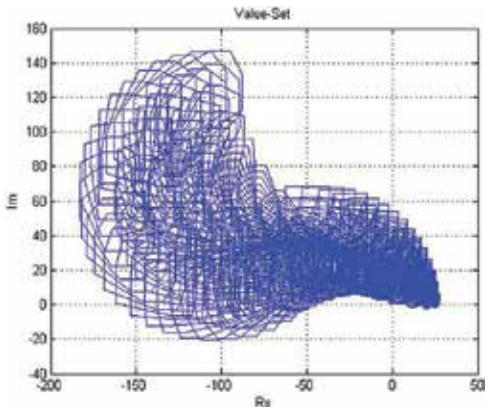


**Figure 9.** Value set with uncertainty in the parameters.

The previous value set was obtained for a value range of $\omega \in [0, 1.5]$, $\tau_d \in [0, 2.8]$ and like the previous case it can be observed that it barely reaches the zero of the complex plain; therefore, it can be assumed that the maximum time delay the control system supports is 2.8 s. Therefore, it can be clearly appreciated that parameter uncertainty decreases the delay margin that the control system supports and it is important to take this into account when the robust stability property is being verified. It is necessary to note that due to the overestimation about the parameters to represent the characteristic equation as a polynomial delay interval, the results obtained only warranty enough robust stability conditions; nevertheless, the next simulation shows how instability is presented for each of the values contained in the uncertainty, on the control system, when having a delay of $\tau_d = 4.1$ s (see **Figure 10**).

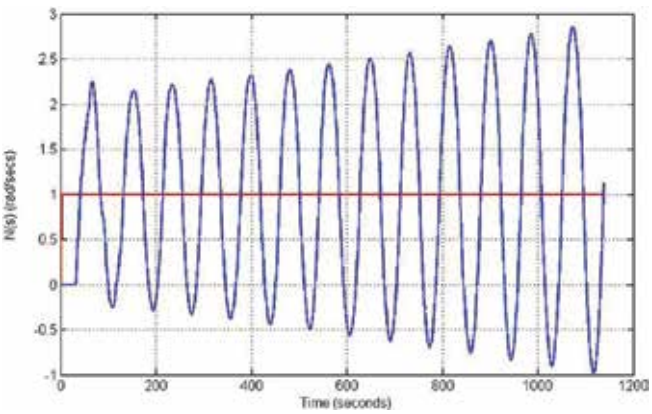


**Figure 10.** Step response with uncertainty in both parameters and time delay.

## 6. Discussion and conclusion of results

A robust stability verification methodology based on a graphic method was mentioned in this chapter. First, the mathematical model with nominal approximated parameters must be obtained; then, a control algorithm connected in feedback with the plant is analyzed when in the plant of the closed-loop system, uncertainty is introduced in both parameters and time delay. The main tools used are the value-set graph and the zero exclusion principle, then the analytical problem to verify the robust stability is transformed into a graphical problem, which consist of checking if the value-set plot for frequency interval does not include the origin. The case of study of an internal combustion motor was presented. The time delay appears when modeling the corresponding section of the engine combustion chamber of the motor. It is important to note that by considering the uncertainty in the parameters of the mathematical model, the time delay influences more in the control stability system; so, it can become significant even when it is very small and therefore the inclusion in the analysis is important. Then, with the tools presented here, a robustness margin for parameters and time delay can be obtained.

## Author details

Gerardo Romero, David Lara*, Irma Pérez and Esmeralda Lopez

*Address all correspondence to: dlara@docentes.uat.edu.mx

Autonomous University of Tamaulipas, Tamaulipas, México

## References

[1] Doyle, J.C., Francis, B.A. and Tannenbaum, A.R. Feedback Control Theory. 1st ed. USA: Dover Publications; 2009. 224 p. ISBN: 978-0486469331

[2] Green, M. and Limebeer, D.J.N. Linear Robust Control. 1st ed. USA: Dover Publications; 2012. 558 p. ISBN: 978-0486488363

[3] Zhou, K., Doyle, J.C. and Glover, K. Robust and Optimal Control. 1st ed. USA: Prentice Hall; 1996. 596 p. DOI: 978-0134565675

[4] Ackermann, J. Robust Control: Systems with Uncertain Physical Parameters. 1st ed. London: Springer Verlag; 1993. 405 p. ISBN: 10.1007/978-1-4471-3365-0

[5] Barmish, B.R. New Tools for Robustness of Linear Systems. 1st ed. ON, Canada: Macmillan; 1994. 394 p. ISBN: 0-02-306055-7

[6] Chapellat, H., Keel, L.H. and Bhattacharyya, S.P. Robust Control: The Parametric Approach. 1st ed. USA: Prentice Hall; 1995. 672 p. ISBN: 978-0137815760

[7] Abate, M., Barmish, B.R., Murillo-Sanchez, C. and Tempo, R. Application of Some New Tools to Robust Stability Analysis of Spark Ignition Engine: A Case of Study. IEEE Transactions on Control Systems Technology. 1994;2(1):22–30. DOI: 10.1109/87.273106

[8] Ranzer, A.A. Finite Zero Exclusion Principle. In: Kaashoek, M.A., editor. Robust Control of Linear Systems and Nonlinear Control. 1st ed. USA: Springer; 1990. pp. 239–245. DOI: 10.1007/978-1-4612-4484-4

[9] Lara, D., Romero, G., Sanchez, A., Lozano, R. and Guerrero, A. Robustness Margin for Attitude Control of a Four Rotor Mini-Rotorcraft: Case of Study. Mechatronics. 2010;20(1):143–152. DOI: 10.1016/j.mechatronics.2009.11.002

[10] Kogan, J. and Leizarowitz, A. Frequency Domain Criterion for Robust Stability of Interval Time Delay Systems. Automatica. 1995;31(3):463–469. DOI: 10.1016/0005-1098(94)00079-X

[11] Romero, G. Análisis de Estabilidad Robusta Para Sistemas Dinámicos con Retardo [Thesis]. San Nicolas de los Garza, Nuevo Leon, México: FIME Universidad Autónoma

de Nuevo León; 1997. 125 p. Available from: http://cdigital.dgb.uanl.mx/te/1020119973/1020119973.html

[12] Romero, G. and Collado, J. Construcción del Value-Set para Sistemas de Control con Retardo en el Transporte. In: Tecnológico de Chihuahua, editor. VIII Congreso Internacional Académico de Ingeniería Electrónica, Electro 96; October 1996; Chihuahua Mexico. Mexico: Tecnológico de Chihuahua; 1996. pp. 228–233. http://www.depi.itch.edu.mx/apacheco/electro/96/

[13] Åström, K.J. and Hägglund, T. PID Controllers: Theory, Design, and Tuning. 1st ed. USA: Instrument Society of America; 1995. 343 p. ISBN: 978-1556175169

*Edited by Moises Rivas López and Wendy Flores-Fuentes*

The need to be tolerant to changes in the control systems or in the operational environment of systems subject to unknown disturbances has generated new control methods that are able to deal with the non-parametrized disturbances of systems, without adapting itself to the system uncertainty but rather providing stability in the presence of errors bound in a model. With this approach in mind and with the intention to exemplify robust control applications, this book includes selected chapters that describe models of H-infinity loop, robust stability and uncertainty, among others.

Each robust control method and model discussed in this book is illustrated by a relevant example that serves as an overview of the theoretical and practical method in robust control.

ISBN 978-953-51-5070-1

Photo by kentoh / CanStock

IntechOpen